

# Design of a Robot-Assisted Gait Trainer



LOPES II

Jos Meuleman



Design of a Robot-Assisted Gait Trainer:  
LOPES II

This research was financially supported by a grant from Dutch Ministry of Economic affairs and Province of Overijssel, the Netherlands (grant: PID082004)

This research and the publication of this thesis was financially supported by MOOG B.V., Nieuw-Vennep, The Netherlands. [www.moog.com](http://www.moog.com)

Their support is gratefully acknowledged.

De promotiecommissie is als volgt samengesteld:

*Voorzitter en Secretaris (Chairman and Secretary):*  
Prof.dr. G.P.M.R. Dewulf      Universiteit Twente

*Promotorenen (Promotors):*  
Prof.dr.ir. H. van der Kooij      Universiteit Twente  
Prof.dr. J.S. Rietman      Universiteit Twente

*Co-Promotor:*  
Dr. E.H.F. van Asseldonk      Universiteit Twente

*Leden (Members):*  
Prof.dr.ir. S. Stramigioli      Universiteit Twente  
Prof.dr.ir. J.Herder      Universiteit Twente  
Prof.dr. S. Geurts      UMC St. Radboud  
Prof.dr. S.K. Agrawal      Columbia University (NY)  
Prof.dr. M. Steinbuch      Technische Universiteit Eindhoven

*Paranimfen:*  
Ralph Marissen  
Floris te Lintelo

Copyright ©2015 J.H. Meuleman, Bennebroek, the Netherlands.  
All rights reserved. No part of this publication may be reproduced or transmitted in any form or by any means, electronic or mechanical, including photocopy, recording or any information storage or retrieval system, without the written permission of the author.

ISBN: 978-90-365-3965-4  
DOI: 10.3990/1.9789036539654

Printed by Gildeprint Drukkerijen BV, Enschede  
[www.gildeprint.nl](http://www.gildeprint.nl)



DESIGN OF A ROBOT-  
ASSISTED GAIT TRAINER:  
LOPES II

PROEFSCHRIFT

ter verkrijging van  
de graad van doctor aan de Universiteit Twente,  
op gezag van de rector magnificus,  
Prof. dr. H. Brinksma,  
volgens besluit van het College voor Promoties,  
in het openbaar te verdedigen  
op vrijdag 13 november 2015 om 16.45 uur

door

**Johannes Hendricus Meuleman**  
geboren op 9 april 1976  
te Amsterdam

Dit proefschrift is goedgekeurd door:  
prof.dr.ir. H. van der Kooij, promotor  
prof.dr. J.S. Rietman, promotor  
dr. E.H.F. van Asseldonk, co-promotor

# Summary

Robot-assisted gait training is rapidly evolving since the last two decades. However the use of robot-assisted gait trainers (RAGT) in clinical practice is limited. Main contributors hereto are the limited effectiveness and limited efficiency. The main challenges in the development of robot-assisted gait trainers are to allow for Assist As Needed (AAN) training and reduction of the idle time of training, i.e., time needed to (de-)install the patient in the RAGT (donning and doffing time). AAN training implies that the patient should have freedom in walking and only receives support on specific (affected) aspects of gait. This in its turn implies that the RAGT must allow for multiple Degrees of Freedom (DoFs) and that the powered DoFs are capable of following the patient's motion, i.e., the DoFs should be transparent, in order to display minimum impedance.

After extensive research on the requirements from the end users i.e., physical therapists, rehabilitation physicians, patients and researchers, the system requirements for the new RAGT, LOPES II, were established: a treadmill-based robot, with mechanics located behind the patient, with minimum amount of clamps. Furthermore the patient must be able to move freely in rotations and translations of all segments and joints, and arm swing must be unhindered. In a study, we have demonstrated that one can walk unhindered with up to 6 kg of inertia added to the pelvis, or 2 kg of inertia added to the ankle. Support must be supplied on the pelvis horizontal translations, hip abduction / adduction (leg sideways) and flexion / extension (swinging the upper leg forward/backward), knee flexion / extension, and foot plantar / dorsiflexion (foot push-off/toelifting).

During the concept phase, the end users frequently evaluated the concepts. This process not only improved the quality of the concepts, but also increased the involvement of the end users in the development process. The best concepts were integrated into a single-legged mechanical proof of

concept. This integrated proof of concept for LOPES II uses a patented shadow leg approach, i.e., a mechanical leg located behind the patient. The patient leg and shadow leg are connected with push-pull rods. Contrary to conventional exoskeletons with a mechanical leg located at the side of the patient leg, the shadow leg requires little alignment. The number of clamps are minimum: a clamp at the pelvis (combined with a harness for safety and bodyweight support), clamps at the lower legs (below the knees), and clamps at the feet (foot brackets). For the clamps at the feet and pelvis we use patented gimbals which allow rotations of feet and pelvis, and make that supportive forces apply in the center of the ankle joints and hip joints. Furthermore the concept contains a seat on which patients can sit during the donning and doffing phase, and rest between trainings.

The integrated proof of principle, together with a list of system requirements, formed the input for the design of the mechatronic prototypes. The mechanical linkage is designed such that powered DoFs are largely decoupled, to avoid complexity in transformation calculations and to have an optimal range of motion for each DoF. The selected actuators are capable of providing sufficient support for severely impaired patients, and they are fast enough to follow motions of fast walking. For control of LOPES II we selected admittance control. This allows for both high impedance (high support) and low impedance (low support), by displaying a (low) virtual mass without friction. Custom-made force sensors located near the clamps provide input for the admittance controller. For safety, we added redundant force and position sensors to detect sensor failure. The development of the resting chair in the linkage has been postponed, in order to maintain focus on the primary function of LOPES II, i.e., assistance of gait.

Two mechatronic prototypes were built and installed in the Roessingh Rehabilitation Center in Enschede, the Netherlands, and the Sint Maartens clinic in Nijmegen, the Netherlands. The linkage for the foot plantar/dorsiflexion had a negative impact on the controllability of the remaining DoFs, due to its weight. Therefore the actuation for foot push-off was removed. We added a passive toe lifter, to allow for gait training for patients with problems with toe lifting (e.g., due to weakness in the dorsiflexor muscles or spasms).

We then started the evaluation of LOPES II, starting with the verification of the system requirements. Measurements of the mechanical stiffness between the actuators and the force sensors showed that LOPES II is not as stiff as required. Furthermore we measured the position accuracy of LOPES II, i.e., how accurate can LOPES II measure the patient joint an-

gles from the motor angle data. The measured position errors are less than the standard deviation of normal walking.

For most DoFs, the impedance of LOPES II is sufficiently low. In minimal impedance mode, the admittance controller displays a virtual inertia with minor damping. For ankle translations (anterior / posterior and mediolateral), LOPES II displays little over the allowable 2 kg. For the knee anterior / posterior translation, LOPES II displays 4.7 kg; little higher than the allowable 4 kg. However for the pelvis anterior / posterior and mediolateral translations, LOPES II displays 40 kg, whereas 6 kg is the allowable inertia to allow for free walking. Examining the gait patterns of healthy subjects, we see that walking in LOPES II in minimal impedance mode, resembles free walking on a treadmill. Particularly for the joint rotations, the correlation is high. For the pelvis translations the correlation is lower, which is also reflected in the relatively high interaction forces on the pelvis (peak-to-peak 100 N). This is attributed to the relatively high virtual mass at the pelvis.

In the next phase we performed pilot studies to evaluate the potential of LOPES II in the clinic. When patients were installed in LOPES II for the first time, the donning time varied from ten to fifteen minutes. For recurring trainings, the donning time varied from five to eight minutes. For first time training the patient limb sizes must be measured, and data must be fed in the computer. More severely impaired patient required longer donning times, due to the fact that they require help in standing. These donning time are considerably lower than the known donning times for existing devices, allowing for more efficient use of training time.

During pilot studies we tested the potential of LOPES II to assist as needed. For this we have developed a graphical user interface, with which the therapist can adjust gait patterns and the support levels for specific aspects of gait. LOPES II is powerful and stiff enough to enforce a walking pattern (high support on all aspects of gait) on a severely affected patient. We also demonstrated that, on the other side of the spectrum, LOPES II can provide selective support to a mildly affected patients.

LOPES II has the potential to perform Assist As Needed training in the clinic. Currently a randomized clinical trial is being performed to compare the effect training with LOPES II with conventional therapy.



# Samenvatting

In de laatste twee decennia heeft robotisch ondersteunde looptraining een sterke ontwikkeling doorgemaakt. Het gebruik van revalidatierobots in de klinische praktijk is echter beperkt. Belangrijkste oorzaken hiervan zijn de beperkte effectiviteit en de beperkte efficiency. De voornaamste twee uitdagingen in de ontwikkeling van robotisch ondersteunde looptraining zijn om tijdens training alleen te ondersteunen daar waar nodig, *Assist As Needed (AAN)*, en het verlengen van de effectieve trainingstijd, voornamelijk door het verkorten van de tijd die nodig is om de patiënt te (de-)installeren in de robot (*doffing time*). AAN training houdt in dat de patiënt voldoende vrijheid moeten hebben tijdens het lopen en daarbij alleen ondersteuning krijgt bij specifieke (aangedane) aspecten van het lopen. Dit houdt vervolgens in dat de robot vrij moet kunnen bewegen in meerdere graden van vrijheid, *Degrees of Freedom, (DoFs)*, en dat de aangedreven DoFs in staat zijn om de beweging van de patiënt te volgen, en een minimale weerstand, *minimal impedance* geven, m.a.w. ze moeten transparant zijn.

Na uitgebreid onderzoek naar de eisen gesteld door de eindgebruikers (fysiotherapeuten, revalidatieartsen, patiënten en onderzoekers) zijn de systeemvereisten voor de nieuwe robotische looptrainer, LOPES II, vastgesteld: een robot met een loopband, met het mechanisme achter de patiënt, met een minimum aantal bevestigingen aan het lichaam. Verder moet de patiënt vrij kunnen bewegen in rotaties en translaties van alle segmenten en gewrichten en de armzwaai moet ongehinderd zijn. In een onderzoek hebben we aangetoond dat men ongehinderd kan lopen als er tot 6 kg massatraagheid wordt toegevoegd aan het bekken, of 2 kg massatraagheid aan de voet. Ondersteuning moet worden geleverd op het bekken in horizontale translaties, heup abductie/adductie (been zijwaarts) en flexie/extensie

(bovenbeen voorwaarts/achterwaarts zwaaien), knie flexie/extensie en voet plantairflexie/dorsaalflexie (voetafzet/tenen optillen).

Tijdens de conceptfase hebben de eindgebruikers regelmatig de concepten geëvalueerd. Dit proces leidde niet alleen tot verbetering van de kwaliteit van de concepten, maar vergrootte ook de betrokkenheid van de eindgebruikers in het ontwikkelingsproces. De beste concepten werden geïntegreerd in een éénbenige mechanische proefopstelling. Deze opstelling heeft een gepatenteerde schaduwbeenbenadering, d.w.z. een mechanisch been achter de patiënt. Het schaduwbeen en het been van de patiënt zijn met elkaar verbonden met trekduwstangen. In tegenstelling tot conventionele robotische looptrainers met een mechanisch been aan de zijkant van het been van de patiënt, vergt het schaduw been mechanisme weinig afstelling. Het aantal bevestigingen is minimaal: een klem in het bekken (gecombineerd met een harnas voor de veiligheid en het leveren van gewichtsondersteuning), klemmen op de onderbenen (vlak onder de knieën), en klemmen bij de voeten (voetbakjes). Voor de bevestigingen bij de voeten en het bekken gebruiken we gepatenteerde gimbals welke rotaties van voeten en bekken toelaten en zorgen dat ondersteunende krachten aangrijpen in het midden van het enkelgewrichten en heupgewrichten. Verder bevat de proefopstelling een stoel waarop de patiënt kan zitten tijdens de (de-)installatie van de robot, en om te rusten tussen de trainingen.

De geïntegreerde proefopstelling, vormde, samen met een lijst van systeemvereisten, de input voor het ontwerp van de mechatronische prototypes. De mechanische structuur is zodanig ontworpen dat aangedreven graden van vrijheid grotendeels ontkoppeld zijn, om complexiteit in berekeningen van de transformaties te voorkomen, en om een optimale bewegingsvrijheid per graad van vrijheid te realiseren. De geselecteerde actuatoren zijn in staat om voldoende steun te leveren aan ernstig aangedane patiënten, en ze zijn snel genoeg om bewegingen van snel lopen te kunnen volgen. Voor de aansturing van LOPES II hebben we voor *admittance control* gekozen. Hiermee kan zowel een hoge impedantie (veel ondersteuning) als lage impedantie (minimale ondersteuning) kan worden gegeven, doordat deze controller een (lage) virtuele massa weergeeft zonder wrijving. Speciaal ontworpen kracht sensoren vlakbij de bevestigingen geven input voor de admittance controller. Voor de veiligheid zijn er redundante kracht en positie sensoren aangebracht, om defecten van sensoren op te detecteren. De ontwikkeling van de stoel is niet meegenomen in dit ontwerp, om de primaire functie van LOPES II, d.w.z. ondersteuning bij het lopen, eerst goed te ontwikkelen.

Twee mechatronische prototypes zijn gebouwd en geïnstalleerd in het Roessingh Centrum voor Revalidatie in Enschede en de Sint Maartenskliniek in Nijmegen. Het mechanisme van de voet plantairflexie/dorsiflexie bleek, vanwege het gewicht, een nadelige invloed te hebben op de aansturing van de overige graden van vrijheid. Daarom is het mechanisme voor de voetafzet verwijderd. In plaats daarvan hebben we een passieve teen lifter toegevoegd die kan worden gebruikt door patiënten met problemen met het optillen van de voet (bijvoorbeeld ten gevolge van zwakte in de dorsiflexor spieren of spasmen).

Vervolgens zijn we begonnen met de evaluatie van LOPES II, te beginnen met de verificatie van de systeemeisen. Na metingen van de mechanische stijfheid tussen de actuatoren en de krachtsensoren is gebleken dat LOPES II niet zo stijf is als vereist. Verder hebben we de positie nauwkeurigheid van LOPES II gemeten, d.w.z. hoe nauwkeurig kan LOPES II de gewrichtshoeken meten op basis van de gemeten motor hoeken. De gemeten fouten zijn kleiner dan de standaard deviatie van normaal lopen.

Voor de meeste graden van vrijheid is de impedantie van LOPES II voldoende laag. In de minimale impedantie modus, geeft de admittance controller een virtuele massa traagheid met een beetje demping. Voor de enkel translaties (anterior/posterior en mediolateraal) voegt LOPES II iets meer dan de toelaatbare 2 kg toe. Voor de knie anterior/posterior translatie voegt LOPES II 4.7 kg toe; iets meer dan de toelaatbare 4 kg. Echter, voor de bekken translaties voegt LOPES II 40 kg toe, terwijl 6 kg de maximaal toelaatbare massa traagheid is om ongehinderd te kunnen wandelen. Onderzoek van de loop patronen van gezonde proefpersonen laat zien dat het lopen in LOPES II in minimale impedantie modus, lijkt op vrij lopen op een loopband. Met name voor de gewrichtsrotaties zijn de correlaties hoog. Voor de bekken translaties zijn de correlaties lager, hetgeen ook blijkt uit de relatief hoge interactiekrachten op het bekken (piek-piek 100 N). Dit wordt toegeschreven aan de relatief hoge virtuele massa bij het bekken.

In de volgende fase hebben we een pilotstudie gedaan om het potentiëel van LOPES II in de kliniek te evalueren. Voor patiënten die voor de eerste keer in LOPES II werden geïnstalleerd varieerde de donning time van 10 tot 15 minuten. Voor de tweede keer duurde het 5 tot 8 minuten. Bij patiënten die voor de eerste keer in LOPES II gingen trainen, moesten de lengtes van de ledematen worden opgemeten en in de computer ingevoerd worden. De donning time van zwaarder aangedane patiënten was langer, omdat zij moeilijk zelfstandig kunnen staan. Deze tijden zijn aanzienlijk korter

dan de tijden voor bestaande apparaten, waardoor LOPES II efficiëntere gebruikmaakt van de trainingstijd.

Tijdens de pilotstudies hebben we de mogelijkheden van Assist as Needed met LOPES II getest. Hiervoor hebben we een grafische gebruikersinterface ontwikkeld, waarmee de therapeut het looppatroon en de mate van ondersteuning voor de specifieke aspecten van het lopen kan aanpassen. LOPES II is krachtig en stijf genoeg om een looppatroon op een zwaar aangedane patiënt op te leggen (hoge ondersteuning op alle aspecten van het lopen). Aan de andere kant van het spectrum hebben we aangetoond dat LOPES II selectief kan ondersteunen bij mild aangedane patiënten.

LOPES II heeft de potentie om Assist as Needed loop training naar de kliniek te brengen. Momenteel wordt een gerandomiseerde klinische studie uitgevoerd om het effect van training met LOPES II te vergelijken met conventionele therapie.

# Contents

<b>Summary</b>	<b>v</b>
<b>Samenvatting</b>	<b>ix</b>
<b>I Thesis</b>	<b>1</b>
<b>1 Gait Training</b>	<b>3</b>
1.1 Rehabilitation after Stroke . . . . .	3
1.2 Robot-Assisted Gait Trainers — Taxonomy . . . . .	5
1.2.1 Exoskeletons on a Treadmill . . . . .	6
1.2.2 Fixed-base End Effector Approach . . . . .	8
1.2.3 Overground Balance Training . . . . .	8
1.2.4 Exoskeleton Suits . . . . .	10
1.3 Challenges in Robot-Assisted Gait Training . . . . .	11
1.4 Thesis Goal . . . . .	13
1.5 Layout . . . . .	14
<b>2 User Requirements &amp; System Layout</b>	<b>15</b>
2.1 About Users, Requirements and Requirement Finding . . . . .	15
2.1.1 Users . . . . .	15
2.1.2 User- & System Requirements . . . . .	15
2.1.3 Requirement Finding for a New Device . . . . .	16
2.1.4 User Centered Design . . . . .	16
2.1.5 Team Expert Choice . . . . .	17
2.1.6 Requirement Finding for LOPES II . . . . .	17
2.2 Main User Requirements . . . . .	17
2.3 Detailing User Requirements . . . . .	19

2.3.1	General Requirements . . . . .	20
2.3.2	Physical Therapist's Requirements . . . . .	20
2.3.3	Patient's Requirements . . . . .	21
2.3.4	Researcher's Requirements . . . . .	21
2.3.5	Requirements from Health Care . . . . .	21
2.3.6	Requirements from Industry . . . . .	22
2.4	Global System Layout . . . . .	22
<b>3</b>	<b>Gait Analysis and Degrees of Freedom</b>	<b>27</b>
3.1	Analysis of Gait . . . . .	27
3.2	Pathological gaits . . . . .	29
3.3	Functions in Gait Training . . . . .	30
3.4	Degrees of Freedom in Gait Training . . . . .	33
3.4.1	Required Powered DoFs . . . . .	36
3.4.2	Required Constrained DoFs . . . . .	38
3.4.3	Required Free DoFs . . . . .	38
<b>4</b>	<b>Concepts</b>	<b>41</b>
4.1	Introduction . . . . .	41
4.2	Theoretical Concepts . . . . .	42
4.2.1	Clamps and Clamp Locations . . . . .	42
4.2.2	Force / Torque Transfer . . . . .	42
4.3	Proofs of Concept . . . . .	45
4.3.1	User Centered Design in the Concept Phase . . . . .	45
4.3.2	Forces on Segments — Proof of Concept 1 . . . . .	46
4.3.3	Foot & Pelvis Gimbal — Proof of Concept 2 and 3 . . . . .	47
4.3.4	Foot Actuation — Proof of Concept 4 . . . . .	50
4.3.5	Chair / Lifting Aid — Proof of Concept 5 . . . . .	51
4.4	Integrated Proof of Concept . . . . .	51
4.5	Conclusion . . . . .	53
<b>5</b>	<b>System Requirements</b>	<b>55</b>
5.1	Anthropometric Data . . . . .	55
5.2	Walking Speed . . . . .	56
5.3	Degrees of Freedom . . . . .	57
5.3.1	Range of Motion . . . . .	58
5.3.2	Speed and Force / Torque . . . . .	61
5.4	Impedance . . . . .	63
5.4.1	Minimal Impedance . . . . .	64

5.4.2	Maximum Impedance . . . . .	65
<b>6</b>	<b>System Design</b>	<b>67</b>
6.1	Scope for the First Prototypes . . . . .	67
6.2	Additional Safety Measures . . . . .	68
6.3	Actuation . . . . .	68
6.4	Sensors . . . . .	69
6.4.1	Sensors on Actuators . . . . .	69
6.4.2	Angular Sensors . . . . .	69
6.4.3	Force Sensors . . . . .	71
6.4.4	Accelerometers . . . . .	73
6.4.5	Real time Platform . . . . .	73
6.5	Treadmill . . . . .	73
6.6	Bodyweight Support Module . . . . .	74
<b>7</b>	<b>Mechanical Design</b>	<b>77</b>
7.1	Main Dimensions . . . . .	77
7.2	Decoupled Linkages . . . . .	80
7.2.1	Thigh Sagittal and Frontal Rotation . . . . .	80
7.2.2	Shank Sagittal Rotation . . . . .	81
7.2.3	Foot Sagittal Rotation . . . . .	82
7.2.4	Pelvis XZ Stage . . . . .	83
7.2.5	Coupling . . . . .	85
7.3	Short Skewed Axis Gimbal at Ankle & Hip . . . . .	85
7.3.1	Description . . . . .	85
7.3.2	Dimensioning a Short Skewed Axis Gimbal . . . . .	86
7.3.3	Hip Gimbal . . . . .	89
7.3.4	Ankle Gimbal . . . . .	90
7.4	Mechanical Design Summary & Analysis . . . . .	91
7.4.1	Physical Mass . . . . .	91
7.4.2	Range of Motion . . . . .	95
<b>8</b>	<b>Controller Design</b>	<b>101</b>
8.1	The LOPES II Controller — An Overview of the Components	101
8.2	Admittance Control . . . . .	104
8.2.1	Theory & History . . . . .	104
8.2.2	Applications . . . . .	106
8.3	Motor Controller . . . . .	108
8.4	Kinematics Transformations . . . . .	109

8.4.1	Degrees of Freedom . . . . .	110
8.4.2	Virtual Rod Elongation . . . . .	112
8.4.3	Iterative Position Solution . . . . .	113
8.4.4	Velocity Solution . . . . .	113
8.4.5	Acceleration Solution . . . . .	114
8.4.6	Force Solution . . . . .	114
8.4.7	Total Transformation . . . . .	115
8.5	Mass Model . . . . .	115
8.5.1	Coordinate Systems for Mass Model . . . . .	115
8.5.2	Inertia Scaling on Contact . . . . .	118
8.5.3	Inertia Compensation with Accelerometers . . . . .	120
8.6	Integration Method . . . . .	121
8.7	PVA Limiter . . . . .	122
8.7.1	Introduction . . . . .	122
8.7.2	Multi DoF Limiter . . . . .	123
8.8	Guard . . . . .	125
8.9	Renderer . . . . .	126
8.10	Gait Controller & GUI . . . . .	127
8.10.1	Graphical User Interface . . . . .	127
8.10.2	Gait Trajectory Controller . . . . .	127
8.11	Conclusion & Discussion . . . . .	130
8.11.1	Kinematics Transformations . . . . .	130
8.11.2	Simplified Mass Model . . . . .	130
<b>9</b>	<b>Realization &amp; Evaluation</b> . . . . .	<b>133</b>
9.1	Built Prototypes . . . . .	133
9.2	Removal of the Foot Rotation Actuation . . . . .	133
9.3	Stiffness . . . . .	135
9.4	Tuning Procedures & Results . . . . .	137
9.4.1	Range of Motion — Position Limits . . . . .	137
9.4.2	Speeds & Accelerations . . . . .	138
9.4.3	Inertia . . . . .	140
9.4.4	Maximum Force / Torque . . . . .	141
9.5	Guard Margins . . . . .	142
9.6	Position Accuracy . . . . .	143
9.7	Minimal Impedance . . . . .	147
9.8	Selective Support — Pilots with patients . . . . .	150
9.9	Interaction Forces . . . . .	154
9.10	Donning Time . . . . .	158

9.11 Usability . . . . .	158
9.11.1 Questionnaire . . . . .	159
9.11.2 Results . . . . .	160
9.12 Discussion . . . . .	160
9.12.1 Stiffness and Position Accuracy of LOPES II . . . . .	160
9.12.2 Transparency of the Admittance Controller . . . . .	162
9.12.3 Maximum Impedance Admittance Controller . . . . .	164
9.12.4 Speed . . . . .	164
9.12.5 Selective Support . . . . .	165
9.12.6 Usability . . . . .	166
<b>10 Discussion, Conclusion &amp; Future Directions</b>	<b>169</b>
10.1 Goals vs Achievements . . . . .	169
10.2 Requirements vs Performance . . . . .	170
10.2.1 System Requirements . . . . .	170
10.2.2 User Requirements . . . . .	171
10.3 LOPES II in Perspective . . . . .	172
10.4 The Design Process . . . . .	174
10.5 Transfer to Other Domains . . . . .	175
10.6 The Future of LOPES . . . . .	176
10.6.1 LOPES III . . . . .	176
10.6.2 Support Plantar / Dorsiflexion . . . . .	178
10.6.3 Chair / Lifting Aid . . . . .	178
10.6.4 Simplified Rod Structure — Coupled Linkages . . . . .	178
10.6.5 Modules . . . . .	179
10.7 The Future of Gait Training . . . . .	180
10.7.1 Research . . . . .	180
10.7.2 Clinic . . . . .	181
10.8 Finally . . . . .	183
<b>Bibliography</b>	<b>183</b>
<b>II Appendices</b>	<b>201</b>
<b>Appendix A Pilot Study on Following and Resisting Forces on the Pelvis</b>	<b>203</b>
<b>Appendix B Effect of Directional Inertias Added to Pelvis and Ankle on Gait</b>	<b>207</b>

<b>Appendix C LOPES II — Design and Evaluation of an Admittance Controlled Gait Training Robot with Shadow-Leg Approach</b>	<b>221</b>
<b>Appendix D Rehabilitation Apparatus with a Shadow Leg</b>	<b>235</b>
<b>Appendix E Parallel Rectangular Manipulator</b>	<b>247</b>
<b>Appendix F Short Skewed Axis Gimbal</b>	<b>263</b>
<b>Appendix G Proximal PD Controller Used as PVA Limiter</b>	<b>281</b>
<b>Appendix H System Usability Scale for LOPES II</b>	<b>291</b>
<b>Dankwoord</b>	<b>295</b>
<b>Biography</b>	<b>299</b>
<b>List of Publications</b>	<b>301</b>

Part I

**Thesis**



# Gait Training

This chapter discusses the need for gait training for stroke survivors and what the current role of robotics in gait training is, and how it preferably would be performed. Although there are numerous different gait disorders, we limit the scope of this thesis to stroke, ranging from severely to mildly impairments. We assume that the majority of other central neurological gait disorders e.g., due to spinal chord injury, the pathologies and training needs are similar to those of stroke survivors and therefore that robot-assisted gait training maybe beneficial for them as well.

## 1.1 Rehabilitation after Stroke

A stroke, or cerebrovascular accident (CVA) is damage of brain tissue by either rupture of a bloodvessel (hemorrhage) or clogging of a bloodvessel (ischæmia). Stroke is the second leading cause of death for adults worldwide ([Krishnamurthi et al., 2013](#)). In the Netherlands in 2012 over 44,000 stroke incidents were hospitalized ([Vaartjes et al., 2013](#)). The number of stroke incidents is increasing ([Krishnamurthi et al., 2013](#)). Additionally the age at which first stroke occurs is decreasing ([Kissela et al., 2012](#)). Consequently we can expect an increase of health-care cost of stroke.

Most recovery occurs in the first three months post stroke ([Jørgensen et al., 1995](#); [Buurke et al., 2008](#)). Part of this recovery is spontaneous recovery ([Cramer, 2008](#)), therapy can improve the recovery ([Colombo et al., 2012](#)). In the Netherlands per year more than 9,000 stroke survivors receive rehabilitation-care ([Kok et al., 2008](#)). Physical therapy training is part of

the rehabilitation process for most stroke survivors, to regain functional recovery.

Recovery of walking ability is a major goal during rehabilitation (Ditunno et al., 2008). 70% of the patients who survive a stroke are unable to walk independently during the first three to four weeks post stroke (Skilbeck et al., 1983). Improvements in walking ability (changes in walking speed, independence of walking) can be caused by recovery of function in the affected leg to premorbid levels or by learning and using compensatory strategies (Dobkin and Carmichael, 2005; Van Asseldonk, 2008). The importance of recovery and compensation in functional improvements is subject of debate (Levin et al., 2008). The current view is that chances of motor recovery decrease with the time post stroke and that it is largely subject dependent which recovery mechanism might be most effective and needs to be promoted during training (Kwakkel and Kollen, 2013). Yet, it is largely unknown which subject characteristics determine the optimal recovery mechanism (Langhorne et al., 2011).

There are several types of gait training, e.g., overground training, treadmill training and body weight support treadmill training. The type, frequency and duration of training depends not only on patient's capability, but also on the policy of the rehabilitation centers, and reimbursement policies.

'Intensity' is often referred to as the duration of a training session. For bodyweight supported treadmill training, the dutch guidelines for physical therapy recommend 20–30 minutes effective therapy time per session (Veerbeek et al., 2014). Kwakkel et al. (1999) have proven that an increased duration of rehabilitation has a positive effect on functional recovery, in terms of activities of daily living (ADL), walking ability, and walking speed. However this definition of intensity does not include the amount of effort the patients have to make during the training. Outermans et al. (2010) examined the effect of 'effort intensity' (toughness) on gait training of stroke survivors. They found that for equal training duration, the high intensity group showed larger improvements in gait speed and gait ability than the low intensity group. These studies indicate that longer and tougher gait training is favorable for gait performance.

Gait training is labor intensive. For more severely impaired patients gait training often requires two physical therapists to provide support (see figure 1.1). The limiting factor in gait training is sometimes the physical capacity of the therapists (Schmidt et al., 2007). Another limiting factor for gait training is budget available for physical therapy (Hesse et al., 2003).



**Figure 1.1:** Body Weight Support Treadmill Training in the Saint Joseph’s Healthcare, London. <https://www.sjhc.london.on.ca/locomotor>

Evers et al. (2004) found that the cost of stroke is approximately 3% of total health care expenditures in eight observed countries. A second limitation of current practice is that applied assistance and consequently therapeutic outcome may vary between therapists (Reinkensmeyer et al., 2004). It is hardly surprising that robots have entered the discipline of gait training: robotic automation has taken over cumbersome, strenuous and expensive manual labor in several other disciplines, therefore robots seem suitable to reduce the physical load and cost of conventional gait training and support in the repetitive training of stepping.

## 1.2 Robot-Assisted Gait Trainers — Taxonomy

By the end of the 20th century the first Robot-Assisted Gait Trainers (RAGT) were built and evaluated. This section gives an (incomplete) overview of RAGTs, categorized by their mechanical layout (see table 1.1)

**Table 1.1:** An overview of existing RAGTs

Device	Type <sup>a</sup>	Powered DoFs <sup>b,c</sup>										Target population <sup>d</sup>
		Hf	Ha	Kf	Af	Pm	Pa	Pt	Po	Fu	Fa	
Lokomat (Hocoma, 2014)		F	F	S	F	C	C	C				Se, Mo
REO Ambulator (Motorika, 2015)	EX, T	P	P		C	C	C	C				Se
Lopes I (Veneman et al., 2007)		F	F	F		F	F	C	C			Mo, Mi
ALEX III (Zanotto et al., 2013)		F	F	F	F	F	F	F	?			Se?, Mo, Mi
PAM POGO (Aoyagi et al., 2007)	EE, T	F	F		F	F	F	F				Mo, Mi
GT1 (Hesse and Uhlenbrock, 2000)	EE, P									P	P	Se, Mo
GEO (Schmidt et al., 2005)										F	F	Se, Mo
KineAssist (Peshkin et al., 2005)	EE, O					F	F					Mi
Thera Trainer e-go (Medica, 2008)						S	S					Mi
Ekso (Ekso-Bionics, 2015)		F	F									SCI
Rewalk (ReWalk, 2015)	EX, O	P	P									SCI
Indego (Parker-Hannifin, 2015)		F	F									SCI
HAL (Cyberdyne, 2014)		F	F	F								SCI, Mi

<sup>a</sup>EX: Exoskeleton; EE: End Effector; T: Treadmill; O: Overground walking; P: Foot plates

<sup>b</sup>Hf: Hip flexion/extension; Ha: Hip abduction/adduction; Kf: Knee flexion/extension; Af: Ankle plantar/dorsiflexion; Pm: Pelvis mediolateral; Pa: Pelvis anterior/posterior; Pt: Pelvis transversal rotation; Po: Pelvis obliquity (frontal rotation); Fu: Foot up/down; Fa: Foot anterior/posterior

<sup>c</sup>F: Force control; P: Position control; C: Constrained; S: Spring (passive);

<sup>d</sup>Se: Severely impaired; Mo: Moderately impaired; Mi: Mildly impaired; SCI: Spinal chord injury only

### 1.2.1 Exoskeletons on a Treadmill

Among the pioneers, the Lokomat<sup>®</sup> by Hocoma, Switzerland (Colombo et al., 2000) is best-known. The Lokomat is an exoskeleton structure located

at the side of the patient legs, mounted with clamps to the lower-leg and upper-leg. The exoskeleton structure supports knee flexion / extension and hip flexion / extension for both legs. The patient is strapped in a harness that provides bodyweight support (BWS) (see figure 1.2a).

Originally the Lokomat was position controlled, but with the progressive insight of research on gait training (Riener et al., 2005), the control has shifted towards force control (Bernhardt et al., 2005). Currently Hocoma is marketleader in robot-assisted gait training, with over 500 Lokomats sold (Hocoma, 2013). The latest version of the Lokomat supports lateral pelvis motion and pelvis transversal rotation.

Lopes I (see figure 1.2b) was built with force control as starting point, to support the paradigm of Assist As Need (AAN) (Emken et al., 2005a). A key feature of AAN is that when the robot does not provide assistance, it does not hinder the patient in its motion, i.e., the robot is ‘mechanically transparent.’ Contrary to the Lokomat, it uses fixed base actuators to reduce the moving mass of the exoskeleton, in order to enhance the mechanical transparency of the system. Bowden cables are used to transfer the torque from the actuators to the patient joints and Series Elastic Actuation is used to control the force (Veneman et al., 2007). A second starting point for Lopes I was to not only support leg motions, but also to support balance and weight shift. Therefore Lopes I has powered i.e., hip and knee flexion / extension, hip abduction / adduction and pelvis translations.

Defining **“Transparency”**, **“Minimal Impedance & “Assist As Needed”**.

In this thesis, we state that a Robot-Assisted Gait Trainer (RAGT) is ‘transparent’ if the patient can walk in the RAGT without being hindered by the RAGT.

This transparency implies that the interaction forces between patient and robot are low, i.e., the robot has a low mechanical impedance. The ‘Minimal Impedance’ mode of a RAGT is the mode in which the controller of the robot aims to be as transparent as possible.

Assist As Needed (AAN) means that the robot only assists on particular aspects of gait e.g., the robot applies a torque on the knee to help the patient to obtain sufficient knee flexion. For the other aspects of gait the robot does not apply forces i.e., it is in minimal impedance mode.

The Active Leg EXoskeleton (ALEX) (Banala et al., 2007) was designed to support a single leg during walking on a treadmill (see figure 1.2c). Similar to the Lopes I the starting points were force control and multiple Degrees of Freedom (DoFs) for the patient. The third generation of ALEX has twelve powered DoFs (Zanotto et al., 2013, 2014). All powered DoFs can be made mechanically transparent with force control, however it is unclear if pelvis frontal rotation and foot endo- / exorotation are free and what the stiffness of the powered DoFs is. ALEX III is currently in development, trials with patients have not been executed.

### 1.2.2 Fixed-base End Effector Approach

A second approach for robot-assisted gait training is to interact with the end effectors only, e.g., feet. Around the turn of the century, Hesse and Uhlenbrock (2000) published the first results of their mechanized gait trainer. This gait trainer later evolved into the GT1 by Reha-Stim, Germany (see figure 1.2d). An additional harness provides safety and BWS. A benefit of end effector approach over the exoskeletons is the easy donning and doffing, i.e., the installation of the patient in the RAGT. The patient has freedom for pelvis motions, but the feet are position controlled, this limits the freedom of the patient and thus the possibilities for Assist As Needed.

The same group later built the Haptic Walker (Schmidt, 2004), which does have force control on the feet (Schmidt et al., 2005). The programmable foot plates allow for simulation of walking on uneven terrain and stairs. The GEO from Reha Technology, Switzerland, is the commercial spin-off (Reha-Technology, 2015)

The PAM & POGO (Reinkensmeyer et al., 2006) (see figure 1.2e) is a combination of two end effector devices. The Pelvis Assist Manipulator (PAM) was designed to support balance on a treadmill (Ichinose and Reinkensmeyer, 2003). The PAM allows for natural motions of the pelvis and arm swing. The Pneumatically Operated Gait Orthosis (POGO) consists of two actuators that are attached to clamps near the knee and the ankle respectively. The PAM & POGO allows for Assist As Needed for both pelvis motions and leg motions.

### 1.2.3 Overground Balance Training

Where the afore mentioned devices are fixed-base gait trainers, the KineAssist™ (HDT Global, Solon, U.S.) supports overground training (see figure

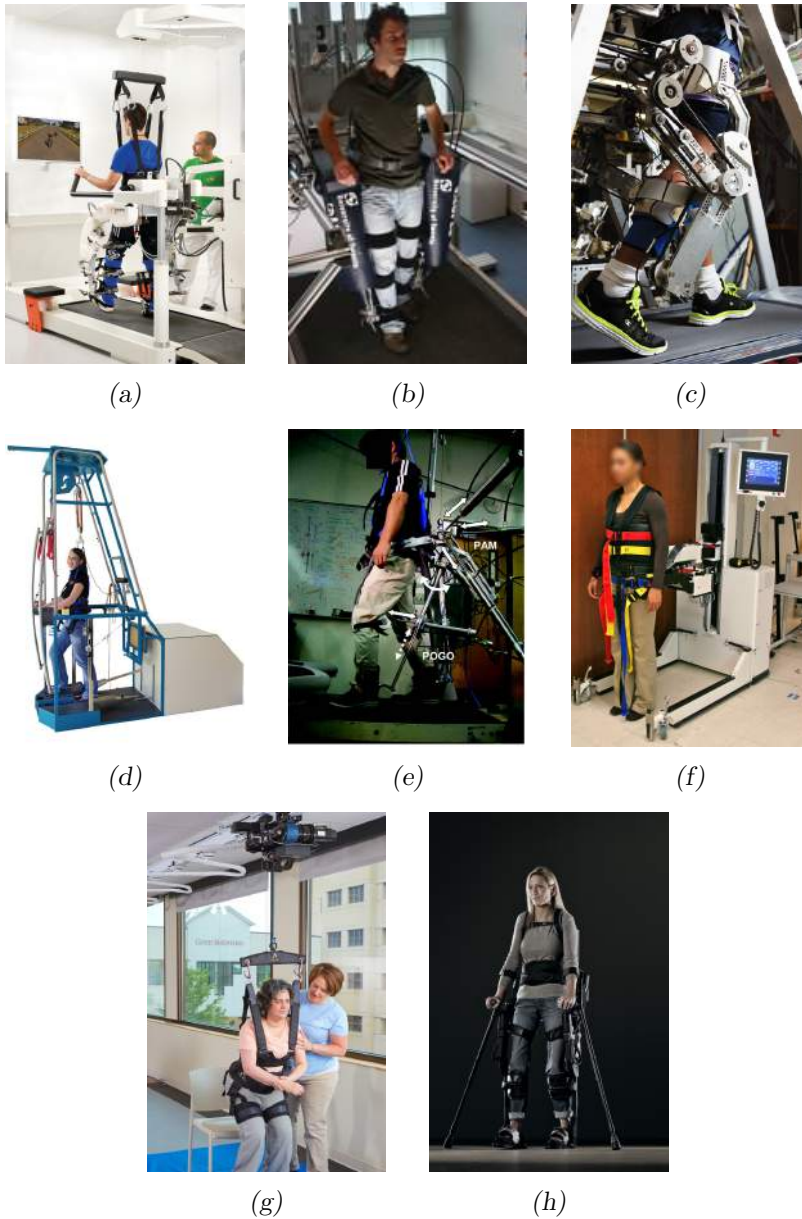


**Figure 1.2:** Existing RAGTs. (a): Lokomat<sup>®</sup> Pro FreeD by Hocoma. Photo courtesy: Hocoma, Switzerland. (b): Lopes I by University of Twente. (c): ALEX III. Photo courtesies: ROAR Lab., Columbia University, Dr. Sunil K. Agrawal. (d): GT1<sup>™</sup> by Reha-Stim. Photo courtesies: Reha-Stim, Germany. (e): The PAM & POGO by University of California. Photo courtesies: U.S. Department of Veterans Affairs, Office of Research and Development, JRRD. (f): KineAssist<sup>™</sup> by HDT Global. Photo courtesy: Photo courtesy: Departments of Physical Therapy and Occupational Therapy, UAB. (g): ZeroG<sup>®</sup> by AreTech<sup>®</sup>. Photo courtesies: Aretech, USA. (h): Ekso<sup>™</sup> by Ekso Bionics<sup>™</sup>. Photo courtesy: Ekso Bionics.

1.2f). Overground training is more realistic than training on a treadmill, e.g., making turns is possible. The layout of the KineAssist is optimized for balance training and weight-shift training: assistive forces are applied to the pelvis and trunk; the legs are not controlled (Peshkin et al., 2005).

The Thera Trainer e-go by Medica (Medica, 2008) is a passive balancer that allows for overground walking. It is suitable for patients that are able to stand, and thus not suitable for the severely impaired patients.

The Float by Lutz Medical Engineering, Switzerland (Vallery et al., 2013) supplies bodyweight support and optionally horizontal forces to the patient's trunk. In a fixed space the patient can train overground walking or walking over obstacles or uneven terrain. It provides no support on the legs and therefore the system is less suitable for the severely impaired patients.

The ZeroG, by Aretech, USA (Hidler et al., 2011) (see figure 1.2g), provides a rail system with bodyweight support. Patients can practice overground walking or walking over obstacles or uneven terrain. It provides no support on the legs and therefore the system is less suitable for the severely impaired patients.

#### 1.2.4 Exoskeleton Suits

The last philosophy discussed here is to support overground training by using exoskeleton suits. At the turn of the century the first version of the HAL robot was published (Okamura et al., 1999), an exoskeleton structure for overground walking.

Similar devices are the Ekso™ (see figure 1.2h) by Ekso Bionics™, the Rewalk™ (Esquenazi et al., 2012) by Argo Medical and the Indego® by Parker, based on the Vanderbilt Exoskeleton (Farris, 2012). All devices are commercially available and all these devices, except the HAL, had a primary function of assistive device for paraplegic patients, but now deliver products for rehabilitation as well (ReWalk, 2015; Ekso-Bionics, 2015; Cyberdyne, 2014). In a pilot study a stroke survivor has trained with a single leg version of the HAL (Kawamoto et al., 2009), receiving support torque on the paretic knee. A limitation of the HAL and the other exosuits is that patients must be able to walk with crutches to maintain balance. For severely and moderately impaired stroke survivors this may be difficult. Furthermore, the current generation of exoskeletons do not offer support in lateral motions and therefore training of weight shift and balance is limited.

## 1.3 Challenges in Robot-Assisted Gait Training<sup>1</sup>

Since the first gait trainers have been developed, the efficacy and effectiveness of robot-assisted gait training has been a topic of research. Studies on effectiveness have shown contradictory results (Hornby et al., 2008; Hidler et al., 2009; Husemann et al., 2007; Pohl et al., 2007; Morone et al., 2012). Recent meta-analyses have shown that for spinal chord injury (SCI) patients robot-assisted gait training has no beneficial effect compared to conventional therapy (Swinnen et al., 2010). However stroke survivors are more likely to walk independently when robot-assisted gait training is added to conventional training (Pohl et al., 2007; Mehrholz et al., 2013).

To improve the efficacy, gait training robots should encourage the patient to actively participate (Schüick et al., 2012; Riener et al., 2005). This can be achieved by an ‘Assist As Needed’ (AAN) approach (Cai et al., 2006; Ziegler et al., 2010; Cao et al., 2014; Emken et al., 2005a). For severely affected patients, this implies that the robot should provide much assistance. This can be achieved with feedforward force (Agrawal and Fattah, 2004; Aoyagi et al., 2007) or with high stiffness (high impedance). For mildly affected patients, the robot should behave mechanically transparently (low impedance) and provide assistance only on aspects that require support. Robot mechanics and control are key-drivers in facilitating AAN (Penny-cott et al., 2012).

Implementation of AAN requires the robot mechanics to allow free motions in all DoFs of gait, and when needed, to provide support in most DoFs. Hindering free motions or constraining DoFs causes changes in gait kinematics (Hidler et al., 2009; Veneman et al., 2008). Constraining mediolateral pelvis motions hinders the training of balance (Westlake and Patten, 2009). Of all devices described in section 1.2 only KineAssist, PAM & POGO and ALEX III seem to allow for free motion in all DoFs. *Free motions* also means that arm swing should be possible, since it is part of normal walking and it contributes to the overall stability of human gait (Bruijn et al., 2010). In most exoskeleton gait training robots arm swing is obstructed by the presence of mechanics beside the hip joints (Hidler et al., 2009). The PAM & POGO allows for arm swing (Aoyagi et al., 2007), and the KineAssist seems to allow for arm swing.

The interaction forces between robot and patient should be force controlled to implement both low and high impedance control (Van Asseldonk

---

<sup>1</sup>Part of this section is taken from Appendix C

et al., 2008; Vallery et al., 2009; Riener et al., 2005). The Lokomat was originally position controlled (high impedance), later force control was applied to the Lokomat (Bernhardt et al., 2005). This reduced the impedance of the Lokomat, however the behavior is not sufficiently transparent (Schüick et al., 2012). Several devices have been designed with low-impedance control as starting point, however, they all compromise on high impedance support: The stiffness of the Series Elastic Actuation in Lopes I is limited (Veneman et al., 2007; Vallery et al., 2008), and therefore the high impedance mode is not stiff enough for training severely impaired patients. Similarly the PAM and POGO perform well in the low impedance control (Aoyagi et al., 2007), but the stiffnesses are limited (Reinkensmeyer et al., 2006) and insufficient for high impedance control in gait training. Sulzer et al. (2009) focused on low impedance for an active knee support, compromising high impedance support. AAN has been tested successfully on stroke-survivors with mild to moderate impairment with the single-sided exoskeleton ALEX (Srivastava et al., 2014). The challenge is to develop a gait training robot that is both sufficiently transparent and sufficiently stiff. Little has been published on the required transparency and stiffness. Regarding the required transparency, we have assessed the maximum allowable inertia at the pelvis and ankle during walking (see Appendix B).

Another aspect that needs improvement to optimize robot-assisted gait training is the donning and doffing time. To increase the usability of gait training robots in practice, the donning time should be reduced. Little has been published about donning time of gait training robots. Nilsson et al. (2014) reported a donning time of 15–20 minutes for the HAL robot, but this includes application of EMG. For Ekso the average set up time is 18 minutes for SCI patients (Kolakowsky-Hayner, 2013). The donning time of the PAM & POGO is up to 30 min (Aoyagi et al., 2007). These donning times are considerable given the duration of training sessions (30–60 minutes). In exoskeleton robots the long doffing/donning times are caused by the need to precisely align the robot joint axes with the human joints to prevent damage and uncomfortable man-machine interaction (Schiele, 2009). Devices that do not have a cuffs to the legs, have shorter donning times. For example, in the KineAssist, the donning time is 5 min (Patton et al., 2008). The lack of leg cuffs however limits the possibilities to support in the leg motions. For severely affected patients, support of leg motions is desirable. Especially for donning of severely affected patients both patient and physical therapist will benefit from a short and comfortable donning procedure.

Summarizing, the current RAGTs are improving, but no device is available that is clinically suitable for training a wide range of patients.

## 1.4 Thesis Goal

Our objective was to design and evaluate a Robot-Assisted Gait Trainer LOPES II that is suitable for (research on) clinical gait training of severely and mildly affected patients, using the AAN paradigm. This objective consists of several sub-goals.

### Usable

For clinical training, it is important that LOPES II is ‘usable’. As [Hesse et al. \(2003\)](#) already pointed out, it is important to realize that a RAGT must be regarded a (sophisticated) *tool* for both the therapist and patient to improve on the patient’s gait and not as a replacement of the therapist. Focus on the usability, i.e., how the system will be used by the therapist and patient in a convenient and effective way is of key importance. Quick donning and doffing has been identified as one aspect of usability, however it is likely that usability comprises more than donning and doffing. Therefore it is key to involve the users of LOPES II throughout the whole design process.

### Multiple Degrees of Freedom

Most current commercially available RAGTs lack the possibility to train balance ([Westlake and Patten, 2009](#)) and weight-shift, while this is recognized as an important goal in gait training ([Matjačić et al., 2014](#)). To facilitate balance training and weight shift, a RAGT should have support and freedom in pelvis translations and rotation and foot placement.

### Assist As Needed — From Minimum Support to Full Support

LOPES II should be suitable for gait training of both severely and mildly affected patients. This requires large autonomy for the patient, with minimal hindrance for the patient. On the other hand, LOPES II should supply support if needed. This requires a controller for LOPES II that can switch from minimal impedance to high impedance.

## 1.5 Layout

Part I of this book contains the thesis. The first chapters are dedicated to the definition of the device that is to be built. **Chapter 2** is devoted to identify the user requirements. What do the users really want? In **chapter 3** the process of gait and gait training is further analyzed to understand the functions that LOPES II must fulfill, resulting in a list of requirements on Degrees of Freedom. The next step is to find a mechanical structure that has these desired Degrees of Freedom (**chapter 4**). Also in this phase, the users are consulted in order to increase the usability of the design and refine the requirements. This part ends with a list of system requirements (**chapter 5**).

The following chapters discuss the design of the device. The global system design (**chapter 6**) discusses the type of actuators and sensors that are used, and where they are positioned in the system. The mechanical design (**chapter 7**) gives dimensions to the system components. It also encompasses workspace calculations. **Chapter 8** describes how the input from the sensors are used to control the actuators, in order to assure both low impedance and high impedance control.

The realization and evaluation of the two LOPES II prototypes are described in **chapter 9**. It starts with a description of the built systems, followed by the verification of the system requirements. Does LOPES II have the required stiffness, range of motion, inertia etc? The last part of this chapter is the validation of the user requirements.

The chapter with the discussion **chapter 10**. Amongst others it discusses to what extent the set goals are met. Subsequently it gives a glimpse of the future of LOPES II. In the closing the conclusions are drawn.

Part II contains publications, submitted manuscripts, patent applications and supplementary material, that are relevant for the thesis.

# User Requirements & System Layout

This chapter describes the main user requirements and lists the priorities. This chapter ends with a global system layout based on the user's choice.

## 2.1 About Users, Requirements and Requirement Finding

### 2.1.1 Users

Eason (1988) identified three types of device-users: The primary users actually use the device; the secondary users use the device occasionally or through intermediaries; the tertiary users are affected by the use or make decisions about the purchase of the device. For a robot-assisted gait trainer this means that physical therapists and patients form the primary users (Lee et al., 2005). On the second level are the researchers and rehabilitation physicians. The board of rehabilitation centers and the manufacturers form the tertiary users.

### 2.1.2 User- & System Requirements

A user requirement is a requirement viewed from the user's point of view; whereas a system requirement is a requirement defining the function or performance of a (sub)system (Maiden, 2008). An additional rule-of-thumb

is that user requirements are not necessarily quantitative, e.g., the user may require a ‘safe’ system that is ‘easy to use’. The system requirements are the quantified version of the user requirements, i.e., the system shall comply with safety standard X, and procedure Y shall take no longer than five minutes. The system requirements are discussed in chapter 5.

### 2.1.3 Requirement Finding for a New Device

For new devices it may be difficult to obtain the requirements. For LOPES II the goal is to build a robot that assists in gait-training. This raises a couple of questions: How do patients learn to walk again, and how can a robot optimally assist? Although there are several devices on the market, robot-assisted gait training is not ubiquitous, and experience is a limited resource for the requirements.

Another reason why existing robot gait trainers may not be suitable for deriving new requirements, lies in the fact that requirements (both user and system) may be concept-specific. This is best illustrated by an example. Suppose that a car designer, wants to address the user requirement “provide safety in a crash”. Hypothetically the concept of an airbag may be an alternative to the seatbelt concept. The concept of the seatbelt has concept-specific requirements as non-cutting belts, strong but easy-click fasteners, whereas the airbag has concept-specific requirements as usage of non-hazardous gases, prevention of suffocation etc. Therefore the requirements drive the concept and the concept drive the requirements. When LOPES II will be based on a non-existing concept, deriving the requirements from an existing concept may lead to an unsuitable product.

The requirements for a new device must be obtained through a different process, where there is iteration between generating concepts and defining requirements.

### 2.1.4 User Centered Design

The term ‘User-Centered Design’ (UCD) was introduced by [Norman and Draper \(1986\)](#). Nowadays UCD is a broad design philosophy with applications. A key feature of UCD is how to involve users throughout the whole design process ([Abrams et al., 2004](#)). This involves extracting the users needs, and validating the designed product to the users needs. [Preece et al. \(2002\)](#) lists methods for user-involvement ranging from interviews and questionnaires to role-playing, simulation and usability testing. Especially

the role-playing and simulation method is of interest for the design of new devices, since it involves prototype evaluation to gain information on the users needs and expectations.

### 2.1.5 Team Expert Choice

A method specifically dedicated to ranking the users needs and evaluating concepts against users needs is Team Expert Choice (TEC) (Hummel et al., 2000). TEC is related to Group Decision Support System (GDSS) (DeSanctis and Gallupe, 1987) GDSS is a method for seeking consensus in decision making. TEC has a focus on the establishment of requirements for a new product where multiple types of users are involved.

In a group session, a team of users ranks a set of user needs with pairwise comparisons. Ranking is done on an individual basis with an electronic keypad. When there is little consensus, discussion may help to come to consensus, or at least come to mutual understanding. The average of the rankings results in weighing factors on user requirements. A similar method can be used to evaluate concepts against requirements: in group sessions users discuss and vote how well a concept will score on a particular requirement compared to another concept or existing situation. This way users will be involved during the requirement phase and concept phase.

### 2.1.6 Requirement Finding for LOPES II

We used interviews, observations and TEC to obtain the main user requirements. Subsequently we designed system solutions, i.e., global system sketches, that were presented and ranked by the users.

## 2.2 Main User Requirements

We interviewed users who had experience with both conventional therapy, Lokomat therapy, and Lopes training. Additionally we interviewed physical therapists and rehabilitation doctors obtain more understanding in the physiological process of rehabilitation. Next we held interviews and group meetings with users (Team Expert Choice, see 2.1.5). In this section we describe the main results of TEC.

With the first Team Expert Choice, a mixed group of eight users attended. Among the users were physical therapists, rehabilitation physicians, a patient with experience in robot-assisted gait training and robot

manufacturers. In a first round of discussion, a list of requirements was defined, categorized in five main groups. It should be noted that this is not the final list of requirements, but a working list, to gain more understanding between the various users. Each participant had a electronic voting box. Pairwise comparisons of the user requirements were displayed on screen. The attendees used the voting box to rank the user requirements. The voting results were showed on screen immediately. Although the voting was anonymous, participants often explained their voting, especially when there was little consensus. In some cases participants changed their votes after discussion.

By far the most important requirement was the Assist As Needed requirement (see figure 2.1). This requirement encompasses quick switching between high and low impedance control, and selective support, i.e., apply support on subtasks of gait.

Comfort was the second most important requirement. In the meeting the term ‘comfort’ was associated with soft clamps, comfort during donning and doffing and the option for the patient to rest between walking sessions.

Several requirements were more or less equally important. Users wanted a transparent robot, such that walking in the robot is similar to walking outside the robot. Although this requirement is related to the Assist As Needed requirement, it was taken as a separate requirement, to emphasize its importance. Of similar importance according to the users, was the efficiency. The efficiency encompasses the training time vs the non-training time (e.g., donning time) and the cost of therapy (number of therapists) to achieve gait improvements. The ratio of donning time and training time was seen as a pitfall (risk) for RAGTs; the reduction of therapy costs was seen as an opportunity since there was a consensus that a RAGT can reduce the number of therapists required to execute gait training. Balance support is one of the few specific gait training functions that was put to the list (contrary to e.g., support in knee-flexion). The reason was that in the discussion there was a firm consensus that the existing RAGT lacked the opportunity to train balance and weight shift, despite its importance in gait and gait training. The requirement of safety encloses prevention of falling and medical certification.

The remaining requirements have either large overlap with afore mentioned requirements or are of lesser importance.

At first glance, the usefulness of TEC seems limited, since most of the requirements have already been identified in literature (see section 1.3). However the discussions in the TEC meeting have revealed the require-

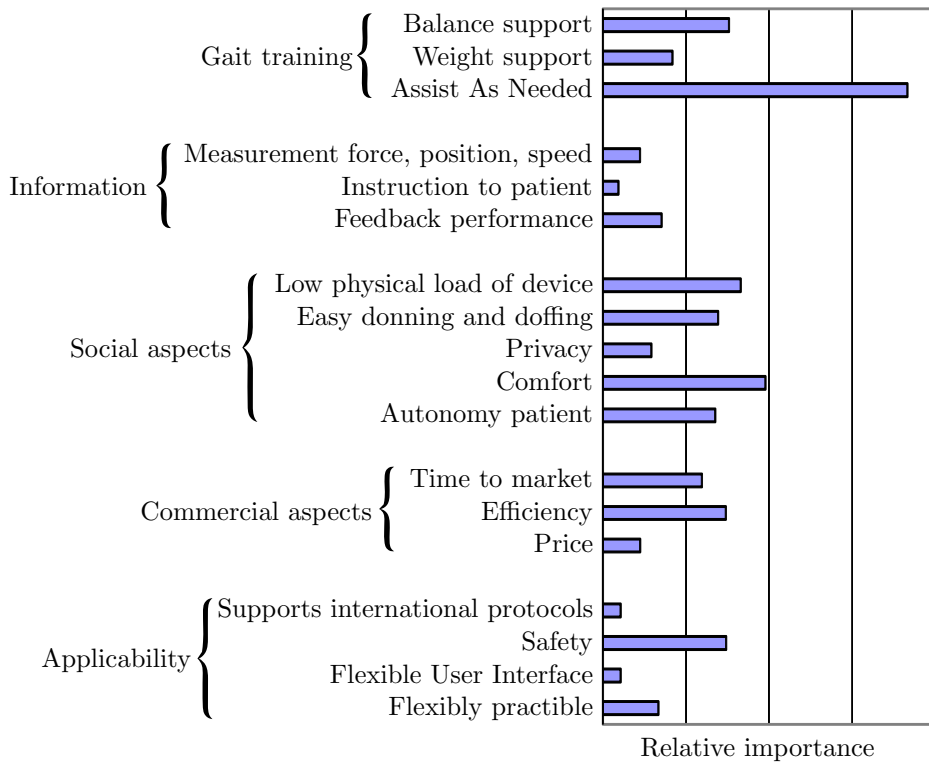


**Figure 2.1:** Requirements of a RAGT and their relative importance.

ment of comfort, and particularly the desire to rest between trainings. We believe that for LOPES II comfort will enhance the usability. Therefore we found the TEC meeting a valuable method for our goal to design a usable LOPES II.

## 2.3 Detailing User Requirements

The TEC gave a good silhouette of the user requirements. With individual conversations, the users requirements were detailed. The following sections give the results per group. The user requirements are numbered with ‘UR’.

### 2.3.1 General Requirements

There was great consensus among the users, confirmed by literature, that LOPES II must be a force controlled controlled RAGT in order to provide Assist As Needed for a wide variety of patients.

#### UR01 Patient in Charge

The patient can walk in the robot with minimal resistance (Patient in Charge)

#### UR02 Robot in Charge

LOPES II can force a gait pattern on the patient (Robot in Charge)

#### UR03 Settable guidance

Guidance force shall be settable per aspect of gait

#### UR04 Variety in walking

In LOPES II a variety in walking shall be possible

Researchers, therapists and rehabilitation doctors stated that recording of the performance of walking is desirable in order to measure progress of individual patients and efficacy of training strategies.

#### UR05 Assessment

The Lopes shall measure patient's performance

The last general requirement may seem 'too obvious to mention', but also these requirements must be mentioned:

#### UR06 Safety

Training shall be safe for the patient and his environment

### 2.3.2 Physical Therapist's Requirements

Physical therapists focused on the usability of LOPES II:

#### UR07 Easy donning and doffing

UR08 Easy, direct and intuitive therapist control over the device and the patient.

Therapists who did have experience with robot-assisted gait training said that they wished that the devices had more control possibilities to manually tailor the training for a patient.

#### UR09 Task specific training

Training (instructions and gait manipulation) shall be task specific.

### 2.3.3 Patient's Requirements

The patients who had no experiences with RAGT, warned that such devices may seem threatening. Patients that did have experience with other devices warned for discomfort during installation and use. Additionally they wished that they had had the possibility to 'play around' and fine-tune gait training to their specific need.

UR10 No discomfort in installation

UR11 Pleasant to use in operation

- (a) No discomfort in physical connection with robot
- (b) Training shall be non threatening
- (c) Training shall be motivating
- (d) The patient should have privacy
- (e) The patient should have independence during training
- (f) Allow resting between trainings
- (g) Optionally program control by the patient

### 2.3.4 Researcher's Requirements

The intended use of the LOPES II prototypes is not only for clinical training, but also on research on recovery mechanisms and training strategies.

UR12 Assessment and Perturbation Research on recovery mechanisms, optimizing functional recovery, patient selection (which patients profit most from robotic therapy)

### 2.3.5 Requirements from Health Care

For hospitals, rehabilitation centers and insurance companies it is important that LOPES II is economically profitable. This means that the investment and operation costs should be acceptable relative to conventional therapy. Investments for such devices is high, therefore it is important that the device has a high utilization rate. By making LOPES II suitable for a wide range of patients this can be achieved. Furthermore it is important that LOPES II provides effective gait training, i.e., that patients will benefit from training in LOPES II. Literature shows that this requires training at a high intensity in terms of duration and effort.

UR13 Effective training

Training shall increase walking functionality

UR14 Wide patient population base

(a) Various gait disorders

(b) Various level of impairments

UR15 Acceptable maintenance costs

UR16 Acceptable investment cost

UR17 Low operating costs

UR18 Acceptable installation efforts

### 2.3.6 Requirements from Industry

Robot-assisted gait training is a rapidly evolving market. Therefore it is important to bring LOPES II to the market as soon as possible to gain market share. The price should also be attractive to cope with competition. It is important to make LOPES II suitable for an international market, since national markets (especially the dutch market) are too small to make a healthy business in robot-assisted gait training. This requires LOPES II to be suitable for international standards and protocols.

UR19 Quick time to market.

UR20 Competitive price.

UR21 International acceptance.

## 2.4 Global System Layout

The next step is to elaborate on the system layout of LOPES II. After the interviews with users, and examining the state of the art of RAGT several fundamental questions arose:

- From what side should the mechanics approach the patient?
- What is the optimal donning procedure?

- Should LOPES II be a treadmill based RAGT or a mobile, overground RAGT?

In a second TEC session twelve users were invited: two patients, three physical therapists, three rehabilitation physicians, one researcher and three representatives of the industry. To find answers these questions, we presented possible system solutions to the users. Subsequently the users ranked the system solutions on selected criteria.

In four groups the users were asked to discuss and rank the solutions, based on the afore mentioned requirements.

“How much do you agree with the following statement?  
Concept A scores better on criterion X than Concept B.”

### **Long-Arm Robot**

The first system solution is the ‘long-arm’ robot (see figure 2.2). The order of operation is: 1) the patient in wheelchair approaches the robot; 2) the clamps, that are connected to long arms, are connected to the patient; 3) the robot pulls the patient to stand; and 4) the training starts.

The mechanics are located in front of the patient. This limits the space for VR projection, however the main console in front of the patient is a suitable place to contain a display with target and feedback. The long (telescopic) arms facilitate the sit-to-standing procedure, and reversely they facilitate resting between trainings, on a chair that is either integrated in the robot, or placed separately.

### **Exoskeleton Chair**

The second system solution is the ‘exoskeleton chair’ (see figure 2.3). The order of operation is: 1) the patient sits down in the robot; 2) in the sitting pose the clamps are attached; 3) the robot pushes the patient to stand; and 4) the training starts.

This solution has the mechanics behind the patient, and consequently offers space in front of the patient that can be used for e.g., Virtual Reality. Another advantage is that this solution offers resting between exercises. The exoskeleton chair does not facilitate in a transfer from the wheelchair to the robot. This must be done by the patient solely, or with help from the physical therapist. For mildly affected patients the attachment of clamps can be done standing.

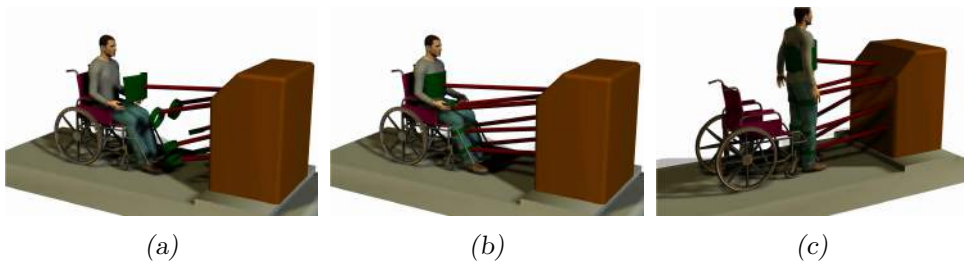


**Figure 2.2:** Concept of ‘long-arm’. (a): Patient rides on the treadmill to the robot. (b): Clamps are mounted to the patient. (c): Robot lifts the patient out of the wheelchair.

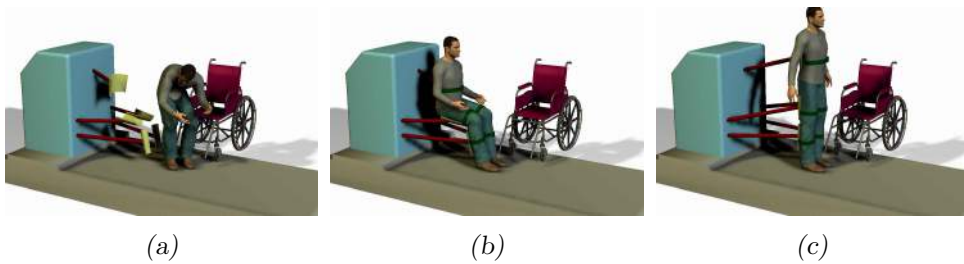


**Figure 2.3:** Concept of ‘exoskeleton chair’. (a): Patients sits down in the robot. (b): Clamps are mounted to the patient. (c): Robot pushes the patient to stand.

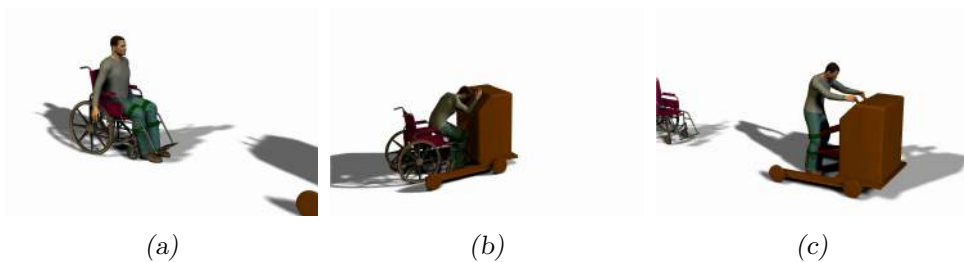


**Figure 2.4:** Concept of ‘compact gait trainer’. (a): Separate clamps are mounted to the patient. (b): Patient rides towards the robot and stands up, optionally using his arms. (c): The clamps are attached to the robot.

### Compact Gait Trainer

The last system solution is the ‘compact gait trainer’ (see figure 2.4). The order of operation is: 1) the clamps are attached to the patient while he is sitting in a wheelchair; 2) the patient rides towards the robot; 3) the patient stands up, optionally with help from the physical therapist; and

4) the training starts. The mechanics are located in front of the patient. The main console in front of the patient is a suitable place to contain a display with target and feedback. The robot does not facilitate in the transfer from sit to stand and vice versa. Resting in the robot is also not possible.

### Discussion & Preference

First the attendees discussed the concepts in four sub groups. Subsequently the sub groups presented their findings in a plenary session, followed by a plenary discussion. There was an extensive discussion on treadmill based robot versus the overground robots. There was a general consensus that overground walking with a mobile RAGT is more task specific, since it allows for making turns and goal oriented walking. Yet, a preference arose for the treadmill, for the following reasons: a) it offers to focus more on the quality of walking; b) it is less distracting for patients with lower FAC score; c) it requires less space than a mobile RAGT; and d) the mobile RAGT is potentially harmful for its environment; and e) the treadmill is deemed more suitable for virtual reality solutions with integrated feedback, such as projection of target and feedback on the treadmill (Houdijk et al., 2012).

Finally the attendees used their electronic voting box (see section 2.2) to evaluate the concepts by means of pair wise comparison, e.g., *‘how well does concept A score on requirement X?’* The exoskeleton chair was favored for most requirements (see figure 2.5). The fact that the mechanics are behind the patient gives a sense of freedom (comfort). The users also liked the idea of projection on the treadmill. This could be beneficial in training specific tasks and could be beneficial for making training challenging for the mildly affected patients. For both the long-arm and the exoskeleton chair, the users liked the possibility to rest between trainings. In the exoskeleton chair a transfer is needed from the wheelchair to the robot. This was not a show-stopper according to the users; the transfer could be made manually, or optionally with existing transfer aids.

Summarizing, there was great consensus that LOPES II should be a treadmill based RAGT with the mechanics located behind the patient, with a possibility for resting between sessions.

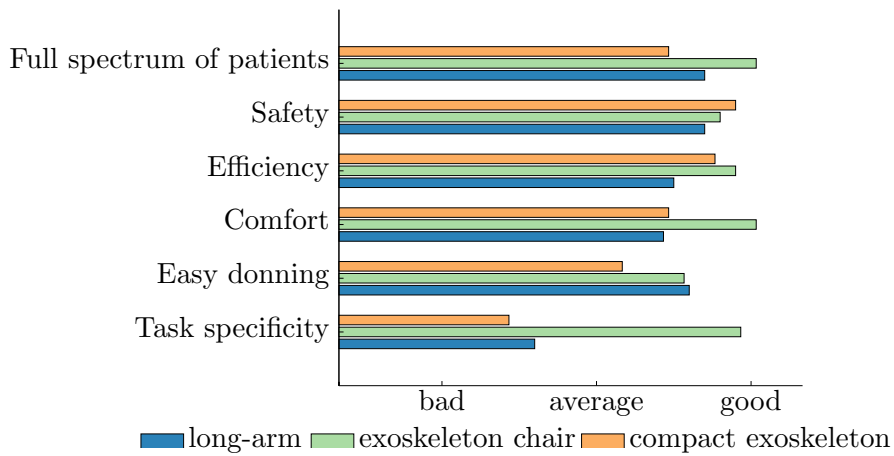


**Figure 2.5:** The users' ranking of the system solutions to a subset of the requirements.

# Gait Analysis and Degrees of Freedom

In the previous chapter the user requirements are listed. This section elaborates on the physical aspect of gait and gait training. LOPES II will provide physical assistance in gait by means of a mechatronic structure. To specify the requirements of the mechatronic structure, it is important to know in which Degrees of Freedom (DoFs) LOPES II must provide assistance, allow free motion, or constrain the motion.

First an analysis is given of normal and pathological gait and gait training. The training functions are prioritized by users in interviews. Subsequently, the desired training functions are linked to DoFs. The priorities in training functions are converted in a DoF priority list.

## 3.1 Analysis of Gait

This section gives a short analysis of the walking pattern. On high level, we can identify three main goals of gait i.e., move the body forward, maintain balance, and adapt to environment (e.g., avoid obstacles). Throughout the gait cycle, several tasks contribute to these goals. For the analysis of gait we will use the breakdown of the phases and tasks as described by [Perry \(1992\)](#) (see figure 3.1).

A gait cycle starts and ends with initial contact. The first task of the gait cycle is the weight acceptance. This involves two phases: initial contact (when the foot touches the floor) and the loading response (from

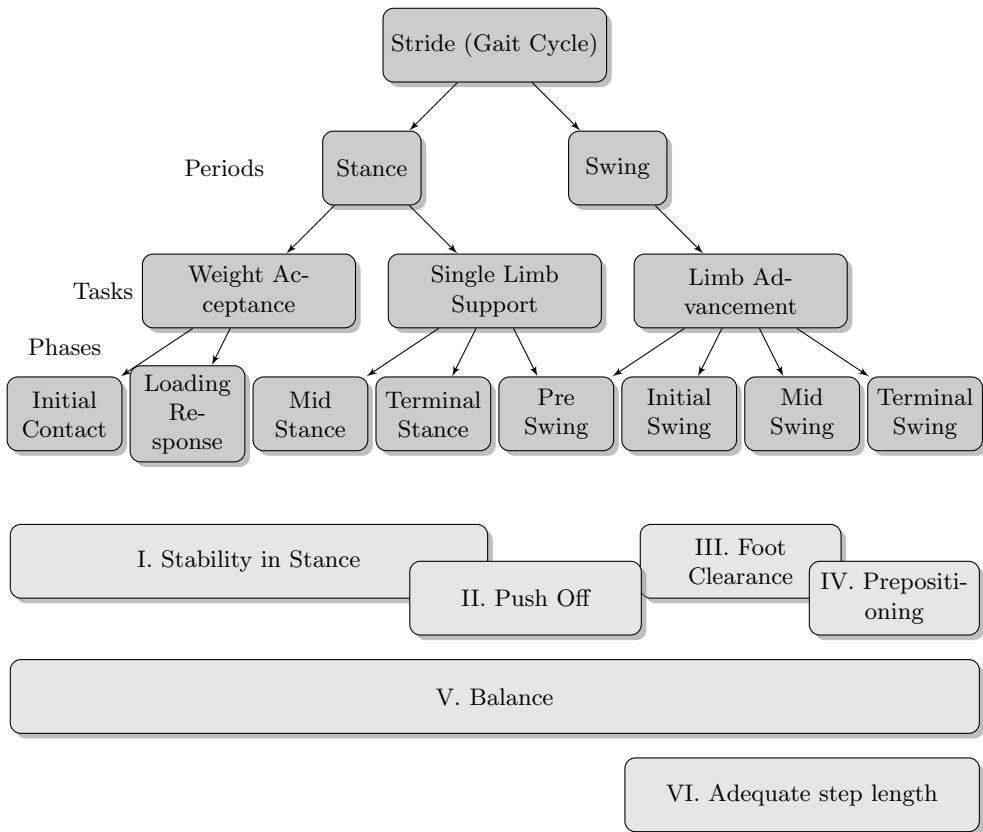


**Figure 3.1:** Divisions of the gait cycle in periods, tasks and phases (Perry, 1992) (dark gray blocks); Subtasks of gait (light gray blocks).

initial contact to toe-off of the contralateral foot). The main challenge is to handle the abrupt change from swing to stance, with maintenance of stability and progression.

The task of single limb support starts when the contralateral foot has been lifted of the ground. During mid stance and terminal stance the leg has to bear the bodyweight and maintain the (dynamic) balance.

As the contralateral foot touches the ground the phase of pre swing starts, as does the task of limb advancement. In this phase the weight is shifted from the ipsilateral leg to the contralateral leg. In the initial swing phase the ipsilateral foot leaves the floor. As the ipsilateral foot is next to

the contralateral, the mid swing phase starts. In the initial and mid swing phases the challenge is to maintain sufficient foot clearance from the floor.

Perry (1992) summarizes the above mentioned challenges and objectives as the *locomotor functions* i.e., 1) propulsion; 2) stance stability; 3) shock absorption; and 4) energy conservation. A slightly different point of view is given by Gage (1993). He introduced the *prerequisites of gait* 1) stance stability; 2) swing phase clearance; 3) foot prepositioning; 4) adequate step length; and 5) energy conservation.

For further analysis of gait we will use a taxonomy that is based on both the prerequisites by Gage and the functions by Perry. To prevent confusion with the afore mentioned taxonomies, the term *subtasks of gait* will be used (see figure 3.1). The subtasks of gait are described below: Starting with initial contact (I) **Stability in stance** is the first subtask; the subtask of (II) **push off** announces the transition from the stance period to the swing period; during the swing period it is important to maintain (III) **foot clearance**; and at the end of swing (IV) **prepositioning** of the foot is required; Throughout the cycle (V) **weight shift** is important to regulate the loading of the legs. And finally in the swing period it is important to generate an (VI) **adequate step length**.

## 3.2 Pathological gaits

In this section various deviations on normal gait are described, in order to gain understanding of goals and methods in gait training. For stroke survivors balance control is less automatic and requires more attention. Additionally stroke survivors use compensatory strategies to maintain balance and propulsion. There are numerous pathological gaits; this section describes the most common gaits for stroke survivors.

Typically stroke survivors have a shorter stance phase for the paretic leg, due to the diminished control over the paretic leg. Speed of walking may be reduced because of general muscle weakness, and especially weakness of the calf muscles for push off. Additionally spasticity may hinder the push off and affects the foot clearance negatively (Lamontagne et al., 2002, 2001). Insufficient push off may also lead to early foot contact of the paretic leg and consequently, shorter step length. Excessive hip pull off may compensate for the lack of push off.

Weakness of the dorsiflexion muscles or spasticity in the plantar flexion muscles may lead to a ‘drop foot’, which causes flat foot landing or forefoot

landing. This absorbs forward kinetic energy. Weakness of the dorsiflexion muscles may also lead to toe drag, resulting in insufficient toe clearance. This may be compensated for by circumduction (swinging the affected leg sideways) or hip hiking (tilting the pelvis in order to lift the hip of the affected swing leg) (Kerrigan et al., 2000).

A common pathology for stroke survivors is a stiff knee gait (Waters et al., 1979), where knee flexion is reduced due to stiffness in the muscles, spasticity in the rectus femoris, or abnormal couplings (synergies). This lack of knee flexion harms the toe clearance in swing, which may be compensated by hip hiking or circumduction.

Hyperextension of the knee may be a result of spasticity in plantar flexion muscles (Olney and Richards, 1996) or limited control over the knee muscles. Hyperextension may be accompanied by a trunk lean-forward occurs when the affected leg is loaded.

Due to limited abductor muscle control the pelvis may be retracted when loaded, and drop when unloaded.

### 3.3 Functions in Gait Training

Gait training of patients with gait disorders, has the goal to improve or maintain, walking speed, stability and flexibility. Functional improvements are facilitated by task specific, intensive training in which the patient provides a large active contribution (Kwakkel et al., 1999). This section elaborates on the specific functions in gait training that are needed to achieve the afore mentioned goals. In interviews physical therapists listed and ranked training functions in gait training. Whether a training function is applied to a patient, depends on his or her severity of impairment (see table 3.1). For the severity of impairment we use the FAC score, since this measure is common for indicating walking functionality for stroke survivors (Holden et al., 1986). In the following section we discuss the functions, grouped by the afore mentioned subtasks of gait. Within each subtask, training functions (marked bold) are related to either support, i.e., support given by LOPES II in performing a task, or freedom, i.e., freedom for the patient to perform a subtask.

#### I. Stability in Stance

For patients it can be difficult or even impossible to bear their own weight. This hinders training of the leg motions of walking. Therefore LOPES II

must **provide body weight support (BWS)**. When the patient is fully paralyzed the required body weight support is estimated at 50%; the remaining support is be provided by support on the joints.

Patients may have difficulty in stabilizing the knee during the stance phase (weight on leg); for a patient with muscle weakness in the knee, with too little extension angle the knee is not capable of bearing the weight and may collapse; too much extension (hyperextension) may result in knee damage. Therefore LOPES II must provide **knee stabilization**.

## II. Push Off

A great part of the propulsion (forward driving force) occurs at the push off of the foot (Neptune et al., 2001). The ankle extends (plantar flexion) and the foot pushes the body forward. To allow normal walking the patient must have **freedom in propulsion**, i.e., forward body movement must be free.

Between the interviewed therapists there was no consensus whether LOPES II should support plantar flexion or not. Research is required to investigate the possibilities for training plantar flexion. This research can be done with LOPES II, if the plantar flexion support is integrated. Therefore it is desirable that LOPES II will **support plantar flexion**.

## III. Foot Clearance

The toes must be lifted during swing phase (dorsiflexion). Too little dorsiflexion may result in toes hitting the floor and therefore the patient may stumble. Passive orthoses keep the foot in a fixed angle relative to the lower leg to compensate for drop-foot. Patients should be able to **wear a foot orthosis** during training in LOPES II. When a patient does not have an orthosis and does not have sufficient dorsiflexion, LOPES II should **support dorsiflexion**. Patients may suffer from a stiff knee. In order to have enough foot clearance, LOPES II must **support knee flexion**.

As a compensatory strategy for lack of knee flexion, patients may use circumduction i.e., swinging the stiff, paretic leg in a hemicircular way, thus creating sufficient foot clearance (Perry, 1992). According to (Kerrigan et al., 2000) circumduction not only involves abduction of the paretic leg, but also pelvis frontal rotation (pelvic obliquity) and pelvis transversal rotation. When sufficient knee flexion is not feasible for a patient, LOPES II must **allow circumduction**. This implies that abduction and

**Table 3.1:** Link between training functions and FAC score: ‘++’ : this training function is important for this FAC score; ‘--’: this training function is never used for this FAC score. Additional weight factors (WF) (0–4) are added for the training functions . Low weight factors are given for functions that have no scientifically proved benefit for training. Similarly additional weight factors (0–4) are given to the FAC score, indicating the target group for training with LOPES II.

		FAC Score	FAC 0	FAC 1	FAC 2	FAC 3	FAC 4	FAC 5
		$W^{FAC}$	3	4	4	4	4	3
	Function	$W^F$						
I	Body weight support	4	++	+	+/-	-	--	--
	Knee stabilization	4	++	++	+	+/-	+/-	-
II	Freedom in propulsion	4	-	+/-	+	++	++	++
	Support in push off	2	+/-	+	+	+	+/-	-
III	Wearing foot orthosis	3	-	+/-	+	+	+	+
	Support in dorsiflexion	2	++	++	++	+	+	+
	Support in knee flexion	4	++	++	++	+	+	+/-
	Allowing circumduction	4	--	+/-	+	+	+	+
	Allowing hip hiking	4	--	+/-	+	+	+	+
	Suppressing circumduction	3	++	++	+	+/-	+/-	+/-
	Suppressing hip hiking	3	++	++	+	+/-	+/-	+/-
	Suppressing pelvic retraction	3	++	++	+	+/-	+/-	+/-
IV	Support stance preparation	4	++	++	+	+	+/-	-
V	Freedom in weight shift	4	-	-	+/-	+	++	++
	Drifting sideways	2	-	+/-	+	+	++	++
	Support in weight shift	3	++	++	+	+	-	-
	Perturbation of balance	2	--	--	-	+/-	+	++
	Freedom of upper body	4	-	+/-	+	+	++	++
	Support in foot placement	3	++	++	+	+	+/-	+/-
VI	Support in step length	3	++	++	+	+	+/-	+/-

pelvis rotations should be possible. Hip hiking (lifting the paretic hip) is another compensation strategy for lack of knee flexion (Kerrigan et al., 2000). **Allowing hip hiking** implies allowing the pelvis rotation in the frontal plane.

In order to train for restitution of gait, it may be desirable to **suppress the compensatory strategies**, such as hip retraction, circumduction and hip hiking.

#### IV. Prepositioning

Before the foot hits the floor, the knee is extended, to prevent collapse. When a patient lacks stability of knee extension, LOPES II must **support stance preparation**.

#### V. Balance

During gait the weight is shifted from one leg to another. The Center of Mass (CoM) of the body is shifted. The patient must have **freedom in weight shift**. Moreover, people do not walk on a straight line; they ‘wander about’. Therefore, patients must have the **freedom in drifting**. For patients with difficulties in weight shift LOPES II must **support weight shift**. Optionally LOPES II has the ability to **provide balance perturbation**, to challenge patients in maintaining their balance.

The upper body has several degrees of freedom relative to the pelvis. These motions play a role in balance and weight shift. To make natural walking possible, LOPES II must provide **freedom of the upper body movements**.

Another important element of balance is the placement of the foot in mediolateral direction. Patients with little balance need **support in foot placement**.

#### VI. Adequate Step Length

When patients have asymmetric step lengths, LOPES II must provide **support in step length**.

### 3.4 Degrees of Freedom in Gait Training

In this section we link the functions as described above to Degrees of Freedom (DoFs). The DoFs are expressed in terms of DoFs of the gait (see figure 3.2). For each DoF the following options are possible in a training function (see table 3.2).

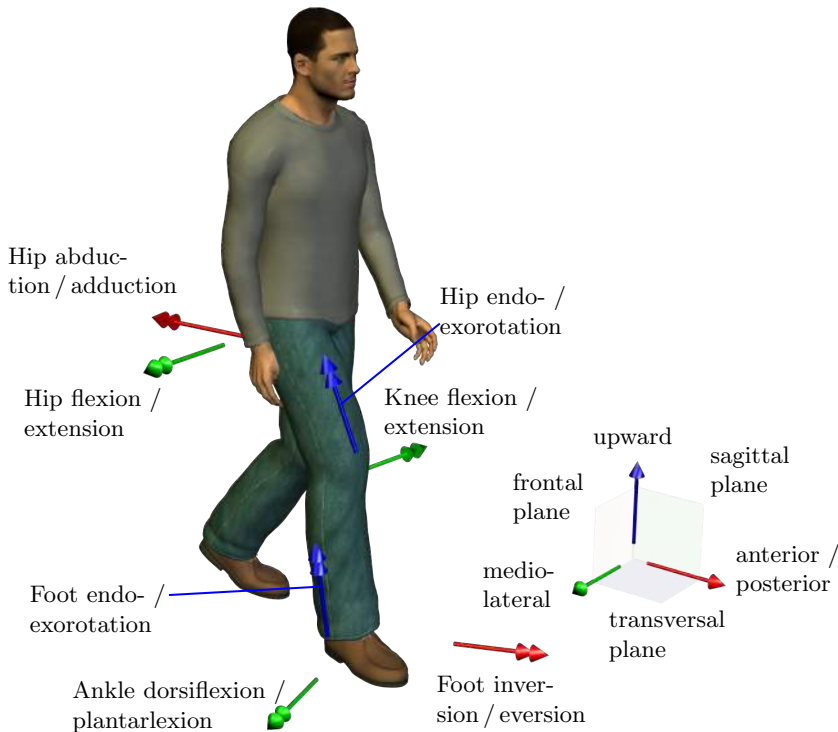


**Figure 3.2:** Degrees of Freedom of the lower extremities and pelvis. The first term is taken as positive direction of the DoF.

- **Powered**  
The DoF requires an actuator to perform the training function
- **Free**  
The DoF must be free (zero impedance) to allow the training function
- **Constrained**  
The DoF has free movement within settable limits. An extreme situation of constrained is when there is no motion possible at all (fixed). The opposite extreme is when the settable limits allow fully free motion.
- **None**  
The DoF has no relation to the training function

**Table 3.2:** Relation between training functions and DoFs. ‘P’: training requires a powered DoF; ‘F’: training requires a free DoF; ‘C’: training requires a constrained DoF.

		Ankle inversion / eversion	Ankle plantar / dorsiflexion	Foot endo- / exorotation	Knee flexion / extension	Hip endo- / exorotation	Hip flexion / extension	Hip abduction / adduction	Pelvis up / down	Pelvis anterior / posterior	Pelvis mediolateral	Pelvis sagittal rotation	Pelvis frontal rotation	Pelvis transversal rotation	Trunk rotations
I	Body weight support				P	P			P						
	Knee stabilization				P										
II	Freedom in propulsion	F		F	F	F				F					
	Support in push off	P	C	F	F	F				F					
III	Wearing foot orthosis	F	F	F											
	Support in dorsiflexion		C												
	Support in knee flexion				P										
	Allowing circumduction					F		F		F		F			
	Allowing hip hiking							F		F		F			
	Suppressing circumduction							C							
IV	Support stance preparation				P										
	Freedom in weight shift							F		F		F			
V	Drifting sideways		F							F		F			
	Support in weight shift							P		P					
	Perturbation of balance									P	P				
	Freedom of upper body								F			F	F	F	F
VI	Support in foot placement	C	C					P							
	Support in step length							P							

It may be impossible to meet all wishes as stated in table 3.2. Therefore we calculate the priorities in DoF requirements, by linking table 3.1 and table 3.2 with the following mathematical procedure: First normalize all weight

**Table 3.3:** Quantization and normalization of symbols

Symbol	Normalized value
'++'	1.0
'+'	0.75
'+/-'	0.5
'.'	0.25
'--'	0.0

factors and relations between FAC and functions from table 3.1 with the values from table 3.3.

Then per DoF, per FAC score, per function, the importance of powering is calculated:

$$W_{i,j,k}^{Powered} = \begin{cases} \hat{W}_i^F \cdot \hat{W}_j^{FAC} \cdot \hat{R}_{i,j}^{FAC\&Func} & \text{if } L_{i,k} = P \\ 0 & \text{otherwise} \end{cases} \quad (3.1)$$

Where  $i$  is the index for function,  $j$  is the index for FAC,  $k$  is the index for DoF,  $\hat{W}^F$  is the normalized weight function vector for training functions,  $\hat{W}^{FAC}$  is the normalized weight function for the FAC,  $\hat{R}^{FAC\&Func}$  is the normalized relation between FAC score and training function, and  $L_{i,k}$  is the link between function and DoF (either 'P', 'F', 'C' or blank) (see table 3.2).

Thus a full 3D matrix is obtained. For each DoF the maximum value is taken, indicating the overall need to power this DoF.

$$w_k^{Powered} = \max \left( W_{*,*,k}^{Powered} \right) \quad (3.2)$$

Analogously the vectors  $w^{Free}$  and  $w^{Constrained}$  are calculated, indicating the need to respectively let DoFs free and to constrain them (see table 3.4). The following sections give more detail on the DoF requirements.

### 3.4.1 Required Powered DoFs

The priority list for powering DoFs is

1. Knee flexion / extension has top priority to be powered for numerous training functions
2. Hip flexion / extension has top priority to be powered for numerous training functions

**Table 3.4:** Prioritized DoF requirements, ‘++’: ‘must-have’; ‘--’: ‘not needed’.

DoF	Powered	Free	Constrained
Ankle inversion / eversion	--	+	+
Ankle plantar / dorsiflexion	+/-	++	+/-
Foot endo- / exorotation	--	+	+
Knee flexion / extension	++	++	--
Hip endo- / exorotation	--	+	--
Hip flexion / extension	+	++	--
Hip abduction / adduction	+	++	+
Pelvis up / down	+	++	--
Pelvis anterior / posterior	+/-	++	--
Pelvis mediolateral	+	++	--
Pelvis sagittal rotation	--	++	--
Pelvis frontal rotation	--	++	+
Pelvis transversal rotation	--	++	+
Trunk rotations	--	++	+

3. Hip abduction / adduction has priority to be powered to support foot placement
4. Pelvis must be supported in upward direction to provide bodyweight support.
5. Pelvis mediolateral (ML) translation has priority to be powered, mainly to support weight shift. Additionally perturbation of balance in the frontal plane can be executed.
6. If it is decided to integrate perturbation of balance of anterior / posterior (AP) direction in the Lopes, the pelvis AP translation must be powered.
7. Whether ankle plantar / dorsiflexion is to be powered or not is subject of debate. The effect of support in plantar flexion in rehabilitation is not clear. Research on this is required. Because LOPES II has the goal to gain technical knowledge of training effects, it is recommended to power the plantar flexion and to perform research on the effect of support.

### 3.4.2 Required Constrained DoFs

The training functions that require DoFs to be constrained, are mainly to suppress compensation strategies. All items have approximately equal priority:

- Trunk rotations must be constrained in order to preserve trunk stability
- Hip abduction / adduction must be constrained to suppress circumduction and hip hiking
- Pelvis frontal rotation must be constrained to suppress hip hiking and pelvic retraction
- Pelvis transversal rotation must be constrained to suppress pelvic retraction
- Ankle plantar flexion must be constrained when the patient has a drop foot, or spasms in absence of a personal AFO.
- Ankle inversion must be constrained to prevent the foot from collapsing during foot placement
- Foot endo- / exorotation must be constrained to provide proper push off and roll-off of the foot, especially when push off is supported.

Note that if DoFs are already powered then these DoFs can be constrained by virtual limits (hip abduction and possibly dorsiflexion). The remaining constrained DoFs require physical end stops.

### 3.4.3 Required Free DoFs

To allow free walking, ideally all degrees of freedom should be free, including the DoFs that are listed in the powered DoFs and the constrained DoFs. It is assumed that these DoFs that require powering or constraining automatically have the option of being free. Note that this implies that limits can be removed on the constrained DoFs and that powered DoFs can be controlled to Zero Impedance. Based on these assumptions, the list of DoFs that are to be free is reduced to the following list

- Hip endo- / exorotation must be free to allow circumduction

- The pelvis sagittal rotation should be free to allow maximum freedom of the upper body. Note: these rotations are a few degrees for healthy persons and in practice are likely to exist within the free play of clamping. For completion, this DoF is mentioned here.



# CHAPTER 4

## Concepts

The user requirements for LOPES II have been defined in the previous chapters. This chapter answers the question *how* these goals are met; Concepts are generated and evaluated frequently with the end users. The chapter ends with a mechanical layout of LOPES II.

### 4.1 Introduction

The powered Degrees of Freedom (DoFs) (see table 3.4) require mechanical connection between actuators and the subject. One of the components of the connection is the clamp, that is connected physically to the subject's body parts. One of the questions that is answered in this chapter is 'what are the best locations on a human body to apply clamps?'

A second component of the connection between subject and actuators is the linkage. In this context, the term 'linkage' refers to any physical connection between the actuators and the clamps in order to transfer force / torque from the actuators to the patient. Additionally, the linkage has the purpose to either bridge a distance, to change a gearing ratio (to increase torque or speed), or both.

The following section discusses theory for both clamping and linkage. Subsequently concepts are generated, built and evaluated.

## 4.2 Theoretical Concepts

### 4.2.1 Clamps and Clamp Locations

Several RAGTs use cylindrical clamps for the upper and lower leg. These clamps are suitable for applying radial forces to the segment, i.e., a force perpendicular to the leg. Shear forces on the surface (forces along the leg, or torsion of the leg) cause sliding of the clamp and discomfort for the subject. Therefore cylindrical clamps should only apply perpendicular forces.

Analogously an upward force on the body, to apply body weight support (BWS), should be applied on a horizontal surface, since an upward force on a vertical surface will cause shear force and thus sliding and discomfort. The number of suitable horizontal surfaces on a human body are limited. Physical therapists advised against the armpits, since hemiplegics may lack strength around the paretic shoulder, and therefore large supportive forces may be harmful. This leaves the perineum and the soles of the feet to apply upward forces. Although support from the perineum may be uncomfortable, it was thought as the best area to apply body weight support.

Mechanical compliance of human tissue may be a limiting factor in the stiffness of the total linkage between actuators and the subject's skeleton structure. This may have a detrimental effect on the 'Robot in Charge' mode (UR02), therefore it is desirable to apply the clamps on the parts of the human where the soft tissues are thin (see figure 4.1a). These areas partially coincide with the areas where the pain pressure threshold is highest (Moreno et al., 2005). Additionally the shoe is a logical place to apply clamp, since it contains reasonably stiff parts.

### 4.2.2 Force / Torque Transfer

From a mechanics point of view, there are three approaches to transfer actuator powers to the human limbs: 1) apply torques on joints; 2) apply torques on limbs; or 3) apply forces on limbs.

Most existing RAGTs have a layout in which knee torques are applied on the joints (Colombo et al., 2000; Motorika, 2015; Veneman et al., 2007; Okamura et al., 1999; Zoss et al., 2006; ReWalk, 2014). The base of the actuator is (directly or indirectly) connected to the upper leg segment; the output of the actuator is connected to the lower leg segment (see figure 4.2a). One way to implement this is to mount the actuator (base) on a seg-

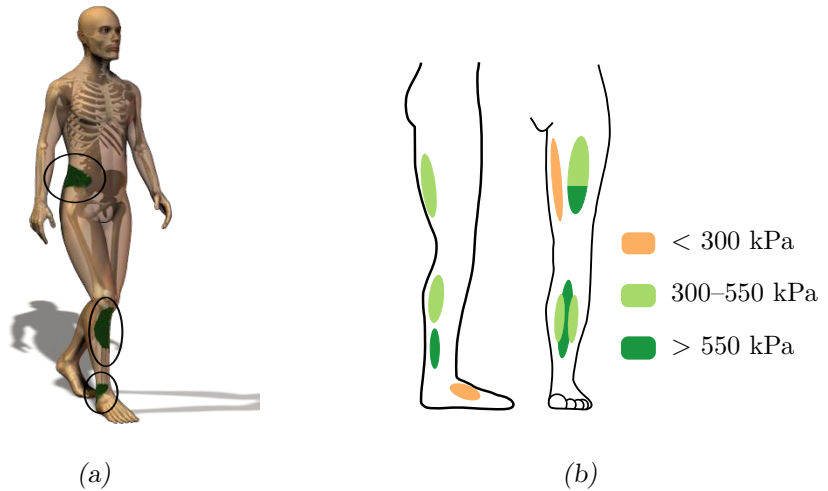


**Figure 4.1:** Fitness for clamping of locations on the lower extremities and pelvis. (a): the areas where the human tissue has lowest mechanical compliance (green areas). (b): Pain Pressure Treshold on lower extremities (Moreno et al., 2005)

ment. Most RAGTs have an actuator for knee flexion / extension mounted on the upper leg segment; the output is connected to the lower leg. A disadvantage of this implementation is that motion of the upper leg requires motion of the (heavy) actuator. Large moving masses have a negative impact on the transparency of the robot (see Appendix B). In Lopes I this disadvantage was mitigated by using fixed base actuators and Bowden cables (Veneman et al., 2005). For example the knee flexion / extension is actuated by connecting the base of the actuator to the upper leg, by means of the Bowden cable sleeve; the output of the actuator is connected to the lower leg by means of the Bowden cable. The Bowden cables however have high internal friction and compliance, which results in play at the joints, furthermore the wear and tear of the Bowden cables is a serious disadvantage. In ALEX III also fixed based actuators are used, but instead of Bowden cables, a complex structure of timing belts and parallelograms assures that the actuator torques are applied on joints (Zanotto et al., 2013).

A second approach is to apply torques to the segments (see figure 4.2b). Several existing RAGTs have implemented the ‘hip torque’ by applying a torque on the upper leg segment, without applying the counter torque on the pelvis segment (Colombo et al., 2000; Motorika, 2015; Veneman et al.,

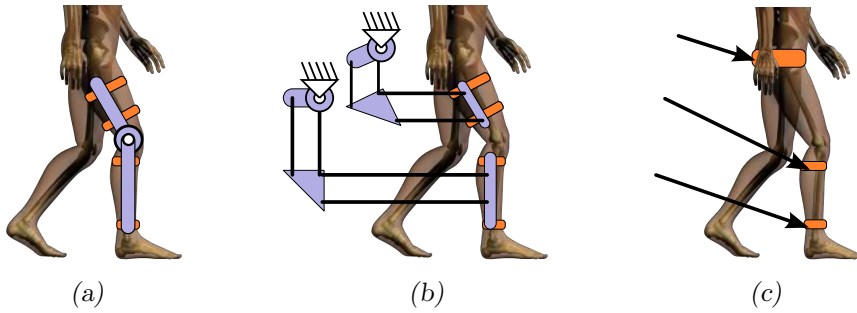


**Figure 4.2:** Concepts for force/transfer to the knee. (a): Torque actuation on the knee with a direct actuator. (b): Torque actuation on the upper and lower leg segment. (c): Force actuation on the segments.

2007). Although with this segment torque it is not possible to control the hip joint torque, the hip angle can be controlled within reasonable accuracy, since the pelvis has limited rotation in the sagittal plane. The torque on the upper leg is the result of two forces on the thigh segment. Usually one force is exerted at the hip, by means of a pelvis belt, and the second force is exerted at the thigh self just above the knee (Colombo et al., 2000; Motorika, 2015; Veneman et al., 2007). This principle of segment torque can be extended to the lower segments as well (lower leg and foot). Per segment two clamps are attached, each exerting a force, equal in magnitude but opposite in sign, and thus exerting a torque on a segment. A joint torque, then is the difference between two segment torques. Transferring the actuator torques to the clamps is can be achieved by connecting fixed base actuators to the segment by means of e.g., parallelogram structures (see figure 4.2b). In order to power the hip flexion / extension, knee flexion / extension, plantar / dorsiflexion and hip abduction / adduction, four double parallelograms structures are needed and six clamps. A benefit of this concept is that there is no exoskeleton structure with joints (hip, knee, ankle) that must be aligned with the patient's joints. A clear disadvantage is that this requires a lot of clamps and moving parts. A second disadvantage is that there is no mechanical limit for joint excursions e.g., knee extension limit. Prevention of excessive flexion and extension of joints requires additional hardware, software checks, or both.

The last approach is to apply forces on the segments (see figure 4.2c). The combination of forces results in torques on the joints. The PAM & POGO (Reinkensmeyer et al., 2006) uses this approach. End effector sys-

tems apply forces to segments as well, i.e., the feet (Hesse and Uhlenbrock, 2000; Schmidt, 2004; Emken et al., 2005b)(see figure 1.2d). However, since they only apply forces to the feet, they do not ‘close the torque loop’ and therefore are incapable of controlling joint or segment torques. A benefit of force approach is that all desired DoFs can be actuated, with a minimum amount of clamps, e.g., with clamp only at the pelvis, knee and ankle, hip flexion / extension and abduction / adduction, knee flexion / extension are controlled. A possible disadvantage is that, if the applied forces have a component tangential to the skin, the clamps will cause undesired shear forces. A second challenge is that the kinematic relation between actuator angles and joint angles is more complex.

Each of the three approaches has its advantages and disadvantages. The joint torque approach is the most ‘pure’ when control of the joints is paramount. However the challenge is to prevent the structure to become too heavy (due to actuator) or too complex (due to sophisticated differential mechanisms). The segment torque is a reasonable alternative for the joint torque: segment torques can be controlled with fairly simple, light-weight structures, and thus the joint torques can be controlled indirectly. The disadvantage is that it requires two clamps per segments. This is expected to have a detrimental effect on the donning time and therefore the usability. The force approach is ranked as favorable approach, since it allows for a minimum amount of clamps (for faster donning). The risk of sliding forces and the complex kinematics are challenges, but not show stoppers.

## 4.3 Proofs of Concept

### 4.3.1 User Centered Design in the Concept Phase

A key principle of User Centered Design is iterative design (Gould and Lewis, 1985). Particularly in software design, the iterative design is a useful tool, e.g., the Agile Manifesto encourages to deliver working software every couple of weeks (Beck et al., 2001). For mechatronic systems the ‘just build’ philosophy of the Agile Manifesto may be less suitable, because mechatronic prototypes cost more time and money to deploy than software prototypes (beta versions). This probably is the reason why all literature that we found on iterative design in combination with robots is limited to its user interface (Green et al., 2000; De Vito Dabbs et al., 2009; Mast et al., 2012).

However, iterative design cycles may be useful in mechatronic systems,

provided that the benefit of the iteration cycles outweighs the cost (time and money) of the iteration cycles.

We have applied the iterative design approach to the mechanical concepts for LOPES II. We made a Proof of Concepts (PoC) for subsystems of LOPES II. For a period of a few months, we built PoCs for subsystems and users evaluated the PoCs. A cycle of building and evaluation typically took two weeks. We used the users' comment to improve or abandon concepts. Finally we integrated the approved PoCs of the subsystems in a complete (mechanical) PoC for a last user validation.

This section discusses the selected concepts for the subsystems and ends with the integrated mechanical PoC.

### 4.3.2 Forces on Segments — Proof of Concept 1

As stated in the section 4.2.2 force actuation on segments is the preferred solution, therefore this was taken as starting point for the actuation of knee flexion / extension and hip flexion / extension.

For this we built a Proof of Concept 1 (PoC1). We built a mechanism with three clamps: a simple bracket at the foot, a brace below the knee and a belt around the waist (see figure 4.3a). To these clamps we attached push-pull rods to apply forces on the clamps. The other end of the rods were connected to levers and a cart. A subject was able to walk freely, only dragging the cart along. Additionally the supportive torques for knee flexion / extension during walking or standing were simulated by a second subject that applied torques to the lever.

We tested this concept on multiple subjects among which physical therapists and rehabilitation physicians. The following limitations were mentioned by the test panel: 1) subjects feared that the supportive knee extension torque could cause hyper-extension of the knee; 2) the knee clamp was sliding up and down along the leg, especially when supportive torques were applied. Apparently the tangential forces on the clamp caused sliding (see figure 4.3b); 3) when applying supportive torque on knee extension, the subject was pushed on the waist bracket, which would push the subject in a hollow back. This is unacceptable, especially for more severely impaired patients; and 4) the feet could not make endo- / exorotation.

To tackle the first item, risk of knee hyperextension, we introduced a 'shadow leg' (see Appendix D). The push-pull rods that are connected to the foot, knee and waist are connected to this mechanical leg, and thus this mechanical leg mimics the motion of the subject (see figure 4.3b). The

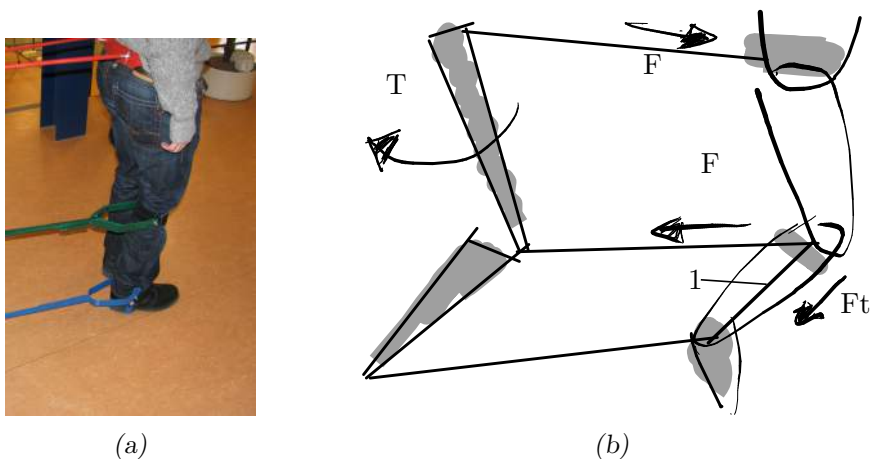


**Figure 4.3:** PoC 1: The concept of the shadow leg. (a): a prototype for applying forces on the leg. (b): Schematics of the shadow. the mechanical leg behind the patient leg mimics the motion of the patient leg. This implementation contains the ‘sliding problem’: A force tangential to the shank ( $F_t$ ) causes friction. A connection between the ankle bracket and knee clamp (1) is needed, to fix the location of the knee clamp.

shadow-leg can contain a physical end stop against knee hyperextension. We did not implement and test the end stop in the concepts, assuming that it will work in the mechatronic prototypes.

The second risk, the sliding of the knee clamp can be prevented by a link between the knee cuff and the foot bracket. This connection can be direct (between the cuffs) or indirect, between the push-pull rods to the knee and ankle (see figure 4.3b). Tests showed that this was a major improvement and that the clamps stayed in place, however there was minor sliding of the knee bracket due to movement of the mechanics. To eliminate the risk of an sliding of the clamps, additional concepts were required.

The two remaining concerns, i.e., hollow back and constrained foot endo/exorotation, are tackled in the following section.

### 4.3.3 Foot & Pelvis Gimbal — Proof of Concept 2 and 3

In the section above, two limitations were not tackled and were related. For the pelvis and hips ideally the supportive force applies to the center of the hip joint without imposing a torque (that forces a hollow back). Additionally the pelvis rotations must have the option to be free (see table

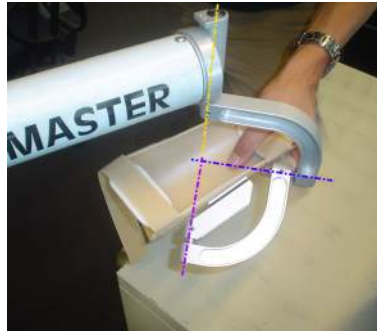


**Figure 4.4:** The skewed axis gimbal with 90 deg segments mounted on the HapticMASTER allowing for rotations of the forearm.

3.4). For the foot bracket ideally the supportive force applies to the center of the ankle-joint without imposing or hindering rotations of the joint. In both cases a force must be applied to a virtual point, i.e., the hip joint and the ankle joint.

This can be solved with a remote center gimbal such as the skewed axis gimbal (Lammertse, 2010). A skewed axis gimbal allows for 3DoF rotation and effectively imposes 3DoF translation to a virtual point. The gimbal contains two arched segments and end effector. Each segment has two pivots which have an axis angle of 90 degrees. On the HapticMASTER (Van der Linde and Lammertse, 2003) a skewed axis gimbal is used as arm rest (see figure 4.4). This way (guiding) forces are applied on the center of mass of the forearm, yet allowing for rotations of the arm. The mechanism approaches the arm from one side, without fully enclosing the arm.

We applied this concept to the foot (PoC2) (see figure 4.5a) and the pelvis (PoC3a) (see figure 4.5b), however we used arched segments with angles smaller than 90 degrees. The advantage is that the segments become shorter and the gimbal becomes more compact and is less enclosing, hence the name ‘Short Skewed Axis Gimbal’ (see Appendix F) The disadvantage is that the for two of the three rotations, the workspace becomes smaller.

For the foot gimbal we choose the primary gimbal axis parallel to the plantar / dorsiflexion axis (see figure 4.5a). This way the range of motion in plantar / dorsiflexion is infinite, whereas for the other DoFs inversion / eversion and endo- / exorotation) the workspace is smaller (see figure 4.5c). All pivots point to the center of the ankle joint. PoC2 proved the feasibility of the concept: it allowed freedom for rotations in all DoFs of the

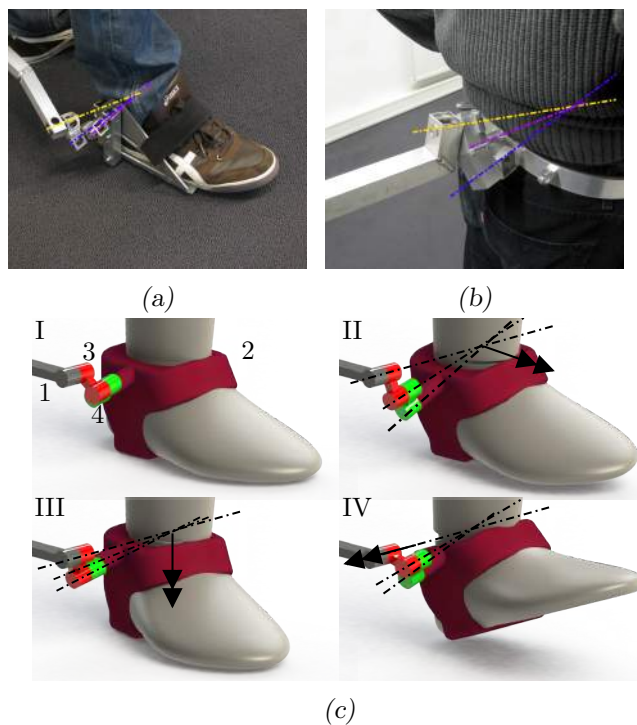


**Figure 4.5:** The skewed axis gimbal applied in concepts for LOPES II: (a): Poc2, the gimbal applied to the ankle, allowing for rotations of the ankle, with applying force in the center of the ankle. (b): Poc3a, the gimbal applied on the pelvis, allowing for rotations of the pelvis while applying force in the center of the pelvis. (c): Schematic drawing of the ankle gimbal. The rod from the shadow leg (1) is connected to the foot bracket (2) with two arched segments (3, 4). The connections between the components are revolutes joints, with axes intersecting in the ankle joint. This allows for rotation of the foot about the three principal axes: inversion / eversion (II), foot endo- / exorotation (III) and foot plantar / dorsiflexion (IV).

foot and when forces were applied to the rod, no parasitic foot rotations were imposed.

For the pelvis we applied the gimbal behind the subject (see figure 4.5b). This way arm swing will not be obstructed by the mechanism. In PoC3a, the remote center of the gimbal is more or less collocated with the center of mass of the subject. This means that forces applied to the rod will exert force in the center of mass of the subject without imposing or hindering rotations. This was confirmed in the tests with PoC3a (see figure 4.5b):

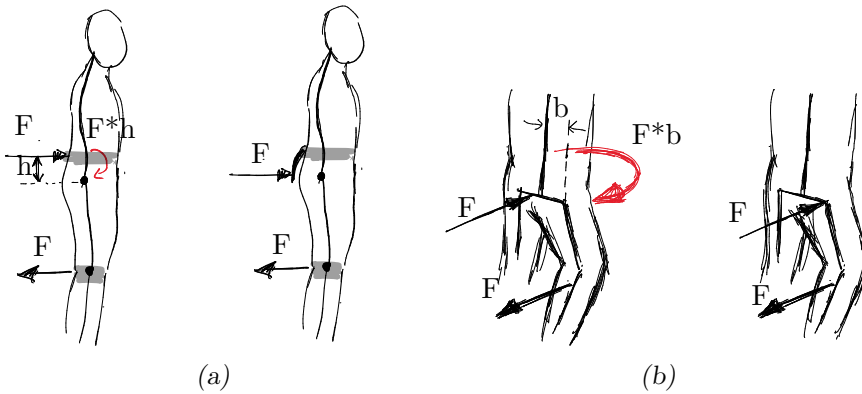
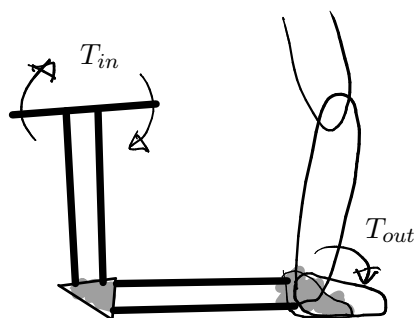


**Figure 4.6:** Effects of the location of center of rotation of the skewed axis gimbal applied to the pelvis. (a): When supporting hip extension, the patient will be forced in hollow back when the force on the pelvis strap is applied too high (left); Assuring that the force is exerted on the hip joint, will avoid this (right). (b): When supporting hip extension, the patient will be forced in transverse rotation the force on the pelvis strap in the center of the two hip joints (left); Assuring that the force is exerted on the hip joint, will avoid this (right).

subjects walked freely with the gimbal attached to their pelvis, while a second subject holding the rod applied forces. Only with exaggerate transverse rotation the gimbal reached the limit of rotation. In the design phase the dimensioning will be done such that the range of motion is acceptable. A second point of concern was the location of the remote center: When applying support torques in hip flexion/extension and knee flexion/extension it is desirable to exert force on the hip joint, but in PoC3a the force is exerted on point at the center of mass. The vertical offset may still cause the undesired hollow back when applying hip extension (see figure 4.6a); the horizontal offset may cause transversal rotation when applying hip extension (see figure 4.6b). Both problems are solved by using a gimbal for each hip, resulting in two rods and two skewed axis gimbals attached to a pelvis brace. This resulted in a new proof of concept (PoC3b) which is an evolution of PoC3a. Of PoC3b no individual picture is given, but it is integrated in following proofs of concept (see section 4.4).

#### 4.3.4 Foot Actuation — Proof of Concept 4

We built a simple bracket for the shoe and applied a parallelogram structure of rods (PoC4) (see figure 4.7). The bracket was actuated manually with a



(a)



(b)

**Figure 4.7:** Concept for push off. (a): the foot bracket is connected to a double parallelogram structure. Input torque ( $T_{in}$ ) will give a torque on the foot ( $T_{out}$ ). (b): The proof of principle for the concept (PoC4).

lever, to test whether this would feel comfortable, and whether one could walk with the bracket normally. Tests were performed with several subjects among which were physical therapists. All responses were positive. When applying plantar flexion torque with the lever, subjects were lifted on their toes. Therefore the concept is expected to be suitable to apply supportive torques.

#### 4.3.5 Chair / Lifting Aid — Proof of Concept 5

It is desirable that the patient can rest in LOPES II during donning and doffing, and between sessions. The challenge was to build a device that fits in the afore mentioned mechanisms. We built a chair of which the seat can tilt in order to push the patient upward. In the prototypes the tilting was done with a pedal. The force applied with the pedal was insufficient to put a fully passive person upright. However therapists agreed that either the body weight support, or the therapist can assist in the standing up, and that this tilting seat was sufficient.

### 4.4 Integrated Proof of Concept

We have integrated the approved proofs of principle in a test cart (see figure 4.9). This cart contains linkage for the pelvis and one leg. We put

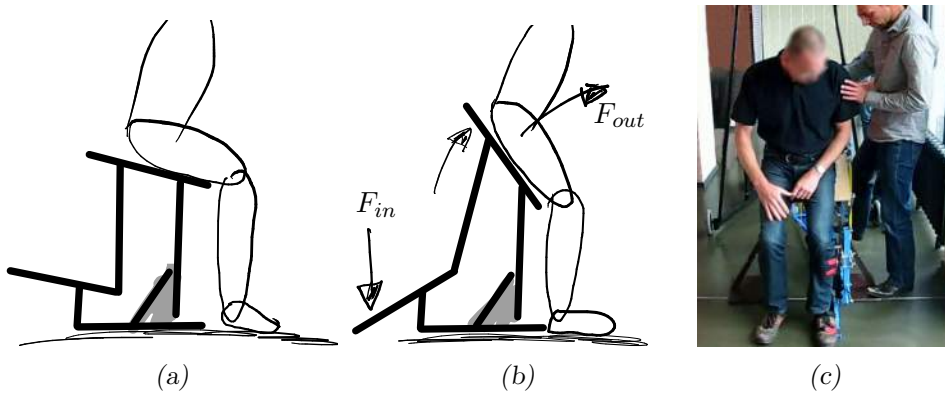


**Figure 4.8:** Concept of lifting chair. (a): Chair in resting pose. (b): Chair in lifting pose.(c): Lifting a subject with the chair (PoC5).

the frame on wheels, instead of using a fixed base frame with treadmill. This facilitated transport to several locations for testing.

The subject's pelvis is clamped with a rigid belt. This belt is to be connected with a harness in the final design. The pelvis belt is connected with two short skewed axis gimbal, each having a hip as the virtual point of rotation (see figure 4.9b). The gimbals are connected with rods to a horizontal stage that allows for pelvis translations. The horizontal stage is suspended from the main frame with rods. Rubber bands are used to balance the rods that are connected to the hip gimbals.

From the horizontal stage the shadow leg is suspended. With parallelogram linkages, levers at the top of the frame are connected to rotations of the lower leg and upper leg. One lever pulls the leg in mediolateral direction (abduction/adduction); one lever pushes and the knee in anterior/posterior direction (flexion/extension); and one lever rotates the lower leg about the lateral axis (flexion/extension).

From the shadow knee and ankle, rods are connected to the patient's lower leg. The foot bracket is connected with a short skewed axis gimbal with the ankle joint as the virtual point of rotation (see figure 4.5a).

The test cart was made of light-weight, aluminium rods. This allows for subjects to walk freely with the cart. The only help needed was a second subject to push the cart forward. Free walking is possible: arm swing is unhindered, free motion is possible in all DoFs. Additionally the 'Robot in Charge' mode can be simulated: a second subject uses the levers to apply

torques (see figure 4.9c). The lifting chair can be used in combination with the test cart.

There was consensus that this concept was the optimal starting point for the mechatronic prototypes.

## 4.5 Conclusion

The integrated proof of concept (Test Cart) seems to be the proper mechanical layout to fulfill the user requirements: the test cart has sufficient DoFs and each DoF can be supported (manually) or left free. Therefore, this mechanical layout is a proper starting point for a robot-assisted gait trainer allowing for both ‘Patient in Charge’ and ‘Robot in Charge’, and Assist-As-Needed training. Nonetheless the detailed design and the controller design will have a great impact on the performance of Assist-As-Needed in the mechatronic prototypes. This will be discussed in the following chapters.

In terms of force / torque actuation, the test cart is a hybrid solution of force on segments and torque on segments. From the force-on-segments principle, we used the minimum amount of clamps connected to rods. On the other hand, due to the shadow leg, each actuators (levers in the test cart) is primarily coupled to a single segment, i.e., a rotation of an actuator causes rotation of a single segment (ignoring small non-linear couplings) (see figure 4.9c).

Furthermore we have demonstrated the value of User Centered Design in the concept phase. The iterative process of UCD can reveal potential negative side effects of new concepts. The first concept of the shadow leg had the risk of pushing subjects in a hollow back. Because in both Lokomat and Lopes I sagittal pelvis rotation is locked, the users that did have experience with these robots, were not triggered to warn for this risk. By involving the users in the concept phase this potential risk surfaced. Similarly, in the PoCs, no end stop against knee extension were incorporated. This triggered the users to emphasize the need for an end stop.

The concepts evolved, due to the UCD. First we had a single gimbal for the pelvis rotations. This concept in combination with the shadow leg revealed that each hip joint requires its own gimbal to prevent parasitic rotations of the pelvis.

Summarizing, UCD helps in gaining insight in the users’ needs and in the evaluation and evolution of concepts.

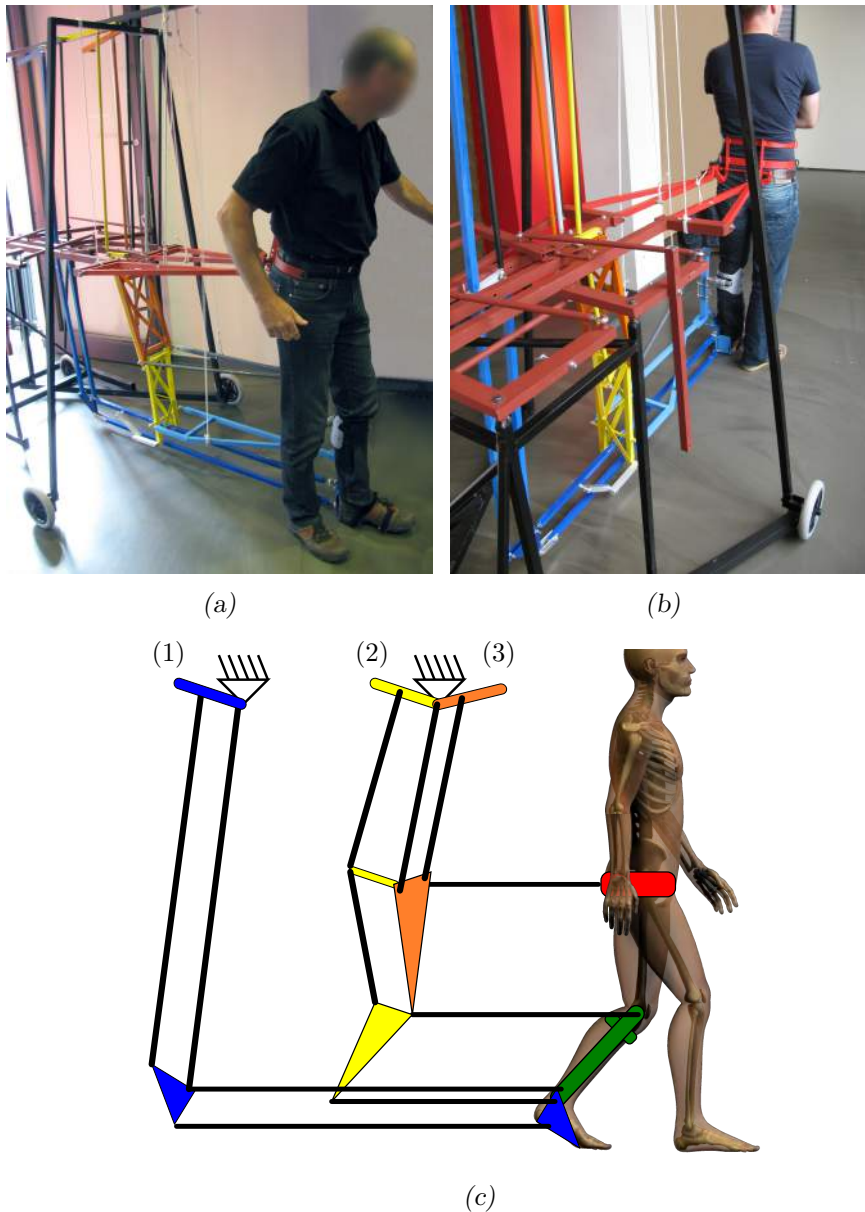


**Figure 4.9:** Integrated proof of principle for pelvis and single leg. (a): Overview of the test cart components: The shadow pelvis (dark red); the shadow thigh (orange); the shadow shank (yellow); The ankle rod (light blue) connecting the shadow ankle to the patient ankle; the knee rod (gray) connecting the shadow knee to the patient knee; the hip rods (red) connecting the shadow pelvis to the patient pelvis; and the foot rotation linkage (dark blue). (b): Double short skewed axis gimbal at the pelvis (PoC3b). (c): Schematic side view of the test cart. A force at the lever (1) results in a torque at the foot. A force at lever (2) results in a torque at the shank. A force at lever (3) results in a torque at the thigh.

# System Requirements

This chapter lists the system requirements of LOPES II. First the anthropometric requirements are defined. Next the requirements on the degrees of freedom are defined: what is the range of motion per DoF.

## 5.1 Anthropometric Data

One of the user requirements is that LOPES II must be suitable for a ‘wide population base’. This implies that LOPES II must be suitable for a wide range of stature and weight. This user requirement is quantified as: ‘LOPES II shall be suitable for  $> 99\%$  of the Western population.’

From the DINED database (TU-Delft, 2015) we selected the male and female databases for North America, North Europe, Central Europe and the Netherlands. For the dutch population databases were available for separate age groups and for 2003 and 2004.

The dimensions that are relevant for the detailed design of LOPES II are stature, mass and dimensions that are related to the lower extremities (see table 5.1). Mass is relevant for the body weight support system (BWS). Additionally forces and torques required to support walking are often related to body mass. Stature determines the height of LOPES II, more specific, it determines how high the BWS is to be located. Assuming that the shadow leg has fixed dimensions and vertical position, the rods between the shadow leg and patient leg will have a slight tilt angle depending on the length of the upper and lower leg and the length of the rods. Ideally these rods are near horizontal. Data for the hip height, length of upper and

**Table 5.1:** Anthropometric data covering 99% ( $\mu \pm 3\sigma$ ) of the European and North-american population

	Min	Max
Stature [mm]	1410 <sup>a</sup>	2088 <sup>b</sup>
Mass [kg]	36 <sup>c,d</sup>	138 <sup>c</sup>
Hip height [mm]	715 <sup>e</sup>	1228 <sup>b</sup>
Hip breadth [mm]	263 <sup>f</sup>	531 <sup>e</sup>
Shank Length [mm]	347 <sup>g</sup>	514 <sup>g</sup>
Thigh Length [mm]	345 <sup>g</sup>	512 <sup>g</sup>
Foot length [mm]	202 <sup>h</sup>	314 <sup>b</sup>
Foot breadth [mm]	74 <sup>h</sup>	123 <sup>c</sup>

<sup>a</sup>Dutch 2004 (60 plus), female

<sup>b</sup>Dutch 2004 (20-30 years), male

<sup>c</sup>Dutch 2003 (31-65 years), male

<sup>d</sup>The values of  $\mu - 3\sigma$  for Dutch 2003 (18-30 years), female and Dutch 2003 (31-65 years), female are 26 kg and 30 kg respectively. These values are regarded as highly unlikely and therefore ignored.

<sup>e</sup>Dutch 2003 (31-65 years), female

<sup>f</sup>North American, female

<sup>g</sup>Values derived from stature [Winter \(1990\)](#)

<sup>h</sup>Dutch 2003 (18-30 years), female

lower leg determine the optimal length of the rods. Data of the upper and lower leg was not available in the DINED database, therefore we used the relative segment lengths ([Winter, 1990](#)) to calculate the absolute segment length for different stature.

For the interfaces with patient, the hip breadth and foot dimensions are relevant.

## 5.2 Walking Speed

Walking speed is an important determinant for the required range of motion (RoM), segment speeds, and segment torques. Training speed vary from very low speeds ( $< 1$  km/h) to high speeds ( $> 5$  km/h). For LOPES II we define the maximum required speed as 1.5 m/s. This is deemed sufficient for nearly all gait training, except for running, which is assumed not be part of gait training with an assistive device.

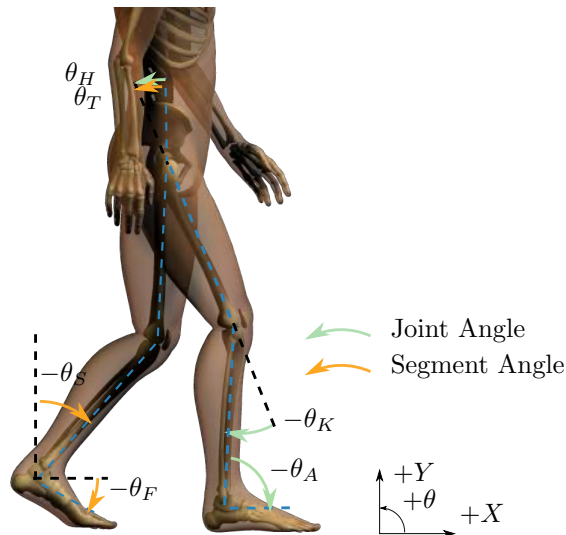


**Figure 5.1:** Joint and segment angles in of the lower extremities in the saggital plane. Segment angles: thigh sagittal angle  $\theta_T$ , shank sagittal angle  $\theta_S$ , and foot sagittal angle  $\theta_F$ ; Joint angles: hip sagittal angle  $\theta_H$  ( $= \theta_T$  since pelvis sagittal angle is assumed to be zero), knee sagittal angle  $\theta_K$  ( $= \theta_T - \theta_S$ ), and ankle sagittal angle  $\theta_A$  ( $= \theta_S - \theta_F$ ).

### 5.3 Degrees of Freedom

This section lists the requirements for the Degrees of Freedom (DoFs). We use three sets of DoFs, each set containing ten DoFs. The first set is contains the absolute segment angles (sagittal angles of thigh, shank, foot, and the frontal angle of the leg) (see figure 5.1) and pelvis horizontal translations. The second set contains the joint angles i.e., the difference between two absolute angles of interconnected segments (see figure 5.1). Furthermore this set contains the pelvis translations as well. The last set contains the joint *translations*, i.e., the absolute positions of the pelvis (X, Z), knee (X), ankle (X, Z) and heel (X).

Results are summarized in table 5.2; the subsections provide the rationale behind the numbers. Where possible we used the 95% confidence interval (C.I.) ( $\mu \pm 2\sigma$ ).

**Table 5.2:** Requirements per degree of freedom in terms of range of motion, torque and speed (powered DoFs only)

DoF	RoM [m;deg]	Force/ Torque [N;Nm]	Speed [m/s;rad/s]
Pelvis anterior / posterior	$\pm 0.3$	500	0.3
Pelvis mediolateral	$\pm 0.15$	500	0.3
Pelvis up / down		1000 <sup>a</sup>	
Pelvis sagittal rotation	$\pm 6$		
Pelvis frontal rotation	$\pm 10$		
Pelvis transversal rotation	$\pm 15$		
Thigh abduction / adduction	19 / 17	60	1.6
Thigh sagittal rotation (min / max)	-28 / +36	60	3.2
Shank sagittal rotation (min / max)	-77 / +31	134	7
Knee flexion / extension	75 / 0		7.3
Foot sagittal rotation (min / max)	-100 / +34	95	9
Foot endo- / exorotation	10 / 20		
Ankle inversion / eversion	10 / 10		

<sup>a</sup>Upward only (body weight support)

### 5.3.1 Range of Motion

A valuable source of information is the Winter data (Winter, 1987). He has recorded sagittal angles of the hip, knee and ankle at various speeds. However for LOPES II the *segment* angles are more relevant than the *joint* angles, since the selected concept largely uses actuation on segments. Therefore we need to convert the joint data to segment data. We calculated the normal distributions of joint angles to normal distributions of segment angles (see figure 5.2). In the calculations we assume that the pelvis sagittal angle is zero and the joint angles are not correlated:

$$N(\mu_{\theta_t}, \sigma_{\theta_t}) = N(\mu_{\theta_h}, \sigma_{\theta_h}) \quad (5.1a)$$

$$N(\mu_{\theta_s}, \sigma_{\theta_s}) = N\left(\mu_{\theta_h} - \mu_{\theta_k}, \sqrt{\sigma_{\theta_h}^2 + \sigma_{\theta_k}^2}\right) \quad (5.1b)$$

$$N(\mu_{\theta_f}, \sigma_{\theta_f}) = N\left(\mu_{\theta_h} - \mu_{\theta_k} + \mu_{\theta_a}, \sqrt{\sigma_{\theta_h}^2 + \sigma_{\theta_k}^2 + \sigma_{\theta_a}^2}\right) \quad (5.1c)$$

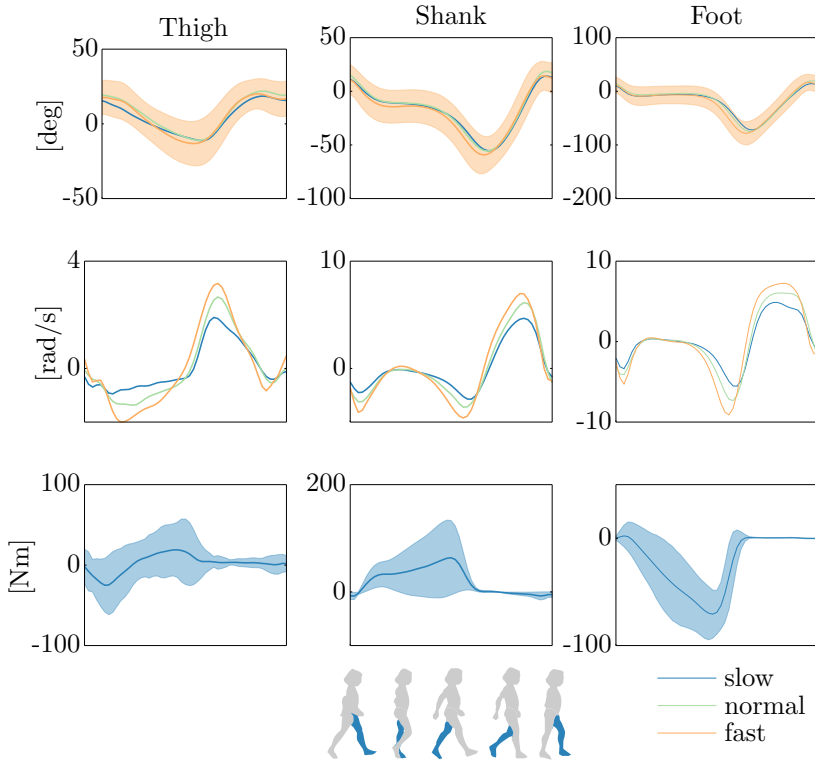


**Figure 5.2:** Sagittal segment angles (average and 95 % C.I.) at slow, normal and fast walking (top); numerical derivative of the average segment angles (middle); Sagittal segment torques at slow walking (mean and 95 % C.I.). All values are derived from Winter (1987).

where  $N(\mu, \sigma)$  denotes the normal distribution with given average  $\mu$  and standard deviation  $\sigma$ ; subscripts  $\theta h$ ,  $\theta k$ , and  $\theta a$  denote the sagittal angles of the hip, knee, and ankle respectively, taken from Winter (1987); subscripts  $\theta t$ ,  $\theta s$ , and  $\theta f$  denote the sagittal angles of the thigh, shank, and foot respectively.

Most likely the joint angles are correlated, but since this correlation is unknown, assuming no correlation will lead to the worst-case estimation of the standard deviation for the segment angles. Consequently this may lead to an overestimation of the required RoM for the distal segments. The following sections describe in detail the required Range of Motion (RoM) per segment. Where relevant we use additional sources to the Winter data.

## Pelvis Translations

For the pelvis AP translation, we require a range of 600 mm. This range is deemed to be sufficient to allow for small variations in speed of the patient during training. In normal gait the pelvis mediolateral translation is only a 40 mm (Saunders et al., 1953). However since we want to allow for drifting sideways, a total range of 300 mm is required.

## Pelvis Rotations

For normal gait the pelvis frontal rotation is  $-4$  deg, i.e., a hip ‘drop’ on the swing side. (Perry, 1992). However, for hip hiking, the pelvis frontal rotation causes a hip ‘lift’ of the paretic leg. Kerrigan et al. (2000) found that the average lift was fairly small ( $+0.2$  deg), but has a large standard deviation (4.4 deg). For LOPES II we take the 95 % C.I. which results in a requirement of  $\pm 10$  deg for pelvis frontal rotation.

In normal gait the transverse rotation of the pelvis is small ( $0.8 \pm 1.7$  deg). In compensatory strategies this rotation is increased ( $7.6 \pm 8.1$  deg). Using the 95 % C.I. would result in a required range of  $\pm 25$  deg. We believe that these values are exceptionally large, and could lead to undesired situations where the patient is not sufficiently oriented in the forward direction. We chose to reduce the required RoM to  $\pm 15$  deg.

For pelvis sagittal rotation, we found no data in literature, however, we analyzed gait recordings and found that a range of  $\pm 6$  deg is likely to cover normal walking.

## Hip / Thigh

The maximum hip flexion in normal walking is 31 deg; maximum hip extension is 28 deg according to the Winter data. However, in stiff-legged gait the 95 % C.I. for hip flexion is 36 deg (Kerrigan et al., 2001).

The required hip / thigh abduction / adduction RoM is defined circumduction. Also in this case, the *thigh* abduction / adduction is more relevant than the *hip* abduction / adduction, since LOPES II will have segment actuation. Fortunately Kerrigan et al. (2000) has researched both the hip abduction / adduction, and the thigh abduction / adduction during circumduction and hip hiking. The maximum abduction (95 % C.I.) is 19 deg; the maximum adduction is 17 deg.

Of the hip / thigh endo- / exorotation little data is available, but the relevance of this angle in the LOPES II concept is limited, since the concept

for the LOPES II contains no clamps on the thigh segment and making turns is not possible. The clamp below the knee actually locks the lower leg and consequently the upper leg in endo- / exorotation. We assume the thigh endo- / exorotation is irrelevant in the design of LOPES II, and therefore will not be discussed in the further design and development as described in this thesis.

### **Knee / Shank**

LOPES II will have a mechanical end stop for hyperextension. The 95 % C.I. for the knee extension 6 deg extension (Winter, 1987), however this may be harmful for several patients. Therefore the required knee extension is set to 0 deg.

For the shank the maximum sagittal rotation (leg forward) is +31 deg; the minimum sagittal rotation (leg backward) is -77 deg.

### **Ankle / Foot**

For the foot the maximum sagittal rotation (toes upward) is +34 deg; the minimum rotation (toes downward) is -100 deg.

According to Perry (1992), the exorotation of the foot is 7 deg in standing. In the concept phase, subjects walked with fixed foot endo- / exorotation, and they found it uncomfortable, even when walking in a straight line. Therefore foot endo- / exorotation should have (limited) freedom. We found no literature on range of motion of foot endo- / exorotation in normal or pathological gait. After discussion with physical therapists and rehabilitation physicians we set the required RoM for the foot endo- / exorotation to 10 deg endorotation to 20 deg exorotation.

For foot inversion / eversion we did not find data either. We set a required range of  $\pm 10$  deg for foot inversion / eversion.

### **5.3.2 Speed and Force / Torque**

For the powered DoFs, it is important that the actuators are fast enough to follow the patient's joint motions. These joint motions are highest at high walking speed. Due to the lack of data on segment speeds, we differentiated the average segment angle patterns derived from the Winter data (see figure 5.2). However, the standard deviation can not be differentiated, and therefore we cannot calculate the 95 % C.I. Therefore, where possible,

we used the Winter data of fast walking (not running), assuming that this will cover the 95 % C.I. of normal walking.

Winter (1987) also recorded the joint torques normalized to body mass at various speeds. To convert these joint torques to requirements for LOPES II, we use the following assumptions: 1) the maximum support LOPES II has to apply is for a completely passive subject of 138 kg; 2) when a subject is completely passive, at least half of its weight is supported by the BWS; 3) the remaining support is applied on the segments, which is estimated at half of the voluntary joint torques (as recorded by Winter); and 4) training at maximum support, occurs at low speed only. With these assumptions, the segment torque requirements are calculated by using the normalized, low-speed torque data with a 69 kg mass. To calculate the normalized distribution of the segment torques from the joint torques, we used a method similar to the calculation of the normalized distribution of the segment RoM (see (5.1)):

$$N(\mu_{Tt}, \sigma_{Tt}) = N\left(\mu_{Th} + \mu_{Tk}, \sqrt{\sigma_{Th}^2 + \sigma_{Tk}^2}\right) \quad (5.2a)$$

$$N(\mu_{Ts}, \sigma_{Ts}) = N\left(-\mu_{Tk} - \mu_{Ta}, \sqrt{\sigma_{Tk}^2 + \sigma_{Ta}^2}\right) \quad (5.2b)$$

$$N(\mu_{Tf}, \sigma_{Tf}) = N(\mu_{Ta}, \sigma_{Ta}) \quad (5.2c)$$

In the following sections, the exact speed and torque requirements are listed per segment.

## Pelvis

On the pelvis speeds, little has been published. We measured speeds of 250 mm/s for both AP and ML direction for treadmill walking at 4.5 km/h. These values are used for the system requirements.

For a requirement on the forces that must be applied on the pelvis, we make a rough guess on the forces that are needed to support or perturb a patient. These forces are estimated at 500 N.

For the bodyweight support we assume that the maximum upward force to be applied is 100 kg, which is approximately 70 % of the body weight of the largest admissible subject (138 kg).

### Thigh

The thigh flexion speed is maximum when swinging forward (3.2 rad/s) (see figure 5.2). The required torque at low speed is 60 N m. For thigh abduction/adduction speed, we assume that the highest speed occurs during circumduction. However, no data is available. Since the abduction/adduction excursion is about half the excursion in flexion/extension, we use half the thigh flexion/extension speed requirement for the required thigh abduction/adduction speed. Data is available for the *hip* abduction/adduction torque, but not for *thigh* abduction/adduction. We will use the thigh flexion/extension torque requirement for the required thigh abduction/adduction torque.

### Shank

The shank sagittal rotation speed is largest when swinging forward (7 rad/s) (see figure 5.2). The required torque at low speed is 134 N m. This occurs during push off.

### Foot

The foot sagittal rotation speed is largest at the push off ( $-9$  rad/s) (see figure 5.2). The required torque at low speed is 95 N m. This occurs during push off.

## 5.4 Impedance

LOPES II must be able to display minimum impedance to allow for ‘Patient in Charge’ (UR01). Transparent behavior of the robot implies that the patient should be able to move freely with minimal resistance (impedance) of the robot (Van Asseldonk et al., 2008). With control strategies the robot impedance can be compensated for largely, but not completely. The remaining impedance can be implemented as an inertia, a damper or a combination of both. If the remaining impedance is sufficiently low, the gait pattern will not notably be affected. When LOPES II is in the ‘Robot in Charge’ mode (UR02), it should be stiff enough to enforce a gait pattern on the patient. We define the required stiffness for the displacement of the pelvis, knee and ankle. The values for required maximum and minimum impedance are listed in table 5.3. The sections below give the rationale for these figures.

**Table 5.3:** The maximum allowable inertia and minimum required stiffness for the translation of the pelvis, knee and foot in LOPES II.

	Inertia [kg;kgm <sup>2</sup> ]	Stiffness [N/mm;Nm/rad]
Pelvis AP	6	50
Pelvis ML	6	50
Knee AP	4	40
Foot AP	2	20
Foot ML	2	20
Foot sagittal rotation	0.006	600

**Table 5.4:** The required measurement accuracy of joint rotations and pelvis translations.

	Required Accuracy
Pelvis anterior / posterior	2 mm
Pelvis mediolateral	2 mm
Hip abduction / adduction	1.4 deg
Hip flexion / extension	2.3 deg
Knee flexion / extension	3.4 deg
Ankle plantar / dorsiflexion	2.5 deg

## Position Accuracy

LOPES II will measure and report the performance of the patient to the therapist, among which the joint angles and positions. The required accuracy of the measured angles and positions must be better than the variability. [Koopman et al. \(2014\)](#) reported the standard deviation of joint patterns averaged across the gait cycle over different walking speeds. For pelvis motions no data is available. We estimate the required accuracy to 2 mm (see table 5.4).

### 5.4.1 Minimal Impedance

We have investigated the effect of directional inertias on the pelvis and foot (see Appendix B). We added inertias to the pelvis in AP direction, ML direction, or both and measured the effect on metabolics, kinematics and muscle activity during walking. In a second experiment we added

inertias to the foot in AP direction during walking. We found that  $\leq 6$  kg of inertia added to the pelvis in AP direction, ML direction, or both, does not affect gait notably. For the foot,  $\leq 2$  kg of AP inertia does not affect the gait notably.

For the knee no data is available. Based on the pelvis and ankle data, we estimate the allowable inertia in AP direction for the knee at 4 kg.

Based in anthropometric data (Winter, 1990) we estimate the average moment of inertia of the foot about plantar flexion axis is estimated at  $0.04 \text{ kgm}^2$ . The just noticeable difference for the foot translational inertia is 0.15 (see Appendix B); we use this factor for the rotation as well, resulting in a maximum allowable inertia of  $0.006 \text{ kgm}^2$ .

### 5.4.2 Maximum Impedance

In the maximum impedance mode LOPES II the actuators are controlled to desired position patterns and thus will force the patient in a predefined gait pattern. For the quantification of the maximum impedance we use a maximum allowable position error at an estimated resistance from the patient. Similar to the minimum impedance we define the maximum impedance at the joint translations, and at the foot sagittal rotation.

During normal walking, patients cannot withstand mediolateral pelvis forces  $> 50 \text{ N}$  (see Appendix A). If we define a positioning error of 1 mm, then the required stiffness for pelvis ML displacement is  $50 \text{ N/mm}$ . Earlier we defined a maximum force of  $500 \text{ N}$ ; this will result in a deflection of 10 mm. For pelvis AP we assume the same values, and thus also  $50 \text{ N/mm}$ .

For knee translation, the required stiffness is highest during stance, to provide extension and to prevent hyperextension of the knee. The maximum knee extension torque in stance is  $1 \text{ N m kg}^{-1}$  (Winter, 1987). For the heaviest case a 138 kg patient then  $138 \text{ N m}$  is the maximum knee torque that is to be delivered if a patient fully bears his own weight. If we assume that 50% body weight is supported is supplied, then the rods of LOPES II have to supply  $69 \text{ N m}$  on the knee extension. For a leg of 1 m, this means that the rod on knee pulls with  $276 \text{ N}$ , and the rods on the hip and ankle push with  $138 \text{ N}$ . If we assume a knee angle error of 2 deg, this means that the knee of a 1 m leg has a displacement error of 8.7 mm. The maximum force with the maximum allowable displacement gives  $32 \text{ N/mm}$ . Since this contains a lot of assumptions, we will use a stiffness of  $40 \text{ N/mm}$ .

For foot translation, the stiffness is most important in terminal swing, where the actual foot positioning takes places. We assume a desired posi-

tioning accuracy of 1 mm with a resistance force of 20 N, thus the required stiffness for the foot translations is estimated at 20 N/mm.

For the foot sagittal rotation we assume a desired positioning accuracy of 1 deg with an average resisting force of 10 N m. This results in a required stiffness of 600 Nm/rad.

# CHAPTER 6

## System Design

This chapter describes the main components of LOPES II, i.e., mechanism layout, actuators, sensors and bodyweight support (BWS). Detailing of the mechanical design and the controller design is described in chapters 7 and 8 respectively.

### 6.1 Scope for the First Prototypes

Due to the complexity of LOPES II, we will first design prototypes with the primary functions. In a later stage we will add the secondary functions. The function of resting and helping the patients to stand is important, but secondary. Therefore the lifting chair is not included in the prototypes. The chair has to fit in / around the rod structure of LOPES II, and therefore it is important to first design the rod structure, to define the envelope for the chair. We believe that LOPES II without lifting chair is usable for the majority of patients. For the more severely impaired patients, the donning process may be more complex and may take longer, consequently affecting the usability of LOPES II. However, the BWS system of LOPES II will be designed such that severely impaired patients can be lifted out off their wheel chair into LOPES II.

## 6.2 Additional Safety Measures

LOPES II is designed according to the Machine Directive (2006/42/EC). This section lists the extra measures that have been taken in order to reduce risks.

Although the actuators are not close to the patient, and the risk of electric shock is very low, we chose to limit the voltages to 60 Vdc to comply with Safety Extra Low Voltage (SELV) according to the medical directive (IEC60601-1, 2005).

The control of LOPES II relies on sensor data (force and position). Sensor errors may lead to dangerous behavior of LOPES II, therefore we chose to have redundancy in the force and position sensors.

## 6.3 Actuation

LOPES II requires actuators that are capable of displaying high impedance and low impedance. High impedance for actuators means that they must be able to display high force and high stiffness. For low impedance it is important that the actuators display smooth behavior, i.e., is shows no disturbances from e.g., gearboxes, torque ripple, stick slip.

For flight simulation similar requirements apply: the actuator that is coupled to the controls of an aircraft must respond smoothly and lightly to the pilots forces, yet it must be able to display extreme forces and stiffnesses in emergency simulations. We decided to use Moog control loading actuators (MOOG, 2009), since they have proven technology in the force controlled flight simulation.

The Moog Control Loading actuators CL-R-E-/MD/40Nm (C40) and CL-R-E-/MD/100Nm (C100) are rotary actuators with gearbox and output lever with torque sensing (see figure 6.1). The C40 and C100 have a maximum output speed of 5.2 rad/s, and a nominal torque of 40 N m and 100 N m respectively. For short duration (< 1 s) the actuators can generate peak torques of twice the nominal torques.

The original actuators are designed for supply voltages of 230 Vac. For the motors we selected the torque constants such that the nominal voltages are less than 60 Vdc in order to comply with SELV.

For the amplifiers we selected Moog Servo Drives (MOOG, 2014a) For the C40 actuators we use the GS392-006 (rated current 6 A); for the C100

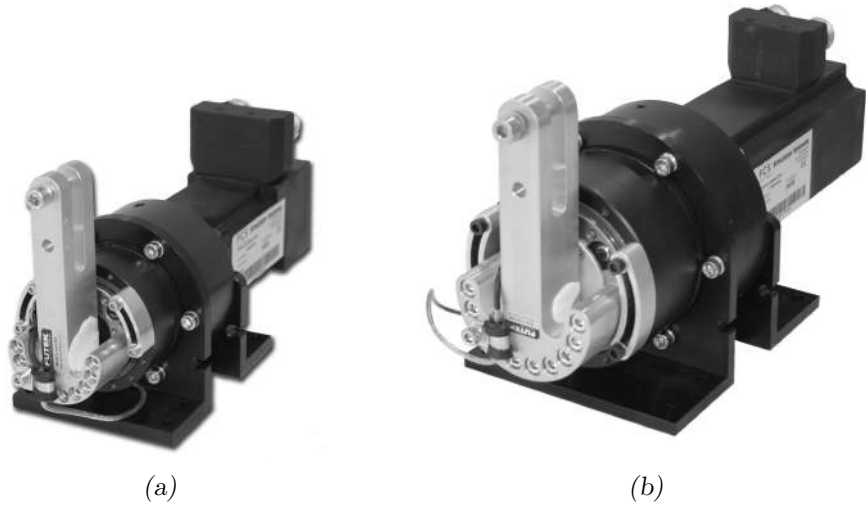


**Figure 6.1:** Moog Control Loading Actuators consisting of motor, gearbox, output lever with torque sensor, and adjustable, mechanical end stops. (a): CL-R-E/MD/40Nm (C40); (b): CL-R-E/MD/100Nm (C100).

we use the GS392-008 (rated current 8 A). The drives are capable of supplying twice the nominal currents for 10 s.

## 6.4 Sensors

### 6.4.1 Sensors on Actuators

The C40 and C100 actuators are equipped with absolute encoders. The repeatability of the position measurement at the lever is 0.02 deg, including sensor resolution, gearbox play and gearbox compliance. Furthermore, the actuators are equipped with torque sensitive levers. The C40 actuator has a torque sensor with a full scale (capacity) of 80 N m; the C100 torque sensor has a capacity of 240 N m. The noise and repeatability are about  $10^{-4}$  of the full scale.

### 6.4.2 Angular Sensors

The encoders in the actuators are insufficient to fully determine the patient posture. The vertical position of the left and right hip, and the transverse pelvis rotation can not be calculated from the the motor angle data alone.

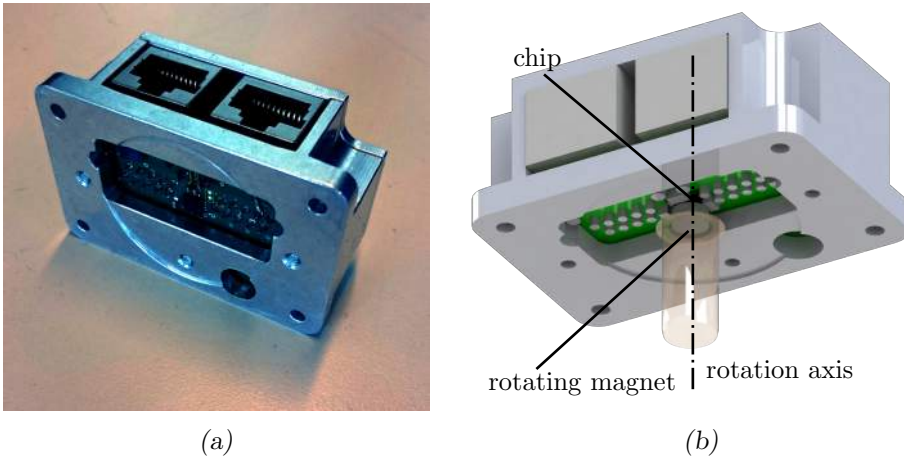


**Figure 6.2:** Magnetic Angular Sensor: the chip measures the rotation of the magnet along the rotation axis. (a): Photo of the manufactured angular sensor; (b): CAD drawing of the working principle of the angular sensor.

Furthermore we stated that we require redundant sensors, i.e., , we require additional sensors to check the motor encoders.

To measure the vertical hip displacements and pelvis rotation, and to have redundancy on the motor encoders, we have developed a contactless angular sensor, based on magnetic sensing (see figure 6.2a). The housing of the sensor is mounted on one body, a 6 mm diameter magnet is placed on a second body. A chip measures the orientation of the magnet in 12 bit resolution, and consequently the sensor measures the relative rotation between the two bodies along a single axis. (see figure 6.2b). For the redundancy we place the angular sensors on the joints of the shadow leg. This way we can detect any deformation or breakage of the linkage between the actuators and the shadow leg. A minor disadvantage is that the relation between the redundant sensors and the primary sensor (i.e., the motor encoders) is non-linear. The redundant sensors measure the knee flexion / extension, hip flexion / extension, and hip abduction / adduction of the shadow leg (see figure 6.3). For the pelvis AP and ML translation, the redundant sensors are located in mechanics of the shadow pelvis.

Additional sensors located in the shadow pelvis measure the tilt angle of the hip rods (see figure 6.3) and pelvis frontal and transversal rotation.

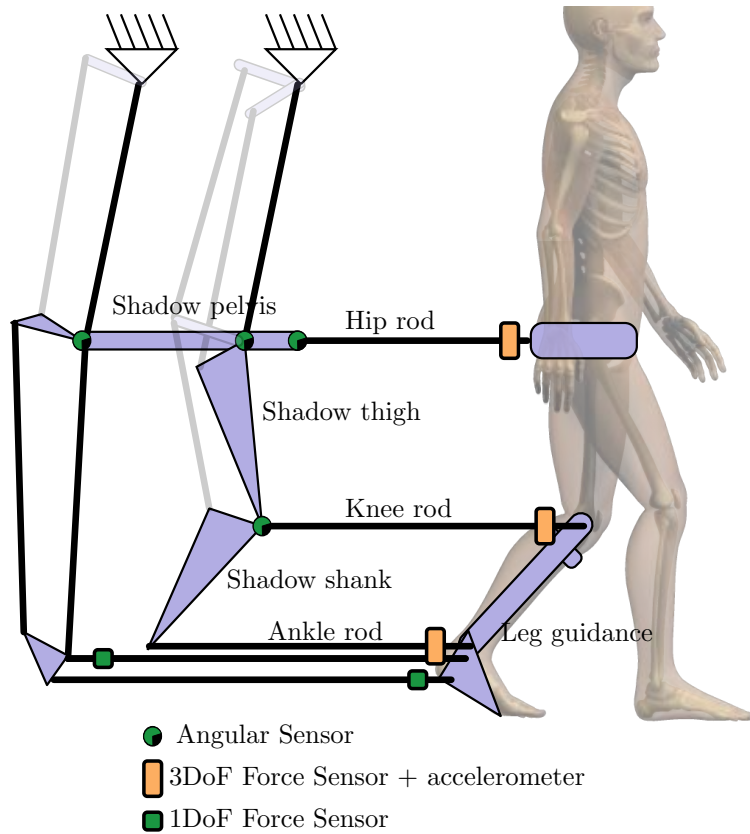


**Figure 6.3:** Location of hip height sensor, redundant sensor for shadow hip flexion / extension and knee flexion / extension, and the 3DoF force sensors on the rods towards the joints.

### 6.4.3 Force Sensors

The force sensors must measure the interaction force between LOPES II and the subject. It is important that these sensors are located as close to the patient as possible, to eliminate disturbing effects such as friction in the linkage and inertia of the linkage. The closest location for force sensing is pressure sensing in the clamps, however we assume that this is not accurate enough to measure the interaction forces. The second closest location is in the mounting between the clamps and linkage. This is feasible, but this would mean that the leg guidance of LOPES II is not force sensitive, i.e., that LOPES II will not respond to forces applied to leg guidance. It is

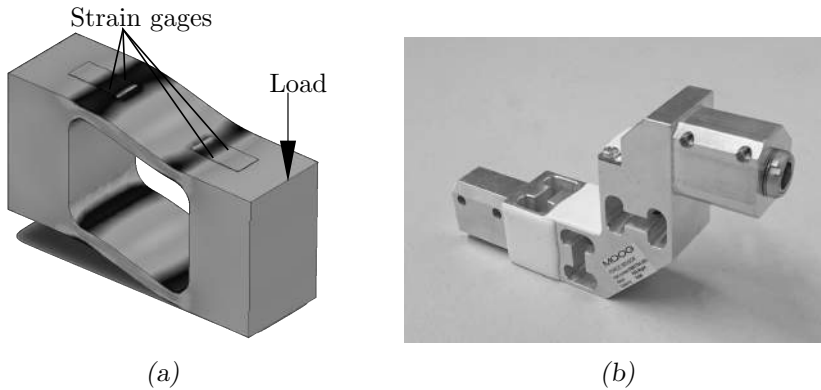


**Figure 6.4:** Force sensor design for LOPES II. (a): Principle of a 1DoF force sensor, sensitive for shear force in one direction. Dark gray indicating high strain, light gray indicating low strain. On the top, in the two areas of high strain, strain gages are glued. (b): Realization of the 3DoF force sensor

imaginable that users may push against the leg guidance e.g., to provide additional assistance, or to position LOPES II during donning. This may lead to unsafe situations, or it may reduce the perceived safety. Therefore we chose to mount the sensors in the hip-, knee-, and ankle rods (see figure 6.3). A compromise of this location is that the measured force is ‘polluted’ with inertia force of the leg guidance and clamps, and friction in the joints between the rods and leg guidance.

At each joint we want to measure the AP and ML forces. In this stage the optimal orientation of the sensor is unknown; that will be determined in the detailed design stage. Therefore we designed a 3DoF sensor that measures three orthogonal forces. The sensor can be mounted in any orientation, to measure the desired forces. The force sensor consists of three force elements, each measuring a shear force in one dimension. A force element contains two parallel thin-walled beams which deflected under shear force. Strain gages mounted on the beam measure the strain in the beams, proportional to the shear force (see figure 6.4a). A single element has four strain grids, which are wired in a Wheatstone bridge configuration, making the sensor is insensitive for other loads than the shear force. A 3DoF force sensor consists of three orthogonal elements (see figure 6.4b). For the hips and knees we use force sensors which are rated for 700 N; for the ankles we use 250 N force sensors.

#### 6.4.4 Accelerometers

The force sensors measure the interaction force between the subject and LOPES II, but also inertia forces of inertias between the subject and the force sensors. When the accelerations of these inertias are measured and the masses are known, the inertia force can be subtracted from the measured force. For this we add 3DoF accelerometers (type MMA7361L, Pololu, Las Vegas, USA) at the force sensors.

#### 6.4.5 Real time Platform

For the real time computer we use Linux based computer that runs on 1024 Hz. For the communication with the drives, treadmill, and sensor analog input components we use EtherCAT. EtherCAT offers for fast communication and drivers are widely available.

### 6.5 Treadmill

For the treadmill we use a treadmill with a large walking surface, to provide sufficient space for the patients to ‘walk around’ during training. Additionally a large area provides a sense of freedom, and it allows for projection of instructions and feedback on the treadmill (Houdijk et al., 2012).

A second requirement for the treadmill is to measure the vertical force and the center of pressure on the treadmill surface.

We used a custom 1.2 m × 2.5 m, instrumented treadmill by Motekforce Link, Amsterdam, the Netherlands. The treadmill is equipped with six force sensors that are placed under the walking surface: a sensor near each corner of the walking surface, and two sensors half way the long edges of the surface.

The treadmill is driven by an AC motor with frequency control. The default maximum speed of the treadmill is 12 km/h. The speed, acceleration and deceleration limits in the treadmill drive are tuned to safe values. We added extra safety to the treadmill control, which allows for a controlled stop within 1 s in case of an emergency stop or a power shutdown. Furthermore the treadmill is equipped with an extra encoder, which serves as redundancy check on the treadmill speed.

## 6.6 Bodyweight Support Module

For the body weight support (BWS) module we use a pneumatic system (see figure 6.5). The BWS module has two pneumatic cylinders; one for the constant force; one to break a fall. The pressure in the constant force cylinder is nearly independent of the extension length of the cylinder and therefore by regulating the pressure in the cylinder, the upward force on the patient is regulated. This means that if the patient moves up and down, he will receive a constant upward force, until the cylinder is fully extended or retracted. The stroke of the constant force cylinder is 200 mm, as is the range in which the constant bodyweight support is supplied.

A second cylinder ('fall-buffer cylinder') is by default fully retracted, due to a constant pressure in the cylinder. In case of a fall of the patient, first the constant force cylinder is fully extended. Then, the buffer cylinder will break the fall with a maximum force, proportional to the pressure in the cylinder. This assures that fall breaking forces will not be excessively (uncomfortably) high.

The pressure in both cylinders is controlled by a panel on the side of LOPES II. The winch is operated by a remote hand held.

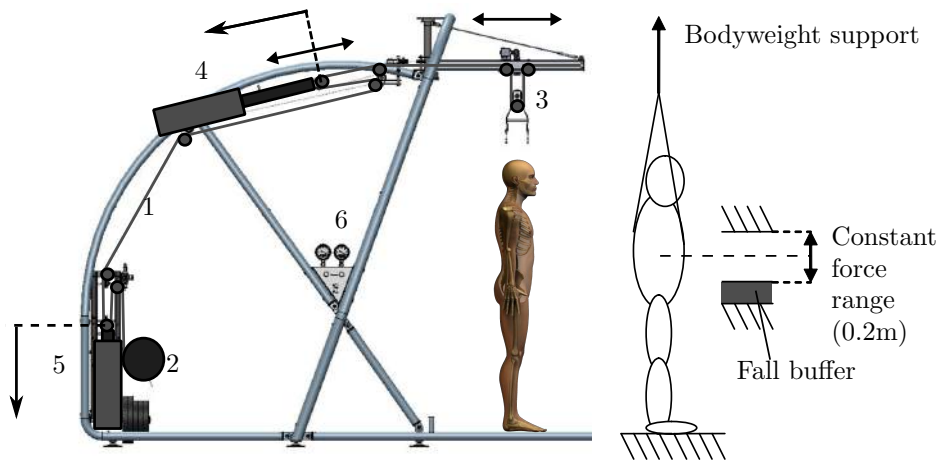


**Figure 6.5:** Bodyweight support system of LOPES II. The harness is connected to a yoke (3) which is suspended from a steel cable (1) that is wound on an electric winch (2) at one end, and fixed at the other end. Two pneumatic cylinders are placed in the cable chain i.e., the constant force cylinder (4) and the fall buffer cylinder (5). The constant force cylinder controls the force in the cable and therewith the upward force on the patient. The pressure in the cylinder is proportional to the upward force on the patient.



# Mechanical Design

In this chapter we describe the mechanical design of the linkages. Crucial in the mechanical design is the dimensioning of the components, since this defines the kinematic relation between actuator and sensor angles, and patient segment angles and positions. With this relation and the required range of motion (RoM) of the patient segments is calculated. Subsequently the linkages are dimensioned i.e., the lengths of the rods and levers. This results in a wireframe of LOPES II, which serves as input for the detailed mechanical design. The detailed mechanical design i.e., selection of bearings, dimensioning components for strength and stiffness, is not discussed. This chapter ends with an analysis of the mechanical design on the physical mass and the range of motion.

## 7.1 Main Dimensions

In this section we state a few main dimensions which form the basis for the dimensioning of the linkage (see figure 7.1).

The vertical rods form the suspension for the shadow pelvis stage from which the shadow legs are suspended. For the vertical rods we take 1 m; this allows the shadow pelvis stage to make horizontal displacement with only little vertical displacement: 20 mm for a horizontal displacement of 200 mm. When LOPES II is unpowered, the pelvis stage is pulled towards the neutral position (pendulum effect). In operation the actuators have to neutralize this pendulum effect, however in practice it may be desirable that the patients are pulled slightly toward the center of the workspace

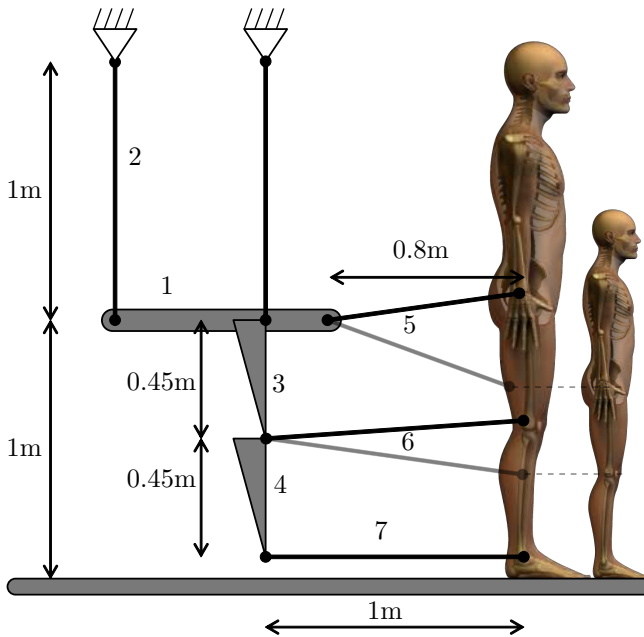


**Figure 7.1:** Main dimensions of LOPES II with the tallest and the shortest patient. The shadow pelvis (1) is suspended from vertical rods (2). The shadow thigh (3) is suspended from the shadow pelvis, and below is the shadow shank (4). The hip rods (5) are connected between the patient's hips and the shadow pelvis. The knee rods (6) are connected to the patient knee and the shadow knee (hinge between shadow thigh and shank). The ankle rod (7) is connected between the patient's ankle and the shadow ankle (end of the shadow shank)

Shorter rods will result in a more compact LOPES II, however the pendulum effect is larger. In the test cart (see figure 4.9) the 1 m seemed to have an acceptable pendulum effect.

For the distance between the shadow leg and the patient leg we choose 1 m. The rods between the shadow leg and patient leg allow for patients of various sizes to train in LOPES II: for a short person, the hip rods will be tilted downward, for a tall person the rods will be tilted upward (see figure 7.1). A tilt of e.g., the hip rod means that the forces applied to the pelvis will have an undesired, vertical component. The longer the rods, the smaller the tilt angle, the smaller the vertical component. However longer rods, will result in a heavier and larger LOPES II. In the test cart we used a distance of 1 m and this seemed to work fine for subjects of various posture. Therefore we use this value for the design of the prototypes as well.

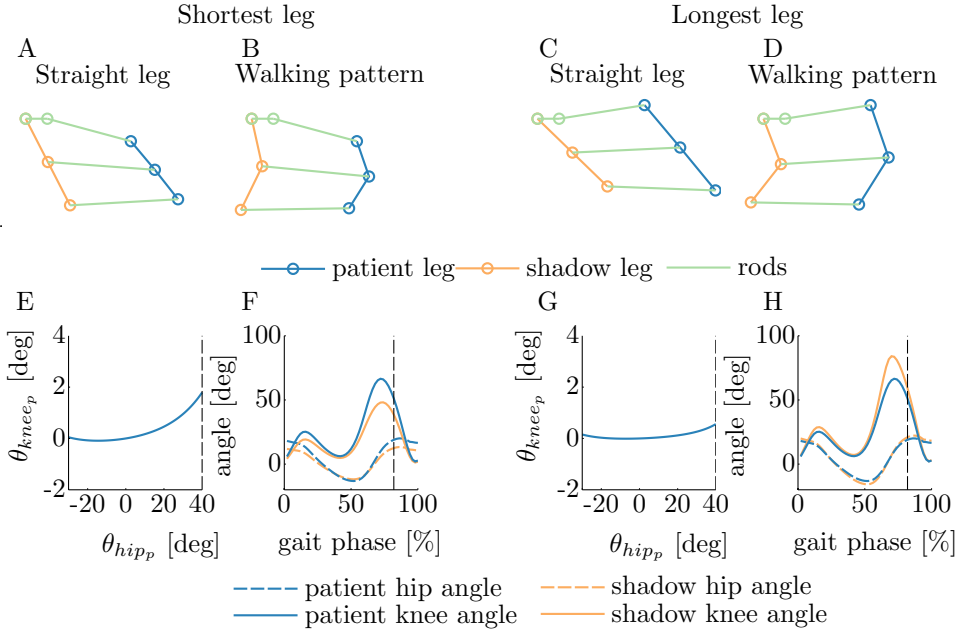


**Figure 7.2:** Relation between shadow leg angles and patient joint angles, depending on the segment length. Top: Two poses for the shortest leg (left) and for the longest leg (right): a straight shadow leg (A, C) (zero knee angle at maximum hip flexion) and pose at 82% of a normal gait cycle (B, D) (Winter, 1987). Bottom: the patient knee flexion angle ( $\theta_{knee_p}$ ) as a function of the hip flexion angle ( $\theta_{hip_p}$ ) when the shadow leg is maintained straight (E, G); and gait patterns of the shadow leg and the patient leg for normal gait (F, H).

For the length of the shadow thigh and shadow shank we use 450 mm. This is approximately 20 mm larger than the average thigh and shank length. For subjects with shank and thigh lengths larger than the shadow shank and thigh, the rotations of the shadow leg are larger than that of the patient leg. By approximation, if the patient thigh is 20% larger than the shadow thigh, the thigh rotation of the shadow thigh is 20% larger (see figure 7.2). We noticed with the test cart that singularities of the linkage may occur at large rotations. Therefore we chose to have a relatively large shadow leg to reduce its rotations and avoid singularities.

The relation between the shadow leg joint angles and the patient joint angles is non-linear (except for the rare case where the patient has equal segments lengths as the shadow segment lengths) (see figure 7.2). The shadow leg contains a mechanical end stop to prevent knee hyperextension.

The shadow leg, contains a physical end stop to prevent knee hyper extension (knee angle 0 deg), however, due to the non-linear kinematic relation, the *patient* knee flexion angle is not necessarily zero when the *shadow* knee flexion angle is zero. To prevent hyperextension at the patient knee, the knee rod is adjustable in length: during the donning, the rod length must be adjusted such that the maximum knee extension of the patient coincides with maximum knee extension of the shadow leg, i.e., when the end stop is reached. When this alignment is done in the standing pose (zero hip flexion), a zero shadow knee flexion will cause a patient approximately zero knee flexion ( $< 2$  deg) for all hip flexion angles, for all leg lengths (see figure 7.2 E and G). In other words, when properly set, the mechanical end stop at the shadow knee will have a similar effect as a mechanical end stop at the patient knee.

## 7.2 Decoupled Linkages

In the concept of the test cart (see section 4.4) each lever (actuator) is coupled to the translation or rotation of one segment. In the test cart there the coupling between the DoFs is small, e.g., rotation of actuator for pelvis AP causes only little rotation of other patient's segments. The main advantage of this decoupling is that it simplifies the kinematic transformation from actuator / sensor angles to segment angles and positions. A disadvantage is that it requires extra links to achieve proper decoupling (see figure 7.3a). When coupling is allowed, the linkage becomes simpler (see figure 7.3b,) however it requires a larger software effort to calculate the kinematics. Additionally, the coupling may introduce coupled dynamic behavior, which in its turn, may raise a challenge in control. Finally the coupling may have a negative impact on the RoM: if a patient DoF rotates due to coupling, its main actuator must have a larger RoM to ensure that the patient has sufficient RoM for all combinations of DoFs. Therefore we aim to have the linkages decoupled as far as possible, since this is estimated having the lowest risk, despite the extra number of parts needed compared to a coupled linkage.

In the following sections we define the linkages per DoF.

### 7.2.1 Thigh Sagittal and Frontal Rotation

For the thigh sagittal rotation we use a C40 with an average gearing of  $\frac{2}{3}$ . This way the continuous actuator torque of 40 N m results in a 60 N m



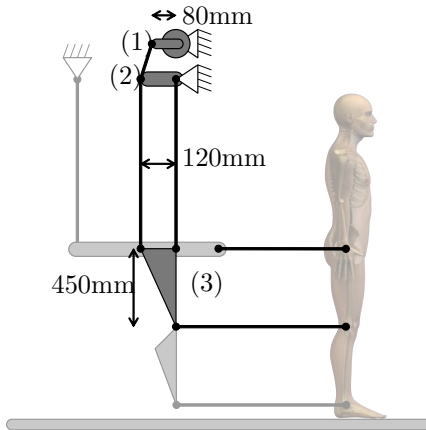


**Figure 7.4:** A C40 actuator (1) is attached to a lever (2) with a gearing of  $2/3$ . From this lever a vertical rod is connected to the shadow thigh (3).

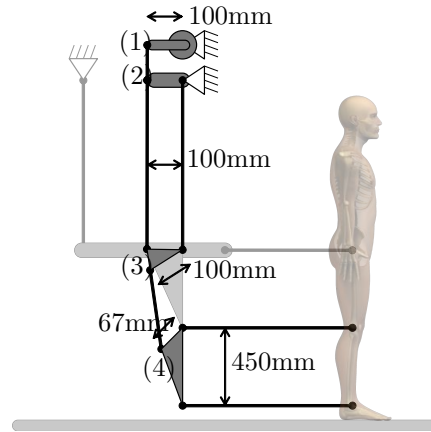


**Figure 7.5:** A C100 actuator (1) is attached to the shadow leg (4) with two levers (2) (3) and three rods. The linkage is parallel (gearing ratio of 1) from (1) to (3); the linkage from (3) to the shadow shank (4) has a gearing is  $3/2$ .

shank contains parallel linkages only. However, the range of motion of the shank is that large, that levers may come close to singular points. Therefore we implement the gearing between the shadow shank and the lever at the shadow hip (see figure 7.5).

### 7.2.3 Foot Sagittal Rotation

For the foot sagittal rotation we use a C100 actuator with an average gearing of  $3/2$ . An actuator speed of 5.2 rad/s results in 7.8 rad/s at the shank. This is insufficient to achieve the required speed of 9 rad/s. In the prototype we will study how this under achievement will affect the usability of LOPES II and if we should change the gearing or use a bigger motor. The actuator peak torque of 200 N m results in a torque of 133 N m at the shank. For a perfect decoupling, the linkage from the top of the frame to the shadow shank contains parallel linkages only. Therefore we implement the gearing in the vertical rods from the shadow pelvis towards the lower triangle of the linkage (see figure 7.6).

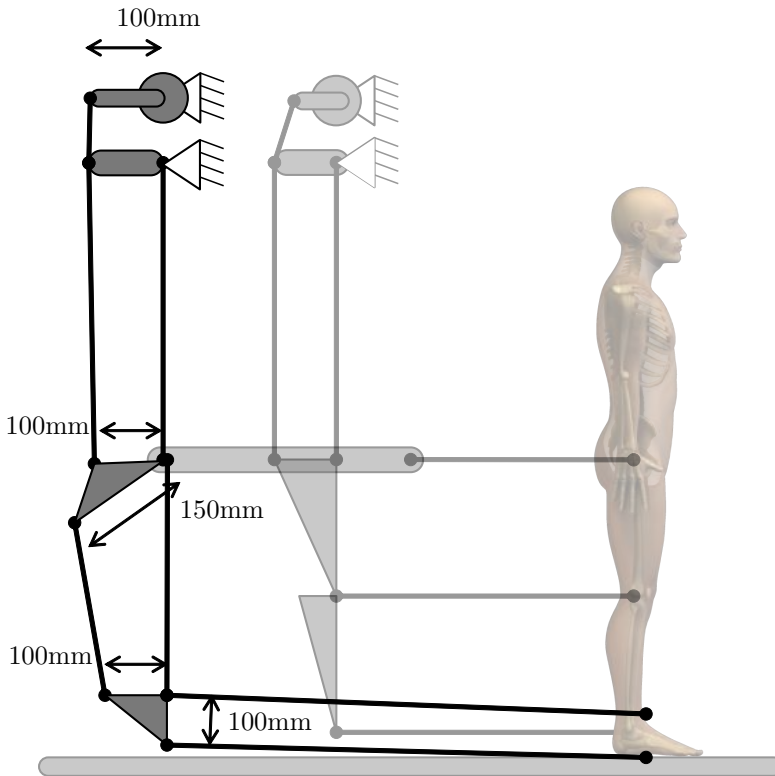


**Figure 7.6:** A C100 actuator (1) is attached to a lever (2), which is connected to a second lever (3) with a gearing of  $\frac{3}{2}$ . From this lever a vertical rod is connected to a triangle (4), which is connected to a foot bracket with two horizontal rods.

#### 7.2.4 Pelvis XZ Stage

We developed a parallel mechanism with two grounded actuators that has a nearly rectangular workspace and is very light weight (see Appendix E). It is based on the Evans linkage that approximates the movement of a straight line. This mechanism is extended with a second degree of freedom, resulting in a 2DoF manipulator.

##### Evans

The Evans mechanism is a ‘nearly straight line linkage’ i.e., a mechanical linkages of which the end effector point moves in a nearly straight line. Point E in figure 7.7 approximates a straight line as lever  $l_1$  rotates. Ideally point D moves horizontally only. This is achieved by making  $l_2$  as long as possible.

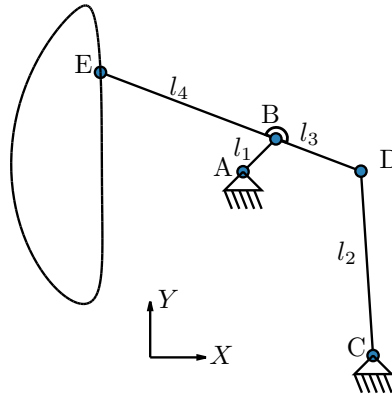


**Figure 7.7:** Straight-line approximation with the Evans-linkage. The right side of the trajectory of point E approximates a straight line.

The optimal relation between  $l_1$ ,  $l_2$  and  $l_3$  is calculated as follows. Consider the mechanism in a starting condition where points A, B, D and E are along the x-axis. For any rotational velocity of the links, the x-component of the velocity of point E is zero for the starting condition. Now select the linkage length such that the x-component of the acceleration of point E is zero as well.

$$\begin{aligned}\ddot{x}_E &= \omega_{l_3}^2 l_4 - \omega_{l_1}^2 l_1 \\ &= 0\end{aligned}\tag{7.1}$$

The rotational velocities of  $l_1$  and  $l_3$  around the starting condition are linearly related by approximation

$$l_1 \omega_{l_1} = l_3 \omega_{l_3}\tag{7.2}$$

Substitution of (7.2) in (7.1) results in:

$$l_4 l_1 = l_3^2\tag{7.3}$$

### Concept of the mechanism

The straight line approximation of the Evans linkage can be used for the forward/backward motion of the pelvis in LOPES II. The length of the rods are selected such that point E lies between point A and D (see figure

7.8a). Segment E-D is actuated in rotation, e.g., by a rotary actuator with push-pull rod.

Now we put point A on an actuated lever instead of the fixed world (see figure 7.8b). This way point A can move sideways and consequently the end effector moves sideways. The resulting workspace of point E has a rectangle-like shape.

For LOPES II it is desirable that the end effector is locked in rotation. Therefore the mechanism is doubled (see figure 7.8c). Around the mid-position (both actuator levers pointing in the lateral direction), actuator one (act1) only causes pelvis displacement in forward direction and actuator two (act2) only in lateral direction. This results in a workspace that is rectangle-like.

## Rectangular Manipulator Applied in LOPES II

The concept of rectangular manipulator has been applied in LOPES II on the actuation of the pelvis in anterior/posterior (AP) direction and mediolateral (ML) direction (see figure 7.9). The end effector is suspended from the frame (not shown in figure 7.9a). The end effector is connected to the pelvis of the subject.

### 7.2.5 Coupling

The workspace of the PRM with the dimensions as described in figure 7.9b for motor angles of  $\pm 1$  rad results in a largely rectangular workspace of the end effector (pelvis) of  $\pm 250$  mm in AP direction and  $\pm 150$  mm in lateral direction (see figure 7.10). The workspace indeed is of rectangular shape, and largely meets the required range of motion (see table 5.2). Near the corners of the workspace, the grid becomes askew, indicating coupling between the degrees of freedom.

## 7.3 Short Skewed Axis Gimbal at Ankle & Hip

### 7.3.1 Description

The concept of the short skewed axis gimbal applied to the hip and ankle is described in section 4.3.3 and Appendix F. This section describes the calculation of the workspace in relation to the gimbal main dimensions.

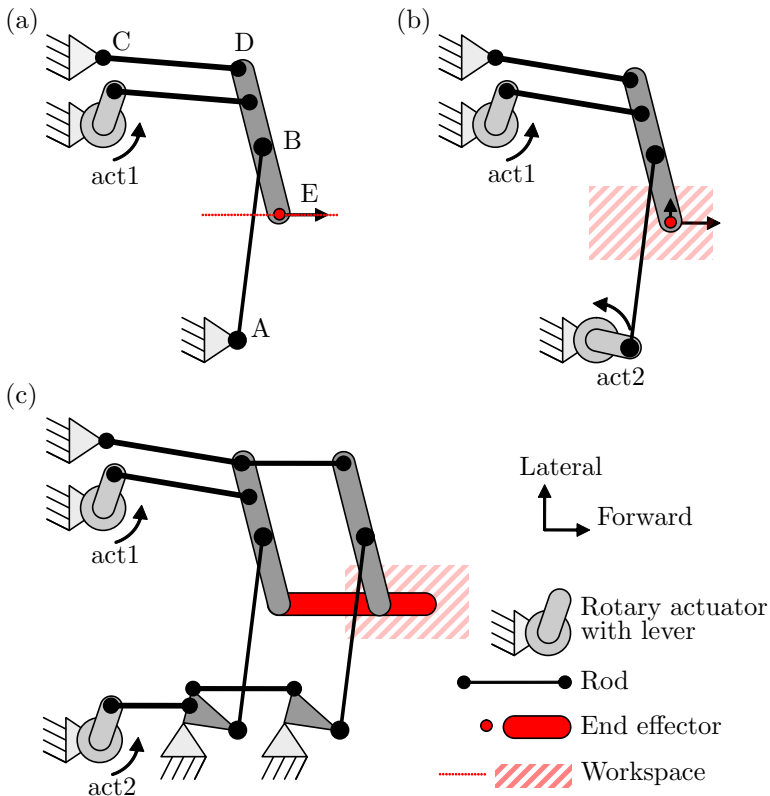


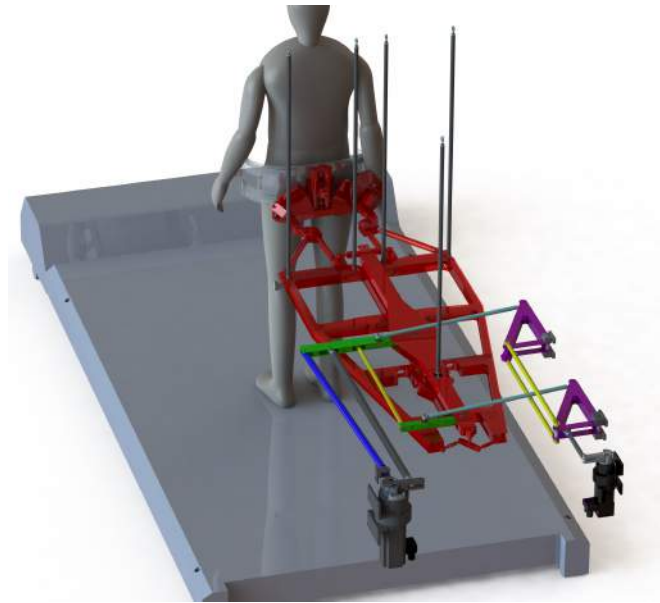
**Figure 7.8:** The Evans mechanism extended to a parallel rectangular manipulator (PRM) for horizontal pelvis manipulation. The 1DoF Evans with actuation (a); the Evans mechanism extended to two actuated DoFs; the mechanism with two actuated DoFs and locked rotation (c).

Subsequently dimensions for both the hip gimbal and ankle gimbal are given.

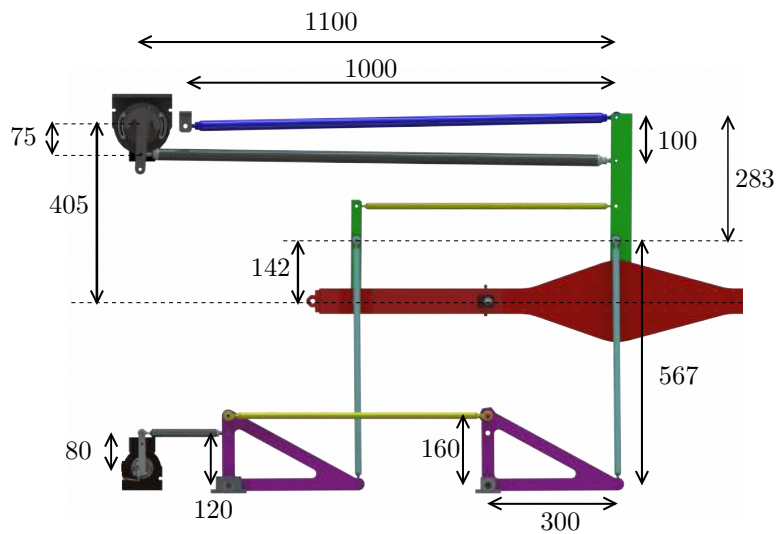
The short skewed axis gimbal consists of a base, two arched segments and an end effector. The four elements are connected with revolute joints; all three joint axes intersect in one point i.e., the remote centre (see figure 4.5).

### 7.3.2 Dimensioning a Short Skewed Axis Gimbal

This section gives the dimensioning guidelines for the gimbal. The main dimensions of the gimbal are the angles of the arched segments and the radii of the segments. Only the angles of the arched segments are relevant



(a)



(b)

**Figure 7.9:** Pelvis AP and ML actuation in LOPES II with PRM. (a): 3D representation. (b): Top view with dimensions in mm.

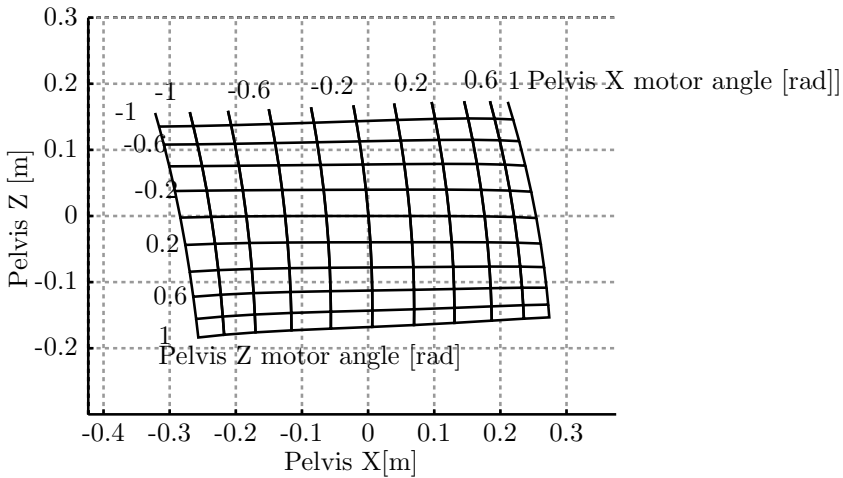


**Figure 7.10:** Workspace of the PRM as used in LOPES II. The grid shows the end effector positions for combinations of motor angles.

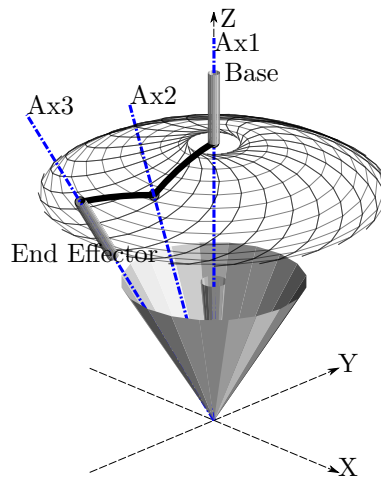


**Figure 7.11:** Example of short skewed axis gimbal with a 20 deg segment (between Ax1 and Ax2) and a 15 deg segment (between Ax2 and Ax3).

for the workspace calculation. We will use an example gimbal with a first segment of 20 deg and a second segment of 15 deg (see figure 7.11).

Align the first axis of the gimbal (Ax1) with the axis that requires the largest range of motion. In the example we will assume this is the Z-axis (see figure 7.11). Then the third axis (Ax3) will move between two cones:

the outer cone having a top angle of  $20 + 15$  deg and the inner cone having a top angle of  $20 - 15$  deg.

At the edges of the workspace for Ax3 i.e., on the cones, the angle between the two segments is 0 deg for the inner cone, and 180 deg for the outer cone. On these edges, the gimbal is in singular position, or gimbal lock, i.e., of the original three rotations only two rotations are available. A special case is when the angles of both segments are equal. Then the inner cone is reduced to a line coinciding with Ax1. Note that in this case the gimbal is also in gimbal lock when the Ax3 is coinciding with Ax1.

In the example the range of motion of the gimbal is infinite for rotation about the Z-axis (coinciding with Ax1). For rotation about the X-axis and Y-axis, the range of motion is  $\pm 35$  deg, but there is a nearly circular dependency between these rotations. Furthermore it should be noted that in the example, there is a ‘dead zone’ (the inner cone) of 5 deg, implication that it not possible to have 0 deg for both X rotation and Y rotation simultaneously.

### 7.3.3 Hip Gimbal

For the pelvis the following rotation ranges of motion are given: pelvis sagittal rotation range  $\pm 6$  deg; pelvis frontal rotation range  $\pm 10$  deg; and pelvis axial rotation range  $\pm 15$  deg (see table 5.2). In the test cart we defined that the pelvis gimbal consists of two hip gimbals that have the center of rotation in the hip joint. Furthermore the gimbals are located behind the patient (see figure 4.9b).

For the primary axis of rotation for the hip gimbal we chose the frontal rotation (along the axis of walking direction). Extra sagittal rotation of the gimbal is required because the primary axis is tilted due to different patients size (see figure 7.1). The hip height varies from 0.715 m to 1.228 m. Therefore the orientation of primary axis ranges from  $-20.9$  deg for the shortest patient to  $16.6$  deg for the tallest patient. For the hip gimbal the required range of motion in sagittal rotation ranges from  $-26.9$  deg to  $22.6$  deg.

We choose to use 17 deg for both segments. For the third axis we use an offset of 12 deg for transversal rotation, to assure that the singular point is close to the edge of the required workspace (see figure 7.12a).

In the detailed design the whole gimbal was rotated along the vertical axis with 10 deg to avoid collisions. This has a negligible effect on the calculations in range of motion (see figure 7.12b).

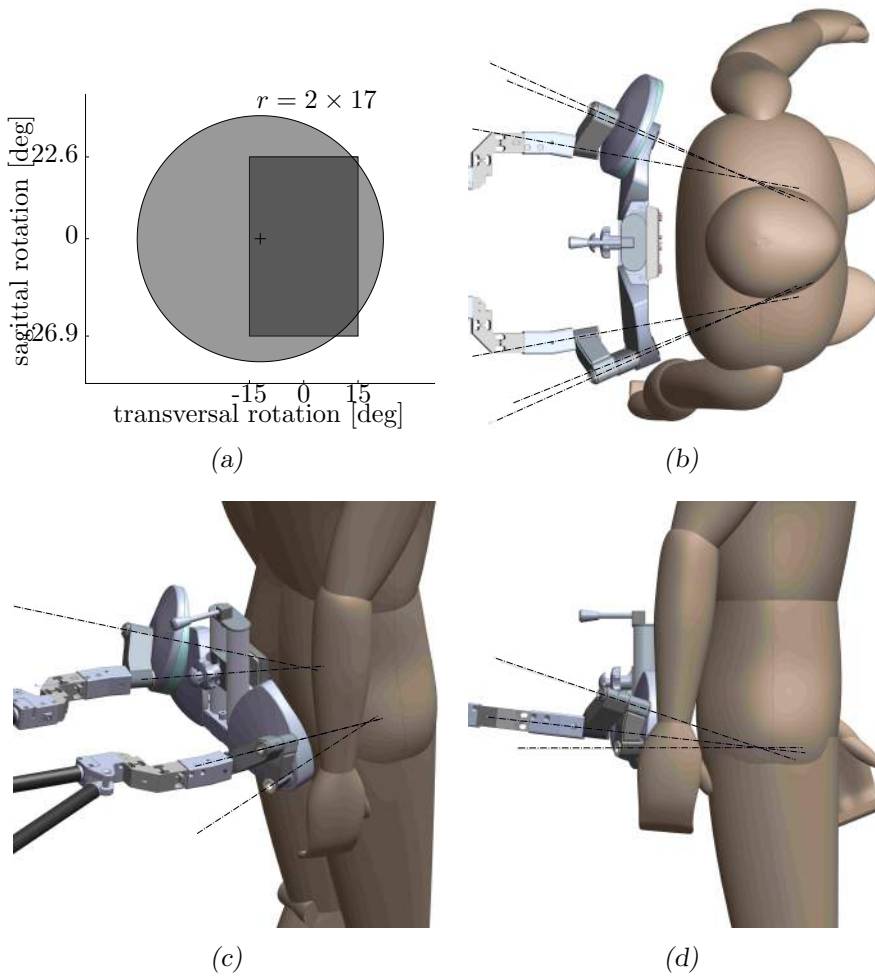


**Figure 7.12:** Short skewed axis gimbal for the hips. (a): Required (rectangle) and realized (circle) workspace for the right hip gimbal in transversal and sagittal rotation. (b): Topview. The primary axis of the hip gimbal is rotated with 10 deg to avoid collisions. (c): Perspective view. The left hip gimbal has a protective cap to prevent finger trapment. On the right hip gimbal this cap is hidden for clarity. (d): Side view. The displayed subject is of average stature, therefore the hip rods are tilted downwards slightly.

### 7.3.4 Ankle Gimbal

For the ankle gimbal the primary axis is the axis of plantar / dorsiflexion, since this requires the largest range of motion 134 deg. The foot inver-

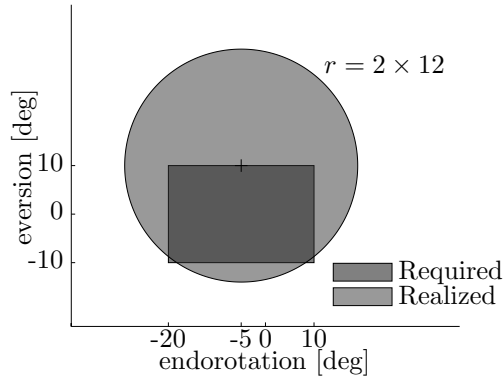


**Figure 7.13:** Required (rectangle) and realized (circle) for ankle gimbals endo-/exorotation and inversion/eversion.

sion requirement is 10 deg and preferably limited to that value in order to prevent collapse. The foot eversion requirement is 10 deg. For foot endo-/exorotation the required rotation is from 10 deg endorotation to 20 deg exorotation.

For the ankle gimbals we tilted the third axis (connected to the foot bracket) (see figure 4.5a) such that the inversion of the foot is limited to 10 deg (see figure 7.13). The third axis also has an offset of 5 deg in the transversal in exorotation to maximize the endo-/exorotation workspace.

## 7.4 Mechanical Design Summary & Analysis

A CAD design of the full LOPES II (excluding plates and railing) is given in figure 7.14. The linkage and actuation for the pelvis and right leg is given in figure 7.15.

### 7.4.1 Physical Mass

In this section we do an analysis of the physical mass of the moving parts of LOPES II. According to (Colgate and Hogan, 1989) passivity of a force controlled system is only guaranteed when the controller inertia (which is perceived by the user) is at least half the physical inertia. An analysis of the physical inertia will give us an indication of the minimal impedance that can be achieved with this mechanical structure. We analysed the CAD design on the physical mass between actuator and force sensor and between force

sensor and patient reflected. The requirements for the minimal impedance are defined at joint translations and foot rotation, therefore we calculate the physical inertias in this frame (see table 7.1).

**Table 7.1:** Reflected mass of the linkage between actuator and force sensor (I) and force sensor and patient (II), at joint displacement (in kg) and foot rotation (in  $\text{kgm}^2$ ). For Pelvis Z the inertia is similar to Pelvis X. For comparison the total allowable mass, as stated in the user requirements (see table 5.3), is added (III). Furthermore the examined the impact of the removal of the foot RZ linkage on the mass reflected on the ankle translations (column “Reduced”).

		Original (with Foot RZ)					Reduced (No Foot RZ)	
		Pelvis X [kg]	Knee X [kg]	Ankle X [kg]	Ankle Z [kg]	Foot RZ [ $\text{kgm}^2$ ]	Ankle X [kg]	Ankle Z [kg]
<b>I</b>	Actuators	1.78	0.84	0.40	0.21	0.08	0.40	0.21
	Pelvis stage	19.12						
	Foot RZ linkage	0.54		1.92	1.71	0.01		
	Shadow leg	1.87	1.65	0.66	2.09		0.66	2.09
	Other	2.72	1.31	0.95	1.31	0.01	0.95	1.31
	<b>Total</b>	<b>26.03</b>	<b>3.80</b>	<b>3.92</b>	<b>5.31</b>	<b>0.10</b>	<b>2.00</b>	<b>3.61</b>
<b>II</b>	Clamps	3.60	0.68	1.90	2.13	0.02	0.69	0.92
	Foot RZ Linkage			0.70	0.92	0.00		
	<b>Total</b>	<b>3.60</b>	<b>0.68</b>	<b>2.60</b>	<b>3.05</b>	<b>0.02</b>	<b>0.69</b>	<b>0.92</b>
	<b>III Allowed</b>	<b>6</b>	<b>4</b>	<b>2</b>	<b>2</b>	<b>0.006</b>	<b>2</b>	<b>2</b>

When examining the masses at the joints and the CAD drawings of the linkages (see figure 7.16 and 7.17) it becomes clear that the pelvis stage (see figure 7.9) forms the main component of inertia for the pelvis translation. When obeying the passivity rules as stated by (Colgate and Hogan, 1989), the virtual mass at the pelvis will be higher than the desired 6 kg. This will be examined in section 9.4.3.

Furthermore it becomes clear that the linkage for the foot rotation (plantar / dorsiflexion) adds a considerable mass in the direction ankle transla-

tion, both between actuator and force sensor and between force sensor and patient. For the zero impedance mode the maximum mass that the patient is allowed to perceive at the ankle is 2 kg (see table 5.3). The clamps (foot-bracket) are heavier than the required value. Removing the linkage for the foot rotation would result in a considerably lower mass of the clamps and also between the force sensor and actuators (see table 7.1) (see figure 7.18). In this stage LOPES II will be equipped with the linkage for foot rotation. In the evaluation phase we will examine whether control strategies may be able to realize an acceptable the perceived mass.

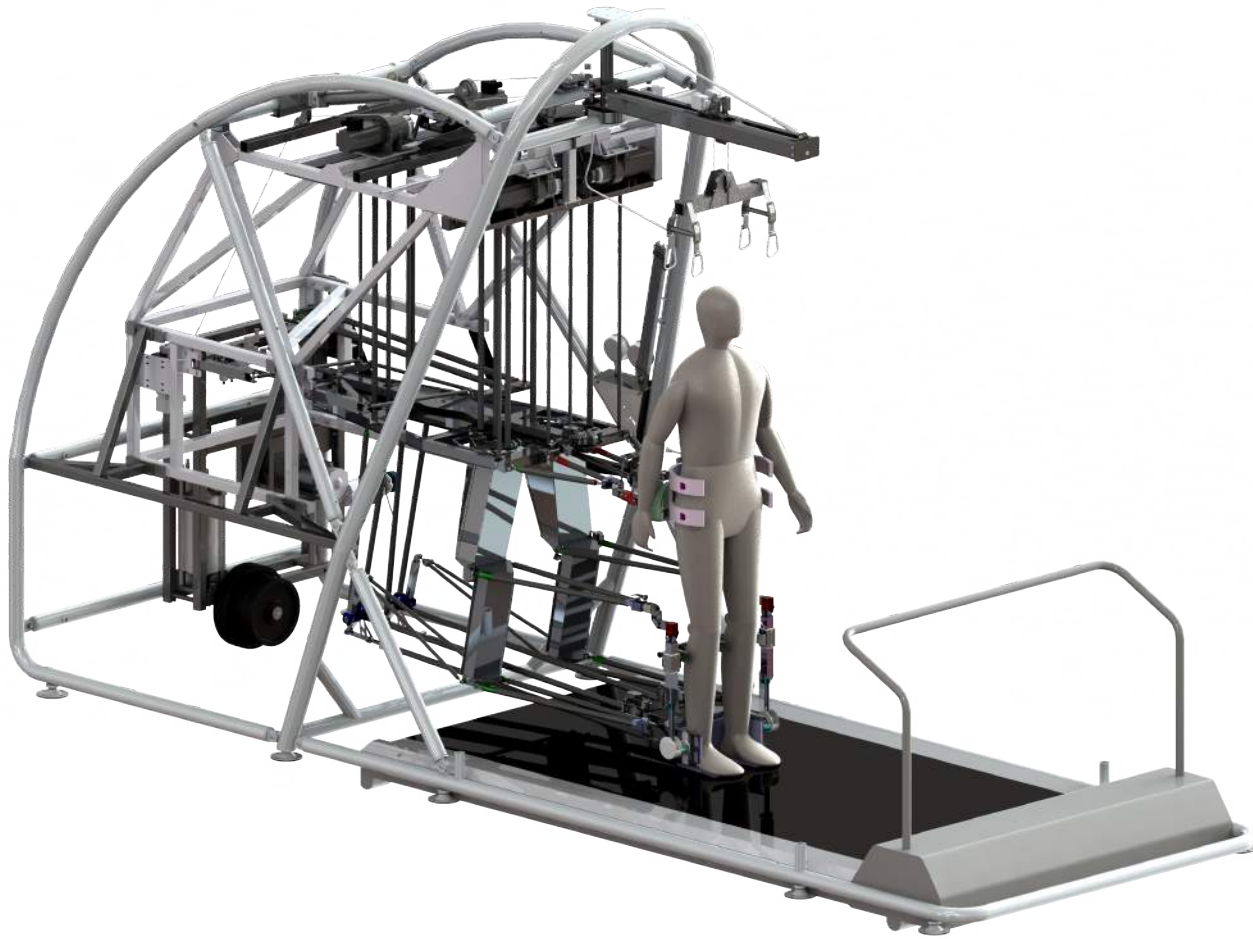


**Figure 7.14:** CAD design of LOPES II with frame (side railing and cover plates on frame are hidden for clarity)

### 7.4.2 Range of Motion

In a motion simulation of the CAD model we verified that most desired ranges of motion can be met regardless the stature of the patient. In this section we will discuss a the ranges of motions that are smaller than required.

The pelvis anterior / posterior motion has been reduced from  $\pm 0.3$  m to  $\pm 0.18$  m, since several collisions occurred in the area of the shadow hips when the pelvis was put in maximum forward or backward position (see figure 7.19a). This reduction of RoM may result in patients reaching the limits of pelvis anterior / posterior motion during walking, and thus consequently limiting their freedom.

A second limitation occurs for the tallest subjects only. The rotation of the knee flexion is limited to 65 deg. When the subject would make a larger rotation knee flexion, the shadow knee would flex more than 90 deg resulting in singular situation when the knee and ankle rods (see figure 7.19b). Therefore we limited this rotation. The consequence is that when the tallest subjects walks fast in LOPES II, he may feel a limitation during swing when the knee flexion is larger than 65 deg, which in practice is quite rare.

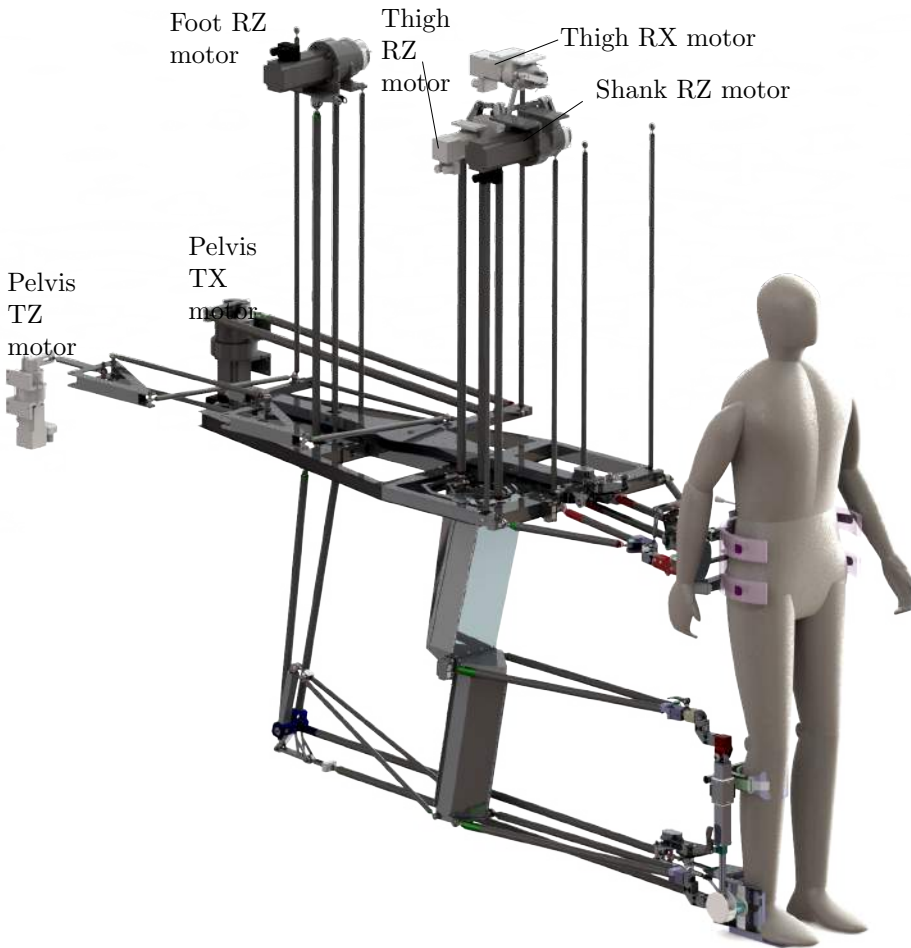
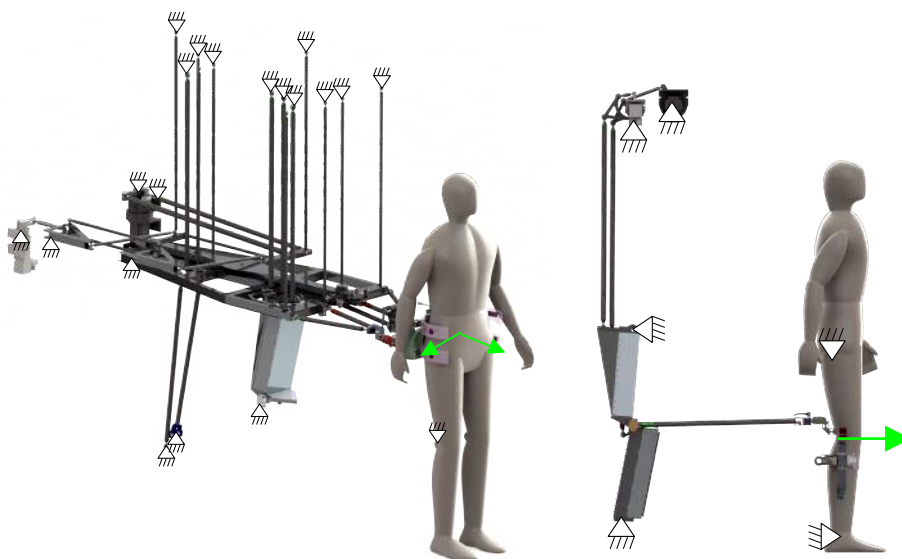
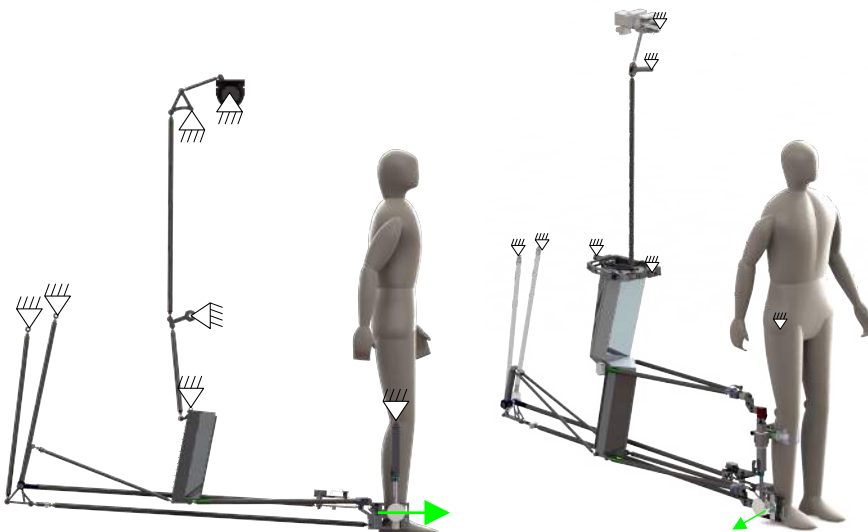


**Figure 7.15:** CAD design of the linkage and actuators for pelvis and right leg



(a) Moving components for pelvis translation (anterior/posterior and mediolateral). M1: 26 kg; M2: 3.6 kg

(b) Moving components for knee anterior/posterior. M1: 3.8 kg; M2: 0.7 kg



(c) Moving components for ankle anterior/posterior. M1: 3.9 kg; M2: 2.6 kg

(d) Moving components for ankle mediolateral. M1: 5.3 kg; M2: 3 kg

**Figure 7.16:** Linkage components that are related to inertia at joint translations. For each DoF the moving components are drawn. For analysis, the components that are not moving are fixed (ground symbol) The total mass between actuators and force sensor is denoted by M1; the mass between force sensor and patient is denoted by M2.

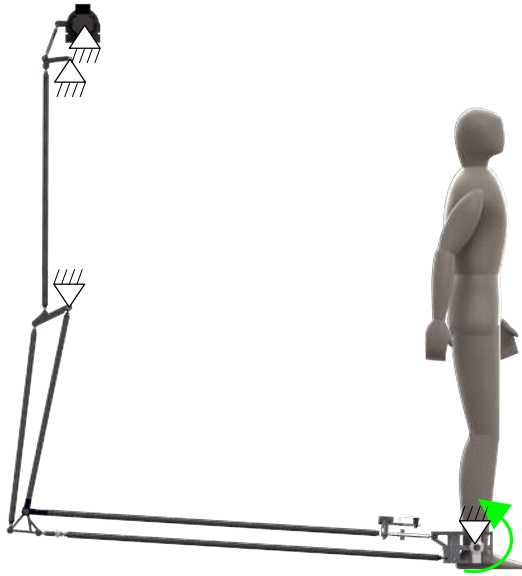
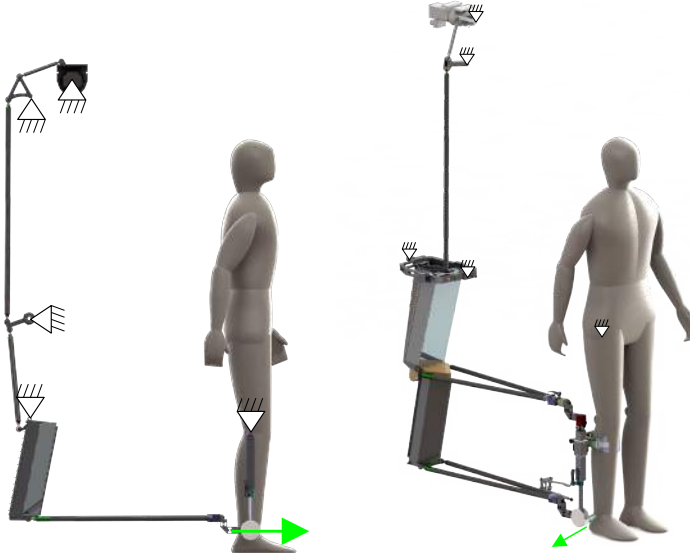


**Figure 7.17:** Linkage components that are related to inertia at foot rotation. The total mass between actuators and force sensor is  $0.1 \text{ kgm}^2$ ; the mass between force sensor and patient is  $0.02 \text{ kgm}^2$ .



(a) Moving components for ankle anterior/posterior. M1: 2.0 kg; M2: 0.7 kg

(b) Moving components for ankle mediolateral. M1: 3.6 kg; M2: 0.9 kg

**Figure 7.18:** Simplification of the mechanics when the mechanism for foot plantar/dorsiflexion is removed. The linkage is simplified and the mass is reduced compared to linkage with the plantar/dorsiflexion mechanism (see figure 7.16c, 7.16d).

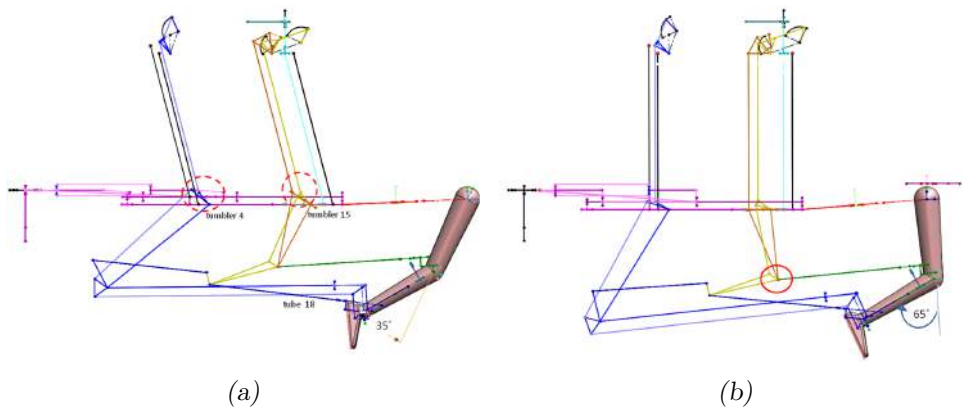


**Figure 7.19:** Critical configurations of the linkage. (a): linkage in near singular position when the pelvis is maximum forward. (b): linkage of shadow shank, knee rod and ankle rod in near singular position when the tallest subject makes maximum knee flexion.



# Controller Design

This chapter describes the design of the controller of LOPES II, and particularly the admittance controller. For LOPES II we chose an architecture containing three computers (see figure 8.1). The first computer is a Graphical User Interface (GUI) with which the operator can define the support and optimize the gait trajectory for the patient. In the GUI, the gait is divided in subtasks (see figure 3.1). Additionally the GUI gives graphical feedback to both the patient and the operator, and recorded data can be analyzed afterwards.

The Gait Trajectory Controller is responsible for translating the desired support to reference patterns for the patient segment angles and stiffnesses.

Finally the Admittance Controller is responsible for the motions and measured data of LOPES II. Additionally it monitors the safety of LOPES II.

This chapter elaborates on the controller components, particularly on the admittance controller.

## 8.1 The LOPES II Controller — An Overview of the Components

The LOPES II controller consists of several components (see figure 8.2). The components are mentioned below and elaborated on in the following sections.

LOPES II uses an admittance controller, consisting of a virtual mass

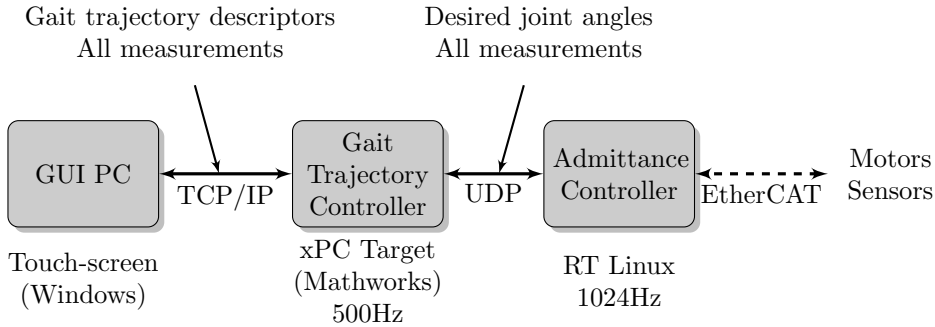


**Figure 8.1:** The three computers used for controlling LOPES II.

**Table 8.1:** Segment Coordinate System

	Short name	Description
1	Pelvis TX	Pelvis anterior / posterior translation
2	Pelvis TZ	Pelvis mediolateral translation
3	Left Thigh RX	Left leg frontal rotation
4	Left Thigh RZ	Left thigh sagittal rotation
5	Left Shank RZ	Left shank sagittal rotation
6	Left Foot RZ	Left foot sagittal rotation
7	Right Thigh RX	Right leg frontal rotation
8	Right Thigh RZ	Right thigh sagittal rotation
9	Right Shank RZ	Right shank sagittal rotation
10	Right Foot RZ	Right foot sagittal rotation

and a double integrator The virtual mass ( $M^{-1}$ ). It receives a force input vector of the renderer and the force sensors, and converts it to a vector of unlimited model acceleration ( $\ddot{x}^U$ ). Section 8.2 describes the background on admittance control, section 8.5 elaborates on the used mass model. The limiter adapt the model acceleration such that model acceleration, velocity and position stay within predefined boundaries (see section 8.7). The limited acceleration ( $\ddot{x}^L$ ) is integrated to velocity en position (see section 8.6).

Where the admittance model is a MIMO system, the motor controllers are SISO systems, i.e., the motor controllers receive scalar set points in terms of position, velocity and acceleration and the control of each motor is independent of the other motor controllers (see section 8.3).

The motors apply forces to the mechanical structure of LOPES II. The

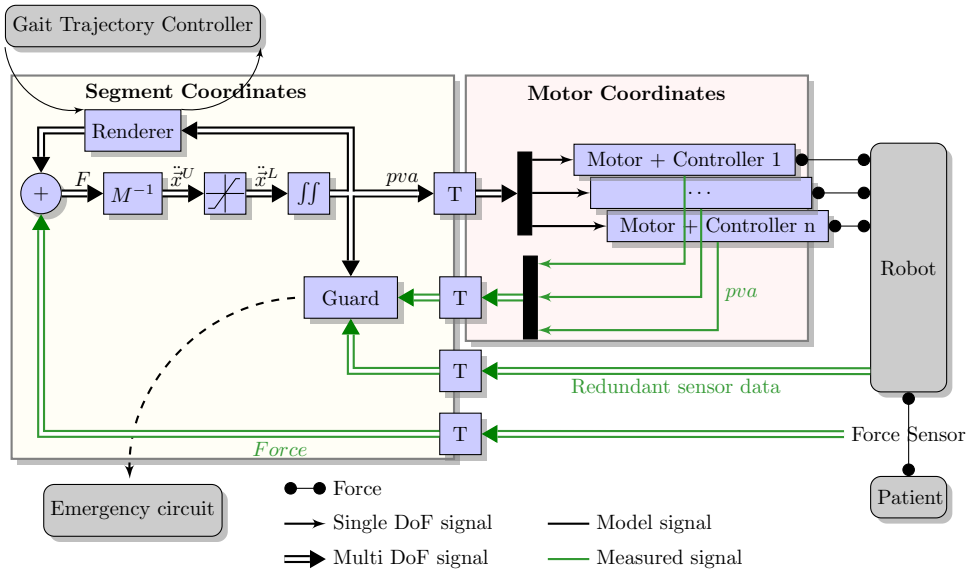


**Figure 8.2:** Controller layout of LOPES II and its relation with its peripherals. The gait controller sets the stiffnesses and positions for the guidance springs in the renderer, which calculates the supporting forces for the patient based on the spring positions and the measured positions. The sum of the renderer force and the measured force are the input for the virtual mass ( $M^{-1}$ ). The resulting model acceleration in segment coordinates ( $a^U$ ) is fed through a limiter to assure the model positions, velocities and accelerations (pva) stay within bounds. The model pva are transformed ( $T$ ) to motor coordinates to serve as set points for the individual motor controllers, which control the robot, which interacts with the patient. The guard triggers the emergency circuit if the errors between the measured pva and model pva, and the errors between measured motor angles with redundant sensor angle data.

patient also exerts forces on LOPES II, which are measured by the force sensor.

Throughout the controller positions, velocities and accelerations are transformed from one coordinate system to another. The mass model runs in segment coordinates (see table 8.1). The kinematic relation between patient segment coordinates and motor coordinates is non linear. This component is addressed separately in section 8.4.

The renderer is the component that applies virtual forces to the mass model, e.g., springs and dampers (see section 8.9). The settings for the

renderer (e.g., spring stiffness and positions) are determined by the gait controller (see section 8.10).

The guard compares model positions with the positions derived from the motor sensors and with the positions derived from the redundant position sensors in the linkage (see figure 6.3). When differences exceed predefined thresholds, the emergency circuit is triggered to stop the system (see section 8.8).

## 8.2 Admittance Control

### 8.2.1 Theory & History

In this thesis we use the following definition for an admittance controller:

*A real time controller that uses operator force (measured by the haptic interface) and virtual forces (generated by a virtual environment), as an input on a virtual mass, to calculate a desired displacement of the haptic interface.*

First records of admittance control go back to 1977. Whitney (1977) was the first to publish a control scheme in which a measured force is used in combination with a double integrator to obtain a desired controller position. In the 1983 patent by Fokker Aircraft, the admittance control is applied to flight simulations (Lam and De Vries, 1983). In the 1980's numerous publications describe admittance control (Maples and Becker, 1986; Hirabayashi et al., 1985; Colgate, 1989), however the term “Admittance Control” was first coined by Glosser and Newman (1994).

Using the admittance model in a closed loop requires a servo loop and force sensors (see figure 8.3). If the servo loop (robot) has a sufficiently high bandwidth, then the operator perceives an admittance controlled device as a free floating mass. A lower virtual mass means that the robot will respond faster to an input force, i.e., the loop gain is higher. A limitation of admittance control is contact instability. In high environment impedances ( $Z^H$ ) e.g., stiff walls, a displacement leads to a high force, which is amplified by the virtual mass to larger displacement. This may lead to instability. Therefore, for a high environmental impedance requires a high virtual mass to maintain stability, however this implies a lower transparency (see figure 8.5).

The opposite of admittance control is impedance control (Hogan, 1984) (see figure 8.4), where measured displacement is used by the controller to

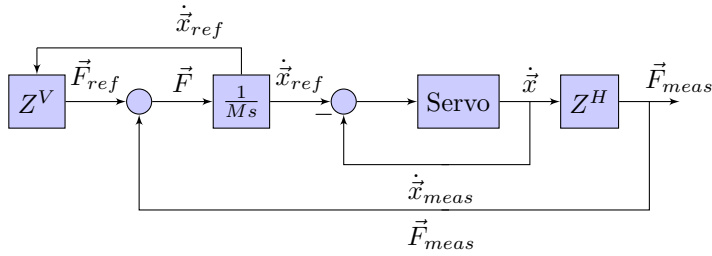


**Figure 8.3:** Admittance control scheme. A virtual impedance ( $Z^V$ ) generates a reference force that is converted to a model acceleration by means of a virtual mass  $M$ . The acceleration is integrated to model velocity, which serves as a setpoint for a servo controller.  $Z^H$  represents the environment impedance of which the interaction force is measured and fed back to the input force.

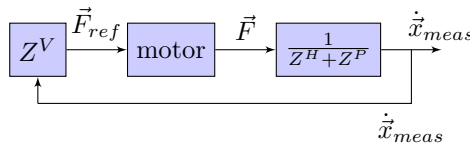


**Figure 8.4:** Impedance control scheme. A virtual impedance ( $Z^V$ ) generates a reference force that is commanded to a torque actuator. The actuator is connected to the robot impedance ( $Z^P$ ) and the environment impedance ( $Z^H$ ).

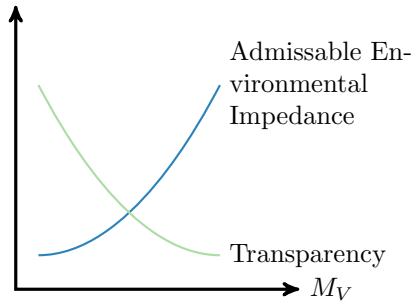


**Figure 8.5:** The trade-off for Admittance Controllers: high transparency requires a low virtual mass, but interaction with high impedance environments (high stiffness) requires a high virtual mass to maintain stability.

calculate a desired force. Admittance control and impedance control are opposing (Lammertse, 2009): a zero gain in admittance control (virtual mass is infinite) means zero displacement and therefore an infinite impedance,

whereas a zero gain in impedance control (zero virtual impedance) implies zero force and therefore only the impedance of the passive device. On the other hand, a high gain in admittance control is achieved by a low virtual mass, and for the impedance controller a high gain corresponds with a high virtual impedance. High control gains lead to instability in both admittance control and impedance control: for impedance control, the smallest measurement displacement should be responded with a high force in order to represent a high stiffness; for admittance control, the smallest force should result in a large displacement in order to display a low inertia. This means that both control paradigms have their limitations on their range of impedance, i.e., Z-width (Colgate and Brown, 1994): for impedance control the control gain sets the upper bound of the Z-width, for admittance control it sets the lower bound of the Z-width.

The lowest impedance for an impedance controlled device as depicted in figure 8.4 is determined by the device impedance, since in pure impedance control, the control gain is zero. For small devices with backdrivable actuators the device impedance is usually low, but for larger devices, the user will perceive the device inertia, device weight, and joint friction. The maximum impedance for an admittance controlled device is determined by the stiffness of the device and the position / velocity loop, therefore a high stiffness, high gearing device with admittance control is capable of displaying an impedance that approaches infinity from the operators perspective. An important property of admittance control is that in the low impedance mode it displays a free floating mass that is perceived without friction (Maples and Becker, 1986) (see figure 8.6). The impedance perceived by the users consists of the virtual mass of the admittance controller and any impedance (e.g., inertia) between the force sensor and the user.

### 8.2.2 Applications

Admittance control is applied in several areas where a high Z-width is required, or when the haptic device is relatively large, or both. One area is the use of admittance control on industrial robots (Glosser and Newman, 1994; Mathewson, 1994; Maples and Becker, 1986; Whitney, 1977) to provide the bulky robots with sensitivity to perform more delicate tasks. In flight simulation the aircraft control must respond smoothly to only a few Newton in normal flight, yet in simulations of emergency situations, the controls must display high stiffness, and must be able to withstand the force of a pilot pulling with all his might. Admittance control has been applied

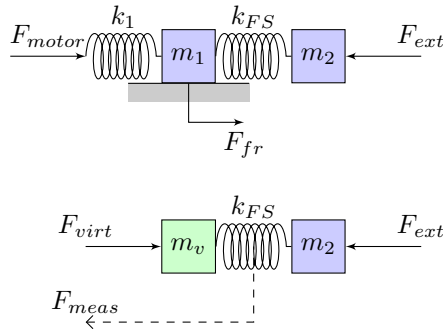


**Figure 8.6:** Free body diagram of robot (above). The robot contains compliance ( $k_1$ ), a force sensor ( $k_{FS}$ ) and inertias ( $m_1$  and  $m_2$ ). Force that apply on the robot are force from the actuator ( $F_{motor}$ ), an external force ( $F_{ext}$ ) e.g., by a human operator, and lastly, internal friction ( $F_{fr}$ ); The admittance controller (below) substitutes the mechanics by a floating virtual mass  $m_v$ .

in flight simulation for more than three decades (Lam and De Vries, 1983; MOOG, 2009). In the simulation of dental procedures it is important that the Z-width is high: the dentist in training must be able to move a burr in free air (no friction and damping), but when in contact with a tooth, he must perceive a high stiffness. The Moog Simodont Dental Trainer is a 3DoF admittance controlled device that displays, both graphically and haptically, the interaction of drilling in a virtual tooth (MOOG, 2014b). In rehabilitation the haptic devices for both the upper and lower extremity, often require a large workspace and therefore the device are often large. Admittance control offers a solution to display a low impedance for rehabilitation devices (Ozkul and Erol Barkana, 2011; Loureiro et al., 2003)

For LOPES II we chose admittance control. We expect that it is suitable to achieve a minimal impedance mode that is sufficiently transparent for free walking. We expect that the admittance controller can compensate for the expected friction in the actuators and linkage, and display an inertia of the DoFs of which the current physical mass (see table 7.1) is currently too high. Furthermore, we expect that the high impedance mode of admittance control is sufficient for the Robot in Charge mode (see UR02).

A challenge lies in the fact that the controller must be both transparent and stable. When a subject walks in LOPES II, the leg that is in stance phase is a high environmental impedance for the controller, i.e.,  $Z^H$  in figure 8.3 is high. This means that a small displacement of LOPES II results in a high force on the leg. This force is the input for the admittance mass

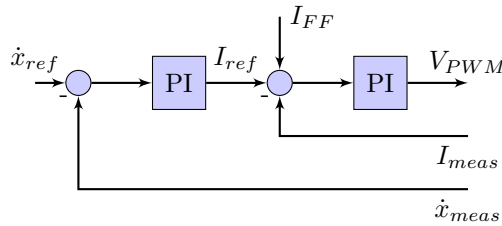


**Figure 8.7:** The control loop of the actuator. The inner loop is a proportional-integral (PI) loop on the current that generates a pulse-width-modulated voltage for the motor ( $V_{PWM}$ ); the outer loop is a PI loop on the velocity. Optionally a current feed-forward setpoint ( $I_{FF}$ ) can be added to the current loop.

(see figure 8.3). If the virtual mass is low (and the force loop gain is high), this may lead to instability of the admittance controller. Therefore, for the stance leg, a high virtual mass to maintain stability is required. A swing leg is a lower impedance for the admittance controller i.e., a displacement of LOPES II may cause interaction force, but not as high as when the leg is in stance. Therefore a higher loop gain (lower virtual mass) is possible for a swing leg (see figure 8.5).

### 8.3 Motor Controller

Each actuator is controlled by a MOOG Servo Drive (MSD) (MOOG, 2014a) (see section 6.3). The drive contains two PI control loops. The inner loop is a current loop, the outer loop is a velocity loop (see figure 8.7). The drive uses an 8kHz switching frequency for both the current loop and the velocity loop.

We tuned both loops with a step response, such that the response time is as fast as possible, with an acceptable overshoot. The actuators are first tuned without load (outside LOPES II) to get a reasonable starting point. When the actuators were placed in LOPES II, we checked the step response performance, and if needed we adjusted the parameters (see figure 8.8a). The pelvis TX actuator has the highest load (see table 7.1), therefore we made a bode plot of this actuator (see figure 8.8b). The velocity controlled actuators behave as a 1 ms time delay, i.e., the magnitude of the transfer is nearly unity, and the phase shift has a linear relation with the frequency:

$$\phi_\omega \approx \tau_{delay} \cdot \omega \quad (8.1)$$

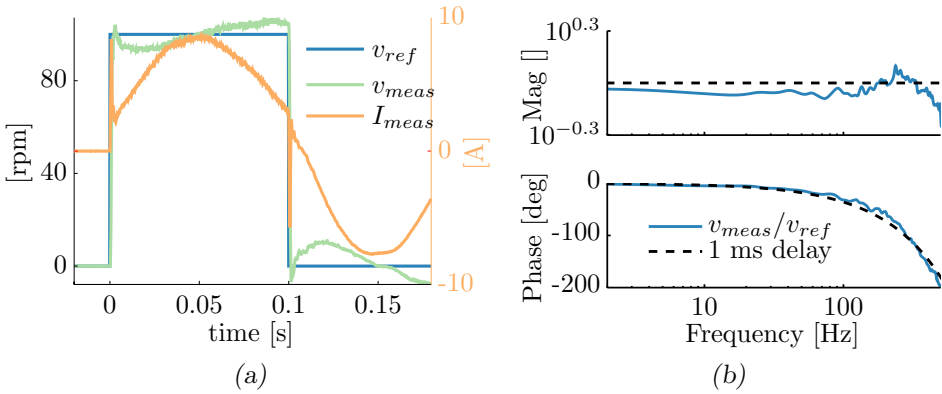


**Figure 8.8:** Tuning result for the pelvis TX actuator built in LOPES II, without a subject in it. (a): Step velocity response; (b): Bode plot of velocity loop (blue). The transfer function of the velocity loop matches the transfer of 1 ms time delay (black dashed line).

The current feed-forward in the actuator control loop (see figure 8.7) is not used, since this does not increase the performance of the velocity loop.

## 8.4 Kinematics Transformations

In the controller of LOPES II, the actuator setpoints in terms of position, velocity and acceleration (pva) are calculated from the segment pva, and the measured actuator pva is converted back to segment coordinates. Additionally sensor angles of the redundant sensors, located in the mechanical structures, are converted to segment pva. And finally the signals from the force sensors are converted to segment forces and torques.

This section discusses these transformations. LOPES II contains ten actuators and three additional sensors (height left hip, height right hip, and pelvis transversal rotation) to calculation the thirteen DoF state of the patient. For most parts in the linkage the transformation is straightforward. The angle from one lever can be calculated from another lever (see figure 8.9a) with simple trigonometry (Meuleman et al., 2013)

For several subsystems of the LOPES II linkage there is interdependency between various states e.g., the transformation from shank motor to shank RZ angle depends on the thigh RZ angle (see figure 7.5). In this particular problem it suffices to first calculate the thigh pva, and then the shank pva.

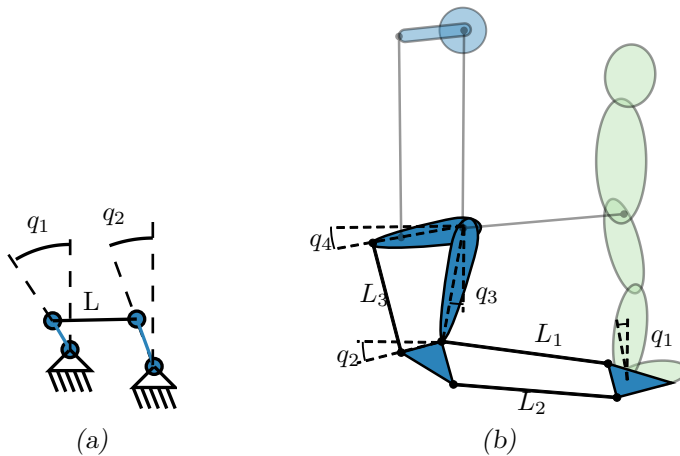


**Figure 8.9:** Linkage examples. (a): a simple two-lever linkage with one degree of freedom and a non linear coupling between  $q_1$  and  $q_2$ ; (b): a more complex linkage with a non linear coupling between a given lever angle ( $q_4$ ) and the output angle i.e., patient foot angle ( $q_1$ ).

This way we calculate the segment pva from motor pva (and vice versa) through solving one DoF linkages.

Some subsystems contain interdependency of two or more states (angles or positions) and thus the transformation is more complex. As an example we use the foot RZ linkage (see figure 7.6). A schematic overview of part of this linkage is given in figure 8.9b . For the backward kinematics i.e., the calculation of the motor angles from end point (patient) angles, is a simple chain of two-lever linkages. However the forward kinematics i.e., the calculation of the foot angle from the given motor angles, is more complex. Therefore we use a numerical, iterative method to solve both the forward kinematics.

### 8.4.1 Degrees of Freedom

Like any mechanism LOPES II contains bodies and joints, but we identify the rod as a special kind of body. The rod consists of tubular body with a spherical joint at one end and one spherical joint or cardanic joint at the other end. The usage of rods is primarily driven because of the high stiffness and strength relative to their weight.

We start by temporary removing the rods. Then the system will have

a set of  $N$  DoFs denoted by  $q$ .

$$\vec{q} = \{q_1, \dots, q_N\}^T \quad (8.2)$$

This set of DoFs contains translations and rotations of all bodies. In the example  $N = 4$ . The system contains a  $M$  rods:

$$\vec{L} = \{L_1, \dots, L_M\}^T \quad (8.3)$$

Since each rod removes one DoF of the total set of DoFs, the mechanical structure with the rods, has  $(P = N - M)$  independent DoFs. In the example  $M = 3$  and thus  $P = 1$ . We define the input states  $\vec{x}$  as a subset of  $\vec{q}$ , of length  $P$

$$\vec{x} = \{x_1, \dots, x_P\}^T \quad \vec{x} \subset \vec{q} \quad (8.4)$$

Provided that there are no singularities, the structure is statically determined when  $\vec{x}$  is provided. The remaining components of  $\vec{q}$  are the driven states, complementary to  $\vec{x}$ . This set is called  $\vec{y}$  and is of length  $M$ .

$$\vec{y} = \{y_1, \dots, y_M\}^T \quad \vec{y} \subset \vec{q} \quad (8.5)$$

Note that in case of forward and backward transformations, as in the example, we are only interested in the a subset of the driven states i.e., the output states  $\vec{z}$ . In this section we define the output states as a subset of  $\vec{y}$ , of the same length as  $\vec{x}$ .

$$\vec{z} = \{z_1, \dots, z_P\}^T \quad \vec{z} \subset \vec{y} \quad (8.6)$$

In the example in case of the forward transformation,  $\vec{x} = q_4$  and  $\vec{z} = q_1$ ; for the backward transformation,  $\vec{x} = q_1$  and  $\vec{z} = q_4$ .

Note that, in the used example, for the forward transformation the input vector  $\vec{x}$  consists of  $q_4$ ; the remaining DoFs form the vector  $\vec{y}$  For the backward transformation  $\vec{x}$  consists of  $q_1$ .

The question is how the driven position ( $\vec{y}$ ), velocity ( $\dot{\vec{y}}$ ), and acceleration ( $\ddot{\vec{y}}$ ) are related to the input position ( $\vec{x}$ ), velocity ( $\dot{\vec{x}}$ ), and acceleration ( $\ddot{\vec{x}}$ ).

$$\vec{y} = f_p(\vec{x}) \quad (8.7a)$$

$$\dot{\vec{y}} = f_v(\vec{x}, \dot{\vec{x}}) \quad (8.7b)$$

$$\ddot{\vec{y}} = f_a(\vec{x}, \dot{\vec{x}}, \ddot{\vec{x}}) \quad (8.7c)$$

where  $f_p$ ,  $f_v$ ,  $f_a$  and  $f_f$  are the unknown functions for position, velocity, and acceleration. Furthermore, we are interested in the force relation between input and output:

$$\vec{F}_z = f_f(\vec{x}, \vec{F}_x) \quad (8.8)$$

### 8.4.2 Virtual Rod Elongation

The relation between a change of the state and a change in the points is defined by trigonometry. We will not go into detail on the trigonometry. For each point the linearized relation between state and point is:

$$\Delta \vec{p}_i = \frac{d\vec{p}_i}{d\vec{q}} \Delta \vec{q} \quad (8.9)$$

where  $\Delta \vec{p}_i$  denotes the displacement vector of point  $i$ ; and  $\Delta \vec{q}$  is a vector containing the change of all DoFs. Rod  $j$  that is connected to points  $a$  and  $b$  and the change in length  $\Delta L_j$  is defined as:

$$\begin{aligned} \Delta L_j &= n_{a \rightarrow b} \cdot (\Delta \vec{p}_b - \Delta \vec{p}_a) \\ &= n_{a \rightarrow b} \cdot \left( \frac{d\vec{p}_b}{d\vec{q}} - \frac{d\vec{p}_a}{d\vec{q}} \right) \cdot \Delta \vec{q} \\ &= \frac{dL_j}{d\vec{q}} \cdot \Delta \vec{q} \end{aligned} \quad (8.10)$$

where  $n_{a \rightarrow b}$  denotes the direction vector, normalized to length from point  $a$  to point  $b$ ;  $\Delta \vec{p}_a$  and  $\Delta \vec{p}_b$  are the displacement vectors of points  $a$  and  $b$  respectively; Applying (8.10) to all rods, results in a matrix

$$\begin{aligned} \Delta \vec{L} &= \frac{dL}{d\vec{q}} \cdot \Delta \vec{q} \\ &= J_{q \rightarrow L} \cdot \Delta \vec{q} \end{aligned} \quad (8.11)$$

where  $J_{q \rightarrow L}$  denotes the Jacobian from states to rod length. This Jacobian is of size  $M \times N$ . Splitting the DoF vector  $\vec{q}$  into  $\vec{x}$  and  $\vec{y}$  gives:

$$\begin{aligned} \Delta \vec{L} &= \frac{dL}{dx} \cdot \Delta \vec{x} + \frac{dL}{dy} \cdot \Delta \vec{y} \\ &= J_{x \rightarrow L} \cdot \Delta \vec{x} + J_{y \rightarrow L} \cdot \Delta \vec{y} \end{aligned} \quad (8.12)$$

Since  $\vec{y}$  is of length  $M$  the Jacobian  $J_{y \rightarrow L}$  is square. Assuming that the system is in non-singular state, the matrix  $J_{y \rightarrow L}$  is invertible. Then (8.12)

can be rewritten as:

$$\Delta \vec{y} = J_{y \rightarrow L}^{-1} \cdot \left( \Delta \vec{L} - J_{x \rightarrow L} \cdot \Delta \vec{x} \right) \quad (8.13)$$

This means that for a small change in rod length and input states, a change for the output states is given.

### 8.4.3 Iterative Position Solution

The solution of (8.7a) can be found iteratively with (8.13). With given input states  $\vec{x}$  and an estimate of output states  $\vec{y}^*$ , the rod lengths are evaluated

$$\vec{L}^* = f(\vec{x}, \vec{y}^*) \quad (8.14)$$

When we compare the estimated rod length  $\vec{L}^*$  with the target rod length  $\vec{L}^{target}$ , we get the virtual change in rod length.

$$\Delta \vec{L} = \vec{L}^{target} - \vec{L}^* \quad (8.15)$$

We use the virtual change of rod length (8.15) in (8.13) to find a delta on the initial estimate of the output positions. This gives a new estimate of the output positions ( $\vec{y}^{\sim}$ ).

$$\vec{y}^{\sim} = \vec{y}^* + \Delta \vec{y} \quad (8.16)$$

This way we have an iterative solution for (8.7a).

For a real-time calculation, the initial estimate of output states is based on the time step. The simplest method is to use the previous outcome.

$$\vec{y}_t^* = \vec{y}_{t-1}^{\sim} \quad (8.17)$$

For a more accurate estimate the velocity and acceleration can be taken into account. This depends on the integration method that is used.

### 8.4.4 Velocity Solution

The velocity solution can be obtained from (8.13) by dividing by  $\Delta t$ .

$$\dot{\vec{y}} = J_{y \rightarrow L}^{-1} \cdot \left( \dot{\vec{L}} - J_{x \rightarrow L} \cdot \dot{\vec{x}} \right) \quad (8.18)$$

In LOPES II the rods have a fixed length and therefore the term  $\dot{\vec{L}}$  is equal to zero. Then we also have the Jacobian ( $P \times M$ ) from input states to output states:

$$\begin{aligned}\dot{\vec{y}} &= J_{y \rightarrow L}^{-1} \cdot -J_{x \rightarrow L} \cdot \dot{\vec{x}} \\ &= J_{x \rightarrow y} \cdot \dot{\vec{x}}\end{aligned}\quad (8.19)$$

This way we have a solution for (8.7b).

### 8.4.5 Acceleration Solution

In (8.11) we divide the delta vectors by a delta time and then differentiate to time.

$$\ddot{\vec{L}} = J_{q \rightarrow L} \cdot \ddot{\vec{q}} + \frac{dJ_{q \rightarrow L}}{dt} \cdot \dot{\vec{q}} \quad (8.20)$$

Now we split the acceleration vector  $\ddot{\vec{q}}$  in the given acceleration of the input DoFs  $\ddot{\vec{x}}$  and the unknown acceleration of the output DoFs  $\ddot{\vec{y}}$ .

$$J_{y \rightarrow L} \cdot \ddot{\vec{y}} = \ddot{\vec{L}} - J_{x \rightarrow L} \cdot \ddot{\vec{x}} - \frac{dJ_{q \rightarrow L}}{dt} \cdot \dot{\vec{q}} \quad (8.21)$$

The time-derivative of the Jacobian can be calculated analytically, but in practice a numerical derivative is faster.

$$\frac{dJ_i}{dt} \approx \frac{J_i - J_{i-1}}{\tau_s} \quad (8.22)$$

This way we have a solution for (8.7c).

### 8.4.6 Force Solution

The solution for (8.8) follows from the conservation of energy.

$$\vec{F}_z^T \cdot \dot{\vec{z}} = \vec{F}_x^T \cdot \dot{\vec{x}} \quad (8.23)$$

The output velocity ( $\dot{\vec{z}}$ ) is a subset of the driven velocity ( $\dot{\vec{y}}$ ) and thus from (8.19) we define:

$$\begin{aligned}\dot{\vec{z}} &= J_{z \rightarrow L}^{-1} \cdot -J_{x \rightarrow L} \cdot \dot{\vec{x}} \\ &= J_{x \rightarrow z} \cdot \dot{\vec{x}}\end{aligned}\quad (8.24)$$

Substituting (8.24) in (8.23) gives:

$$\vec{F}_z = \vec{F}_x \cdot J_{z \rightarrow x}^T \quad (8.25)$$

This way we have a solution for (8.8).

### 8.4.7 Total Transformation

The total transformation, both forward and backward, is a component-wise transformation, i.e., if possible the system is broken down in 1DoF problems i.e., solving the transformation from one state (rotation or translation) to another. If this is not possible we use the method of virtual rod elongation to solve a subsystem. We used the virtual rod elongation on three subsystems (see figure 8.10). The largest subsystem in the transformation is of size  $M = 4$ . This is the linkage between the patient pelvis and the LOPES frame, consisting of the hip rods, shadow pelvis and the vertical rods. For the pelvis stage (see figure 7.9), we use the linear approximation since the mechanism itself is fairly decoupled (see figure 7.10).

With the component wise transformation we also obtain Cartesian coordinates of the patient's leg joints and of the shadow leg joints. From these coordinates we obtain the orientation of the force sensors that are mounted in the rods between the shadow leg and patient leg, and consequently we convert the measured forces to measured segment torques, that form the input for the admittance model together with the rendered forces (see figure 8.2).

## 8.5 Mass Model

The virtual mass converts the forces, both virtual and measured, to virtual acceleration.

$$\ddot{\vec{x}}_{model} = M_V^{-1} \left( \vec{f}_{meas} + \vec{f}_{virt} \right) \quad (8.26)$$

Since the virtual mass represents a model, we will call this acceleration the model acceleration. However for readability we will omit the subscript *model* in this section. For a single DoF system the relation between input force and model acceleration is straightforward. The force is divided by the virtual mass resulting in an acceleration. This implies that a low mass results in a high gain from force to displacement. High gains may lead to instability. For transparency it is key to find the lowest virtual mass at which the admittance controller is still stable. In the following sections we describe the theory and practice of the virtual mass model of LOPES II.

### 8.5.1 Coordinate Systems for Mass Model

LOPES II is a multi-DoF system, i.e., the input force and the output acceleration are both vectors with ten elements in segment coordinates (see

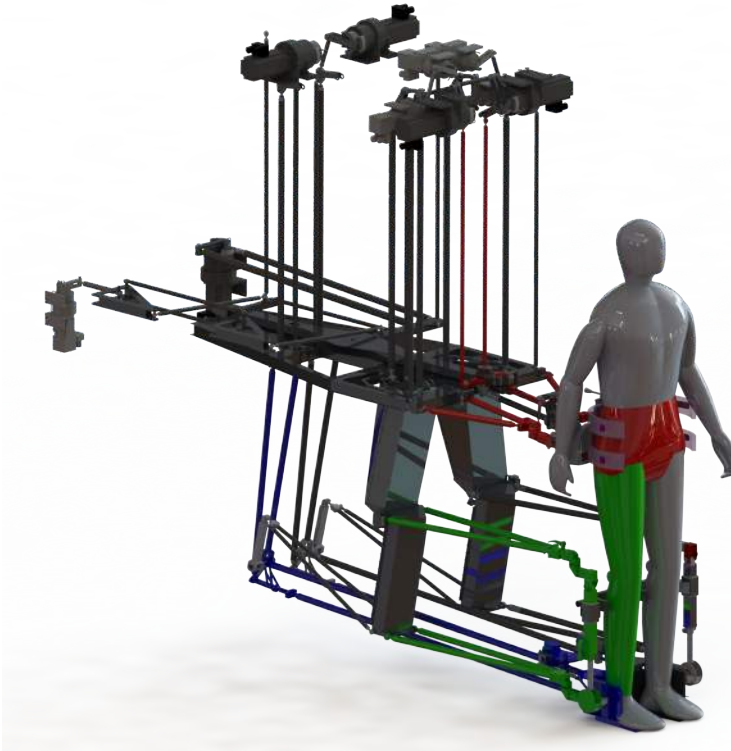


**Figure 8.10:** Subsystems of which the kinematics are solved using the method of virtual rod elongation. The linkage for the foot rotation between patient foot and shadow pelvis (blue); subsystem consisting of the patient upper leg, lower leg, and the interconnecting rods (green); and the linkage between the patient's pelvis, and the 'ground' (at the top) consisting of the hip rods, shadow pelvis and vertical rods (red).

table 8.1). The virtual mass then is a ten by ten matrix. If the virtual mass is a diagonal matrix, then each component of the force is connected to a single element of the acceleration vector.

$$\ddot{x}_i^S = \frac{1}{m_i^S} f_i^S \quad (8.27)$$

where  $^S_i$  denotes DoF  $i$  of the segment coordinate system.

This means that e.g., a force on the pelvis anterior / posterior direction causes an acceleration on the pelvis in anterior / posterior direction only, and that a sagittal torque of the upper leg only causes a sagittal rotation

acceleration of the upper leg, and the lower leg remains its velocity (see figure 8.11a).

For the implementation in LOPES II we chose to use the Cartesian Mass Model. In this model the admittance model displays a point mass at the joints i.e., the pelvis in both anterior / posterior and mediolateral direction, the knee in anterior / posterior direction, the foot in anterior / posterior and mediolateral direction and the heel in anterior / posterior direction (see figure 8.11b). Note that another implementation of the Cartesian Mass Model contains an mediolateral translation of the knee instead of the ankle. We chose for the mediolateral translation of the ankle instead of the knee since the mediolateral translation of the ankle (or foot) is relevant in foot placement. Similarly we could have chosen the toe up / down translation as an alternative to heel anterior / posterior translation. We chose for heel anterior / posterior translation since this more related to the physical implementation of a horizontal rod in anterior / posterior direction connected to the heel (see figure 7.6).

When using the Cartesian mass model, the mass matrix in segment coordinates is non diagonal. We calculate the mass matrix in segment coordinates with the following steps. The mass matrix in Cartesian coordinates ( $M^c$ ) is given, and it is a diagonal matrix.

$$F^c = M^c \cdot \ddot{x}^c \quad (8.28)$$

The superscript  $c$  denotes the Cartesian coordinate system. The matrix is converted to a full matrix in segment coordinates with the following steps. The transformation of velocities from segment coordinates ( $\dot{x}^s$ ) to Cartesian coordinates ( $\dot{x}^c$ ) :

$$\dot{x}^c = T^{s \rightarrow c} \cdot \dot{x}^s \quad (8.29)$$

The transformation matrix  $T^{s \rightarrow c}$  is dependent on the position, however for simplicity we take a position invariant and time invariant transformation matrix. From the consolidation of energy it follows that:

$$F^s = (T^{s \rightarrow c})^T \cdot F^c \quad (8.30)$$

The transformation of acceleration from segment coordinates ( $\ddot{x}^c$ ) to Cartesian coordinates ( $\ddot{x}^s$ ):

$$\ddot{x}^c = T^{s \rightarrow c} \cdot \ddot{x}^s \quad (8.31)$$

Substituting (8.31) and (8.28) in (8.30) in gives:

$$F^s = (T^{s \rightarrow c})^T \cdot M^c \cdot T^{s \rightarrow c} \cdot \ddot{x}^s \quad (8.32)$$

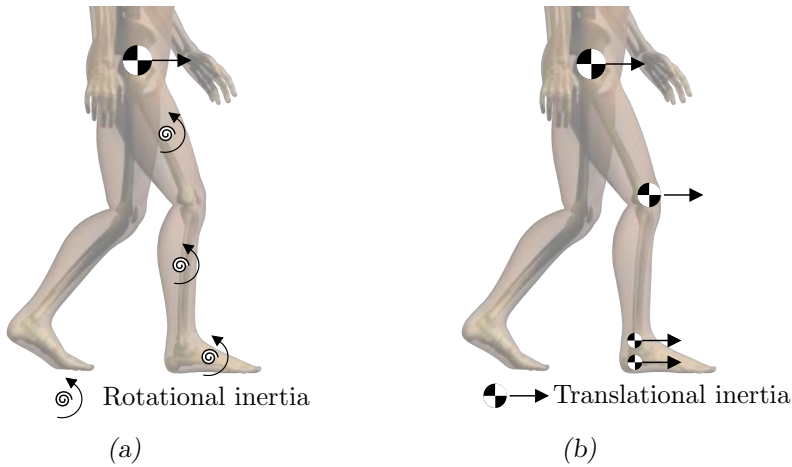


**Figure 8.11:** Coordinate systems for the mass model. (a): Segment Mass Model: The mass model consists of translational inertia's at the pelvis in anterior / posterior direction and mediolateral direction (not drawn), sagittal moments of inertia at the upper leg, lower leg and foot, and a frontal rotational inertia for the total leg (not drawn); (b): Cartesian Mass Model: The mass model consists of translational inertia's (point masses) at the pelvis, knee, ankle and heel in anterior / posterior direction and for the pelvis and ankle in mediolateral direction (not drawn).

where the segment mass matrix is constructed from the (diagonal) Cartesian mass matrix. The inverse of (8.32) is:

$$\ddot{x}^s = T^{c \rightarrow s} \cdot M^{c-1} \cdot (T^{c \rightarrow s})^T \cdot F^s \quad (8.33)$$

### 8.5.2 Inertia Scaling on Contact

As described in section 8.2.1, admittance controllers may require a high virtual mass to maintain contact stability with high impedances, whereas a low virtual mass is required to achieve transparency. In LOPES II the stance leg is a high impedance for the admittance controller, since the foot is relatively rigidly connected to the ground (treadmill surface). In case of the Cartesian mass model, the virtual mass of ankle displacement in  $x$  (anterior / posterior) and  $z$  (mediolateral) direction is connected to the high impedance of the treadmill surface. Increasing the virtual mass at the ankle displacement may be necessary to maintain stability. For the swing leg, the virtual mass should be sufficiently low to obtain transparency.

To maintain transparency in swing and stability in stance we use inertia scaling on contact. For this method it is important to determine if the leg is in contact with the ground i.e., the contact factor per leg. We used the following method to determine the contact factor. From the kinematics transformations we obtain the Cartesian position of the left and right ankle. From the patient's foot length we make an estimate of the location of the toes. The treadmill delivers the center of pressure (CoP) on the treadmill surface. We calculate the distance between the CoP and the heel and toe of both feet (see figure 8.12). We take the sum of the distance heel – CoP, and toe – CoP, minus the distance heel–toe (length of the foot).

$$d = \|\vec{p}_{CoP} - \vec{p}_{heel}\| + \|\vec{p}_{CoP} - \vec{p}_{toe}\| - l_{foot} \quad (8.34)$$

This sum is the ‘elliptical distance’ i.e., , all points with equal value for  $d$  form an ellipsoid. Note that the value of  $d$  is zero for any CoP between the heel and the toe. For larger distances between CoP and the heel and toe,  $d$  is equal to the double distance.

Then we define the contact factor  $cf$  as follows as the relative distance of the foot to the CoP:

$$cf_{right} = \frac{d_{left}}{d_{left} + d_{right}} \quad (8.35a)$$

$$cf_{left} = \frac{d_{right}}{d_{left} + d_{right}} \quad (8.35b)$$

Note that the sum of the contact factors is unity if the CoP, heels and toes have real coordinates. In the contact factor calculation, an extra condition is built in when then treadmill is unloaded and thus when the CoP can not be calculated. In that case, the contact factor for both feet is set to zero.

In the mass matrix, we introduce the inertia scaling:

$$m_i^{scaled} = m_i^{default} (1 + cf_l \cdot g_{l,i} + cf_r \cdot g_{r,i}) \quad (8.36)$$

where  $m_i^{default}$  is the optimal virtual mass for DoF  $i$  in the swing phase (leg is not in contact with floor);  $cf_l$  and  $cf_r$  are the contact factors for the left and right foot respectively;  $g_{l,i}$  and  $g_{r,i}$  are the scaling gains for left and right contact respectively for DoF  $i$ ; and  $m_i^{scaled}$  is the resulting scaled virtual mass for DoF  $i$ . If for example the scaling gain on left contact is four then, when the left leg is in stance, the used virtual mass for DoF  $i$  is five times the default tuned

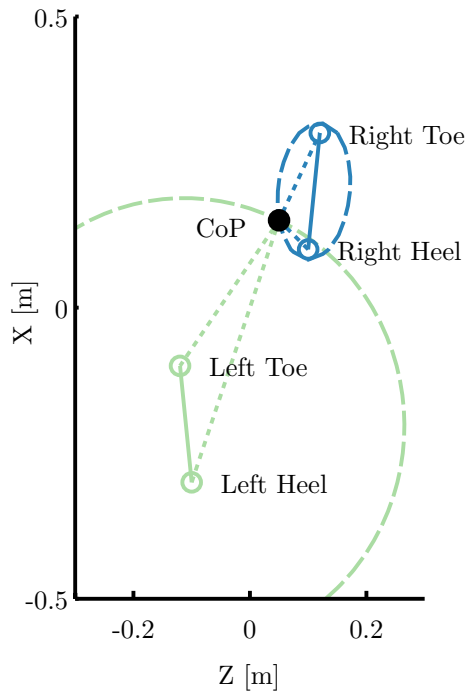


**Figure 8.12:** Top view of the two feet on the treadmill. The dotted lines are the distances between the CoP and the heel and toes of both feet. The dashed lines are ellipses where the sum of CoP–heel distance and CoP–toe distance is constant.

This adaptation of the mass model allows for having low virtual mass for a swinging leg, and a high virtual mass for a stance leg. Consequently it requires two tuning procedure. First tune the mass model such that it is stable for a swing leg, then tune the scaling gains such that mass model is stable for stance leg.

### 8.5.3 Inertia Compensation with Accelerometers

A disadvantage of the admittance control scheme as depicted in figure 8.6, is that the mass between the force sensor and the operator is not compensated, and therefore is part of the inertia that the user will perceive. As listed in table 7.1, these masses are considerable, especially at the foot. Accelerometers can (partially) compensate for this mass. The difference between the measured force at the force sensor and the interaction force between the robot and user is inertial force of the mass between the force

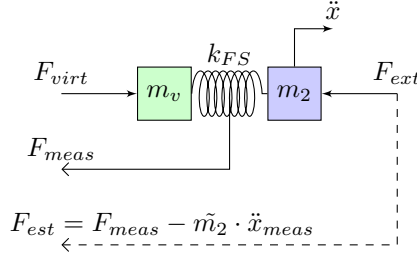


**Figure 8.13:** An accelerometer mounted on the inertia between the force sensor ( $m_2$ ) measures the acceleration ( $\ddot{x}_{meas}$ ) of  $m_2$ , to make a better estimate ( $F_{est}$ ) of the external force ( $F_{ext}$ ), by compensating for the (estimated) inertial forces.

sensor and the operator, assuming that there is no other impedance such as friction. Then an estimate of the interaction force between the operator and the robot can be obtained by subtracting an estimate of the inertial forces off the measured force (see figure 8.13)

$$F_{est} = F_{meas} - \tilde{m}_2 \cdot \ddot{a}_{meas} \quad (8.37)$$

where  $\tilde{m}_2$  is an estimate of the mass between the operator and force sensor ( $m_2$ ). A limitation of this method is that both the accelerometer and force sensor must provide accurate signals. Noise, phase shift and non-linearity may limit the use of this method. Therefore it may be necessary to use a lower value for  $\tilde{m}_2$ .

## 8.6 Integration Method

The admittance controller runs on a real time computer with a fixed update rate (1024 Hz) (see figure 8.1). This implies that the continuous integrators from the admittance controllers (see figure 8.3), must be converted to discrete integrators. The integration rules for the admittance controller are derived from the Velocity Verlet method (Swope et al., 1982). In the Velocity Verlet method the velocities are calculated at the ‘half-time’ step, i.e., the velocity between two discrete time steps:

$$\dot{x}_{k+\frac{1}{2}} = \dot{x}_{k-\frac{1}{2}} + \Delta t \cdot \ddot{x}_k \quad (8.38a)$$

$$x_{k+1} = x_k + \Delta t \cdot \dot{x}_{k+\frac{1}{2}} \quad (8.38b)$$

where  $\Delta t$  is the controller time step; subscript  $k$  denotes the states from the previous time step; and subscript  $k+1$  denotes the states from the new

time step. The velocity at time step  $k+1$  is calculated by taken the average of the velocities at  $k + \frac{1}{2}$  and  $k + \frac{3}{2}$ :

$$\dot{x}_{k+1} = \dot{x}_{k+\frac{1}{2}} + \frac{\Delta t}{2} \ddot{x}_{k+1} \quad (8.39)$$

However this requires new acceleration data ( $\ddot{x}_{k+1}$ ), which is available in the next loop cycle.

For LOPES II we use simplified integration rules as used in the Haptic-MASTER (Van der Linde and Lammertse, 2003):

$$\dot{x}_{k+1} = \dot{x}_k + \Delta t \cdot \ddot{k}_t \quad (8.40a)$$

$$x_{k+1} = x_k + \Delta t \cdot \dot{x}_{k+1} \quad (8.40b)$$

The difference of the used integration method wit the velocity Verlet method is that we use the ‘wrong’ time index for the velocity. However, we use an update rate of 1024 Hz, implying that the timing error is  $< 1$  ms.

## 8.7 PVA Limiter

### 8.7.1 Introduction

The goal of the controller is to make the robot move according to the model position, velocity and acceleration (pva). Then the model pva must contain ‘reasonable’ values e.g., the motors must be able to make desired velocities, the desired joint angles must be safe for the patient. Therefore the PVA limiter checks whether the acceleration from the mass model will cause a violation of these limits on acceleration, velocity and position (see figure 8.14). The first step is to check per DoF whether the accelerations are acceptable (“Limiter ” in figure 8.14). Per joint DoF the limiter checks if the model acceleration exceeds the limit. Then it checks if the velocity needs to be limited, and if so model acceleration is adjusted. The last check is if the DoF , with the desired speed and position, and with maximum allowed deceleration will not exceed the position limit. If so, then the (unlimited) model acceleration ( $\ddot{x}^U$ ) is adjusted ( $\ddot{x}^L$ ). For the single DoF limiter we use the pva limiter based on the Proximal PD controller (see Appendix G). Finally we check whether the limitation in one DoF causes a limit violation in other DoFs and optionally we distribute the acceleration such that all limits are respected (“Acceleration Distribution” in figure 8.14). This is described in section 8.7.2. Next to the limiters on the human joints, we

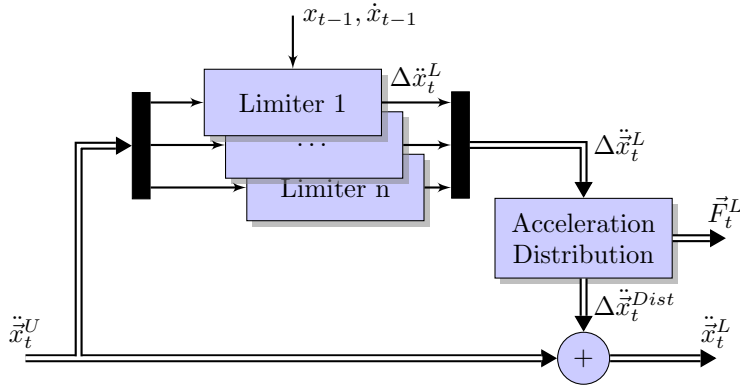


**Figure 8.14:** Schematic function of the limiters. First for each joint the acceleration is validated: will this acceleration cause a violation of a position-, joint-, or acceleration limit? If so, then the acceleration for the individual DoF is corrected ( $\Delta \ddot{x}^L$ ). Subsequently the limiter force ( $\vec{F}_t^L$ ) is calculated and the accelerations are distributed over the DoFs in such a way that all limits are respected.

have limiters on the actuators to assure that their set points stay within their mechanical end stops.

### 8.7.2 Multi DoF Limiter

The single DoF limiters apply to the joint rotations and the pelvis translations. The mass model of LOPES II however is based on translations of point masses. This means that a knee torque causes an acceleration of the point masses at the ankle, hip and knee. When for example the knee is limited when approaching the maximum knee extension, the limiter torque causes accelerations on the point masses at the ankle, hip and knee. Looking again at joint coordinates, this means that there is an acceleration of the hip flexion as well. In other words, the acceleration of the knee caused by the knee limiter, is distributed over other DoFs. This ‘distributed acceleration’ may violate the acceleration limit of the hip flexion. Therefore it is insufficient to regard the limiters as a SISO system, but the total effect of all limiters should be accounted for. This is the step of ‘acceleration distribution’ (see figure 8.14).

The solution of this MIMO problem is described below. The first step is to introduce a limiting force. This means that the single DoF limiter

causes a change in acceleration, which is caused by the limiting force.

$$\begin{aligned}\Delta\ddot{x}_i^L &= \ddot{x}_i^L - \ddot{x}_i^U \\ &= \gamma \cdot F_i^L\end{aligned}\quad (8.41)$$

where  $\gamma$  is the unknown relation between the limiting force ( $F_i^L$ ) and the resulting correcting acceleration ( $\Delta\ddot{x}_i^L$ ) for a single DoF. The relation between force and acceleration is determined by the mass model.

$$\Delta\ddot{x}^L = M^{j-1} \cdot \vec{F}^L \quad (8.42)$$

Where  $M^j$  denotes the mass matrix in joint coordinates. Similar to the transformation of the Cartesian mass model to segment coordinates, we use (8.32) to convert the mass model to joint coordinates.

The mass model is non diagonal, i.e., a limiting force on one DoF  $i$ , not only causes acceleration in DoF  $i$ , but possibly also in other DoFs. Therefore we have to solve the complete system of limiters to find the force that causes the limitations ( $\vec{F}_{lim}$ ) and how these acceleration limitations are distributed over the DoFs ( $\vec{x}^{Dist}$ ). If a DoF is limited, we know the distributed acceleration, since it is defined by its own limiter ( $\Delta\ddot{x}_i^{Dist} = \Delta\ddot{x}_i^L$ ), but the force that causes this limitation is yet unknown ( $F_i^L \neq 0$ ). For a DoF that is not limited ( $\Delta\ddot{x}_i^L = 0$ ), the limiting force is zero ( $F_i^L = 0$ ), but the distributed acceleration is unknown ( $\Delta\ddot{x}_i^{Dist} = 0$ ). The total system to be solved is:

$$\begin{Bmatrix} 0 \\ B \cdot \vec{x}_{lim} \end{Bmatrix} = \begin{bmatrix} (M)^{-1} & -I \\ I - B & B \end{bmatrix} \cdot \begin{Bmatrix} \vec{F}_{limiter} \\ \vec{x}_{dist} \end{Bmatrix} \quad (8.43)$$

with

$$B_{i,i} = \begin{cases} 1 & \text{if DoF } i \text{ is limited} \\ 0 & \text{otherwise} \end{cases} \quad (8.44)$$

If we eliminate the limiting force, this system reduces to:

$$\vec{x}^{Dist} = [B + (I - B) M]^{-1} \vec{x}^L \quad (8.45)$$

Now we know how the limiting accelerations of the complete system and we can correct the model acceleration with the distributed acceleration:

$$\vec{x}^L = \vec{x}^L + \Delta\vec{x}^{Dist} \quad (8.46)$$

The next step is to validate this distribution. For each DoF we check whether the new model acceleration violates the acceleration limits. If

so, then the original state of this DoF changes from unlimited to limited ( $B_{i,i} = 1$ ).

A second step is that the force and the distributed acceleration are equal in sign. This is needed since other limiting DoFs may cause a distributed acceleration such that the DoF would be pulled out of its limit, but the system treats the DoF as limited, and therefore calculates a limiting force that pushes the DoF in its limit. In this case the original state of this DoF changes from limited to unlimited ( $B_{i,i} = 0$ ).

If either of these checks cause a change in  $B$  the system of (8.45) must be solved again. Hence the solution of the limiter distribution is an iterative process.

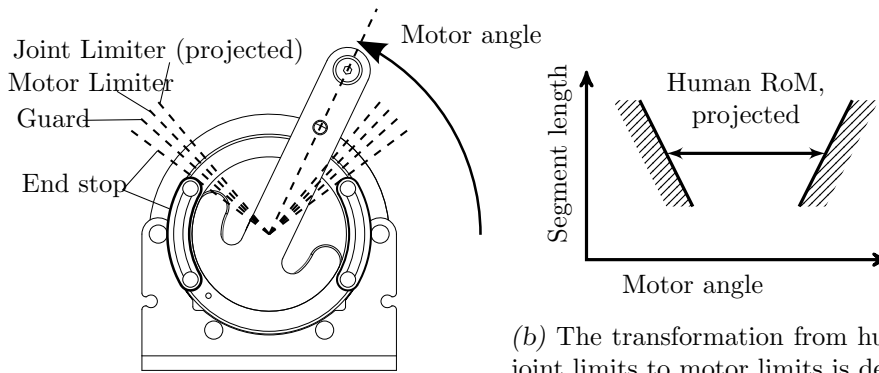
## 8.8 Guard

The guard executes several tasks to check whether the measured data and actuators are reliable. Each task of the guard can put the system to halt when triggered.

Each actuator has settable physical end stops, which physically limit the rotation of the motor axis. Just within the end stops is the drive guard i.e., when the motor angle reaches the guard position, the drive activates the emergency circuit. The motor controller in the real-time software has a PVA limiter (see section 8.7). The position limits are located within the guards to prevent the guards from being triggered. Finally there are limiters on the human joint excursion and pelvis translations. Most actuators are primarily coupled to a single joint e.g., the motor for Thigh RZ rotation is primarily coupled to the thigh flexion. Therefore we project the joint limiters in motor space (see figure 8.15a). However, the relation (kinematics) between motor angles and joint angles is non-linear and dependent on segment length (see section 7.1) (see figure 8.15b).

Second, the measured angles and velocities from the motors are compared with their set point angle and velocity, which are generated by the virtual masks model. The measured values and set points should be nearly similar, since the motor is tuned to follow set points and the limiter in the model assures that the motor set points are feasible. The maximum allowable position errors for the motors are 0.02 rad.

A third check is performed redundant angular sensors that are located on several locations in LOPES II (see figure 6.3). With the kinematics transformations the angles of all mechanical joints in LOPES II are cal-



(a) The inner limits of the motor angle are determined by the limiters on human joints, transformed to motor coordinates. The motor limits are a little wider. Just outside the motor limiters are the guards that stop the motor. The outer limits are physical end stops.

(b) The transformation from human joint limits to motor limits is dependent on segment length, e.g., a longer thigh length requires larger rotation for the Thigh RZ motor, and thus the human joint RoM, defined by the human joint limits, projected in motor space depends on patient's segment length.

**Figure 8.15:** End stops, limiters and guards in motor coordinates

culated. These angles are compared with the angles from the redundant sensors.

## 8.9 Renderer

The renderer calculates the virtual forces from virtual objects such as springs and dampers. The input for the object is model position and velocity ( $pv_{model}$ ) and the object position and velocity ( $pv_{object}$ ).

$$F_{object} = f(pv_{model}, pv_{object}) \quad (8.47)$$

The objects that are used in LOPES II are springs, dampers and bias forces in the segment coordinate system. Additionally we have joint springs for the knee flexion / extension and ankle plantar / dorsiflexion. For example a damped, linear spring, with stiffness  $k$  and damping  $b$ , is rendered by the following function.

$$F_{spring} = -k(x_{model} - x_{spring}) - b(\dot{x}_{model} - \dot{x}_{spring}) \quad (8.48)$$

The objects contain additional nonlinear parameters such as maximum force, and for a spring, a deadband.

The gait controller (see figure 8.1) updates the object pv and the properties, such as stiffness and damping. This way, the gait controller can control e.g., the patient knee flexion/extension by commanding the position and stiffness of a virtual knee spring. For the spring objects not only the position can be commanded but also the speed. This allows for smooth motion of high stiffness springs. If the high stiffness spring position is updated with position at a low update rate, this may cause a grinding feeling on LOPES II, due to the discrete jumps of the spring position. By commanding a speed to the spring instead of a position, the motion of the spring is smooth, because the renderer integrates the spring velocity to a new spring position each time step (1024 Hz).

The output of the renderer is the sum of all object forces.

$$F_{renderer} = \sum_{i=1}^{N_{objects}} F_{object}(i) \quad (8.49)$$

For each segment this renderer force is clipped at a maximum force to limit the forces on the patient.

## 8.10 Gait Controller & GUI

### 8.10.1 Graphical User Interface

In the GUI, the gait is divided in subtasks (see figure 3.1). The amount of support (expressed as a percentage of the maximum support) and the reference trajectory can be adjusted for each gait subtask and each leg individually. This *selective support* (Koopman et al., 2013a) makes it possible to give support on only one subtask while giving complete freedom for the patient on the other subtasks, e.g., only supporting the patient in lifting his left foot during swing phase.

### 8.10.2 Gait Trajectory Controller<sup>1</sup>

The gait trajectory is generated by a Simulink model running on an embedded xPC Target PC (Mathworks Inc., Natick, MA, USA). For each joint, a trajectory is generated as a piecewise third order polynomial fitted between *key events* as described in Koopman et al. (2014). The key event positions (timing and amplitude), and thus the trajectories, are dependent

---

<sup>1</sup>Part of this section is taken from C

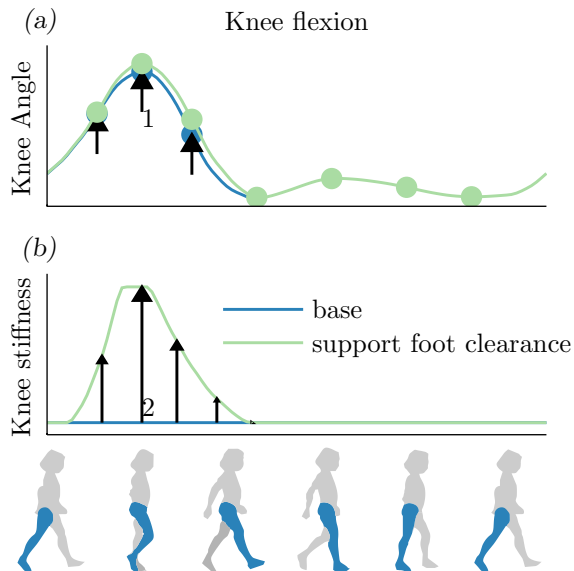


**Figure 8.16:** Reference trajectory for the knee angle (a) and the support on the knee angle (b). The key events are plotted as dots in the angle trajectory. If the foot clearance is increased, specific key events are displaced (arrow 1), resulting in a modified reference trajectory for knee flexion in swing phase. If the support for foot clearance is increased, the stiffness of knee spring increases in swing phase (arrow 2).

**Table 8.2:** List of available sliders for adjusting the gait trajectory and support.

Gait subtask	Support Adjustment	Parameter adjustment
General	Yes	Walking velocity Hip extension offset
Weight shift	Yes	Amplitude <sup>a</sup> Timing Duration <sup>a</sup> Step width
Foot clearance	Yes <sup>a</sup>	Knee flexion in mid swing <sup>a</sup>
Stance	Yes <sup>a</sup>	Knee flexion in mid stance <sup>a</sup>
Prepositioning	Yes <sup>a</sup>	Knee flexion in end swing <sup>a</sup>
Step length	Yes <sup>a</sup>	Step length <sup>a</sup>

<sup>a</sup>adjustable for left and right leg separately

on walking velocity and patient length. The subtasks of gait are linked to the key events such that when the operator adjusts a parameter of a subtask, specific key events move relatively to their original location (see arrow 1 in figure 8.16a), resulting in a modified gait trajectory for DoFs that are related to the specific subtask.

The joint trajectories are sent to the Admittance Controller which interprets them as the equilibrium position of a (critically damped) virtual spring. The spring stiffness  $K$  is related to the desired support  $G$  (in percent) as follows:

$$K = K_{\max} \left( \frac{G}{100} \right)^2 \quad (8.50)$$

with  $K_{\max}$  a predefined maximum stiffness. The reason for the nonlinearity is that, since  $K_{\max}$  is high,  $\frac{1}{2}K_{\max}$  still *feels* very stiff; while we wanted 50% of the stiffness to feel significantly less stiff than 100% stiffness.

The support can be adjusted for each gait subtask individually, resulting in a gait-phase dependent stiffness (see table 8.2). This results in a time-varying stiffness (see figure 8.16b).

Apart from generating the gait trajectories and stiffness trajectories, the Simulink model also has various safety checks and a state machine for the transitions between different modes (self test, motors off, standing still, training etc.).

## 8.11 Conclusion & Discussion

### 8.11.1 Kinematics Transformations

We use a component-wise, iterative solution for both the forward and backward kinematics. For the smallest possible subsystem we solve the kinematics by means of virtual displacements of rods. In a simulation we applied the method of virtual displacement to the total system of LOPES II. This system contains 34 unknown states ( $M = 34$ ). The simulations are promising and accurate. However the implementation in the real time controller needs acceleration, since the virtual displacement method add 80 % to the cpu load, whereas the component-wise transformation only adds 20 % on the loop load. This increase causes system overruns, when the controller executes extra tasks such as limiters, renderer or state changes, which causes the guard to stop the system. Optimization of the real time algorithm may improve the speed. Then the one-step transformation is preferred over the component-wise transformation, since for the programmer, the one-step method is a simpler way to program the kinematics and less sensitive to mistakes in calculations.

### 8.11.2 Simplified Mass Model

The used mass model is the Cartesian mass model i.e., displacements of point masses at the joints. The exact conversion from Cartesian coordinates to segment coordinates depends on the position and is non-linear (see figure 8.17). However in the calculation of the mass matrix we use a constant (linear) transformation matrix from Cartesian coordinates to segment rotations and translations (fixed segments lengths, instead of projected segment lengths). This simplification has the consequence that at larger rotations of the segments, when the projected joint distance deviates substantially from the absolute joint distance, larger point masses are perceived by the user. However, if we would use the non-linear transformation, the elements of the segment mass matrix would be lower at large rotations, possibly causing instabilities in the admittance loop. Furthermore using the non-linear transformation would be pressing on the CPU load of the real time controller, since the mass matrix must be calculated and inverted real time. The inverse of the linearized transformation has an exact solution and therefore is less time consuming in the real time loop.

If we would have used the segment mass model, the above mentioned

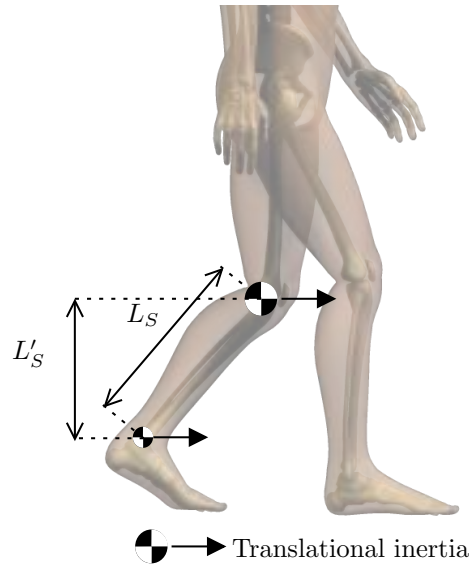


**Figure 8.17:** The relation between Cartesian point masses and segment mass model (moments of inertia of segments). The conversion of Cartesian mass to segment mass requires the usage of the vertical distance between the joints ( $L'_S$ ). In the simplified conversion we use the absolute distance between the joints ( $L_S$ ).

effect would not occur. However the segment mass model has the important disadvantage that when applying inertia scaling on a stance leg, the virtual mass of the pelvis effectively increases as well. A hybrid mass matrix, consisting of point masses and moments of inertia, may be a suitable alternative for the Cartesian mass model. The hybrid mass matrix has more resemblance with the human mass distribution, since the human segments also consist of translational inertias and moments of inertia. Then for the hybrid mass matrix the inertia scaling on contact should only apply on the point masses, and not on the moments of inertia. Due to the complexity of this mass matrix and its inverse we have not implemented it. When the transformation method is improved, this mass matrix may be implemented easier. Until then, the Cartesian mass matrix is used.



# Realization & Evaluation

This chapter describes the built and tuned mechatronic prototypes. The chapter starts with a description of the system and from technical evaluations (verification of the system requirements), we end with evaluation by users (validation).

## 9.1 Built Prototypes

Two identical prototypes were built. The first was installed at the Roessingh Rehabilitation Center in Enschede, the Netherlands (see figure 9.1). The second was installed at the Sint Maartens clinic in Nijmegen, the Netherlands.

## 9.2 Removal of the Foot Rotation Actuation

LOPES II was designed and built with a linkage for actuation of the foot sagittal rotation (foot RZ) (see figure 9.2a). However the foot bracket and linkage for foot rotation was heavy and the stiffness of the linkage for the lower leg showed some compliance (see section 9.3). When using the admittance controller, the controller was only stable with 4 kg at the ankle translation, whereas 2 kg is the maximum allowable inertia (see table 5.3). Furthermore still additional dampers were required to dampen oscillations. The large weight of the foot bracket (2.6 kg, see table 7.1) is located between the force sensor and the subject. This weight could not be compensated for completely, and this deteriorated the mechanical transparency. We



**Figure 9.1:** LOPES II at Roessingh Rehabilitation Center, Enschede the Netherlands. Picture: Gijs van Ouwkerk

suspected that the stiffness of the lower leg rotation was insufficient (as will be confirmed in section 9.3). This limited stiffness in combination with a high mass is likely the cause that the system is difficult to control in force loop, and is only stable with very low gains (and thus high masses).

Due to the negative impact of the foot RZ (plantar / dorsiflexion) linkage on the transparency of LOPES II and particularly the lower leg, we decided to remove the foot RZ linkage and continue with a 8DoF powered system without the foot RZ actuation, with a simplified, light weight foot bracket.

The new foot bracket is a simple carbon bracket that only clamps at the heel (see figure 9.2b). The interface with the mechanics of LOPES II is unchanged i.e., the spherical gimbal (see figure 9.2c), therefore the new bracket has the same workspace in foot endo- / exorotation and inversion / eversion. A limitation of the loss of the actuation in foot RZ is that LOPES II is unable to provide support in push-off and toe lifting. Especially the latter is



(a) First foot bracket with support in plantar / dorsiflexion.



(b) Second foot bracket without support in plantar / dorsiflexion.



(c) Detail on the second foot bracket and its interface with the ankle gimbal.



(d) Separate toe lift support.

**Figure 9.2:** Foot brackets of LOPES II

a serious limitation for patients with a drop foot (see section 3.2). Therefore we modified the lower leg clamp to allow to apply toe-lifters when the patient needs them (see figure 9.2d).

### 9.3 Stiffness

We measured the stiffness of LOPES II with a Control Force Measurement (CFM) kit (MOOG, 2009). The CFM records force of a force sensor and displacement of a stringpot i.e., a string wound on a drum that is pre-tensioned with an electro motor with encoder. We mounted a clamp with force sensor and the string on the force sensors of LOPES II at the ankle, knee

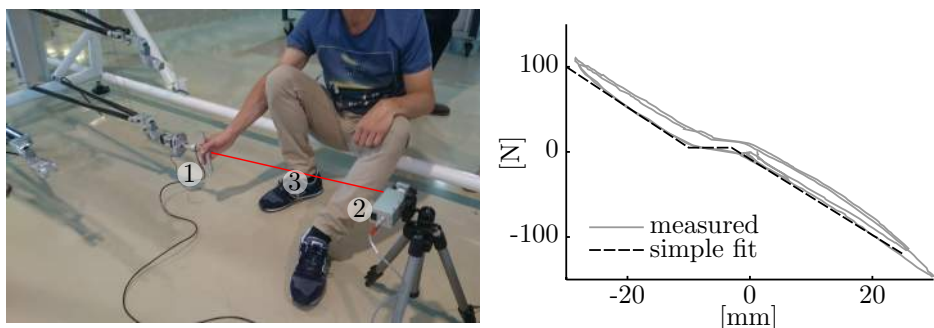
**Table 9.1:** Measured free play and stiffness of LOPES II at the joint translations.

	Free play [mm]	Stiffness [N/mm]	
		measured	required
Pelvis TX	1	34.7	50
Pelvis TZ	1	22.6	50
Knee TX	2.5	14.9	40
Foot TX	7	4.6	20
Foot TZ	7	3.3	20

and hip joint. The actuators of LOPES II are put in position control, thus the measured stiffness is the total stiffness from actuator to force sensor. We then manually pulled and pushed the force sensor, while the CFM kit records force and displacement (see figure 9.3a). This way we obtained force-position plots for the joint displacements ankle TX and TZ, knee TX and pelvis TX and TZ.

The position plots show stiffness (force proportional to displacement), deadband (zero stiffness) and hysteresis (the force position relation at increasing force slightly differs from decreasing force) (see figure 9.3b). The stiffness is attributed to the mechanical stiffness in the system. The deadband is attributed to the physical free play in the system, partially due to the sleeve bearings. The hysteresis is attributed to the friction in the system. For each measurement we do a simple fit of a spring with a deadband, i.e., in the deadband, the force remains constant, outside the deadband, the force is proportional to the displacement (see figure 9.3b).

For all joint displacements we estimate the stiffness and free play (see table 9.1). Comparing the fitted stiffness with the required stiffness as stated in section 5.4.2, we conclude that LOPES II is not as stiff as required. Especially for the distal DoFs the stiffness falls short. This implies that the Robot in Charge mode is not as stiff as required and that patients still have considerable freedom to deviate from the prescribed gait patterns when the support is set to maximum. The deadband is caused by free play in the system. Particularly sleeve bearings at several locations contribute to the deadband. The freeplay also influences the control of LOPES II, as it deteriorates the positioning accuracy. The effect that the free play and lack of stiffness have on the positioning accuracy is discussed further in section 9.6.



(a) Setup for stiffness measurement on ankle TX with CFM force sensor (1) and CFM stringpot (2), the string (3) and CFM force sensor are mounted on the LOPES II force sensor at the ankle.

(b) Stiffness plot of left Ankle TX with measured data (solid gray) and a simple deadband spring fit (dashed black).

**Figure 9.3:** Stiffness measurements on LOPES II.

## 9.4 Tuning Procedures & Results

This section discusses the tuning of LOPES II, i.e., the process of identifying the optimal controller settings.

### 9.4.1 Range of Motion — Position Limits

This section discusses the range of motion (RoM) for the patient joint angles (and pelvis translations). The patient RoM is determined by wanted and unwanted limitations in the linkage and motors. This section describes these limitations

The set joint limiters of LOPES II are listed in table 9.2. For several DoFs the RoM is smaller than required. This has several reasons. For the pelvis AP translations, on several locations in the mechanism rods were colliding depending on the state of the remaining DoFs. We chose to limit the pelvis AP RoM instead of the other colliding DoFs, since the pelvis AP RoM was deemed as less important than the other RoMs. The users consented in this.

The abduction / adduction RoM is also less than required. The abduction limit was lowered because the shadow leg and rods collided with the side railing when the subject was making large adduction while walking at the edge of the pelvis ML RoM. The adduction limit was lowered to limit the collision between the two shadow legs. With a limited adduction there

**Table 9.2:** Range of Motion for the pelvis translations and joint excursions

		Limit	Required
Pelvis	Forward [mm]	0.15	0.3
	Backward [mm]	0.19	0.3
Pelvis	Left [mm]	0.14	0.15
	Right [mm]	0.14	0.15
Hip	Abduction [deg]	11.5	19
	Adduction [deg]	8.6	17
Hip	Flexion [deg]	37.2	36
	Extension [deg]	14.3	28
Knee	Flexion [deg]	74.5	75
	Extension [deg]	0	0

is still collision possible, but the legs can not cross anymore and the RoM is still sufficient to walk foot for foot.

The hip extension is limited because of a collision in the linkage near the thigh RZ motor. A lever ((2) in figure 7.4) collided with the end stop on the motor. This reduced the RoM of the thigh RZ motor and consequently the hip extension.

## 9.4.2 Speeds & Accelerations

This sections lists the limits on speed and accelerations on the human joints and pelvis translations. These limitation are driven by the performance of the actuators. We used a sine sweep to seek the boundaries of the performance of each actuator.

For each actuator we applied a sine sweep in position mode, while maintaining the other actuators on a fixed position. LOPES II was empty while performing the sweeps.

The sweep is symmetric (up and down), with fader at start and end, i.e., the position starts at zero then increases in amplitude in frequency, until the maximum frequency is met, then the frequency decreases. The position sine sweep amplitude is limited such for the entire sweep the position, velocity and acceleration do not exceed predefined limits (see figure 9.4).

With each sine sweep we increased the velocity and acceleration limits until the position error (motor set point angle and motor measured angle) was too high and triggered the position error guard (0.02 rad).

For each actuators we set the velocity and acceleration limits slightly

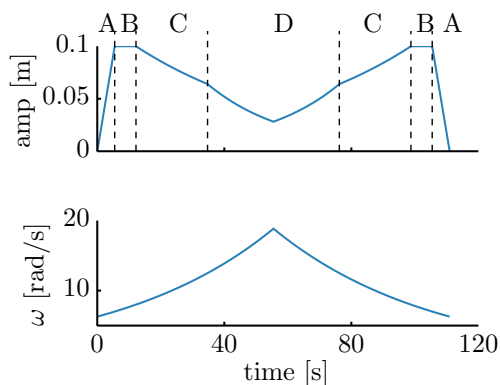


**Figure 9.4:** Example sweep signal amplitude (top) and frequency (bottom). In the first phase (A) the amplitude is faded in, in the second phase (B) the amplitude is limited by a maximum position amplitude; as the frequency increases, in the third phase (C) the amplitude is limited by a maximum velocity; in the fourth phase (D) the amplitude is limited by a maximum acceleration; then the frequency decreases passing the afore mentioned phases in reverse order.

below the performance limits. Next we translated the actuators' velocity and acceleration limits to human joint velocity and acceleration limits (see table 9.3). For this transformation we used the average segment lengths and the average gearing between actuators and patient segments.

By using a symmetric sine sweep, the higher frequencies were played a little longer. The drives can supply a peak current for a short period ( $< 1$  s). By using the symmetric sweep, the maximum acceleration (and thus maximum current) last longer than the peak current duration, and so we are confident that the actuators can make the maximum acceleration for a longer period. An additional benefit of using the symmetric sweep is that the system stops smoothly. An asymmetric sweep ends after the highest frequency with a loud bang, which is easily confused with an emergency stop e.g., due to the position guard being triggered.

For the pelvis the a speed of 0.3 m/s was required, however we set the speed limit to 0.7 m/s, since in practice we often reached the speed limit, which hindered free walking.

For all DoFs we nearly reach the required speed limits. These limits were defined by fast walking (see section 5.3.2). This means that during fast walking velocity limits may be reached.

For taller subjects the velocity limits of the actuators may be reached

**Table 9.3:** Velocity and accelerations for the pelvis translations and joint excursions

		Limit	Required
Pelvis AP	[m/s]	0.7	0.3
	[m/s <sup>2</sup> ]	10	
Pelvis ML	[m/s]	0.3	0.3
	[m/s <sup>2</sup> ]	6	
Hip abduction / adduction	[rad/s]	1.5	1.6
	[rad/s <sup>2</sup> ]	30	
Hip flexion / extension	[rad/s]	3	3.2
	[rad/s <sup>2</sup> ]	30	
Knee flexion / extension	[rad/s]	7	7.3
	[rad/s <sup>2</sup> ]	100	

at lower speeds, due to the effect of segment length on the gearing between motors rotation and segment rotation.

### 9.4.3 Inertia

For the mass model in the admittance controller we use the Cartesian mass mode, i.e., point masses at the pelvis, knee and ankle (see section 8.5). With trial and error we established the lowest virtual masses at which LOPES II still behaves stable. The Cartesian mass model displays 2 kg at the foot and 5 kg at the knee if the leg is in swing phase (see table 9.4). At the pelvis displacement the virtual mass is 40 kg, which is still considerably higher than the target value. We use limited dampers to dampen small oscillations (see table 9.5). Additionally a soft virtual spring ( $k = 10 \text{ N m}^{-1}$ ) is put on the pelvis translations to prevent drift.

With the virtual masses as described above, LOPES II is stable in swing phase. In stance phase, contact instability occurs, and the system starts to oscillate. Therefore we increase the inertia for the stance (inertia scaling). Again the values are established with trial and error. For the ankle displacements we use an inertia scaling gain of five, for the knee we used a gain of three to assure stability for the leg in stance phase (see table 9.4).

The use of the accelerometer allows for compensation of the mass between the force sensor and subject. For most DoFs the compensation is

**Table 9.4:** Masses in LOPES II (in kg).  $M_v$  is the virtual mass in swing;  $M_c$  is the physical mass of the material between force sensor and patient (e.g., clamps);  $M_{acc}$  is the mass that is compensated with the measured acceleration;  $\Sigma M_p$  is the total mass that is perceived by the patient during swing ( $M_v + M_c - M_{acc}$ ); and  $M_{req}$  is the maximum allowable mass taken from the requirements.

		Pelvis TX	Pelvis TZ	Knee TX	Ankle TX	Ankle TZ
(+)	$M_v$	40	40	5 <sup>a</sup>	2 <sup>b</sup>	2 <sup>b</sup>
(+)	$M_c$	3.6	3.6	0.7	0.7	0.9
(-)	$M_{acc}$	3	3	1	0.5	0.5
(=)	$\Sigma M_p$	40.6	40.6	4.7	2.2	2.4
	$M_{req}$	6	6	4	2	2

<sup>a</sup>in stance 15 kg

<sup>b</sup>in stance 12 kg

**Table 9.5:** Additional virtual objects in LOPES II in minimal impedance mode: spring stiffness  $k$ ; spring damping coefficient  $\zeta$ ; Damper coefficient  $b$ ; Damper max force  $f_c$ .

	Pelvis TX	Pelvis TZ	Thigh RX	Thigh RZ	Shank RZ
$k$	10 N/m	10 N/m			
$\zeta$	1	1			
$b$	100 Ns/m	100 Ns/m	1 Nms/rad	1 Nms/rad	1 Nms/rad
$f_c$	5 N	5 N	0.5 N m	0.5 N m	0.1 N m

little less than the physical mass, only for the knee we overcompensate the physical mass (see table 9.4).

Adding up all masses, it is clear that we almost meet the requirements for the foot and the knee, but the virtual mass for the pelvis translations is nearly seven times too high.

#### 9.4.4 Maximum Force / Torque

The forces and torques that LOPES II can apply to the patient are limited in the renderer 9.6. The Shank RZ torque is limited to 70 N m whereas 134 N m was required. The torque on the shank is limited by the continuous current that the drive can supply. The drive and motor can supply double the continuous torque for a short period ( $< 1$  s). Making the maximum

**Table 9.6:** The maximum renderer force.

	Max. force / torque[N;N m]	Required force / torque[N;N m]
Pelvis TX	500	500
Pelvis TZ	500	500
Thigh RX	60	60
Thigh RZ	60	60
Shank RZ	70	134

renderer torque dynamic i.e., taking notice of the duration of peak torque increases the torque performance of LOPES II. We have not implemented this yet, therefore, to prevent position tracking errors, we limit the shank torque to 70 N m. (see table 9.6).

## 9.5 Guard Margins

The guards compare two position values and trigger the emergency circuit if the difference exceeds a predefined margin.

In the structure of LOPES II we placed extra angular sensors as redundancy for the motor encoders (see figure 6.3). The maximum allowable position error for the redundancy check is 0.1 rad-0.2 rad. This margin is fairly high compared to the position errors on the motor controller. This has several causes. The redundant sensor angles have a fair amount of noise. Therefore the data is low-pass filtered, which causes a large tracking error at higher speeds. Furthermore, LOPES II contains (unwanted) free play and compliance (see table 9.1), which is not accounted for in the kinematics transformations. All factors added make that the allowable position error must be set to values up to 0.2 rad. However we believe that this does not harm the safety of LOPES II. If a motor sensor ‘misbehaves’ and this is detected by neither the internal guards in the drive, nor by the position error guard, LOPES II will make an error of 10 deg before the redundancy guard stops the system.

## 9.6 Position Accuracy<sup>1</sup>

Since the position sensors of LOPES II are not collocated with the patient's segments, we want to verify whether the patient's segment angles are calculated correctly. Several factors may negatively affect the accuracy of the calculated segment positions and angles i.e., calculation mechanical compliance in the structure of LOPES II, and mechanical compliance between LOPES II and the human skeleton structure (e.g., clamps and human tissue). We used an optical tracking system (Visualeyez VZ4000, PTI, Burnaby, Canada) to determine the accuracy of segment positions and angles calculated by LOPES II based on the motor angles (LOPES controller data). We applied cluster markers (frames with three markers) on the feet, lower legs, upper legs and sternum. Individual markers were put on the knee (lateral epicondyle) and hip (greater trochanter). We put additional markers on mechanical structure close to the patient i.e., the leg guidance and on the rods that are connected to the pelvis (see figure 9.5).

Two healthy subjects walked at two speeds (1.5 km/h and 2.5 km/h) in LOPES II with different support levels (0%, 10% and 100%). The optical tracking data was sampled at a rate of 90 Hz. In post processing data was filtered for spikes (50 mm), gaps up to 30 samples were interpolated, data was low-pass filtered with a second-order Butterworth filter at 10 Hz. The LOPES controller data (recorded at 1024 Hz) and optical data were re-sampled to 100 Hz, synchronized and cut into steps. Segment angles and positions were calculated from the positions of the markers on the subject (subject marker data). We also calculated the segment angles and positions from the markers on the LOPES structure (LOPES marker data).

To assess the inaccuracies we calculated the root mean square error (RMSE) between LOPES controller data and LOPES marker data. Subsequently we calculated the position accuracy up to the clamps i.e., the RMSE between the LOPES controller data and LOPES marker data, to assess the inaccuracy caused by the control loop and mechanical structure (e.g., free play and mechanical compliance).

The RMSE between LOPES controller data and subject marker data is 1–2 degrees for the segment rotations and 7–8 mm for pelvis translations (see figure 9.6). Although the subjects are firmly strapped in LOPES II, a great part of the error can be attributed to the clamps and human tissue: for the pelvis ML translation, the position accuracy up to the clamps is

---

<sup>1</sup>Part of this section is taken from Appendix C

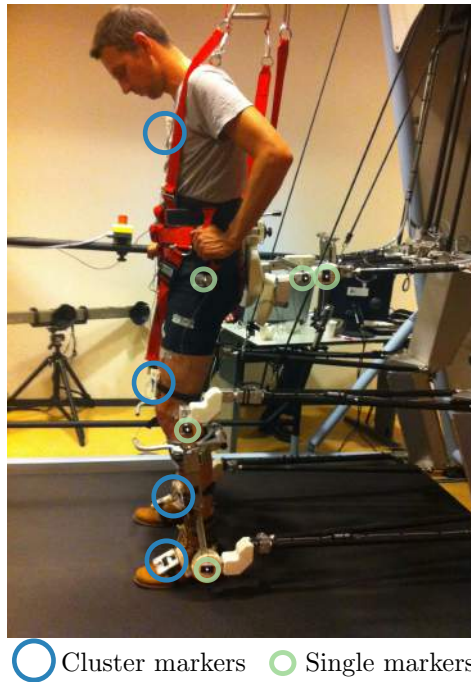


**Figure 9.5:** Subject in LOPES II. Markers are placed on both the subject and on the LOPES structure, to measure the position inaccuracy, caused by mechanical compliance in the LOPES structure and by the clamps and human tissue.

2 mm. Therefore we conclude that the compliance of the harness and human tissue are the main contributors of the position inaccuracy. In AP direction, the position accuracy up to the harness is 5 mm. In AP direction, the connection is much stiffer than in ML direction, and only accounts for 2 mm of the inaccuracy. For the shank, the accuracy up to the clamps is 1 degree, which is half of the total position accuracy of the shank rotation.

For further examination we look in detail at the data from a single case i.e., subject 2 walking at 2.5 km/h (see figure 9.7a). In the time plot we see some discrepancy between LOPES controller data and Subject marker data. This implies that there is a certain inaccuracy in the reconstruction of the patient segment angles and positions from the motor angles. The fact that the LOPES marker data and the LOPES controller data show larger similarity indicates that the inaccuracy is largely caused between the clamps the human skeleton structure. When observing the agreement plots (error versus average) (Altman and Bland, 1983) (see figure 9.7b) we see

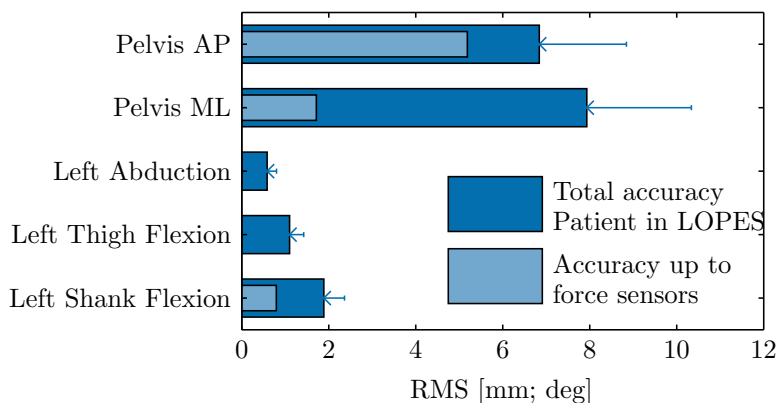


**Figure 9.6:** Dark: Root mean square error between LOPES controller data (segment angles and position calculated by LOPES II) and markers on the subject; Light: RMSE between LOPES controller data and markers on the LOPES structure (near the clamps).

that the position error is position and direction dependent. For the shank flexion the agreement between LOPES controller data and subject marker data show near vertical edges at the maximum and minimum flexion. This indicates that there is free play: as the direction of motion changes (from maximum flexion or extension back to the zero flexion) the error (difference between LOPES controller data and subject marker data) changes rapidly because of the free play.

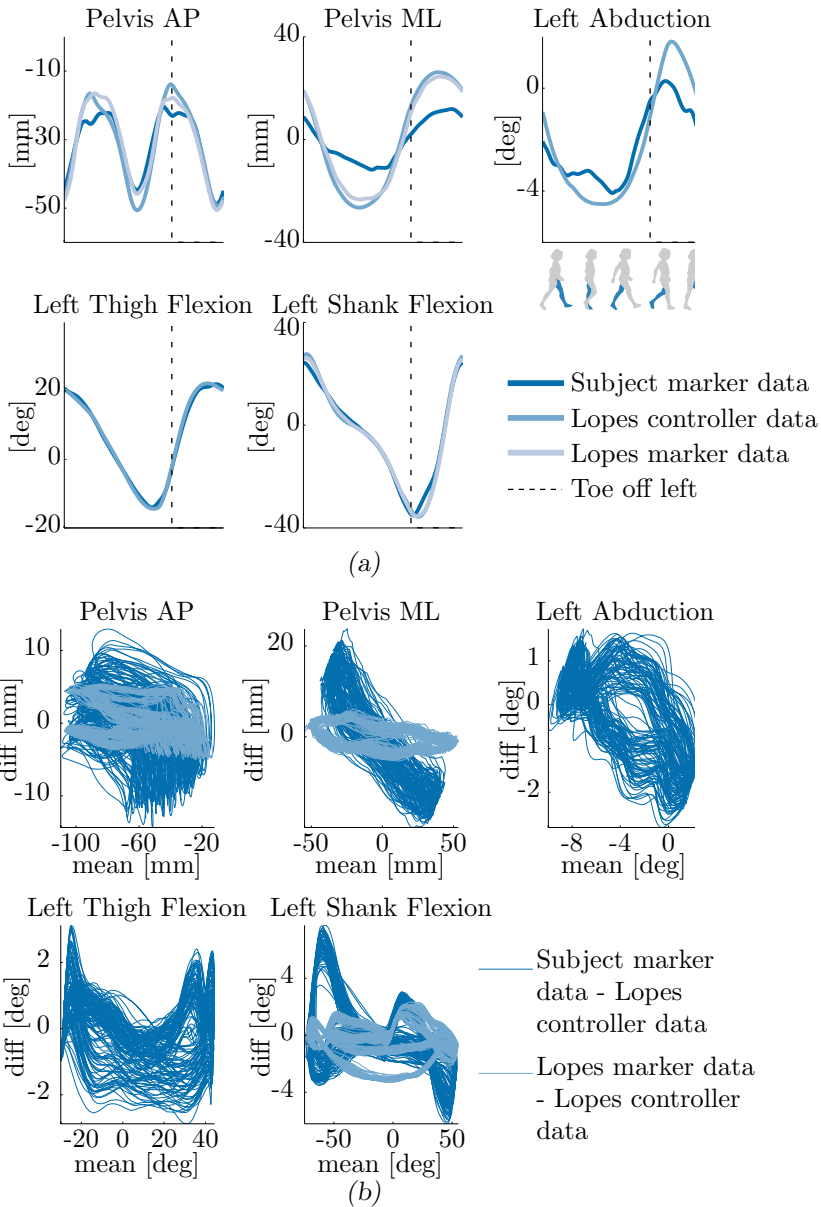


**Figure 9.7:** Subject 2, walking at 2.5 km/h in LOPES II with full support. Joint and segment trajectories are calculated from marker data on the subject (Subject marker data), markers on the LOPES structure near the clamps (LOPES marker data) and by LOPES II from motor angles (LOPES controller data). (a): Average pelvis and joint trajectories; (b): Agreement plots (difference versus average) of LOPES controller data and Subject marker data (dark blue); and of LOPES controller data and LOPES marker data (light blue).

## 9.7 Minimal Impedance<sup>1</sup>

The minimal impedance mode (MI) of LOPES II (0% support) was evaluated by comparing gait patterns of the subjects walking in minimal impedance mode in LOPES II with free walking (FW) on a treadmill. We used the same marker layout and waling velocities as described in section 9.6.

Gait patterns in minimal impedance mode resemble gait patterns of free walking (see figure 9.8). For the joint angles and trunk and pelvis ML motion, the correlation between minimal impedance and free walking is high ( $> 0.8$ , see table 9.7), and the RMSE of the difference of the gait patterns is a few degrees. For trunk and pelvis AP motion the correlation is lower, especially at higher speeds.

An explanation for the difference in correlation between pelvis AP and ML motion can be found in the acceleration. The acceleration in AP direction is higher (see Appendix B) and consequently the interaction forces (needed to accelerate the virtual mass) are higher. This is confirmed by the force patterns in figure 9.8 and the peak-to-peak values of the interaction forces (see table 9.8). For the joints the interaction torques are considerably lower during swing than during stance (see table 9.8). Although the accelerations of the swing leg are higher than the accelerations of the stance leg, the virtual mass during swing is considerably lower than during stance (see table 9.4), and therefore the interaction forces are lower.

---

<sup>1</sup>Part of this section is taken from Appendix C

**Table 9.7:** Correlation (top) and RMSE (bottom) of gait patterns between free walking and minimal impedance walking for two subjects at two speeds.

	S1		S2	
	1.5 km/h	2.5 km/h	1.5 km/h	2.5 km/h
Pelvis AP	0.84	0.33	0.91	0.62
Pelvis ML	1	0.82	0.96	0.99
Trunk AP	0.75	0.61	0.86	0.35
Trunk ML	1	0.80	0.93	0.95
Left abduction	0.95	0.84	0.93	0.88
Left hipflexion	1	0.98	0.99	1
Left kneelexion	0.99	– <sup>a</sup>	0.99	0.99
Left plantarflexion	0.87	– <sup>a</sup>	0.9	0.82
Pelvis AP [mm]	12.3	11.9	9.2	10.9
Pelvis ML [mm]	3.4	11.0	7.2	2.7
Trunk AP [mm]	4.3	5.0	4.9	5.7
Trunk ML [mm]	11.5	12.9	14.4	5.7
Left abduction [deg]	1.3	1.6	1.6	1.5
Left hipflexion [deg]	1.0	2.6	1.2	1.4
Left kneelexion [deg]	2.4	– <sup>a</sup>	2.3	2.7
Left plantarflexion [deg]	3.5	– <sup>a</sup>	3.7	4.6

<sup>a</sup>Too many missing markers on the left shank

**Table 9.8:** Peak-to-peak interaction forces/torques in minimal impedance walking for two subjects at two speeds. For abduction, hip flexion and knee flexion, the interaction torques are split in swing phase (Sw.) and stance phase (St.)

		S1		S2	
		1.5 km/h	2.5 km/h	1.5 km/h	2.5 km/h
Pelvis AP [N]		107.6	169.2	125.7	266.8
Pelvis ML [N]		55.2	76.1	52.0	87.6
Left abduction [Nm]	Sw.	3.3	7.8	5.4	18.1
	St.	14.2	13.6	8.4	28.9
Left hipflexion [Nm]	Sw.	20.6	33.3	21.9	39.8
	St.	32.9	69.1	41.3	99.3
Left kneelexion [Nm]	Sw.	8.4	8.7	12.8	22.6
	St.	9.0	21.1	14.2	29.2

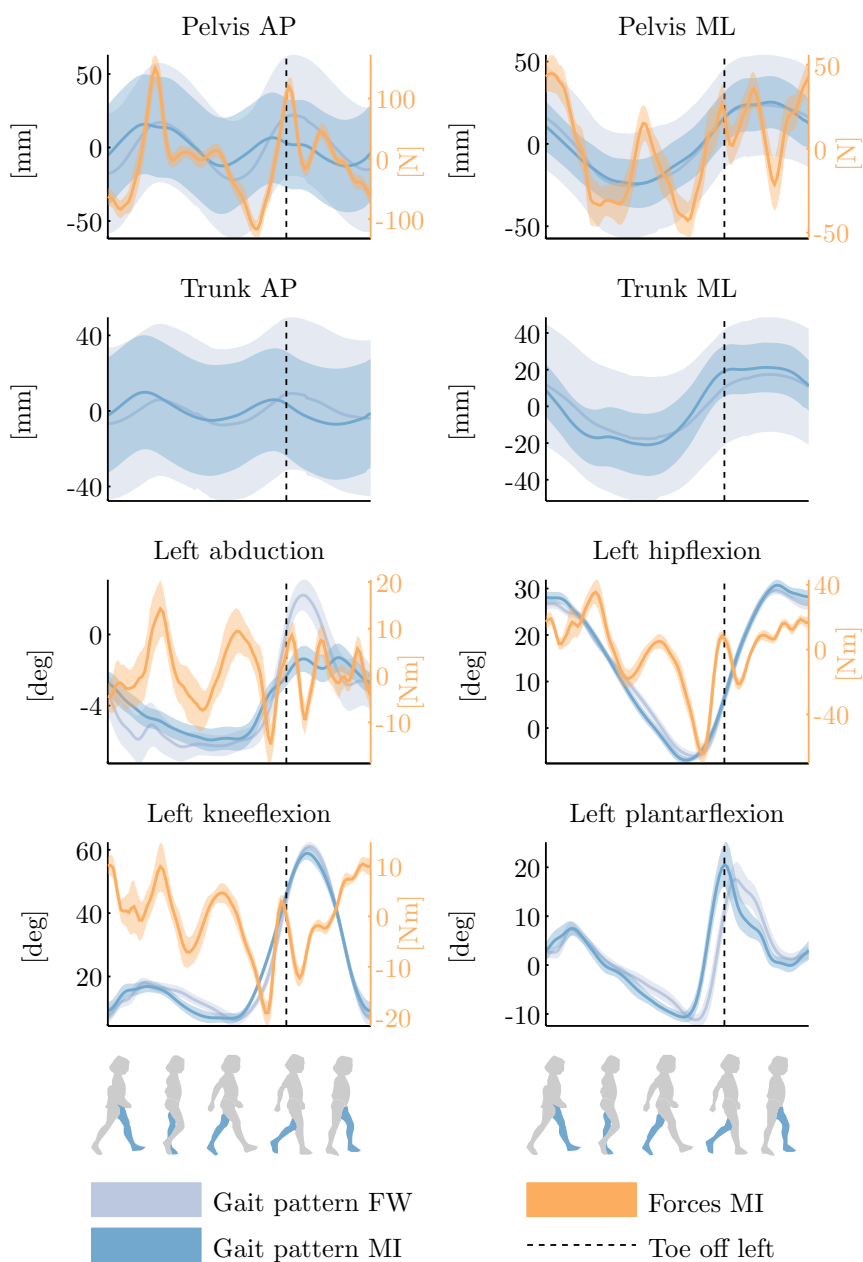


**Figure 9.8:** Gait pattern of subject 2 at 2.5 km/h free walking outside LOPES II on a treadmill (FW) (light blue), and in LOPES II with minimal impedance (MI) (dark blue); Interaction forces in MI are plotted red; Toe-off left is indicated by the dashed line; at the left of the toe-off line, the left leg is in stance; at the right of the toe-off line, the left leg is in swing.

## 9.8 Selective Support — Pilots with patients<sup>1</sup>

We performed exploratory studies with stroke survivors and SCI patients. We will discuss three extreme cases: a severely impaired SCI patient (lesion level C1, FAC 0), and two mildly impaired stroke survivors (FAC 5).

The first case we discuss here, is a SCI patient (FAC 0; 114 kg) walked in LOPES II with a general support of 80 % and 40 % bodyweight support (BWS) at 0.7 km/h (see figure 9.9). The patient's joint angles and pelvis translations followed the reference trajectories. Since the support is implemented as springs, the interaction forces are largely proportional to the tracking errors. This is reflected in the pelvis AP force: the subject was leaning backward (negative interaction force). Consequently the measured trajectory of pelvis AP was a little behind its reference trajectory. This also resulted in more abduction of the left leg, especially during left stance phase: interaction torque of 40 N m and a tracking error of 2 deg. In swing the subject is able to follow the reference trajectory: the interaction torque and tracking error approach zero.

The second case, is a stroke survivor (FAC 5) who walked in LOPES II at 1.5 km/h, first with 10 % support and 0 % BWS. The subject showed a stiff-knee gait on the right leg and used a little circumduction (5 deg abduction) as compensation strategy. Subsequently we applied selective support on the foot clearance, i.e., support (high stiffness) on the paretic knee flexion during the swing phase. The paretic knee showed an increased knee flexion from 42–51 deg (see figure 9.10). Despite the increased support in knee flexion during the swing phase, the interaction torque did not increase. This can be attributed to an intuitive response of the subject to minimize the interaction force. Though the support occurred only during the swing phase, the pelvis ML translation increased to the paretic side and the paretic adduction increased during stance phase of the paretic leg. This indicates that the subject took more weight on the paretic leg, during support on toe clearance.

Next we added selected support on the weight shift. This means that the stiffness for pelvis ML and for the abduction/adduction of both legs was increased for the complete gait cycle. The pelvis ML motions increased (see figure 9.10). Contrary to the support on foot clearance, the subject did not minimize the interaction forces. Due to the increase in stiffness in

---

<sup>1</sup>Part of this section is taken from Appendix C

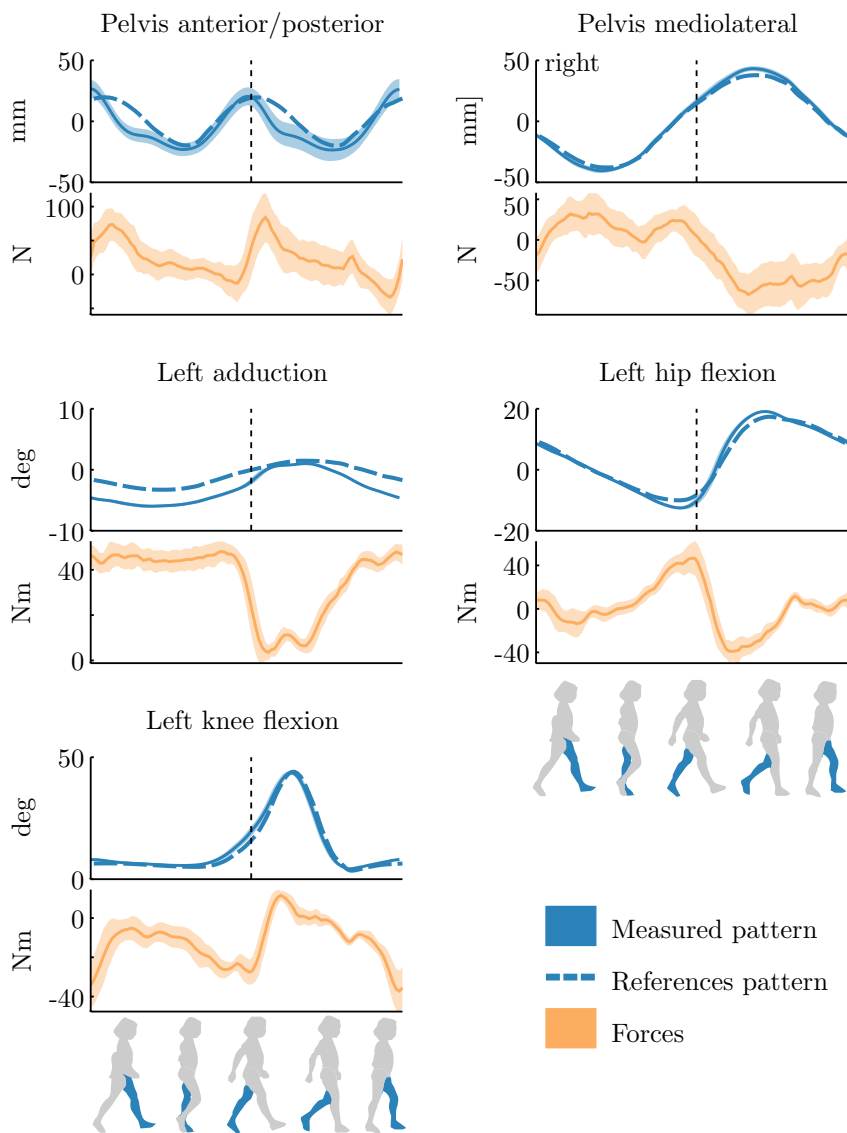


**Figure 9.9:** Gait pattern and interaction forces of a 114 kg SCI patient (FAC 0) walking in LOPES II with 80 % support and 40 % bodyweight support at 0.7 km/h.

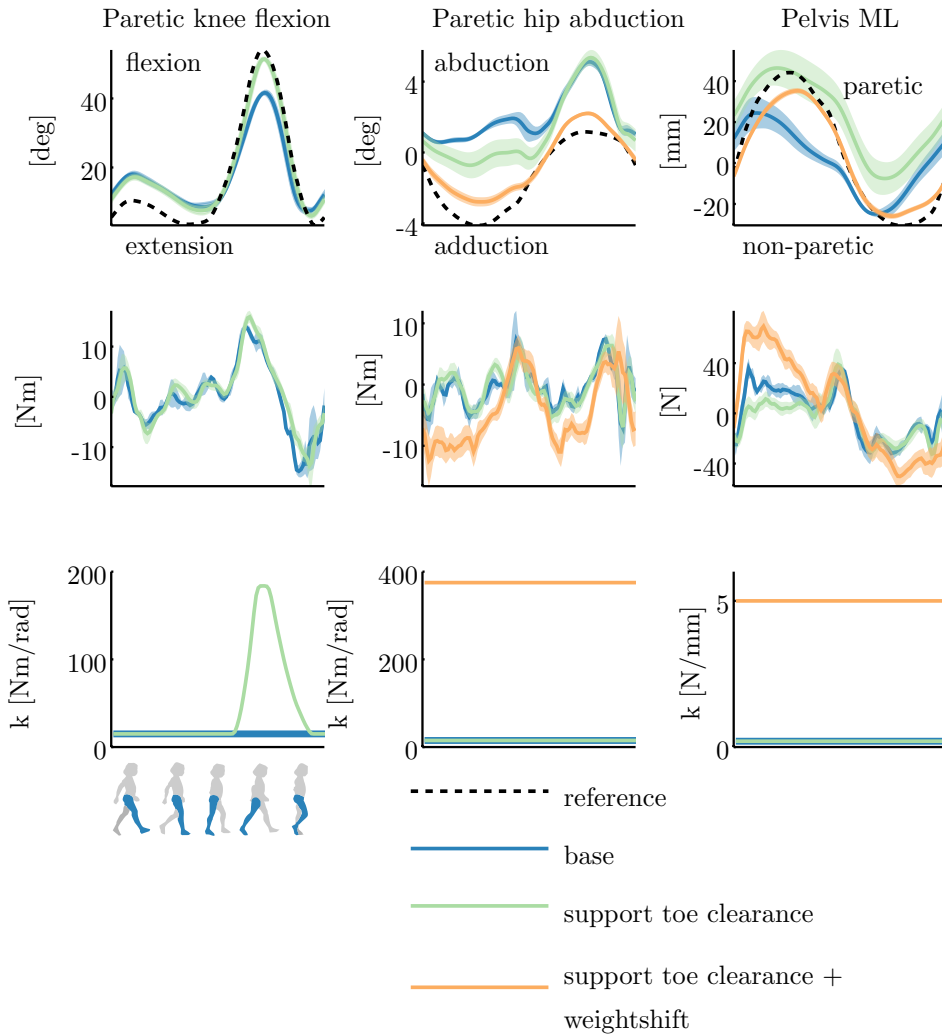


**Figure 9.10:** Assist As Needed with a chronic stroke survivor (FAC 5), 1.5 km/h. Joint angles, interaction torques and virtual spring stiffness are shown for different support conditions. The spring stiffness is denoted by ‘ $k$ ’, the spring’s reference trajectory denoted by ‘reference’. For clarity we omitted the support toe clearance plus weight shift (red line) for knee flexion plots, since the lines are similar to the lines of support toe clearance.

abduction, the paretic abduction decreased to 2 deg, partially canceling the circumduction.

A third case we discuss here is a stroke survivor with left side paresis,

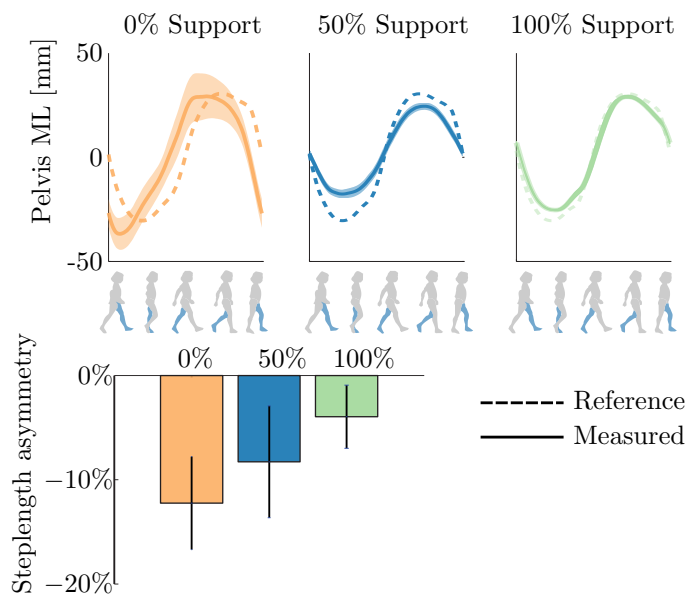


**Figure 9.11:** Stroke survivor (FAC 5) walking with 0 %, 50 % and 100 % support in weight shift only at 1.5 km/h. Above: trajectories of pelvis in mediolateral direction; below: step length asymmetry.

FAC 5, walking at 1.5 km/h. The patient shows asymmetric step length (12 % asymmetry, baseline). When only support in the weight shift is applied, this not only affects the mediolateral pelvis motions, but it also decreases the asymmetry in step length (see figure 9.11). The support in weight shift encourages the patient to bear more weight on the paretic leg.

## 9.9 Interaction Forces

This section gives a further analysis of the interaction forces. From the sessions with healthy subjects and patients, we have recordings of the interaction forces ( $\vec{F}_{meas}$ ), segment angles ( $\vec{x}$ ), speeds ( $\dot{\vec{x}}$ ), and acceleration ( $\ddot{\vec{x}}$ ). Additionally we know the settings of the virtual objects and the virtual mass, and thus we can calculate how much each object contributes to the interaction forces.

The guidance force is executed by a spring. The spring force  $\vec{F}_{spring}$  is dependent on the stiffness, damping ratio, spring position and velocity (see section 8.9)

For the inertial forces from the admittance controller we have :

$$\vec{F}_{mass} = M(\vec{x}, C\vec{o}P) \cdot \ddot{\vec{x}} \quad (9.1)$$

where the mass matrix  $M$  contains inertia scaling which is dependent on the foot positions (derived from  $\vec{x}$ ) and the recorded center of pressure ( $C\vec{o}P$ ) on the treadmill.

Finally there is a default damper (see table 9.5) active in LOPES II, causing force  $F_{damp}$ .

For two cases we compare these object- and inertia forces with the measured interaction forces. First we examine the gait pattern and interaction forces of a healthy subject walking in LOPES II with 10% support at 2.5 km/h (see figure 9.12). The sum of the virtual forces (from virtual objects and masses) largely matches the measured interaction forces. This means that the interaction is almost completely account for the interaction forces. However there are a few parts of the gait where the sum of the virtual forces does not match the measured force i.e., the knee extension in late stance, and the hip extension in late stance (see figure 9.12). This mismatch is caused by the joint limiters. When the hip approaches the maximum hip extension (14deg, see table 9.2), the limiter starts to decelerate the hip. The limiting torque is distributed over the DoFs (see section 8.7.2), and therefore also causes an acceleration on the shank, and thus the knee. The limiter states are not recorded, and therefore we cannot reconstruct the limiters' braking forces. This unknown limiting force now 'pollutes' the inertia force, since this force is simply the product of the acceleration and the mass matrix, and therefore the deceleration by the limiter is falsely plotted as a force due to the acceleration of the virtual mass.

For the healthy subject the support is low, and therefore the interaction forces are largely caused by the inertia forces. At the pelvis in AP and ML direction a small part of the interaction force is generated by the default spring and damper (see table 9.5). Furthermore we see oscillations in the interaction force in nearly all DoFs.

Second we examined the gait pattern and interaction forces of an SCI subject walking in LOPES II with 80% support at 0.7 km/h (see figure 9.13). The sum of the virtual forces largely matches the measured interaction forces. Only in around the left toe off, there is a mismatch, probably due to the hip extension limiter, as described in the case with the healthy subject. Since the speed is low, the accelerations are low, and consequently the inertial forces. The largest part of the interaction force comes from the support force. Furthermore the oscillations in the interaction force are much smaller compared with the healthy subject at higher speed and lower support.

Summarizing, when the support is low and the speed is high, the interaction force consists mainly of inertial force i.e., the force that is needed to accelerate the virtual mass of the admittance controller. When support is high and the speed is low, the interaction force mainly consists of support force i.e., force caused by the guidance spring to provide support to the subject. For the rotations of the leg segments we see that in the low support - high speed case the interaction forces are lower than during the high support - low speed case. However for the pelvis forces the interaction forces in the low support - high speed case are higher than in the high support - low speed case. This is caused by the high inertia of the admittance controller in the pelvis translations.

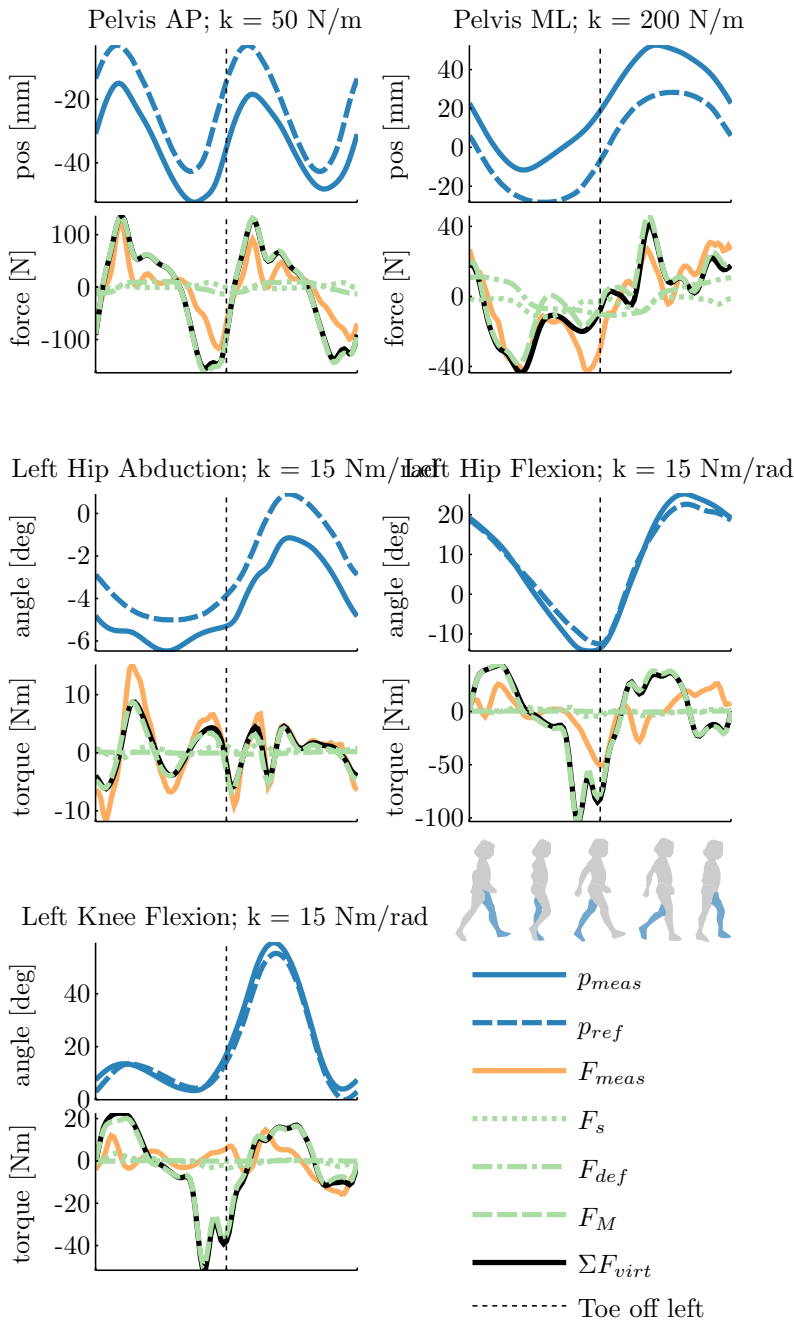


**Figure 9.12:** Joint trajectories and interaction force / torque of a healthy subject with 10% support at 2.5 km/h. The support spring trajectory is denoted by  $p_{ref}$ ; the support spring force is denoted by  $F_s$ ; the force of the default damper and spring is denoted by  $F_{def}$ ; the inertia force is denoted by  $F_M$ ; and the sum of all virtual forces is denoted by  $\Sigma F_{virt}$ .

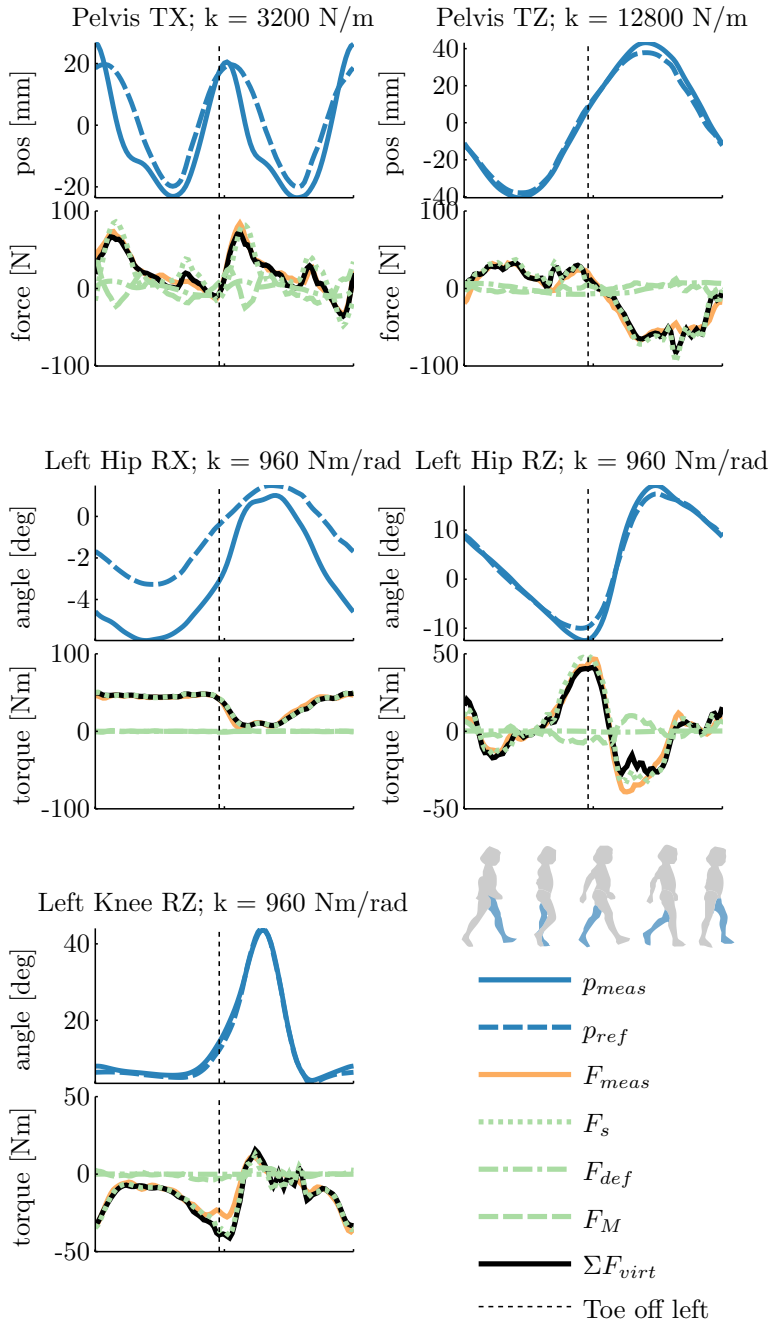


**Figure 9.13:** Joint trajectories and interaction force/torque of an SCI patient with 80% support at 0.7 km/h. The support spring trajectory is denoted by  $p_{ref}$ ; the support spring force is denoted by  $F_S$ ; the force of the default damper and spring is denoted by  $F_{def}$ ; the inertia force is denoted by  $F_M$ ; and the sum of all virtual forces is denoted by  $\Sigma F_{virt}$ .

## 9.10 Donning Time<sup>1</sup>

We recorded the donning time for several stroke patients (N=13) with Functional ambulation category (FAC) scores ranging from 0 to 4. The donning procedure for patients who perform training with LOPES II for the first time consists of five steps: 1) the therapist measures the length of the upper leg, lower leg and foot length; 2) the measured data and other patient data e.g., weight, posture is fed into computer; 3) the patient is prepared to get into LOPES II i.e., getting to stand from wheelchair, optionally apply a sling for the paretic arm and put into standing position. For patients with FAC 0 the harness is applied in the wheelchair and the body weight support (BWS) system is used to lift the patient out of the wheelchair into LOPES II. Additionally the leg guidance (see figure 6.3) is set to the length of the lower leg; 4) the therapist straps the patient in LOPES II. This is done while the patient is standing, if needed the BWS is used; 5) LOPES II is put in an active mode from which the training can start.

For recurring training, steps one and two of the donning procedure are not needed, since the settings are stored in the database, resulting in a shorter donning time. Therefore we did a recording of the recurring donning time for six patients.

The average first donning time is eleven minutes and two seconds. The average recurring donning time is six minutes and four seconds (see figure 9.14). For patients with FAC 2–4 the donning time for first training meets the goal of 10 minutes. For patients with FAC 0 donning time was longer (14–15 minutes), due to the use of the lift. For recurring trainings (no limb measurement needed) the donning time was 5–8 minutes. This approaches the desired donning time of 5 minutes for recurring patients. A limitation is that no data was available of recurring training of FAC 0 patients. There seems to be a trend that a higher FAC score shortens the donning time, but there were too few measurements to statistically confirm this trend.

## 9.11 Usability

The ultimate evaluation is the validation. “did we build the right LOPES?” This question must be answered by the users.

---

<sup>1</sup>Part of this section is taken from Appendix C

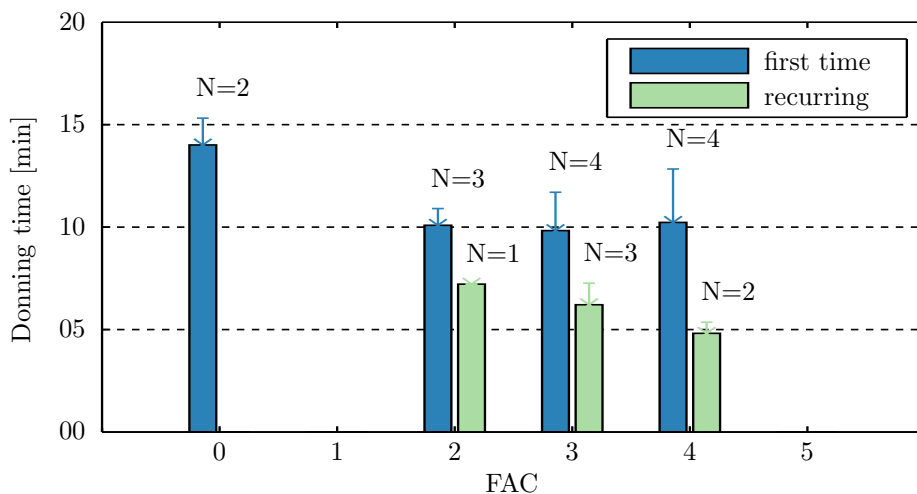


**Figure 9.14:** Donning time grouped by FAC score and separated in first training and recurring training. For FAC 0 a lift was used to transfer the patients from wheelchair to LOPES II.

### 9.11.1 Questionnaire

We use the System Usability Scale (SUS) (Brooke, 1996) to ask users their opinion on several aspects of the use of LOPES II. The SUS uses a generic questionnaire with ten questions, that can be answered with a five point scale. For the questions, see appendix H. The SUS aims to rate the following properties of the device:

- Effectiveness  
Can users successfully achieve their objectives?
- Efficiency  
How much effort and resource is expended in achieving those objectives?
- Satisfaction  
Was the experience satisfactory?

In addition to the SUS we asked the user's function (e.g., therapist, patient, researcher) and we left room for extra remarks. We asked our contacts in the rehabilitation centers to spread the questionnaire amongst people who had worked with LOPES II.

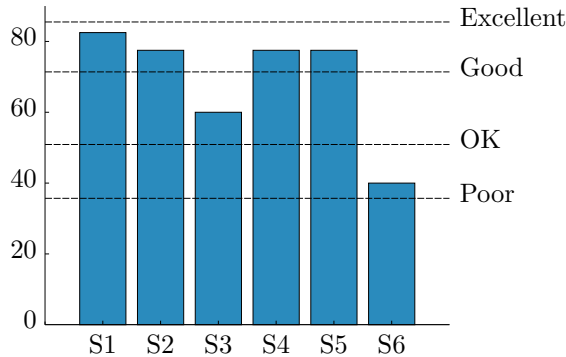


**Figure 9.15:** Usability of LOPES II, according to six users, with qualitative comparison (Bangor et al., 2009)

### 9.11.2 Results

We received answers from six respondents, five therapists and one researcher. One of the reasons for this low number, was that the questionnaire started after the pilot studies. Many of the patients who participated in the pilot studies, were no longer in the rehabilitation centers when we performed the questionnaire, and thus we could not contact them for the questionnaire. A second reason was, that only a small group of therapists had been trained to use LOPES II at the time the questionnaire was taken. The answers of the questionnaire are converted to a ranking (see figure 9.15). For interpretation of the ranking we use the qualification from Bangor et al. (2009).

The ranking shows large variance, ranging from 40 to 82.5. The qualitative interpretation ranges from ‘poor’ to ‘excellent’. Apart from respondent six, the ranking is positive.

## 9.12 Discussion

### 9.12.1 Stiffness and Position Accuracy of LOPES II

Measurements of the static stiffness between the actuators and the force sensors showed that LOPES II is not as stiff as required. Furthermore we measured the position accuracy of LOPES II, i.e., how accurate can LOPES II measure the patient segment positions from the motor angle data. The position accuracy of the pelvis in AP and ML direction is 7–8 mm RMSE, and for the joint rotations 1–2 deg. Partially the inaccuracy can

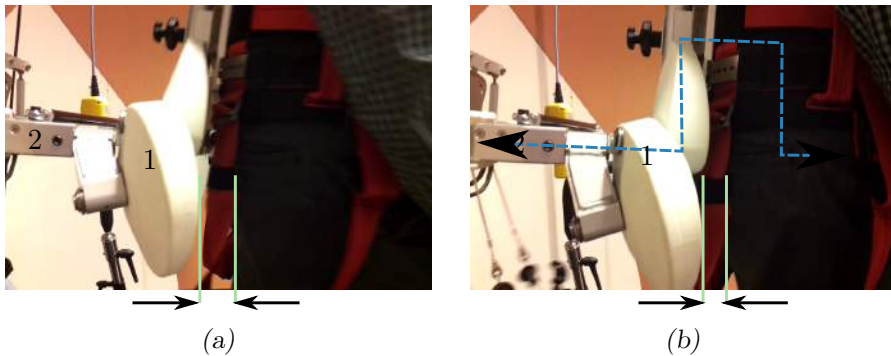


**Figure 9.16:** Pictures of the pelvis, hip gimbal (1) and force sensor (2), when a subject walks in LOPES II, just before toe off (a) and just after toe off (b). The gap between the gimbal and the buttocks changes (distance between green lines). The blue dotted line indicates the ‘force connection’ between force sensor and hip, i.e., the physical connection that transfers the force.

be explained by the limited, static stiffness between motor and force sensor. However a greater part of the inaccuracy is due to the compliance between the force sensors and the human skeleton structure. This includes gimbals (at hip and ankle), clamps (foot bracket, leg clamp, harness) and human tissue. Although the subjects were firmly strapped in LOPES II during the trials, there was no rigid connection between LOPES II and the patient’s skeleton structure i.e., the clamping of the patient’s feet, legs and pelvis was not stiff enough.

The average trajectories and agreement plots (see figure 9.7) give some insight in the nature of the inaccuracy. For pelvis AP translation, small, short oscillations are visible in the average trajectory at maximum pelvis translations around heel strike (see figure 9.8). This means that there is mechanical compliance or free play between the force sensor and the (markers on the) pelvis. Stills from a video recording reveal that there is free play between the gimbals and the pelvis (see figure 9.16). The hip gimbals are connected to the harness at a relatively high point (belly button height). This means that the connection between the force sensor takes a ‘detour’ (see figure 9.16). The connection between the force sensor and the subject’s pelvis contains several elements that show free play i.e., the sleeve bearings in the hip gimbal and, the connection plate in the harness. That this connection is not rigid is clear around heel strike and toe off, when the human pelvis (and hips) suddenly accelerates. Then the speed of the pelvis

changes sign, then the free play changes direction and the (high) virtual mass of the pelvis AP hits the end of the free play, resulting in a push against the subject. This causes an oscillation on the patient pelvis in AP direction. This makes that the patient perceives a push at the pelvis at each step.

We compare these values with the required accuracies (see table 5.4). For pelvis translations we stated a required accuracy of 2 mm. For both pelvis anterior / posterior (6.8 mm) and pelvis mediolateral (7.9 mm) LOPES II does not comply. For hip abduction / adduction the required accuracy is 1.41 deg and the accuracy of LOPES II is 0.6 deg. For hip flexion / extension the required accuracy is 2.34 deg and the accuracy of LOPES II is 1.1 deg. We can not compare the shank angle accuracy with the required accuracy for knee flexion / extension, but the given the (required knee accuracy 3.42 deg, achieved shank angle accuracy 1.9 deg) we believe that the shank accuracy complies with the required accuracy. Summarizing the accuracy of the segment angles calculated by LOPES II is less than normal intra-subject variability.

Improvement of the position accuracy requires improvement of the stiffness and reduction of the free play in the structure. We found free play in the sleeve bearings in several places in the linkage. Although the free play for each component is low (estimates of 0.1 – 0.5 mm), the sum of all components add up to considerable free play. Furthermore the gearing of the linkage magnifies the free play in some cases e.g., for the shank rotation, the free play at the end of the motor is amplified five times at the ankle displacement. Finally a more rigid connection between the LOPES structure and the patient skeleton structure is desired. This requires an improvement of the clamping at the pelvis, legs and feet.

### 9.12.2 Transparency of the Admittance Controller

We use an admittance controller for the control of LOPES II. With most DoFs the achieved impedance is (almost) as low as required (see table 9.4). However there are several remarks to be made here. First, for the pelvis translations, the virtual mass is roughly seven times higher than required.

Second, admittance control bears the promise that the dynamic mass between the actuator and the force sensor can be reduced. In our experience with the HapticMASTER we found a reduction is of factor of ten for the vertical axis (physical mass 30 kg, virtual mass 3 kg). However, according to Colgate and Hogan (1989) a factor two is maximum, when passivity must

be guaranteed. In LOPES II no reduction seems possible, and for the pelvis translations, the admittance mass is even larger than the physical mass. We have no solid explanation for these high virtual masses, however, we believe that mechanical compliance and free play in the linkage and clamps are (partially) liable (see figure 9.16). The lack of transparency was confirmed by the subjects who noted that LOPES II was pushing them during walking in minimal impedance mode. Especially in pelvis AP direction, disturbing forces were perceived. The measured interaction force at the pelvis confirms this, since this force shows damped oscillations, which are triggered at each heel strike (see figures 9.8 and 9.12). At higher speeds the accelerations and consequently the inertial forces are higher and therefore more disturbing. Also the other DoFs have some free play (see table 9.1), and they also show oscillations, particularly at higher speeds (see figure 9.12). However due to the coupled nature of the masses of LOPES II (both physical mass and controller mass), oscillations in one DoF may induce oscillations in other DoFs. We believe that the transparency of LOPES II is currently limited due to the free play and the limited stiffness.

The limitations on the transparency suggest that impedance control might be the better strategy for LOPES II, since for pelvis translations the mechanical mass is lower than the virtual mass. However, for foot translations total physical mass between motor and patient is higher (2.7 kg for ankle TX, 4.5 kg for ankle TZ) (see table 7.1) than the perceived mass of the admittance controller (2.2 kg for ankle TX and 2.4 kg for ankle TZ), and thus for these DoF a (small) reduction of the mass is possible. Furthermore, the stick-slip friction in the rod-ends and the friction in the actuator gearbox, would be perceived by the user when using classic open loop impedance control i.e., without compensation for plant dynamics and friction. This will have a detrimental effect on the perceived transparency of LOPES II. Friction compensation can limit the negative consequence of friction. The force sensors on the actuators may be used to compensate for the gearbox friction. A second concern with impedance control is the limited maximum impedance. As described in section 8.2, the stiffness of impedance controllers is limited. Therefore an impedance-controlled LOPES II may not be sufficiently stiff.

Another strategy is to extend the admittance controller with a time-based passivity controller to suppress instabilities (Hannaford and Ryu, 2002). Further research will have to deliver the optimal control strategy that provides both sufficient transparency and high stiffness control.

**Table 9.9:** Controller stiffness of LOPES II.

DoF	Maximum stiffness
Pelvis AP	5 N/mm <sup>a</sup>
Pelvis ML	20 N/mm
Abduction	1500 Nm/rad
Thigh flexion	1500 Nm/rad
Knee flexion	1500 Nm/rad

<sup>a</sup>The controller is capable of rendering higher stiffness ( $> 20$  N/mm), but we chose 5 N/mm since this felt more in balance with the stiffnesses of the other DoFs.

### 9.12.3 Maximum Impedance Admittance Controller

For nearly all DoFs LOPES II can supply the required force / torque (see table 9.6). Only for the shank, the required torque was set to 134 N m, whereas LOPES II can only deliver 70 N m. This performance limit is caused by the continuous torque the motor and drive can supply. For short duration, higher torques can be supplied, but this is not incorporated in the renderer's torque limit yet.

In the pilot trials this has caused a limitation in only a few cases. In one case a large ( $> 100$  kg) SCI patient showed strong spasms on the knee. During support in knee flexion in swing phase, LOPES II support was clipped to 70 N m. This implied that LOPES II was not able to give sufficient support in toe clearance, whereas a stronger LOPES II may have been able to do so. We believe that the performance limit of 70 N m is sufficient for the majority of the targeted patients, but in order to train a wide variety, the performance must be increased. However 140 N m seems too much. Therefore we propose a requirement of 100 N m for the next generation of RAGT.

With trial and error we established the maximum stiffness LOPES II should have in the Robot in Charge mode (100% support) (see table 9.9).

### 9.12.4 Speed

Walking in LOPES II is currently limited to 3 km/h, whereas  $> 5$  km/h was required. We limited the speed, because walking at higher speeds causes oscillations in LOPES II, as described in the section 9.12.2. We believe that if the transparency is increased, walking at higher speeds in LOPES II is possible.

**Table 9.10:** Maximum segment speeds at fast walking derived from the Winter data ( $\omega_{max}^{50\%}$ ) and an estimate of the 95 % C.I. of the maximum segment speeds ( $\omega_{max}^{95\%}$ ).

	DoF	$\omega_{max}^{50\%}$ [rad/s]	$\omega_{max}^{95\%}$ [rad/s]
Thigh sagittal rotation (min / max)		3.2	5.8
Shank sagittal rotation (min / max)		7	10
Foot sagittal rotation (min / max)		9	12

Increasing the transparency may not be sufficient to assure a higher walking speed. Currently the speeds of the joints are currently barely sufficient for fast walking (see table 9.3). However in the calculation of the speed requirements, we had no data on the standard deviation of speed, and consequently we could not calculate the 95 % confidence interval (C.I.) for speed. Due to the lack of data on segment speeds, we differentiated the average segment angle patterns derived of fast walking from the Winter data (see figure 5.2). In hindsight we could have made an estimate of the 95 % C.I., by multiplying the average maximum speed with a gain  $\lambda > 1$ , based on the ratio of the average RoM and the 95 % C.I. RoM:

$$\lambda = \frac{RoM_{\mu \pm 2\sigma}}{RoM_{\mu}} \quad (9.2)$$

$$\omega_{95\%CI}^{max} \approx \lambda \omega_{\mu}^{max} \quad (9.3)$$

The values for  $\lambda$  for the thigh, shank and foot are 1.8, 1.4, and 1.4 respectively. The estimated 95 % C.I. speeds are listed in table 9.10. The actuators are now tuned to their maximum performance. This implies that, if the speeds of the segments should be higher, different actuators or different gearing is required.

### 9.12.5 Selective Support

The goal was to provide robotic gait training for a wide range of patients from mildly to severely impaired. LOPES II is powerful and stiff enough to enforce a walking pattern on a severely affected patient (SCI lesion level C1; FAC0; 114 kg).

We also demonstrated that, on the other side of the spectrum, LOPES II can provide selective support to a mildly affected patients (FAC5). For the first stroke survivor we applied support on toe clearance. This resulted in

the anticipated effect on the supported aspect of gait. The patient seemed to adapt to support on toe clearance since the interaction torques did not change. Remarkably the stroke survivor also showed minor changes in aspects of walking that were not supported directly. We assume that when subjects receive selective support, they adapt different aspects of their gait pattern, also aspects that are not supported directly, to find a new optimal gait pattern. For this process the minimal impedance of LOPES II is paramount, since it gives the patient the freedom to adapt his gait pattern.

For the second stroke survivor we only applied support in the weight shift. This resulted in a change in the supported degree of freedom (pelvis mediolateral). Additionally there seemed to be a transfer to the step length, since the asymmetry in step length decreased with increasing support in weight shift. These cases show that LOPES II is capable of providing Assist As Needed.

### 9.12.6 Usability

In general therapists and patients are enthusiastic about LOPES II. This is confirmed by the usability questionnaire, although the number of respondents (six) is too low to make a solid conclusion on the usability of LOPES II. From respondent five and six we quote parts of the (translated) remarks they filled in at the end of the questionnaire

Quote Respondent five:

*Of the unfortunately limited of trials, the donning procedure was quick, and no re-adjustment during training was needed. The optimization and familiarization of the support by the robot took less time than in Lokomat. The possibilities in controlling the pelvis appear to be therapeutically effective and noticeable when looking at the patient walking, and are also experienced by the patient during and after training. The remark 'I walk like before' is typical for the quality of the individual adaptation possibilities of LOPES II. I find it very regrettable that we cannot use LOPES II in therapy yet [due to regulations], since we know how to work with the device, and it works the way we want, with only little failures*

For the pilot studies we received permission from the Medical Ethical Technical Committee (METC) since the LOPES II prototypes have no medical

certification. The METC approval gave some room to explore the use LOPES II, but due to the regulations, the room is limited.

Quote Respondent six:

*A major disadvantage of LOPES II is that, when re-initialization of LOPES II is needed, the patient must be doffed and donned, before continuing training.*

In the LOPES controllers multiple safety features are active, since we are working with patients in a prototypes. One of the safety features requires a self-test of the system when a guard is triggered. Unfortunately this sometimes happens during training, which is frustrating for both therapist and patient.

Although the two responses are quite different they agree that it is a limitation that LOPES II is still in a prototype stage. Bug fixing and medical certification will have a considerable impact on the usability and will open up the possibilities to use the full capacity of AAN training in LOPES II. The majority of the users agree that LOPES II is promising.



# CHAPTER 10

## Discussion, Conclusion & Future Directions

In this chapter we draw up the balance. We evaluate LOPES II against the original goals, and subsequently we propose some future directions for robot-assisted gait training. Additionally we evaluate the design process of LOPES II.

### 10.1 Goals vs Achievements

To what extent have the set goals been met? This is answered in this section.

The main goal was:

*Design and evaluate Robot-Assisted Gait Trainer LOPES II, suitable for (research on) clinical gait training of severely and mildly affected patients.*

We have developed, built and installed two prototypes of LOPES II. We performed pilot studies with stroke survivors and SCI patients. The efficacy of gait training in LOPES II is currently topic of research in the ZonMW translational research project ARTS.

The prototypes are approved by the Medical Ethical Technical Committee for the pilot studies and for the follow up research. The prototypes do not have medical CE, and therefore they cannot be used in daily clinical practice yet.

A subgoals was to build a device with multiple degrees of freedom. LOPES II has eight powered degrees of freedom: pelvis anterior / posterior and mediolateral, hip abduction / adduction, hip flexion / extension, and knee flexion / extension. Furthermore pelvis rotations, and foot rotations are left free and arm swing is unhindered. This makes it possible to walk in LOPES II with a gait close to normal gait and allow compensatory strategies.

A second subgoal was to perform Assist as Needed training. In pilot studies several patients have tried LOPES II, with walking capability from FAC 0 to FAC 5. The selective support allows for customizing the support to the patient's needs. Severely impaired patients walked in LOPES II with high support on all aspects of gait; mildly impaired patients received little support and on specific aspects only. This implies that LOPES II is capable of facilitating Assist as Needed training.

The last subgoal was to build a *usable* device. The users are enthusiastic about LOPES II. One therapist remarked in the usability study the following:

*I find it very regrettable that we cannot use LOPES II in therapy yet [due to regulations], since we know how to work with the device, and it works the way we want . . . .*

We conclude that LOPES II, despite the shortcomings that are ubiquitous in prototypes, LOPES II is a usable device for assist as needed gait training.

## 10.2 Requirements vs Performance

### 10.2.1 System Requirements

The system requirements are the quantification of the user requirements. In the evaluation we have tested to what extent LOPES II meets the system requirements. In most cases the LOPES II achieved the system requirements, in some cases LOPES II does not comply with the requirements. In this section we briefly discuss the aspects on which LOPES II can be improved.

The goal was that LOPES II is capable to be fully transparent i.e., that it does not affect the patient's gait pattern. The transparency of LOPES II is not as good as required. First, the virtual mass of the pelvis is higher than allowed. Second, when subjects were walking in the minimal

impedance mode, the interaction forces are considerable, particularly at the pelvis. And third, subjects also said that LOPES II is ‘heavy’, i.e., they feel its inertia, particularly at the pelvis. The transparency can be improved by reduction of the free play and increase of the stiffness. Additionally the control of LOPES II may be improved. For instance, the admittance control loop may be extended with passivity strategies (Hannaford and Ryu, 2002) to suppress oscillations, allowing a lower virtual mass. A second strategy is to use the cyclic nature of walking to provide acceleration feed forward on the virtual mass (Van Dijk et al., 2013). Finally alternative control strategies such as impedance control may also provide improvement of transparency, especially in pelvis motions, where the virtual mass of the admittance controller (40 kg) is higher than the physical mass reflected on the pelvis (26 kg). However, friction compensation then is needed, since the friction in the gearboxes is considerable and impedance control may not be able to provide the required stiffness.

The range of motion (RoM) of most Degrees of Freedom (DoFs) is sufficient, however, for some DoFs the RoM is limited. The pelvis anterior / posterior translation is limited to 0.34 m, whereas 0.6 m is required. This slightly limits the freedom for the patient *where* to walk on the treadmill. Also for the hip abduction / adduction the RoM is less than required. The abduction is limited to 11.5 deg, whereas 19 deg is required. This does not affect normal walking, only when using circumduction, the abduction limit may be reached. The adduction is limited to 8.6 deg, whereas 17 deg is required. We have not noticed any hinder from this limitation. The hip extension is limited to 14.3 deg, whereas 28 deg is required. During slow walking (< 2 km/h) this limitation is hardly a problem; at higher speeds, this limit is sometimes reached.

Furthermore walking in LOPES II is currently limited to 3 km/h, whereas 5 km/h was required. This is mainly due to the limited transparency. Therefore we are certain that the faster walking is possible if the transparency is improved.

### 10.2.2 User Requirements

Did we accomplish everything that the users wanted? In this section we reflect on the user requirements as stated in section 2.2.

LOPES II facilitates Assist as Needed, provides weight support and balance support. LOPES II measures interaction forces and joint excursions as needed for assessment, research. The graphical user interface provides

feedback for the patient and the therapist. The therapist can easily adjust the support per aspect of gait. This allows for a flexible training, which is easily adjusted to the patient's needs.

We aimed to develop LOPES II such that training for the patient and the therapist is attractive. The shadow leg structure reduces the need for alignment of the mechanics with the patient and therefore there is no risk of discomfort for the patient due to misalignment. The donning and doffing time of LOPES II is short, allowing more time for training. This is also beneficial for the efficiency of LOPES II.

A few user requirements we did not meet. LOPES II is still a prototype, and therefore not commercially available. The major limitation for this is the medical certification. LOPES II complies with the machinery directive and partially with the standards for medical certification, and was approved by the medical ethical technical committee. However LOPES II is not medically certified. Future development is needed to turn LOPES II into a medically certified, commercially available robot-assisted gait trainer.

### 10.3 LOPES II in Perspective

In chapter 1 we reviewed the existing Robot-Assisted Gait Trainers (RAGT). Now that the LOPES II prototypes are built, we can compare LOPES II with the existing RAGTs (see figure 10.1).

The first generation of RAGTs have limited degrees of freedom and are mainly position controlled (Colombo et al., 2000; Hesse and Uhlenbrock, 2000). These limitations imply that they are less suitable for the mildly impaired patient, who require more degrees of freedom and Assist as Needed. For the severely impaired patients these robots are suitable for imposing the movement of gait. Therefore we group the early trainers as 'Stepping trainers' (see figure 10.1).

The early stepping trainers are slowly evolving into devices with force control (Schmidt et al., 2005; Bernhardt et al., 2005). Additionally the latest Lokomat has an extra powered degree of freedom in the pelvis mediolateral direction. This allows for training of weight shift, however the feet are still fixed in mediolateral direction and therefore the task of mediolateral foot placement, also crucial in balance control, cannot be trained in Lokomat. Several exoskeleton gait trainers have been built that support both weight shift and mediolateral foot placement (Zanotto et al., 2013; Grosu et al., 2012), however, these systems are not commercially available.

Overground exoskeletons are gaining ground in rehabilitation. The HAL by Cyberdyne, Japan (Cyberdyne, 2014), Esko by Ekso Bionics, USA (Ekso-Bionics, 2015), Rewalk by Rewalk Robotics, USA (ReWalk, 2015), and the Indego by Parker Hannifin, USA (Parker-Hannifin, 2015) are all commercially available. These exoskeletons allow for overground walking and provide support in hip and knee flexion/extension, some in ankle plantar/dorsiflexion as well. However, none of them provide support in abduction/adduction, and weight shift. The patient requires crutches to maintain balance. For SCI patients, this is no limitation, but for stroke survivors, this may be difficult, when they have an impaired arm. These limitations make that the overground exoskeletons can only cover a part of the gait training. Combination with bodyweight support extends the possibilities of gait training, since that the patient does not need to use crutches (Cruciger et al., 2014). However this combination does not support weight shift and mediolateral foot placement, and therefore is still limited in the training coverage.

At the other end of the spectrum we see ‘interactive treadmills’ to train subjects by means of treadmills on balance platforms, equipped with virtual reality (MotekforceLink, 2015; Sloot et al., 2014). By means of perturbations subjects are challenged to maintain balance during walking. Optical tracking systems and force plates provide data on the posture of subjects and consequently their quality of balance, which is used as feed back to both the patient and the therapist. This is suitable for patients who can walk without aids i.e., the mildly impaired patients. For the more severely impaired patients this type of training is less suitable, due to the fact that maintaining balance may be too challenging for them. Furthermore they require assistance in making steps, which, apart from bodyweight support, is not incorporated in the balance trainers.

A different kind of trainers are the overground weight support systems (Hidler et al., 2011; Vallery et al., 2013). These devices allow for overground walking with adjustable bodyweight support. The bodyweight support provides a safe environment to practices stepping, and if needed it reduces the weight bearing for the patient. However they provide no support for the leg motions, and therefore only cover a fraction of the required training, especially for the severely impaired patients.

With LOPES II we aimed to cover the complete spectrum. This is partially succeeded. With LOPES II we are able to train in Robot in Charge mode, therefore we are able to cover the spectrum of the stepping trainers. At the other end of the spectrum we partially cover the training

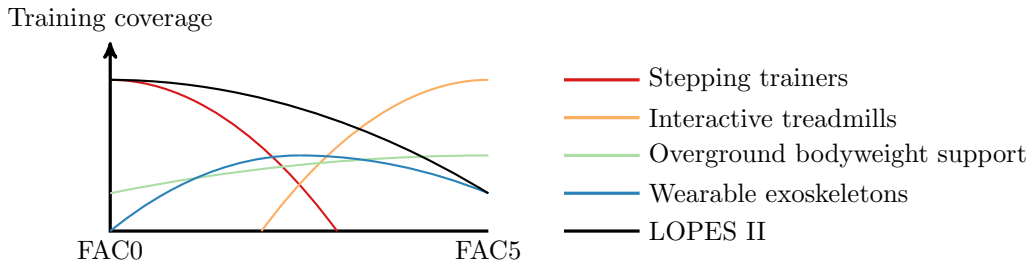


**Figure 10.1:** Suitability (training coverage) of RAGTs as function of FAC.

needs of the mildly impaired patients. With LOPES II balance training is possible, by applying supportive or perturbing forces on the pelvis. The force control and multiple powered DoFs allow for AAN training. The transparency and walking speed of LOPES II are limited and therefore the mildly impaired patients may not have the freedom and speed they require. Improving on the transparency will make LOPES II more suitable for the mildly impaired patients. However LOPES II will not be able to cover all their training needs, such as walking over obstacles and rough terrain, and making turns.

## 10.4 The Design Process

The process of Team Expert Choice helped in discovering the user requirements, but the process as used was fairly rigid. When a set of requirements was chosen for the pair-wise comparison, there was little room to alter the set. The real benefit of TEC was that it encouraged the discussion between different users, not only to sort requirements, but also to trigger brainstorming.

The phase of quick prototypes can be seen as the mechanical equivalent of the software iterations as described in UCD (Gould and Lewis, 1985) and Agile (Beck et al., 2001). UCD revealed negative side effects of new concepts. The first concept of the shadow leg had the risk of pushing subjects in a hollow back. By involving the users in the concept phase this potential risk surfaced. The risk was mitigated by using spherical gimbals which apply force to the hip joints.

Another benefit from the quick prototypes and the TEC is that the physical therapists and patients are involved throughout the design process, and feel responsible for the design as it is. One involved physical

said: “This is our device, we have been involved from the beginning.” The involvement increased mutual understanding between the design team and the end users. It offered the design team the opportunity to focus on what was really important, and the end users understood that some requirements were easier to comply with than others.

The quick prototypes with its iterations ended with an unpowered, one-legged Test Cart. During the detailed design of the mechanics and mechatronics design, there was little room for demonstrations and evaluations by users. We believe that if the user centered approach, i.e., give demos and respond to user evaluations, was extended to the mechatronic design and detailed mechanic design, LOPES II would have been more usable. This implies that we would have mechatronic proofs of principle of (parts of) the test cart. However, this would have required a revision of the project plan, which was not feasible.

It is fair to say that even the process itself was subject to iterations, i.e., the steps as described above were not predefined at the start. The idea to introduce the phase of quick prototypes arose after the second TEC, when the outline of LOPES II was roughly defined, and various concepts were to be evaluated.

Concluding, like in software, iterative design process is suitable for building new devices, where requirements are largely unknown. It is important to realize upfront that iterations and continuous evaluation initially cost time and money, but it helps in building the right product (Travis, 2009). Finally it should be noted, that with the design as described in this thesis, the design process itself is not finished; with the current LOPES II a new tool is available to do further research on robotic aided gait training and this will inevitably lead to new or changed requirements.

## 10.5 Transfer to Other Domains

Not only the above described design process, but also several components of LOPES II may be of interest for other domains. First we will discuss the mechanical components. The push-pull rods offer an attractive solution for mechatronic devices where low-weight and high-stiffness is required. It should be noted that push-pull rods are already widely used in several fields such as aircraft simulators and industrial pick-and-place robots (Delta robots), but scarcely in the field of rehabilitation robots. Push-pull rods in general are stiffer than Bowden cables and less subject to wear. More

specific, the shadow *leg* approach may be converted to a shadow *arm* robotic arm trainers. Similarly to gait trainers, arm trainers donning times will improve when no exact alignment is required.

The patented short skewed axis gimbal allows for (limited) rotations in three dimensions and applies force in a remote center point, without having large mechanics around the center point. In LOPES II the gimbal is applied at the ankle joint and pelvis, to allow for rotations of the ankle and the pelvis and apply supportive forces in the center of the ankle and center of the hip joint. For assistive or therapeutic devices for the upper extremities the gimbal may be useful as well e.g., to apply force in the center of the lower arm or hand, without imposing rotations.

The patented parallel rectangular manipulator is used for the pelvis actuation in LOPES II in anterior / posterior and mediolateral direction. It is a parallel 2DoF mechanism with a nearly rectangular workspace. The actuators are grounded, which makes the mechanism light-weight. For e.g., pick and place applications it is often desirable to have quick, and therefore lightweight mechanisms. When near rectangular workspace is required, the parallel rectangular manipulator may be an attractive solution of pick and place robots.

Of the controller components the method of virtual rod elongation is of use for kinematic transformation of many different mechatronic systems. The method is an iterative method that is capable of calculation the kinematic relations in complex system containing both serial and parallel kinematic chains. Finally the PVA limiter can be used as a set point limiter in any model following device since it offers a robust set point limitation that respects the limits in position, velocity and acceleration. This property makes the PVA limiter also suitable for position control of mechatronic systems.

## 10.6 The Future of LOPES

### 10.6.1 LOPES III

LOPES II generally meets the requirements, but the limited stiffness is deemed as the culprit of the oscillations and limitation of the transparency. In a follow up project we designed and built a follow-up prototype, LOPES III. It has the same wireframe as LOPES II, i.e., the location and length of the rods and levers is unchanged. However we increased the stiffness of the elements that showed the largest mechanical compliance. These

**Table 10.1:** Stiffness  $k$  [N/mm] and free play  $s$  [mm] of LOPES III compared with LOPES II.

	LOPES II		LOPES III		Required
	s	k	s	k	k
Pelvis TX	1	34.7	0.5	32.5	50
Pelvis TZ	1	22.6	0.5	20	50
Knee TX	2.5	14.9	0.5	18	40
Foot TX	7	4.6	2	7	20
Foot TZ	7	3.3	2	5.4	20

elements are related to the shank rotation. Furthermore we removed all sleeve bearings with ball bearings, which are located in several places in LOPES II, affecting all DoFs. These measures are intended to increase the stiffness of LOPES III and most likely improve on the transparency and the position accuracy.

At the time of writing, we have no result on the total performance improvement, however we do have data of the stiffness and free play measurements (see table 10.1). Although the stiffness are still not as high as required, a considerable enhancement of the stiffness of the foot in anterior / posterior (Foot TX) direction and in mediolateral (Foot TZ) direction is achieved. On the knee translation the stiffness is increased slightly, and for the pelvis motions, the stiffness is largely unchanged. Furthermore, the free play is reduced considerably in LOPES III, particularly at the lower extremities.

In LOPES II we also found free play in the connection between the hip force sensors and the patient's pelvis (see section 9.12.1), which we ascribed to the sleeve bearings in the hip gimbal. In LOPES III we replaced the sleeve bearings by ball bearings, and we made a more direct and rigid connection between the gimbal and the patient's pelvis. We have not quantified the improvement, but manual test of the LOPES III components indicate that also here the free play is reduced considerably, and the first tests with control that lower virtual inertia in the pelvis is possible.

We believe that, compared with LOPES II, LOPES III will have better transparency and position accuracy, and that walking at higher speeds is possible, thanks to the improvement in stiffness and reduction of free play.

### 10.6.2 Support Plantar / Dorsiflexion

Support in plantar /dorsiflexion was originally designed and built in LOPES II. However we removed the plantar /dorsiflexion linkage and foot bracket due to its negative impact on the transparency of LOPES II in general, and particularly on the shank rotation. As a countermeasure we modified LOPES II such that foot lifters can be used if the patient requires support in foot lift (dorsiflexion). Support in plantar flexion is currently not possible in LOPES II. For LOPES III we intend to implement support in plantar /dorsiflexion in a later stage.

### 10.6.3 Chair / Lifting Aid

A second functionality that was requested by users, but not implemented yet, is the chair with lifting aid. Especially for the severely impaired patients, resting on a chair during donning and doffing, and between training is desirable. In the integrated proof of concept, a chair was incorporated in the design. This chair also offered aid during standing up. Although the chair is desirable, we gave it less priority than the support during walking, and therefore we did not incorporate the chair in the design of LOPES II.

Severely impaired patients (FAC0, FAC1) have walked in the LOPES II prototypes. Instead of the chair, therapists now use the BWS to lift patients in and out of LOPES II. However we believe that a chair in LOPES II, with lifting function will improve the comfort for the patient and therapist, and shorten the donning time. Therefore we highly recommend to incorporate a chair with lifting aid in future versions of LOPES.

### 10.6.4 Simplified Rod Structure — Coupled Linkages

In the mechanical design of LOPES II we aimed for decoupled linkages, i.e., each motor is primarily coupled to a single segment. This implies that a translation / rotation of one DoF, barely has effect on other DoFs. Decoupling simplifies the programming of the kinematics. However, we developed a new method to program the kinematics in an easy way, regardless the complexity or coupling of the total linkage (see section 8.4).

If the requirement of decoupling is abandoned, the linkage of LOPES II can be simplified on several points. First of all, the actuators for the shanks and the thighs can be connected directly to the vertical rods (see figure 10.2). Similarly the pelvis stage (see figure 7.9) can be simplified, when allowing coupling between the pelvis anterior / posterior (TX) and pelvis

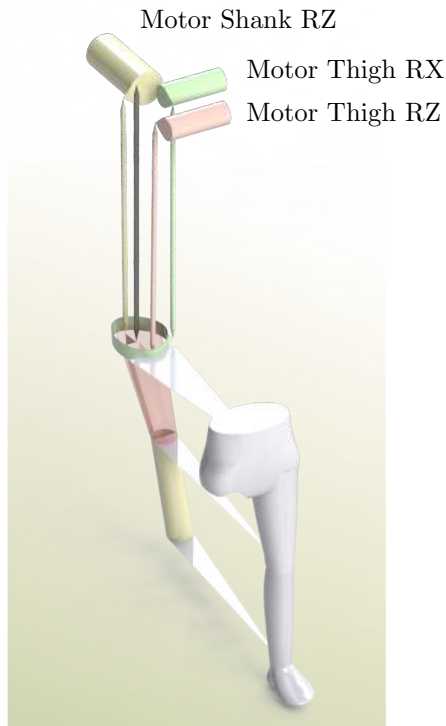


**Figure 10.2:** Concept for new design of LOPES with a simplified rod structure at the actuators. The linkage contains coupling, i.e., when the pelvis moves forward or sideways, small leg rotations will occur. The kinematics calculation must compensate for this.

mediolateral (TZ). All kinematics couplings can be corrected for in the control software.

This saves several rods and levers, consequently reducing the manufacturing costs and mass and free play in the system, and thus improving the overall performance.

### 10.6.5 Modules

A future direction for LOPES II may also be a modular approach. LOPES II was built to apply support of pelvis motions, and motions of both legs. A logic spin-off from LOPES II is a balance trainer, which support on pelvis motions only. The gimbals can be used to assure that the supportive forces apply in the center of mass of the patient and that

rotations of the pelvis are free. A second spin-off is a single-legged therapeutic device, offering support for only one leg (e.g., for hemiplegic patients). These two modules can be the components for a modular version of LOPES II. Additional modules consists of the afore mentioned chair and foot plantar / dorsiflexion module.

## 10.7 The Future of Gait Training

### 10.7.1 Research

The field of gait training is evolving. Several types of robot-assisted gait trainers are being developed and research on the mechanisms behind rehabilitation is marching forward. The fundamental research and device development can amplify each other. Research results may define new device requirements and new devices may allow for new research. In fact, the relationship between Research and Development is indispensable:

Quote (Krebs and Hogan, 2009):

*Contrary to our initial expectations, the major hindrance to the development and deployment of robots for therapy was not engineering, but the lack of strong evidence supporting many current rehabilitation practices. In many cases, conventional practices lack the support of empirical evidence or any other scientific basis. As a result there was no clear design target for the technology nor any reliable gold standard against which to gauge its effectiveness. In fact, the biggest hurdle we faced in the development of therapeutic robotics was the validation of movement therapy per se. But every challenge is also an opportunity: robots provide an ideal platform for objective, reproducible, continuous measurement and control of therapy.*

With LOPES II we have developed a sophisticated tool which can leverage research on the efficacy of gait training strategies.

Assist As Needed (AAN) is one of the most important topics of research on gait training of the last decade. In turn, the latest robot-assisted gait trainers nearly all allow for AAN. However, proper AAN requires a device to be both transparent and stiff. Particularly the transparency is a major challenge in the development of robot-assisted gait trainers (Pennycott et al., 2012). With the development of LOPES II we believe that we are close to the desired transparency without compromising the stiffness.

For stroke, a topic of research is restitution versus compensation (Van Asseldonk, 2008; Levin et al., 2008). Conventional strategies are focused on restitution, however for stroke survivors, full restitution may not be possible. Patients adopt compensation strategies to compensate for the lack of restitution. If the adoption and training of compensatory strategies is encouraged by therapists and clinicians, then the robot-assisted gait trainers should also be able to facilitate and train these strategies. With LOPES II for example circumduction is possible, and technically it is possible to provide assistance in circumduction. However, protocols to train compensatory strategies (i.e., reference patterns and adjustable assistance) have not been implemented in the user interface yet, and therefore research on the effects of training circumduction can not be performed yet.

Another challenge for robot-assisted gait training is to incorporate training of balance control during walking in robot-assisted gait training. Balance is an important aspect of gait and consequently, for subjects with gait impairment, there is a need to train balance (Westlake and Patten, 2009). Studies on the assistance of balance during walking for subjects with gait impairments are limited to the use of force plates with bio-feedback (Yavuzer et al., 2006; Liston and Brouwer, 1996; Nichols, 1997; Geiger et al., 2001). A few studies discuss algorithms on the physical assistance of balance in gait (Li and Vallery, 2012; Koopman et al., 2013b). However we found no studies on physical balance assistance during walking for subjects with gait impairments. With robot-assisted gait trainers like LOPES II it is possible to provide support in the pelvis ML direction and in ML foot placement. Research on physical balance assistance during walking for the impaired, should, and probably will, be topic of future research, to improve the gait training. Furthermore, a great part of the mechanisms behind restitution are unknown. Robot-assisted gait training may serve as a useful tool in the research on rehabilitation.

### 10.7.2 Clinic

In the first three months post-stroke the training has the highest effect (Zeiler and Krakauer, 2012), but especially in the first weeks post stroke, the patient requires highest support. In conventional gait training, the therapist sometimes is the limiting factor. The patient could benefit from longer training or more support, but the therapist may simply lack the strength or endurance to provide this. Robot-assisted gait training can

automate the labor and therefore have a positive impact on the work the therapist.

Another driving factor of the future of gait training is the cost of health care. With the aging society, the cost of health care is increasing rapidly. Technological developments may have a positive impact on the cost of gait training. In conventional gait training, sometimes two or more therapists are allowed for training the more severely impaired patients. Robot-assisted gait training may reduce this therapist-patient ratio to one, or even below one, by having one therapists, training two or more patients simultaneously. Literature on the economic aspects of robotic gait training is scarce. [Morrison \(2011\)](#) calculated that the return on investment with robot-assisted gait training with Lokomat is less than two and a half year, assuming that the Lokomat replaces three therapist aides. This assumption is rather optimistic. Additionally the cost of donning time was not included in this study. Therefore these figures are merely an indication of the return on investment. Robot-assisted gait training can reduce labor cost, especially if in the future cheaper devices will become available. For LOPES II we have not established the sales price for series production, however we do believe that the return on investment will be competitive with that of other devices. This is leveraged by the fact that the donning time in LOPES II is shorter and therefore less time is lost.

For the upper extremities, [Wagner et al. \(2011\)](#) have studied the financial feasibility of robot-assisted therapy for the upper extremities. They compared intensive arm training with robots with arm training without robots. After 36 weeks, the quality of life for both groups was similar, however the cost of robotic training was lower. We must be careful to project these results on the robot-assisted gait trainer, however we expect to see a similar trend in gait training when this were to be studied. The impact of automation of labor in gait training is expected to have a considerable impact on the cost of gait training.

Robot-assisted gait training may improve the duration and strength of training and possibly the quality of training. On the other hand robots are rarely as flexible as humans. From observations we learned that gait training is not predefined; it is based on the actual performance, the therapist adapts the support to the patient's capacity. In the pilot studies with LOPES II this was also the case. The therapists adapted the amount of support and the reference patterns constantly, often in consultation with the patient. Also in the future, we believe that the therapist is required during robot-assisted gait training. As [Hesse et al. \(2003\)](#) pointed out, it

is important to realize that a RAGT is a *tool* for the therapist and not the *replacement* of the therapist.

## 10.8 Finally

We believe that ultimately robot-assisted gait training will be an effective and efficient tool to help the therapist to provide gait training, provided that the robot-assisted gait trainers a) provide Assist As Needed in an intuitive way; b) allow for and assist in balance training; and c) allow for and assist in compensation strategies. We believe that, with LOPES II, developed with all these requirements in mind, is the next milestone towards effective and efficient robot-assisted gait training in both clinic and research.



# Bibliography

- Abras, C, Maloney-krichmar, D, and Preece, J (2004). *User-Centered Design*. Thousand Oaks: Sage Publications.
- Agrawal, SK and Fattah, A (2004). Gravity-balancing of spatial robotic manipulators. *Mechanism and Machine Theory*, 39(12):1331–1344.
- Altman, DG and Bland, JM (1983). Measurement in medicine: the analysis of method comparison studies. *The Statistician*, 32(July 1981):307–317.
- Aoyagi, D, Ichinose, WE, Harkema, SJ, Reinkensmeyer, DJ, and Bobrow, JE (2007). A robot and control algorithm that can synchronously assist in naturalistic motion during body-weight-supported gait training following neurologic injury. *Neural Systems and Rehabilitation Engineering, IEEE Transactions on*, 15(3):387–400.
- van Asseldonk, EHF (2008). *Restitution and compensation in the recovery of function in the lower extremities of stroke survivors*. PhD thesis, University of Twente.
- van Asseldonk, EHF, Veneman, JF, Ekkelenkamp, R, Buurke, JH, van der Helm, FCT, and van der Kooij, H (2008). The Effects on Kinematics and Muscle Activity of Walking in a Robotic Gait Trainer During Zero-Force Control. *Neural Systems and Rehabilitation Engineering, IEEE Transactions on*, 16(4):360–370.
- Banala, SK, Agrawal, SK, and Scholz, JP (2007). Active Leg Exoskeleton (ALEX) for gait rehabilitation of motor-impaired patients. *2007 IEEE 10th International Conference on Rehabilitation Robotics, ICORR'07*, pages 401–407.

- Bangor, A, Kortum, P, and Miller, J (2009). Determining what individual SUS scores mean: Adding an adjective rating scale. *Journal of Usability Studies*, 4(3):114–123.
- Beck, K, Beedle, M, Van Bennekum, A, Cockburn, A, Cunningham, W, Fowler, M, Grenning, J, Highsmith, J, Hunt, A, Jeffries, R, Kern, J, Marick, B, Martin, RC, Mellor, S, Schwaber, K, Sutherland, J, and Thomas, D (2001). Agile Manifesto. Online: <http://agilemanifesto.org/>.
- Bernhardt, M, Frey, M, Colombo, G, and Riener, R (2005). Hybrid force-position control yields cooperative behaviour of the rehabilitation robot LOKOMAT. In *Rehabilitation Robotics, 2005. ICORR 2005. 9th International Conference on*, pages 536–539.
- Brooke, J (1996). SUS-A quick and dirty usability scale. *Usability evaluation in industry*, 189(194):4–7.
- Bruijn, SM, Meijer, OG, Beek, PJ, and van Dieën, JH (2010). The effects of arm swing on human gait stability. *The Journal of Experimental Biology*, 213(23):3945–3952.
- Buurke, JH, Nene, AV, Kwakkel, G, Erren-Wolters, V, IJzerman, MJ, and Hermens, HJ (2008). Recovery of Gait After Stroke: What Changes? *Neurorehabilitation and Neural Repair*, 22(6):676–683.
- Cai, LL, Fong, AJ, Otsoshi, CK, Liang, Y, Burdick, JW, Roy, RR, and Edgerton, VR (2006). Implications of Assist-As-Needed Robotic Step Training after a Complete Spinal Cord Injury on Intrinsic Strategies of Motor Learning. *The Journal of Neuroscience*, 26(41):10564–10568.
- Cao, J, Xie, SQ, Das, R, and Zhu, GL (2014). Control strategies for effective robot assisted gait rehabilitation: The state of art and future prospects. *Medical Engineering & Physics*, 36(12):1555–1566.
- Colgate, E (1989). On the Intrinsic Limitations of Force Feedback Compliance Controllers. *Robotics Research*, 14:23–30.
- Colgate, E and Hogan, N (1989). An analysis of contact instability in terms of passive physical equivalents. In *Robotics and Automation, 1989. Proceedings., 1989 IEEE International Conference on*, pages 404–409. IEEE Comput. Soc. Press.

- Colgate, EJ and Brown, MJ (1994). Factors affecting the Z-Width of a haptic display. In *Robotics and Automation, 1994. Proceedings., 1994 IEEE International Conference on*, pages 3205–3210. IEEE Comput. Soc. Press.
- Colombo, G, Joerg, M, Schreier, R, and Dietz, V (2000). Treadmill training of paraplegic patients using a robotic orthosis. *Journal of Rehabilitation Research and Development*, 37(6):693–700.
- Colombo, R, Sterpi, I, Mazzone, A, Delconte, C, and Pisano, F (2012). Robot-aided neurorehabilitation in sub-acute and chronic stroke: Does spontaneous recovery have a limited impact on outcome? *NeuroRehabilitation*, 33(4):621–629.
- Cramer, SC (2008). Repairing the human brain after stroke: I. Mechanisms of spontaneous recovery. *Annals of Neurology*, 63:272–287.
- Cruciger, O, Tegenthoff, M, Schwenkreis, P, Schildhauer, Ta, and Aach, M (2014). Locomotion training using voluntary driven exoskeleton (HAL) in acute incomplete SCI. *Neurology*, 83(5):474.
- Cyberdyne (2014). HAL Medical. Online: [http://www.cyberdyne.jp/english/products/LowerLimb\\_medical.html](http://www.cyberdyne.jp/english/products/LowerLimb_medical.html).
- De Vito Dabbs, A, Myers, BA, Mc Curry, KR, Dunbar-Jacob, J, Hawkins, RP, Begey, A, and Dew, MA (2009). User-centered design and interactive health technologies for patients. *Computers, Informatics, Nursing : CIN*, 27(3):175.
- DeSanctis, G and Gallupe, RB (1987). A foundation for the study of group decision support systems. *Management Science*, 33(5):589–609.
- van Dijk, W, van der Kooij, H, Koopman, B, and van Asseldonk, EHF (2013). Improving the transparency of a rehabilitation robot by exploiting the cyclic behaviour of walking. In *Rehabilitation Robotics (ICORR), 2013 IEEE International Conference on*, pages 1–8. IEEE.
- Ditunno, PL, Patrick, M, Stineman, M, and Ditunno, JF (2008). Who wants to walk? Preferences for recovery after SCI: a longitudinal and cross-sectional study. *Spinal cord: the official journal of the International Medical Society of Paraplegia*, 46(7):500–506.

- Dobkin, BH and Carmichael, S (2005). Principles of recovery after stroke. *Recovery after Stroke*, pages 47–66.
- Eason, K (1988). *Information technology and organisational change*. Taylor & Francis/Hemisphere, Bristol.
- Ekso-Bionics (2015). Ekso Bionics - Our Story. Online: <http://intl.eksobionics.com/ourstory>.
- Emken, JL, Bobrow, JE, and Reinkensmeyer, DJ (2005a). Robotic movement training as an optimization problem: Designing a controller that assists only as needed. In *Rehabilitation Robotics, 2005. ICORR 2005. 9th International Conference on*, pages 307–312.
- Emken, JL, Wynne, JH, Harkema, SJ, and Reinkensmeyer, DJ (2005b). A robotic device for measuring and manipulating stepping. *IEEE Transactions on Robotics*, 22(1):185–189.
- Esquenazi, A, Talaty, M, Packel, A, and Saulino, M (2012). The ReWalk Powered Exoskeleton to Restore Ambulatory Function to Individuals with Thoracic-Level Motor-Complete Spinal Cord Injury. *American Journal of Physical Medicine & Rehabilitation*, 91(11):911–921.
- Evers, SMAA, Struijs, JN, Ament, AJHA, Van Genugten, MLL, Jager, JC, and Van Den Bos, GAM (2004). International comparison of stroke cost studies. *Stroke*, 35(5):1209–1215.
- Farris, RJ (2012). *Design of a powered lower-limb exoskeleton and control for gait assistance in paraplegics*. PhD thesis, Vanderbilt University.
- Gage, JR (1993). Gait analysis. An essential tool in the treatment of cerebral palsy. *Clinical orthopaedics and related research*, 288:126–134.
- Geiger, RA, Allen, JB, O’Keefe, J, and Hicks, RR (2001). Balance and mobility following stroke: effects of physical therapy interventions with and without biofeedback/forceplate training. *Physical therapy*, 81(4):995–1005.
- Glosser, G and Newman, W (1994). The implementation of a natural admittance controller on an industrial manipulator. In *Robotics and Automation, 1994. Proceedings., 1994 IEEE International Conference on*, pages 1209–1215.

- Gould, JD and Lewis, C (1985). Designing for usability: key principles and what designers think. *Communications of the ACM*, 28(3):300–311.
- Green, A, Hüttenrauch, H, Norman, M, Oestreicher, L, and Eklundh, KS (2000). User centered design for intelligent service robots. In *Robot and Human Interactive Communication, 2000. RO-MAN 2000. Proceedings. 9th IEEE International Workshop on*, pages 161–166.
- Grosu, V, Brackx, B, Van Ham, R, Van Damme, M, Vanderborght, B, and Lefeber, D (2012). Electronic hardware architecture of step rehabilitation robot ALTACRO. In *National Congress on Theoretical and Applied Mechanics*, pages 1–5.
- Hannaford, B and Ryu, JH (2002). Time-domain passivity control of haptic interfaces. *Robotics and Automation, IEEE Transactions on*, 18(1):1–10.
- Hesse, S, Schmidt, H, Werner, C, and Bardeleben, A (2003). Upper and lower extremity robotic devices for rehabilitation and for studying motor control. *Current Opinion in Neurology*, 16:705–710.
- Hesse, S and Uhlenbrock, D (2000). A mechanized gait trainer for restoration of gait. *Journal of Rehabilitation Research and Development*, 37(6):701–708.
- Hidler, J, Brennan, D, Black, I, Nichols, D, Brady, K, and Nef, T (2011). ZeroG: overground gait and balance training system. *Journal of Rehabilitation Research and Development*, 48(4):287–298.
- Hidler, J, Nichols, D, Pelliccio, M, Brady, K, Campbell, DD, Kahn, JH, and Hornby, TG (2009). Multicenter randomized clinical trial evaluating the effectiveness of the lokomat in subacute stroke. *Neurorehabilitation and Neural Repair*, 23(1):5–13.
- Hirabayashi, H, Sugimoto, K, Arai, S, and Sakaue, S (1985). Virtual Compliance Control of Multiple Degree of Freedom Robot. *Transactions of the Society of Instrument and Control Engineers*, 22(3):95–102.
- Hocoma (2013). Media Release Hocoma celebrates the sale of the 500 th neurorehabilitation robot Lokomat . Online: <http://www.hocoma.com/media-center/media-releases/media-release/hocoma-celebrates-the-sale-of-the-500th-neurorehabilitation-robot-lokomatR/4850da3e2f58fb360a9853ce071911f4/>.

- Hocoma (2014). Technical Data Lokomat Pro Manufacturer of the Lokomat Pro. Online: [http://www.hocoma.com/fileadmin/user/Dokumente/Lokomat/TECH\\_L6\\_140317\\_en.pdf](http://www.hocoma.com/fileadmin/user/Dokumente/Lokomat/TECH_L6_140317_en.pdf).
- Hogan, N (1984). Impedance control: An approach to manipulation. In *American Control Conference, 1984*, pages 304–313.
- Holden, MK, Gill, KM, and Magliozzi, MR (1986). Gait assessment for neurologically impaired patients. Standards for outcome assessment. *Physical Therapy*, 66(10):1530–1539.
- Hornby, TG, Campbell, DD, Kahn, JH, Demott, T, Moore, JL, and Roth, HR (2008). Enhanced gait-related improvements after therapist- versus robotic-assisted locomotor training in subjects with chronic stroke: A randomized controlled study. *Stroke*, 39:1786–1792.
- Houdijk, H, van Ooijen, MW, Kraal, JJ, Wiggerts, HO, Polomski, W, Janssen, TWJ, and Roerdink, M (2012). Assessing gait adaptability in people with a unilateral amputation on an instrumented treadmill with a projected visual context. *Physical Therapy*, 92(11):1452–1460.
- Hummel, JM, Van Rossum, W, Verkerke, GJ, and Rakhorst, G (2000). The effects of team expert choice on group decision-making in collaborative new product development: a pilot study. *Journal of Multicriteria Decision Analysis*, 9(August 1999):90–98.
- Husemann, B, Müller, F, Krewer, C, Heller, S, and Koenig, E (2007). Effects of locomotion training with assistance of a robot-driven gait orthosis in hemiparetic patients after stroke: a randomized controlled pilot study. *Stroke*, 38(2):349–354.
- Ichinose, W and Reinkensmeyer, D (2003). A robotic device for measuring and controlling pelvic motion during locomotor rehabilitation. In *Engineering in Medicine and Biology Society, 2003. Proceedings of the 25th Annual International Conference of the IEEE*, pages 1690–1693.
- IEC60601-1 (2005). IEC 60601-1: 2005 Medical electrical equipment—Part 1: General requirement for basic safety and essential performance.
- Jørgensen, HS, Nakayama, H, Raaschou, HO, and Olsen, TS (1995). Recovery of walking function in stroke patients: the Copenhagen Stroke Study. *Archives of Physical Medicine and Rehabilitation*, 76(1):27–32.

- Kawamoto, H, Hayashi, T, Sakurai, T, Eguchi, K, and Sankai, Y (2009). Development of single leg version of HAL for hemiplegia. In *Engineering in Medicine and Biology Society, 2009. EMBS 2009. Annual International Conference of the IEEE*, pages 5038–5043.
- Kerrigan, DC, Frates, EP, Rogan, S, and Riley, PO (2000). Hip hiking and circumduction: quantitative definitions. *American Journal of Physical Medicine & Rehabilitation*, 79(3):247–252.
- Kerrigan, DC, Karvosky, ME, and Riley, PO (2001). Spastic paretic stiff-legged gait: joint kinetics. *American Journal of Physical Medicine & Rehabilitation*, 80(4):244–249.
- Kissela, BM, Khoury, JC, Alwell, K, Moomaw, CJ, Woo, D, Adeoye, O, Flaherty, ML, Khatri, P, Ferioli, S, De Los Rios La Rosa, F, Broderick, JP, and Kleindorfer, DO (2012). Age at stroke: Temporal trends in stroke incidence in a large, biracial population. *Neurology*, 79(17):1781–1787.
- Kok, L, Houkes, A, and Niessen, N (2008). Kosten en baten van revalidatie. *SEO-rapport*.
- Kolakowsky-Hayner, Sa (2013). Safety and Feasibility of using the Ekso™ Bionic Exoskeleton to Aid Ambulation after Spinal Cord Injury. *Journal of Spine*.
- Koopman, B, van Asseldonk, EHF, and van der Kooij, H (2013a). Selective control of gait subtasks in robotic gait training: foot clearance support in stroke survivors with a powered exoskeleton. *Journal of Neuroengineering and Rehabilitation*, 10(1):3.
- Koopman, B, van Asseldonk, EHF, and van der Kooij, H (2014). Speed-dependent reference joint trajectory generation for robotic gait support. *Journal of Biomechanics*, 47(6):1447–1458.
- Koopman, B, Meuleman, JH, van Asseldonk, EH, and van der Kooij, H (2013b). Lateral balance control for robotic gait training. In *Rehabilitation Robotics (ICORR), 2013 IEEE International Conference on*, pages 1–6.
- Krebs, HI and Hogan, N (2009). Therapeutic Robotics: A Technology Push. *Proceedings of the IEEE*, 94(9):1727–1738.

- Krishnamurthi, RV, Feigin, VL, Forouzanfar, MH, Mensah, Ga, Connor, M, Bennett, Da, Moran, AE, Sacco, RL, Anderson, LM, Truelsen, T, O'Donnell, M, Venketasubramanian, N, Barker-Collo, S, Lawes, CMM, Wang, W, Shinohara, Y, Witt, E, Ezzati, M, Naghavi, M, and Murray, C (2013). Global and regional burden of first-ever ischaemic and haemorrhagic stroke during 1990-2010: Findings from the Global Burden of Disease Study 2010. *The Lancet Global Health*, 1(5):e259–e281.
- Kwakkel, G and Kollen, BJ (2013). Predicting activities after stroke: What is clinically relevant? *International Journal of Stroke*, 8(1):25–32.
- Kwakkel, G, Wagenaar, RC, Twisk, JWR, Lankhorst, GJ, and Koetsier, JC (1999). Intensity of leg and arm training after primary middle-cerebral-artery stroke: A randomised trial. *Lancet*, 354:191–196.
- Lam, W and de Vries, L (1983). Flight simulator. Online: <http://www.google.com/patents/US4398889>.
- Lammertse, P (2009). Admittance control and impedance control - a dual, with an application to master slave telemanipulation.
- Lammertse, P (2010). Skewed-axis three degree-of-freedom remote-center gimbal. Online: <http://www.google.com.ar/patents/WO2010140016A1?cl=en>.
- Lamontagne, A, Malouin, F, and Richards, CL (2001). Locomotor-specific measure of spasticity of plantarflexor muscles after stroke. *Archives of Physical Medicine and Rehabilitation*, 82(12):1696–1704.
- Lamontagne, A, Malouin, F, Richards, CL, and Dumas, F (2002). Mechanisms of disturbed motor control in ankle weakness during gait after stroke. *Gait & Posture*, 15(3):244–255.
- Langhorne, P, Bernhardt, J, and Kwakkel, G (2011). Stroke rehabilitation. *The Lancet*, 377(9778):1693–1702.
- Lee, M, Rittenhouse, M, and Abdullah, Ha (2005). Design Issues for Therapeutic Robot Systems: Results from a Survey of Physiotherapists. *Journal of Intelligent and Robotic Systems*, 42(3):239–252.
- Levin, MF, Kleim, Ja, and Wolf, SL (2008). What do motor "recovery" and "compensation" mean in patients following stroke? *Neurorehabilitation and neural repair*, 23(4):313–319.

- Li, D and Vallery, H (2012). Gyroscopic assistance for human balance. *Advanced Motion Control (AMC), 2012 12th IEEE International Workshop on*, pages 1–6.
- van der Linde, R and Lammertse, P (2002). The HapticMaster, a new high-performance haptic interface. *Proc.*, pages 1–5.
- van der Linde, R and Lammertse, P (2003). HapticMaster a generic force controlled robot for human interaction. *Industrial Robot: An International Journal*, 30(6):515–524.
- Liston, RAL and Brouwer, BJ (1996). Reliability and validity of measures obtained from stroke patients using the balance master. *Archives of Physical Medicine and Rehabilitation*, 77(5):425–430.
- Loureiro, R, Amirabdollahian, F, Topping, M, Driessen, B, and Harwin, W (2003). Upper limb robot mediated stroke therapy GENTLE/s approach. *Autonomous Robots*, 15(1):35–51.
- Maiden, N (2008). User requirements and System Requirements. *Software, IEEE*, 25(2):90–91.
- Maples, JA and Becker, JJ (1986). Experiments in force control of robotic manipulators. *Robotics and Automation. Proceedings.*, 3:695–702.
- Mast, M, Burmester, M, Krüger, K, Fatikow, S, Arbeiter, G, Graf, B, Kronreif, G, Pignini, L, Facal, D, and Qiu, R (2012). User-centered design of a dynamic-autonomy remote interaction concept for manipulation-capable robots to assist elderly people in the home. *Journal of Human-Robot Interaction*, 1(1):96–118.
- Mathewson, BB (1994). *Integration of force strategies and natural admittance control*. PhD thesis, Case Western Reserve University.
- Matjačić, Z, Olenšek, A, and Zadavec, M (2014). Robot Supported Gait Rehabilitation: Clinical Needs, Current State of the Art and Future. In *Replace, Repair, Restore, Relieve-Bridging Clinical and Engineering Solutions in Neurorehabilitation*, volume 7, pages 75–80. Springer.
- Medica (2008). THERA-Trainer e-go. Online: <http://www.thera-trainer.de/english/professional/gait/thera-trainer-e-go/index.html>.

- Mehrholz, J, Elsner, B, Werner, C, Kugler, J, and Pohl, M (2013). Electromechanical-assisted training for walking after stroke (Review). *The Cochrane Library*, (7):9–10.
- Meuleman, JH, van Asseldonk, E, and van der Kooij, H (2013). Novel actuation design of a gait trainer with shadow leg approach. In *Rehabilitation Robotics (ICORR), 2013 IEEE International Conference on*, Seattle.
- MOOG (2009). Moog Control Loading Solutions. Online: <http://www.moog.com/literature/ICD/Moog-Test-ControlLoadingSolutions-Overview-en.pdf>.
- MOOG (2014a). Programmable Multi-Axis Servo Drive System. Online: <http://www.moog.com/literature/ICD/Moog-ServoDrives-MSDSeries-Catalog-en.pdf>.
- MOOG (2014b). Simodont Dental Trainer. Online: [http://www.moog.com/literature/ICD/Datasheet\\_Moog\\_Simodont\\_Dental\\_Trainer.pdf](http://www.moog.com/literature/ICD/Datasheet_Moog_Simodont_Dental_Trainer.pdf).
- Moreno, JC, Brunetti, FJ, Pons, JL, Baydal, JM, and Barberà, R (2005). Rationale for multiple compensation of muscle weakness walking with a wearable robotic orthosis. *Proceedings - IEEE International Conference on Robotics and Automation*, 2005(April):1914–1919.
- Morone, G, Iosa, M, Bragoni, M, De Angelis, D, Venturiero, V, Coiro, P, Riso, R, Pratesi, L, and Paolucci, S (2012). Who may have durable benefit from robotic gait training?: a 2-year follow-up randomized controlled trial in patients with subacute stroke. *Stroke; a journal of cerebral circulation*, 43(4):1140–2.
- Morrison, Sa (2011). Financial Feasibility of Robotics in Neurorehabilitation. *Topics in Spinal Cord Injury Rehabilitation*, 17(1):77–81.
- MotekforceLink (2015). Grail. Online: <http://www.motekforcelink.com/product/grail/>.
- Motorika (2015). REO Ambulator. Online: <http://www.motorika.com/?categoryId=90004>.
- Neptune, RR, Kautz, SA, and Zajac, FE (2001). Contributions of the individual ankle plantar flexors to support, forward progression and swing initiation during walking. *J Biomech*, 34(11):1387–1398.

- Nichols, DS (1997). Balance retraining after stroke using force platform biofeedback. *Physical therapy*, 77(5):553–558.
- Nilsson, A, Vreede, KS, Häglund, V, Kawamoto, H, Sankai, Y, and Borg, J (2014). Gait training early after stroke with a new exoskeleton the hybrid assistive limb : a study of safety and feasibility. *Journal of neuroengineering and rehabilitation*, 11(92).
- Norman, DA and Draper, SW (1986). User Centere System Design - New Perspectives on Human-Computer Interaction. *Hillsdale, New Jersey*.
- Okamura, J, Tanaka, H, and Sankai, Y (1999). EMG-based prototype powered assistive system for walking aid. In *Proc. Asian Symp. on Industrial Automation and Robotics*, pages 229–234.
- Olney, SJ and Richards, C (1996). Hemiparetic gait following stroke. Part I: Characteristics. *Gait & posture*, 4(2):136–148.
- Outermans, JC, van Peppen, RPS, Wittink, H, Takken, T, and Kwakkel, G (2010). Effects of a high-intensity task-oriented training on gait performance early after stroke: a pilot study. *Clinical rehabilitation*, 24:979–987.
- Ozkul, F and Erol Barkana, D (2011). Design of an admittance control with inner robust position control for a robot-assisted rehabilitation system RehabRoby. *2011 IEEE/ASME International Conference on Advanced Intelligent Mechatronics (AIM)*, pages 104–109.
- Parker-Hannifin (2015). Indego’s Features — Parker Indego. Online: <http://www.indego.com/indego/en/Product>.
- Patton, J, Brown, Da, Peshkin, M, Santos-Munné, JJ, Makhlin, A, Lewis, E, Colgate, EJ, and Schwandt, D (2008). KineAssist: design and development of a robotic overground gait and balance therapy device. *Topics in stroke rehabilitation*, 15(2):131–139.
- Pennycott, A, Wyss, D, Vallery, H, Klamroth-marganska, V, and Riener, R (2012). Towards more effective robotic gait training for stroke rehabilitation : a review. *Journal of neuroengineering and rehabilitation*, pages 1–13.
- Perry, J (1992). *Gait Analysis: Normal and Pathological Function*, volume 12. SLACK Incorporated.

- Peshkin, M, Brown, Da, Santos-Munné, JJ, Makhlin, A, Lewis, E, Colgate, JE, Patton, J, and Schwandt, D (2005). KineAssist: A robotic over-ground gait and balance training device. *Proceedings of the 2005 IEEE 9th International Conference on Rehabilitation Robotics*, 2005:241–246.
- Pohl, M, Werner, C, Holzgraefe, M, Kroczeck, G, Mehrholz, J, Wingendorf, I, Hoölig, G, Koch, R, and Hesse, S (2007). Repetitive locomotor training and physiotherapy improve walking and basic activities of daily living after stroke: a single-blind, randomized multicentre trial (DEutsche GAngtrainerStudie, DEGAS). *Clinical rehabilitation*, 21(1):17–27.
- Preece, J, Rogers, Y, and Sharp, H (2002). *Interaction Design: Beyond human computer interaction*. John Wiley & Sons, Inc.
- Reha-Technology (2015). G-EO System - Reha Technology. Online: <http://www.rehatechnology.com/en/products.html>.
- Reinkensmeyer, DJ, Aoyagi, D, Emken, JL, Galvez, Ja, Ichinose, W, Ker-danyan, G, Maneekobkunwong, S, Minakata, K, Nessler, Ja, Weber, R, Roy, RR, Leon, RD, Bobrow, JE, Harkema, SJ, and Edgerton, VR (2006). Tools for understanding and optimizing robotic gait training. *The Journal of Rehabilitation Research and Development*, 43(5):657.
- Reinkensmeyer, DJ, Emken, JL, and Cramer, SC (2004). Robotics, motor learning, and neurologic recovery. *Annual review of biomedical engineering*, 6:497–525.
- ReWalk (2014). ReWalk Personal Exoskeleton System Cleared by FDA for Home Use. Online: <http://www.rewalk.com/news/press-releases/rewalk-personal-exoskeleton-system-cleared-by-fda-for-home-use/>.
- ReWalk (2015). ReWalk - Rehabilitation. Online: <http://www.rewalk.com/products/rewalk-rehabilitation/>.
- Riener, R, Lünenburger, L, Jezernik, S, Anderschitz, M, Colombo, G, and Dietz, V (2005). Patient-cooperative strategies for robot-aided treadmill training: first experimental results. *IEEE transactions on neural systems and rehabilitation engineering : a publication of the IEEE Engineering in Medicine and Biology Society*, 13(3):380–94.

- Saunders, JB, Inman, VT, and Eberhart, HD (1953). The major determinants in normal and pathological gait. *J Bone Joint Surg Am*, 35-A(3):543–558.
- Schiele, A (2009). Ergonomics of exoskeletons: Objective performance metrics. In *EuroHaptics conference, 2009 and Symposium on Haptic Interfaces for Virtual Environment and Teleoperator Systems. World Haptics 2009. Third Joint*, pages 103–108.
- Schmidt, H (2004). HapticWalker - A novel haptic device for walking simulation. In *EuroHaptics Conference, 2004*, pages 60–67.
- Schmidt, H, Hesse, S, Bernhardt, R, and Krüger, J (2005). HapticWalker A Novel Haptic Foot Device. *ACM Transactions on Applied Perception (TAP)*, 2(2):166–180.
- Schmidt, H, Werner, C, Bernhardt, R, Hesse, S, and Krüger, J (2007). Gait rehabilitation machines based on programmable footplates. *Journal of neuroengineering and rehabilitation*, 4:2.
- Schück, A, Labruyère, R, Vallery, H, Riener, R, and Duschau-Wicke, A (2012). Feasibility and effects of patient-cooperative robot-aided gait training applied in a 4-week pilot trial. *Journal of neuroengineering and rehabilitation*, 9(1):31.
- Skilbeck, CE, Wade, DT, Hewer, RL, and Wood, Va (1983). Recovery after stroke. *Journal of neurology, neurosurgery, and psychiatry*, 46(June 1982):5–8.
- Sloot, LH, van der Krogt, MM, and Harlaar, J (2014). Effects of adding a virtual reality environment to different modes of treadmill walking. *Gait & posture*, 39(3):939–45.
- Srivastava, S, Kao, PC, Kim, SH, Stegall, P, Zanutto, D, Higginson, J, Agrawal, S, and Scholz, J (2014). Assist-as-Needed Robot-Aided Gait Training Improves Walking Function in Individuals Following Stroke. *IEEE transactions on neural systems and rehabilitation engineering : a publication of the IEEE Engineering in Medicine and Biology Society*, 4320(c):1–9.
- Sulzer, JS, Roiz, Ra, Peshkin, Ma, and Patton, JL (2009). A Highly Back-drivable, Lightweight Knee Actuator for Investigating Gait in Stroke.

- IEEE transactions on robotics : a publication of the IEEE Robotics and Automation Society*, 25(3):539–548.
- Swinnen, E, Duerinck, S, Baeyens, JP, Meeusen, R, and Kerckhofs, E (2010). Effectiveness of robot-assisted gait training in persons with spinal cord injury: a systematic review. *Journal of rehabilitation medicine*, 42(6):520–6.
- Swope, WC, Andersen, HC, Berens, PH, and Wilson, KR (1982). A computer simulation method for the calculation of equilibrium constants for the formation of physical clusters of molecules: Application to small water clusters. *The Journal of Chemical Physics*, 76(1).
- Travis, D (2009). The Fable of the User-Centred Designer. *Userfocus*, page 42.
- TU-Delft (2015). DINED. Online: <http://dined.io.tudelft.nl/dined/#>.
- Vaartjes, I, Koopman, C, Dis, IV, Visseren, F, and Bots, M (2013). Hart- en vaatziekten in Nederland. *Incidentie en prevalentie van hart- en vaatziekten in Nederland*.
- Vallery, H, Duschau-wicke, A, and Riener, R (2009). Generalized Elasticities Improve Patient-Cooperative Control of Rehabilitation Robots. In *International Conference on Rehabilitation Robotics*, pages 535–541.
- Vallery, H, Lutz, P, Von Zitzewitz, J, Rauter, G, Fritschi, M, Everarts, C, Ronsse, R, Curt, a, and Bolliger, M (2013). Multidirectional transparent support for overground gait training. *IEEE International Conference on Rehabilitation Robotics*.
- Vallery, H, Veneman, J, van Asseldonk, E, Ekkelenkamp, R, Buss, M, and van Der Kooij, H (2008). Compliant actuation of rehabilitation robots. *Robotics & Automation Magazine, IEEE*, 15(3):60–69.
- Veerbeek, J, Van Wegen, E, Van Peppen, R, Hendriks, H, Rietberg, M, Van der Wees, P, Heijblom, K, Goos, A, Hanssen, W, Harmeling-van Der Wel, B, De Jong, L, Kamphuis, J, Noom, M, Van der Schaft, R, Smeets, C, Vluggen, T, Vijsma, D, Vollmar, C, and Kwakkel, G (2014). KNGF-richtlijn Beroerte. *Koninklijk Nederlands Genootschap voor Fysiotherapie*.

- Veneman, J, Ekkelenkamp, R, Kruidhof, R, van der Helm, F, and van der Kooij, H (2005). Design of a Series Elastic and Bowdencable-Based Actuation System for Use As Torque-Actuator in Exoskeleton-Type Training Robots. *9th International Conference on Rehabilitation Robotics, 2005. ICORR 2005.*, pages 496–499.
- Veneman, JF, Kruidhof, R, Hekman, EEG, Ekkelenkamp, R, Van Asseldonk, EHF, and van der Kooij, H (2007). Design and Evaluation of the LOPES Exoskeleton Robot for Interactive Gait Rehabilitation. *Neural Systems and Rehabilitation Engineering, IEEE Transactions on*, 15(3):379–86.
- Veneman, JF, Menger, J, van Asseldonk, EH, van der Helm, FC, and van der Kooij, H (2008). Fixating the pelvis in the horizontal plane affects gait characteristics. *Gait Posture*, 28(1):157–163.
- Wagner, TH, Lo, AC, Peduzzi, P, Bravata, DM, Huang, GD, Krebs, HI, Ringer, RJ, Federman, DG, Richards, LG, Haselkorn, JK, Wittenberg, GF, Volpe, BT, Bever, CT, Duncan, PW, Siroka, A, and Guarino, PD (2011). An economic analysis of robot-assisted therapy for long-term upper-limb impairment after stroke. *Stroke*, 42(9):2630–2632.
- Waters, RL, Garland, DE, Perry, J, Habig, T, and Slabaugh, P (1979). Stiff-legged gait in hemiplegia: surgical correction. *The Journal of Bone & Joint Surgery*, 61(6):927–933.
- Westlake, KP and Patten, C (2009). Pilot study of Lokomat versus manual-assisted treadmill training for locomotor recovery post-stroke. *Journal of neuroengineering and rehabilitation*, 6:18.
- Whitney, DE (1977). Force Feedback Control of Manipulator Fine Motions.
- Winter, DA (1987). *The biomechanics and motor control of human gait*. University of Waterloo Press.
- Winter, DA (1990). *Biomechanics and Motor Control of Human Movement*. Nueva York, EUA : Wiley.
- Yavuzer, G, Eser, F, Karakus, D, Karaoglan, B, and Stam, HJ (2006). The effects of balance training on gait late after stroke: a randomized controlled trial. *Clinical rehabilitation*, 20(11):960–969.

- Zanotto, D, Stegall, P, and Agrawal, SK (2014). Adaptive Assist-As-Needed Controller to Improve Gait Symmetry in Robot-Assisted Gait Training. In *Robotics and Automation (ICRA), 2014 IEEE International Conference on*, pages 724–729.
- Zanotto, D, Stegall, P, Member, S, and Member, SKA (2013). ALEX III : A Novel Robotic Platform with 12 DOFs for Human Gait Training. In *ICRA*, pages 3899–3904.
- Zeiler, S and Krakauer, J (2012). The interaction between training and plasticity in the post-stroke brain. *Changes*, 29(6):997–1003.
- Ziegler, MD, Zhong, H, Roy, RR, and Edgerton, VR (2010). Why variability facilitates spinal learning. *The Journal of neuroscience : the official journal of the Society for Neuroscience*, 30(32):10720–6.
- Zoss, AB, Kazerooni, H, and Chu, A (2006). Biomechanical design of the Berkeley lower extremity exoskeleton (BLEEX). *Mechatronics, IEEE/ASME Transactions on*, 11(2):128–138.

Part II

Appendices



# APPENDIX **A**

## Pilot Study on Following and Resisting Forces on the Pelvis

Meuleman, J.H. and Kruithof, R. and Asseldonk, E.H.F. van and Kooij, H. van der (2012) Pilot Study on Following and Resisting Forces on the Pelvis. In: International Conference on NeuroRehabilitation - ICNR 2012, 14-11-2012 - 16-11-2012, Toledo, Spain (pp. 149 - 153).

# Pilot Study on Following and Resisting Forces on the Pelvis

Jos H. Meuleman, Reinoud Kruithof, Edwin H. F. van Asseldonk, Herman van der Kooij

**Abstract**— To apply guiding forces in gait training, it is important to know the forces that can be perceived (perception threshold) and the forces a patient cannot resist (resistance threshold). In a pilot study we applied lateral forces on the pelvis by means of a virtual spring on three healthy subjects standing. We measured forces on the pelvis and lateral position on the pelvis. When instructed to follow the exerted forces, the subjects started moving when forces reached 12.5 N. When instructed to resist forces, the subjects were capable of resisting forces up to 40-60 N.

## I. INTRODUCTION

**I**N gait training robots the paradigm is shifting from position control [1] to interaction control [2-4]. The algorithms apply corrective forces based on position or angle errors between target patterns and actual patient performance. To implement interaction control, not only target patterns are required, also knowledge on the effects of corrective forces.

To promote active participation, it is relevant to make a distinction between guiding forces, that give a hint to the patient and enforcing forces, that ‘override’ the patient’s contribution [5]. To develop a strategy based on guiding forces, it is important to know how subjects respond to forces.

This paper describes a pilot study on how subjects respond to guiding- and enforcing forces on the pelvis during stance. Results can be used in the development of strategies on balance training during gait [6].

We performed an experiment in which we applied lateral forces to the pelvis of healthy subjects. The subject was instructed either to follow the force or to resist the force. The goal of the tests is to identify a minimum amount of force that makes the subject voluntarily follow the force (perception threshold), and maximum amount of force that the subject can resist (resistance threshold). These thresholds can be used in the design of control strategies for training weight shift and balance control in gait.

## II. METHODS

We used an admittance controlled servomotor (Moog C40 actuator), connected to the pelvis with a waist strap. The setup is capable of displaying a virtual spring on the pelvis

This study was supported by a grant from Dutch Ministry of Economic affairs and Province of Overijssel, the Netherlands (grant: PID082004).

Jos H. Meuleman is with Moog Robotics, Nieuw-Vennep, The Netherlands ([jmeuleman@moog.com](mailto:jmeuleman@moog.com)).

Jos H. Meuleman, Reinoud Kruithof, Edwin H.F. van Asseldonk and Herman van der Kooij are with the Department of Biomechanical Engineering, University of Twente, Enschede, The Netherlands.

(see Fig. 1). The spring stiffness and the position of the base point of the spring were controlled in the experiments.

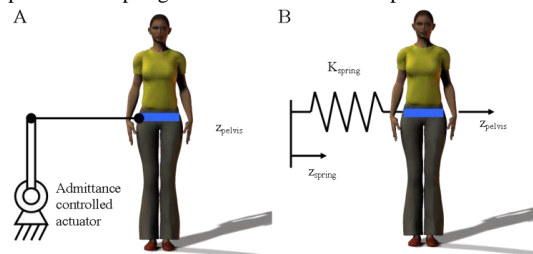


Fig. 1. Setup for applying force to the pelvis. A) Admittance controlled actuator with lever and rod connected to belt. B) Virtual spring attached to the pelvis.

We performed two tests. In the first test, we asked three subjects (length  $1.88 \pm 0.03$  m; body mass  $77.00 \pm 2.65$  kg) to follow the force that they felt on the pelvis. The guiding force was generated by a virtual spring (see Fig. 1B). The base point of the spring moved randomly to either left or right for 12 cm in five seconds. The test is considered quasistatic since the motions are slow (2.4 cm/s).

When the subject stands still, the force slowly increases until the perception threshold is reached, and then the subject follows the force. In order to assess how well the subjects can follow the force, we used various spring stiffnesses: the subject adapts his pelvis position to minimize the interaction force. Higher spring stiffness, requires either more accurate positioning or results in more fluctuation in the interaction force. In ten trials the following spring stiffness values were used in increasing order: 0, 12.5, 31.52, 62.5, 125, 312.5, 625, 1250, 3125 and 6250 N/m.

In the second test the conditions and subjects were equal to the first test, the instruction however was to resist the force. The destabilizing effect of the resistance force is dependent on the base of support and the location of the center of mass relative to the base of support. We instructed the subjects to stand with the feet next to each other and keep the body upright. The force slowly increases, while the subjects stand still. When the resistance threshold is met, the subjects can no longer resist the force and will move with the force.

The subject position and measured force from the tests were recorded at a frequency of 100Hz. The data was multiplied by the sign of the spring speed, to convert all data to positive values. In the following force test, we defined the perception threshold as the first peak in the measured force, since this indicates the start of following the force.

For the resisting force test a similar approach is taken,

except that the peak force represents the maximum force the subject can resist. When the peak is reached, the subject cannot resist the force and follows the movement. Consequently the measured force decreases.

### III. RESULTS

#### A. Guiding forces – perception threshold

For lower spring stiffness no clear trend in the response was visible, indicating that the subjects did not feel the force. From stiffnesses of 312.5 N/m the perception threshold emerged: the force increased to 10-15 N, then the subject started to follow the spring (Fig. 2 A-D). In most cases the interaction force oscillates around 12.5 N (Fig. 2 A), however in some cases the force drops to zero or even below zero (Fig. 2 B, subject 1) indicating that the subject moves ahead of the spring. The fluctuation of the force after the threshold is reached appears to be independent of the spring stiffness, the position error decreases with increasing spring stiffness.

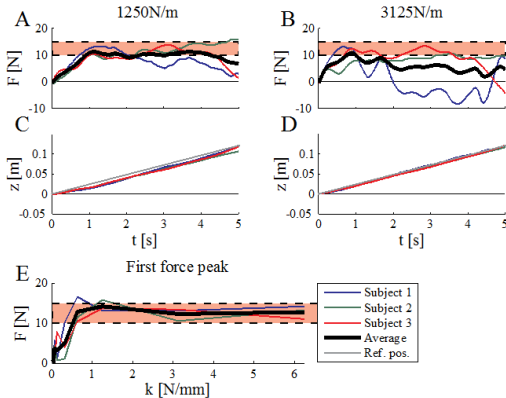


Fig. 2. Responses to an encouraging force on the pelvis, generated by a moving spring: measured force on pelvis with spring stiffnesses of 1250 N/m (A) and 3125 N/m (B); pelvis lateral position response with spring stiffness of 1250 N/m (C) and 3125 N/m (D); first force peaks per trial (E).

#### B. Enforcing force – resistance threshold

When resisting soft springs the subjects hardly moved, and thus were able to resist the force. From stiffnesses of 62.5 N/m upward resisting became more difficult, resulting in lateral displacement of the pelvis (see Fig. 3 A and C).

Subjects 1 and 3 were able to withstand a force of 40-60 N; when that force was reached, they were forced to follow the spring. Subject 2 showed a larger variance and also lost balance in the 3125 N/m trial (see Fig. 3 Error! Reference source not found. B & D from 4.2 s).

### IV. DISCUSSION

One limitation of our study is that only three subjects participated. The outcomes of the tests are merely an indication. Especially in the resistance tests the body weight and length are of influence on the amount of force a person

can resist. However, these results provide sufficient information to build tests where dynamic following- and resisting forces are applied during walking.

A possible explanation for the variance of subject 2 in the resistance test is the trunk orientation. This was not measured, but by leaning towards the force, the subject can resist higher lateral forces. Although the subjects were instructed to stay upright, minor deviations of the trunk orientation may affect the resistance threshold.

Whether the found resisting force threshold also applies for walking is questionable, since the base of support and the dynamics of the center of mass vary.

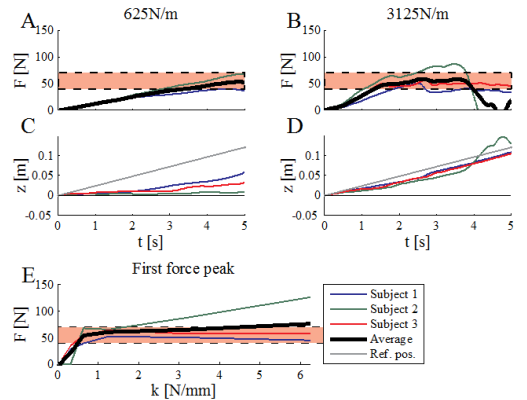


Fig. 3. Responses to resisting force on the pelvis, generated by a moving spring: measured force on pelvis with spring stiffnesses of 250 N/m (A) and 1250 N/m (B); pelvis lateral position response with spring stiffness of 250 N/m (C) and 1250 N/m (D); first force peaks per trial (E).

### V. CONCLUSION

On the pelvis subjects perceive forces of 12.5 N upward, and are capable of resisting forces of 40-60 N, when both feet are placed next to each other. For gait training this means that when guiding forces on the pelvis are used, they should be 12.5 N or more. The resistance threshold for walking depends on the timing of the disturbance force, but is expected to have an order of magnitude of 50 N.

### REFERENCES

- [1]. Colombo, G., et al., *Treadmill training of paraplegic patients using a robotic orthosis*. J Rehabil Res Dev, 2000. **37**(6): p. 693-700.
- [2]. Cai, L.L., et al., *Implications of Assist-As-Needed Robotic Step Training after a Complete Spinal Cord Injury on Intrinsic Strategies of Motor Learning*. The Journal of Neuroscience, 2006. **26**(41): p. 10564-10568.
- [3]. Marchal-Crespo, L. and D.J. Reinkensmeyer, *Review of control strategies for robotic movement training after neurologic injury*. J Neuroeng Rehabil, 2009. **6**: p. 20.
- [4]. Reinkensmeyer, D., et al., *Tools for understanding and optimizing robotic gait training*. J Rehabil Res Dev, 2006. **43**(5): p. 657-70.
- [5]. Perez, M., et al., *Motor skill training induces changes in the excitability of the leg cortical area in healthy humans*. Exp Brain Res, 2004. **159**(2): p. 197-205.
- [6]. Aoyagi, D., et al., *A robot and control algorithm that can synchronously assist in naturalistic motion during body-weight-supported gait training following neurologic injury*. IEEE Trans Neural Syst Rehabil Eng, 2007. **15**(3): p. 387-400.



# APPENDIX **B**

## **Effect of Directional Inertias Added to Pelvis and Ankle on Gait**

Meuleman, J. H., van Asseldonk, E. H. F., & van der Kooij, H. (2013). The effect of directional inertias added to pelvis and ankle on gait. *Journal of Neuroengineering and Rehabilitation*, 10(1), 40. doi:10.1186/1743-0003-10-40

RESEARCH

Open Access

# The effect of directional inertias added to pelvis and ankle on gait

Jos H Meuleman<sup>1,2\*</sup>, Edwin HF van Asseldonk<sup>2</sup> and Herman van der Kooij<sup>2,3</sup>

## Abstract

**Background:** Gait training robots should display a minimum added inertia in order to allow normal walking. The effect of inertias in specific directions is yet unknown. We set up two experiments to assess the effect of inertia in anteroposterior (AP) direction to the ankle and AP and mediolateral (ML) direction to the pelvis.

**Methods:** We developed an experimental setup to apply inertia in forward backward and or sideways directions. In two experiments nine healthy subjects walked on a treadmill at 1.5 km/h and 4.5 km/h with no load and with AP loads of 0.3, 1.55 and 3.5 kg to the left ankle in the first experiment and combinations of AP and ML loads on the pelvis (AP loads 0.7, 4.3 and 10.2 kg; ML loads 0.6, 2.3 and 5.3 kg). We recorded metabolic rate, EMG of major leg muscles, gait parameters and kinematics.

**Results & discussion:** Adding 1.55 kg or more inertia to the ankle in AP direction increases the pelvis acceleration and decreases the foot acceleration in AP direction both at speeds of 4.5 km/h. Adding 3.5 kg of inertia to the ankle also increases the swing time as well as AP motions of the pelvis and head-arms-trunk (HAT) segment. Muscle activity remains largely unchanged.

Adding 10.2 kg of inertia to the pelvis in AP direction causes a significant decrease of the pelvis and HAT segment motions, particularly at high speeds. Also the sagittal back flexion increases. Lower values of AP inertia and ML inertias up to 5.3 kg had negligible effect.

In general the found effects are larger at high speeds.

**Conclusions:** We found that inertia up to 2 kg at the ankle or 6 kg added to the pelvis induced significant changes, but since these changes were all within the normal inter subject variability we considered these changes as negligible for application as rehabilitation robotics and assistive devices.

**Keywords:** Inertia, Kinematics, Pelvis, Metabolic rate, Locomotion, Leg loading, Emg, Robotic gait trainers

## Background

In Robot aided gait training the trend is moving from position controlled robots as the early Lokomat [1] towards force controlled robots [2]. Where position controlled robots impose a gait pattern on a patient, force controlled robots offer the possibility to provide corrective- or guiding forces when needed. These "Assist As Needed" control algorithms [3-5] facilitate active participation, which have a positive effect on the rehabilitation process [6]. A pre-requisite for assist as needed is that the robot does not affect gait when no assistance is needed, i.e., the robot must

be able to minimize the interaction forces. This is known as "zero impedance control" [3] or transparent mode.

The target of transparent mode is to minimize interaction force between robot and subject; however zero interaction is impossible if the interaction force itself is the input for the control. The remaining impedance can be expressed in mechanical impedances such as inertia, damping, friction, stiffness, and combinations. Performance of gait training robots and other devices for force interactions with humans is often expressed in these mechanical impedances. Most impedances can be compensated for completely with control algorithms, such as admittance control [7]. Inertia, however usually cannot be compensated for completely, especially when passivity has to be guaranteed [8]. In robotic gait rehabilitation, this means that the inertia of the robot is

\* Correspondence: jmeuleman@moog.com

<sup>1</sup>Moog Robotics, Nieuw-Vennep, The Netherlands

<sup>2</sup>Department of Biomechanical Engineering, University of Twente, Enschede, The Netherlands

Full list of author information is available at the end of the article

perceived by the patient. Therefore it is important to know the effect of added inertia on gait, more specific, the effect of added inertia on legs and trunk.

Several studies have investigated the effect of mass added to body parts. These studies can be divided in two groups. The first group applied weights to body parts. These weights introduced inertia and a downward force due to gravity. In these studies it cannot be distinguished if the found effects are elicited by pure inertia or weight. The second group did compensate for the weight e.g. by means of body weight support, thus these studies assessed the effect of pure inertia. Adding inertia of 25-50% to the trunk of body mass resulted in an increase of energetics [9] and muscle activity [10]. Gait parameters remained unchanged [11] or change hardly (<3% [10]). The effect of inertia only on gait kinematics has not been assessed, however the effect of added weight has. The gravity component of the added weight has a significant effect on gait [9], therefore the found effects caused by added weight are likely to differ from effects caused by pure inertia. Table 1 summarizes the found effects of added inertia in previous studies.

No literature was found on the effect of inertia added to the legs, only the effects of adding weight to legs have been assessed. Browning et al. showed that 4 kg attached to the ankle caused an increase of metabolic rate (36%) which is close to the effect of adding 16 kg added on the waist (32%) [12]. Royer and Martin [13] added weight in several distributions: the total weight remained constant (5.64 kg), while the moment of inertia with respect to the hip joint varied. The largest increase was found in metabolic rate (+8.2%) when 2.82 kg was added to the proximal shank; other effects remained small. Though the weights added to the feet and legs are considerably less than the weights added to the pelvis by Grabowski [9], the effect of gravity on these added weights is expected to be considerable

To design robots for gait training, it is important to assess the effect of added inertia on gait, and ideally the

inertia that the robot displays to the subject is so low that the effect on gait is negligible. Our objective is to establish this threshold for added inertia. The above-mentioned studies give an indication of this threshold, but there are some limitations. First, in all studies on ankle and leg loading, weight is added instead of inertia. Second, all studies that assessed the effect of added inertia on the trunk/pelvis did so by adding weights to a subject and compensating for the gravity of the weight by a body weight support system. A body weight support suspended on a fixed point has an equivalent of a stabilizing effect as a spring in a horizontal plane. Furthermore Aaslund and colleagues [14] have shown that the harness itself, without applying body weight support, has an effect on gait kinematics. Third, no study assessed the effect of inertia on gait kinematics. Fourth, in the different studies relatively large added inertias (~20 kg) were added on the trunk, whereas interaction control algorithms are expected to be able to reduce the displayed inertia to values below 10 kg [15,16]. The fifth limitation is that all studies applied equal inertia in all three translational degrees of freedom dimensions, while each controlled degree of freedom can be tuned independently, resulting in different inertias in different degrees of freedom. The last limitation is that the existing studies did not establish a threshold below which added inertia leaves gait unaffected, and thus below which a robot is transparent, and above which gait is affected.

The aim of this paper is to assess the effect of inertia added to the pelvis and the ankle. The first experiment adds inertia on the pelvis in anterior posterior (AP) and mediolateral (ML) direction; the second experiment adds inertia in AP direction on the ankle. We quantified the effect of inertia on gait parameters, gait kinematics, energetics, and muscle activity. These parameters are commonly used in gait analysis [9-11], and therefore are selected in our study, assuming that this set of parameters suffice in quantifying changes of gait. Moreover, a threshold is estimated for the allowable inertia of the gait training robot, below which walking in the gait training robot resembles normal walking. This serves as a recommendation for the design of transparent gait training robots.

We hypothesize that adding inertia elicits an increase of energetics or a decrease in gait motions (joint rotations, segment motions) or both. We base this on Newton's second law:

$$F = m a$$

When inertia increases the first possible effect is that the subject exerts more force (muscle activity and energetics) to maintain the motion (acceleration). For extra inertia on the ankle, we expect an increase of muscle activity for push -off and stance preparation, since the acceleration and deceleration are highest in these phases.

**Table 1 Effect of added inertia during walking**

Quantity	Effect of 25% body mass added to the trunk	Effect of mass added to the foot 4 kg
Metabolic rate	+18% [9]	+36% @ 4 kg at foot [12] +8.2% @2.8 kg at proximal shank [13]
Muscle activity	+21% Soleus [10]	~0 [13]
Gait parameters	~0 [11] - 3% [10]	+2% swing time +1% Stride time @2.8 kg at proximal shank [13]
Gait kinematics	Unknown	Unknown

The second possible effect is that acceleration will decrease when a mass increases, while the subject maintains his effort (no change in energetics and muscle activity). For loads on the pelvis this implies smaller motions of the pelvis and trunk. For the ankle this would imply shorter stride length, but this inadvertently leads to an increase in cycle time (if speed is kept constant).

Finally we hypothesize that the effect of inertia is larger at high speeds, since in general accelerations of the segments are higher at high speeds, thus the absolute effect of a change in inertia is likely to elicit a larger absolute change in energetics.

## Method

### Subjects

Both experiments were executed with nine healthy subjects. All subjects signed an informed consent before the experiment. See Table 2 for subject data.

### Apparatus

To add pure inertia, we designed a mechanism that connects the subject to two modules with adjustable inertias through a light-weight pelvis strap or ankle strap. The pelvis strap contains a light-weight bar, a rigid belt, and a trapezium construction, that allows pelvis rotation in the coronal plane.

A single module of adjustable inertia consists of a horizontal bar connected with spherical joints to a stand at one end and to the pelvis strap at the other end. Dumbbell weights are mounted on the bar. A steel wire is connected to the stand and the joint with the strap to assure vertical fixation of the bar, allowing only rotation of the bar and module around the vertical axis of the stand. The location of the dumbbell weight on the bar determines the added inertia to the segment, according to (1).

$$M_{direction}^{segment} = \xi^2 M^{dumbbell} + M_{direction}^{apparatus} \quad (1)$$

$M_{direction}^{segment}$  denotes the added inertia on the segment in a specific direction;  $M^{dumbbell}$  is the mass of the dumbbell weights;  $M_{direction}^{apparatus}$  is the inertia of the construction without the dumbbell weights at the segment (ankle 0.3 kg; pelvis anterior-posterior 0.58 kg; pelvis mediolateral 0.41 kg). Parameter  $\xi$  is the effective inertia gearing of the

dumbbell weights, determined by the location of the dumbbell weight on its bar (see Table 3).

For the pelvis experiment we used two modules to apply AP load and ML load independently (see Figure 1 and Additional file 1); for the ankle experiment a single module was used to apply inertia in AP direction only (see Figure 2). In both studies, the inertia in other translations and rotations added by the apparatus is negligible.

We used loads that are similar to the loads used in the study of Browning and colleagues [12] (2 – 4 kg on the foot; 4 – 16 kg on the waist).

### Recordings

The effects of added inertia were assessed by quantifying kinematics, muscle activity and energetics.

### Kinematics and gait parameters

Motions were measured using an optical tracking system (Vicon Oxford Metrics, Oxford, UK). Twenty one reflective markers were attached to the human body; these markers were attached on both sides of the subject. Four markers were placed on the upper extremity (shoulders, front trunk and back trunk), five markers were placed on the pelvis (sacrum, left and right anterior superior iliac spine, left and right posterior superior iliac spine), on each leg seven markers were placed (femur, knee, tibia, malleolus, heel, fifth metatarsal joint). In both experiments two extra markers were placed on the apparatus, one on the stand and one on the strap near the ankle or pelvis. All markers were recorded at a sampling rate of 120 Hz by means of optical tracking.

### Muscle activity

The muscle activity was measured by recording the electromyography (EMG) from eight different muscles of the right leg: (1) the gluteus maximus, (2) gluteus medius, (3) rectus femoris, (4) vastus lateralis, (5) biceps femoris (6) gastrocnemius medialis (7) soleus, and (8) tibialis anterior. The analogue signals were sampled at 1024 Hz and recorded with a Bagnoli system (Delsys, Boston, USA). Amplified EMG data was synchronized with the VICON System. Electrodes were placed over the muscle bellies according to the Seniam guidelines [17].

**Table 2 Subjects data**

	Ankle experiment	Pelvis experiment
Sex	7 men; 2 women	7men; 2 women
Weight	72.4 ± 12.5 kg	74.9 ± 9.0 kg
Height	1.81 ± 0.09 m	1.80 ± 0.10 m
Age	25.1 ± 5.2 years	30.9 ± 10.3 years

**Table 3 Parameter values for pelvis AP and ML loading and ankle AP loading**

	AP load on pelvis		ML load on pelvis		AP load on ankle			
	$\xi$	$M_{AP}^{pelvis}$	$\xi$	$M_{ML}^{pelvis}$	$\xi$	$M_{AP}^{boot}$		
1	0.10	0.7 kg	1	0.12	0.6 kg	1	0.0	0.3 kg
2	0.50	4.3 kg	2	0.36	2.3 kg	2	0.50	1.5 kg
3	0.80	10.2 kg	3	0.57	5.3 kg	3	0.80	3.5 kg

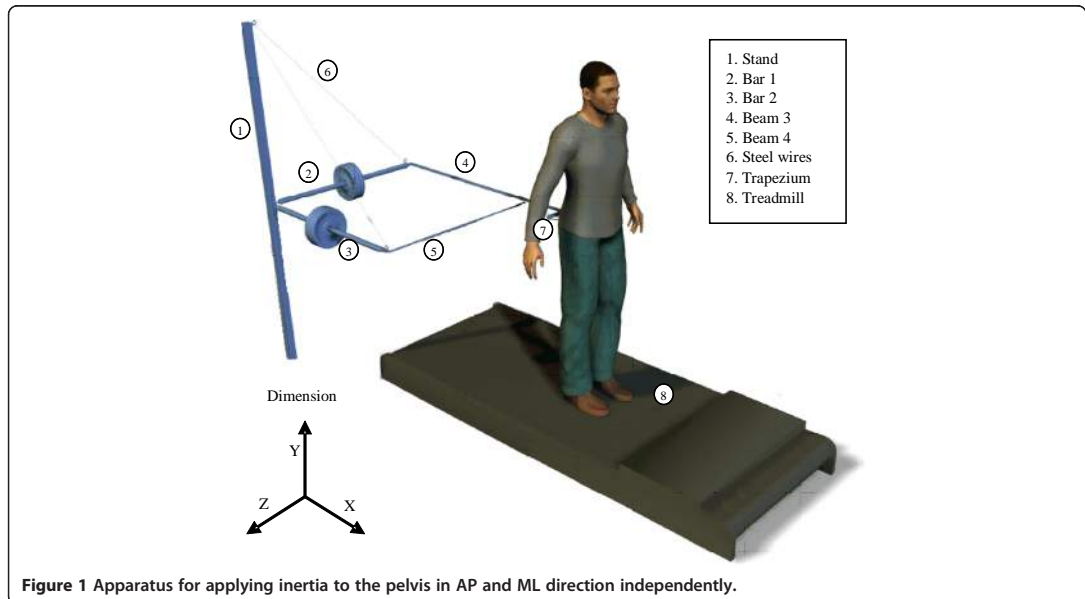


**Figure 1** Apparatus for applying inertia to the pelvis in AP and ML direction independently.

### Energetics

The energy expenditure was measured by the Oxycon Pro system (Jaeger, Hoechberg, Germany). Subjects were connected to the Oxycon with a flexible tube making an airtight seal to a facemask, measuring oxygen consumption (VO<sub>2</sub>) and volume expiration (VE). The heart rate of the subjects was measured at the index finger by a pulse-oximeter. Every five seconds (0.2 Hz) all parameters were measured and stored on the personal computer that was connected to the Oxycon.

### Experimental protocol

Both experiments started with two conditions in which subjects were walking on a treadmill at 1.5 km/h and 4.5 km/h without being attached to the system, called “no load” conditions (NL). These trials were followed by a randomized sequence of the added inertia- and speed conditions. In the pelvis experiment subjects walking with every combination of three loading conditions in AP and ML direction (see Table 3). In the ankle experiment, three loadings were applied in AP direction (see Table 3). Combining the loading conditions with speeds, resulted in 18 different loaded conditions for the pelvis-experiment and six loading conditions for the ankle-experiment. All trials consist of 3 minute walking.

### Data analysis

The last 12 VO<sub>2</sub> samples (1 minute) were converted to VO<sub>2</sub> rate per subject weight.

All kinematics and EMG data were split into individual stride cycles, determined by movement of the left heel marker [18]. Only the last 30 seconds of each trial was analyzed to eliminate the transition effects.

Marker data was converted to joint- and segment kinematics using custom written software, resulting in flexion and abduction of the left hip, left knee flexion, left plantar flexion, and back sagittal- and frontal rotation. For the pelvis and trunk the AP and ML motions and for the left foot the AP motion are analyzed in terms of position and acceleration. For the joint angles and segment motions, the range of motion (RoM) was

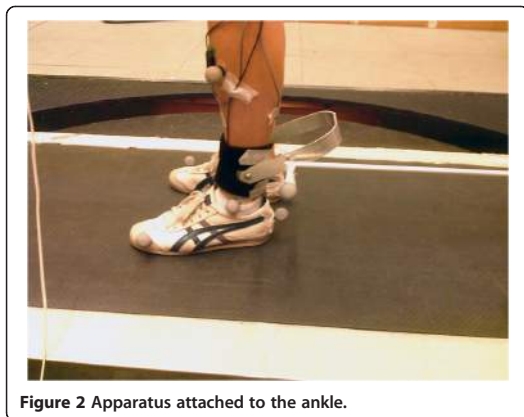


**Figure 2** Apparatus attached to the ankle.

calculated as the difference between the maximum and minimum value within a stride cycle.

We calculated the following gait parameters: cycle time [s], double stance time [s], swing time left [s], stance time left [s], step width [m] and stride length [m].

The raw EMG data was band passed filtered at 10–25 Hz with a second order (zero-lag) Butterworth filter. The filtered EMG data per subject per muscle was normalized to its maximal activity over the last 30 seconds. Mean muscle activity was calculated over seven intervals per step as described by Van Asseldonk [3]. The mean activity per interval was averaged per subject per trial. The double stance starting at left heel strike ending with toe off right defines *initial loading*; the stance phase is divided in two periods of equal length: *mid stance*, *terminal stance*. The double stance from heel strike right to toe off left defines the *pre swing*; the swing phase is divided in three periods of equal length: *initial swing*, *mid swing* and *terminal stance*. The intervals are described in Figure 3.

### Statistical analysis

The results of our research will be used as requirements gait training robots that are transparent. This implies walking in the gait training robot should resemble free walking. To quantify this resemblance we first checked the statistical significance first. However, this method does not take into account the variance within a subject (i.e. variance between steps). Even if differences are consistent, as they are significant, they may be small relative to the normal variance within a subject. Since our focus is to state requirements for gait training robots that allow normal walking and thus also the variability of normal walking, any effect that is smaller than the variability of walking is deemed ‘negligible’.

First we tested whether the NL conditions differed significantly from the BLSN condition to assess whether merely attaching the mechanical setup already affected the walking pattern. Subsequently we assessed the effects of the different loads.

To assess whether inertia had a significant effect on gait, we performed a two-way (velocity, AP load) repeated

measures (ANOVA) in the ankle experiment; we used a three-way (velocity, AP load, ML load) in the pelvis experiment. We examined the main effects of load and the interaction effects between load and speed. Pair wise comparisons were performed on main- and interaction effects that are significant.

The intra subject variability (ISV) is calculated as twice the standard deviation in the baseline condition for a single subject. For data that is cut into steps (all except energetics) the standard deviation is taken over the number of steps. For the energetics the standard deviation is taken over the number of samples. If a parameter change due to added inertia does not exceed the averaged intra-subject variability the effect is judged as ‘negligible’.

$$ISV = 2 \frac{1}{nSubjects} \sum_{i=1}^{nSubjects} \sigma_{BSLN}^{iSubject} \quad (4)$$

In total we observed 31 parameters: energetics (1 parameter), gait parameters (6 parameters), joint angles (6 parameters), segment translation (5 parameters) and accelerations (5 parameters), and EMG activity (8 parameters). In both experiments 261 tests are performed: 31 parameters are observed + 56 muscle-phase combinations, resulting in 87 main effects, 174 interaction effects with speed (high and low speed).

## Results

### Baseline validation

#### Effect of apparatus on the ankle

When the apparatus was attached to the subject’s ankle with the inertia of the apparatus only (minimal added inertia), no significant increase is found in energetics and gait parameters relative to the free walking on the treadmill. Hip flexion range of motion however increased significantly ( $p = 0.009$ ). The motions of the pelvis segment increased significantly in AP direction in position range of motion (RoM) ( $p = 0.008$ ) and acceleration RoM ( $p = 0.006$ ). The head-arm-trunk (HAT) position RoM increased significantly ( $p = 0.028$ ). There is also a significant interaction effect with speed on the range of motion of the pelvis ( $p = 0.025$ ) and HAT ( $p = 0.028$ ). The post hoc tests showed the increase at low speed (see Table 4).

The soleus shows a significant ( $p = 0.005$ ) increase of mean activity due to the apparatus and moreover, the apparatus has a significant ( $p = 0.011$ ) interaction effect with phases, and pair wise comparisons show significant increase in pre swing, initial swing and mid swing. The gluteus maximus and the gastrocnemius medialis show a significant interaction effect ( $p = 0.041$  and  $p = 0.037$  respectively) on phase  $\times$  speed  $\times$  load. Pair wise comparison shows only a significant decrease ( $p = 0.028$ ) of gluteus maximus in mid stance at slow speed.

None of the changes exceeded the intra subject variability.

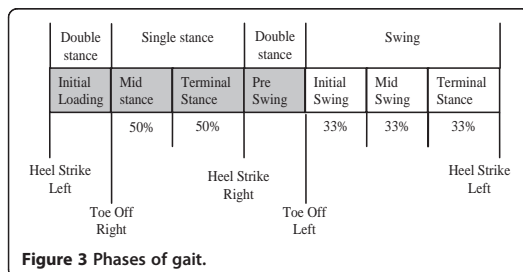


**Table 4 List of significant effects of baseline validation**

Measure	Parameter	Speed	NL	BSLN
<b>Energetics</b>	-		-	-
Gait parameters	-		-	-
Joint angles	LHip flexion RoM [deg]		33.2 ± 3.9	34.4 ± 3.7*
Segment motions	Pos pelvis AP RoM [mm]		45.0 ± 10.2	50.3 ± 6.4*
		1.5 km/h	50.1 ± 12.6	58.4 ± 7.8*
	Pos HAT AP RoM [mm]		34.3 ± 8.0	39.0 ± 6.9*
		1.5 km/h	38.4 ± 10.2	46.2 ± 11.3*
	Acc pelvis AP RoM [m/s <sup>2</sup> ]		3.49 ± 0.67	3.71 ± 0.67*
EMG	Soleus		0.10 ± 0.02	0.11 ± 0.02*
	Soleus - pre swing		0.103 ± 0.036	0.122 ± 0.043*
	Soleus - initial swing		0.055 ± 0.021	0.066 ± 0.026*
	Soleus - mid swing		0.054 ± 0.019	0.069 ± 0.028*
	Gluteus maximus - mid stance	1.5 km/h	0.125 ± 0.050	0.114 ± 0.050*

\* Significantly different from NL ( $p < 0.05$ ).

Minimum added inertia is compared with no load; The table lists significant main effects (independent of speed) and significant interaction effects with speed, but only at speeds that were significant in pair wise comparisons.

#### Effect of apparatus on the pelvis

When the apparatus was attached to the subject's pelvis with the inertia of the apparatus only (minimal added inertia), no significant increase is found in energetics relative to the free walking on the treadmill. Of the gait parameters, only the stride length showed a significant increase of load ( $p = 0.024$ ) and load  $\times$  speed ( $p = 0.030$ ) (see Table 5). The pair wise comparison showed a significant increase at slow speed.

Of the joint angles, plantar flexion range of motion increased significantly ( $p = 0.010$ ). The hip flexion range of motion has a significant interaction effect with speed ( $p = 0.028$ ), but no significance was found in the pair wise comparisons.

There was a significant interaction effect of load and speed on the pelvis AP position RoM ( $p = 0.002$ ) and the head-arm-trunk (HAT) segment ( $p = 0.029$ ). In both cases pair wise comparison showed an increase at slow speed. The pelvis acceleration range of motion increased significantly ( $p = 0.048$ ) with  $0.13 \text{ m/s}^2$ .

The EMG showed a significant ( $p = 0.047$ ) effect on the soleus (from 0.087 to 0.091) and a significant ( $p = 0.042$ ) interaction effect of phase, load and speed at the biceps femoris. The pair wise comparison showed a significant decrease of the biceps femoris in mid stance during fast walking.

Of all significant changes, only the stride length and foot RoM at low speed exceeded the averaged intra subject variability.

#### Effect of inertia on the ankle in AP direction

Adding inertia in AP direction on the ankle causes a significant increase in metabolic rate ( $p = 0.001$ ), and in

interaction with speed ( $p = 0.006$ ). The pair wise comparison revealed a significant increase at high speed only (see Table 6).

In the muscle activity there is an interaction effect of AP inertia with phase on the gluteus medius ( $p = 0.045$ ), the vastus lateralis ( $p < 0.001$ ), the soleus ( $p = 0.020$ ) and the tibialis anterior ( $p < 0.001$ ), but pair wise comparisons revealed significant decrease only of soleus in terminal stance and the tibialis anterior in initial swing and mid swing.

The double stance time decreased significantly ( $p = 0.008$ ), whereas the swing time increased ( $p < 0.001$ ), and has an interaction effect with speed ( $p = 0.028$ ). The stride length decreased significantly ( $p = 0.009$ ), but pair wise comparison showed not significant changes.

Of the joint angles, we found significant decreases in the knee flexion ( $p = 0.001$ ) and the plantar flexion ( $p = 0.010$ ). Also significant interaction effects with speed appeared at both trunk frontal ( $p = 0.025$ ) and sagittal rotation ( $p = 0.011$ ), but the pair wise comparisons revealed no significant differences, also no clear trends are visible.

The pelvis and HAT segment motions AP increased significantly in position (pelvis  $p < 0.001$ ; HAT  $p = 0.009$ ) and acceleration (pelvis  $p < 0.001$ ; HAT  $p = 0.001$ ); for both segments the acceleration also has a significant interaction effect with speed (pelvis  $p = 0.001$ ; HAT  $p = 0.042$ ), which is significant only at high speed according to pair wise comparison.

The HAT segment position RoM in ML direction changed significantly ( $p = 0.035$ ) due to load, but no consistent increase or decrease. Also pair wise comparison did not reveal significant differences.

**Table 5 List of significant and appreciable effects of baseline validation**

Measure	Parameter	Speed	NL	BSLN
<b>Energetics</b>	-		-	-
Gait parameters	Stride length [m]		0.67 ± 0.04	0.70 ± 0.05*
		1.5 km/h	0.52 ± 0.06 (0.05)	<b>0.58 ± 0.08*</b>
Joint angles	Left plantar flexion RoM [deg]		25.2 ± 3.5	28.0 ± 5.4*
	LHip flexion RoM [deg]	1.5 km/h	29.8 ± 2.5	31.7 ± 3.7
		4.5 km/h	42.0 ± 3.4+	42.4 ± 3.5
Segment Motions	Pos pelvis AP RoM [mm]	1.5 km/h	53.5 ± 10.0	63.5 ± 11.7*
	Acc pelvis ML RoM [m/s <sup>2</sup> ]		1.50 ± 0.22	1.63 ± 0.29*
	Pos HAT AP RoM [mm]	1.5 km/h	41.3 ± 8.9	48.8 ± 9.3*
	Pos Left foot RoM [mm]	1.5 km/h	546.71 ± 77.23 (41.23)	<b>612.50 ± 88.64*</b>
EMG	Soleus		0.09 ± 0.02	0.09 ± 0.02*
	Biceps femoris – mid stance	4.5 km/h	0.14 ± 0.05	0.12 ± 0.05*

\* Significantly different from NL ( $p < 0.05$ ).

**Bold:** change larger than the average intra subject variability given in brackets.

Minimum added inertia is compared with no load; the table lists significant main effects (independent of speed) and significant interaction effects with speed, but only at speeds that were significant in pair wise comparisons.

Finally the left foot RoM decreased significantly in position RoM ( $p = 0.015$ ) and acceleration RoM ( $p < 0.001$ ). The acceleration has a significant interaction effect with speed ( $p < 0.001$ ), at both speeds as revealed by pair wise comparison, but the decrease is considerably larger at high speeds (see Table 6).

Of the significant changes due to adding 1.55 kg to the ankle, only two exceed the average intra-subject variability: at high speed the acceleration range of motion in AP direction of the pelvis and the left ankle. Adding 3.5 kg caused more changes that exceeded the ISV: the increase in swing time, the increase of pelvis- and HAT acceleration in AP direction, the decrease of the foot acceleration and the decrease of the tibialis anterior in initial swing. All these effects except for EMG are plotted in Figure 4.

#### Effect of inertia on the Pelvis in AP direction

Adding inertia in AP direction on the pelvis during walking on a treadmill has no effect on energetics.

Of all the gait parameters only the stance time shows a significant ( $p = 0.050$ ) interaction effect with speed, though a clear trend is not visible and also not revealed by pair wise comparisons (see Table 7).

The hip abduction, -flexion and knee flexion decrease at significantly ( $p = 0.002$ ,  $p = 0.014$  and  $p = 0.03$ ) due to a load at the pelvis in AP direction. The trunk sagittal rotation increases significantly ( $p = 0.002$ ). This has a significant interaction effect with speed as well ( $p = 0.003$ ). Pair wise comparisons show that the increase is larger at high speed.

The pelvis and HAT motions in AP direction both decrease significantly in position RoM (pelvis  $p < 0.001$ ; HAT:  $p = 0.003$ ) and acceleration RoM (both  $p < 0.001$ ). For both segments the acceleration RoM also has an interaction effect with speed (both  $p = 0.003$ ). Pair wise comparison reveals that for the pelvis this occurs at high speed and high load only and for the HAT segment this occurs at both speeds, high load only, but the decrease is larger at high speeds (see Table 7).

The vastus lateralis has a significant interaction effect with speed and phase ( $p = 0.050$ ). Pair wise comparison reveals a decrease during mid stance at slow speed, though this is not a clear consistent decrease (see Table 7). During terminal swing a decrease of activity is found at high speed. Both gastrocnemius medialis and soleus show a significant interaction effect with phase ( $p = 0.018$  and  $p = 0.022$  respectively); both muscles showed an increase during mid stance.

In short, although adding 4.3 kg to the pelvis in AP direction caused significant effects, none of these effects exceeded the averaged ISV. Adding 10.2 kg however did cause changes larger than the ISV: the increase of the trunk sagittal rotation, the acceleration in AP direction of pelvis and HAT segments (see Figure 5).

#### Effect of inertia on the pelvis in ML direction

Adding inertia to the pelvis in ML direction during walking has no effect on energetics, gait parameters and joint angles. Of the segment motions only the acceleration range of motion of the pelvis and HAT segment

**Table 6 Significant main effects and speed interaction effects of inertia added to the ankle**

Measure		Speed	0.3 kg	1.55 kg	3.50 kg	
Energetics	VO2 [ml/min/kg]		10.96 ± 1.92	11.58 ± 1.93	12.26 ± 1.96*+	
		4.5 km/h	13.56 ± 2.40	14.46 ± 2.21	15.65 ± 2.45*+	
Gait parameters	Double stance time [s]		0.32 ± 0.04	0.30 ± 0.04*	0.29 ± 0.04*	
		Swing time left [s]		0.43 ± 0.02	0.47 ± 0.02*	<b>0.50 ± 0.03*</b>
			1.5 km/h	0.49 ± 0.05	0.54 ± 0.05*	<b>0.60 ± 0.05*</b>
Joint- & Segment angles	Stride length [m]	4.5 km/h	0.37 ± 0.01	0.39 ± 0.01*	<b>0.41 ± 0.04*</b>	
			(0.04)			
			0.66 ± 0.05	0.66 ± 0.05	0.62 ± 0.04	
		1.5 km/h	5.73 ± 1.91	5.69 ± 2.11	6.23 ± 2.37	
		4.5 km/h	8.98 ± 1.61	9.48 ± 2.24	8.48 ± 1.91	
		1.5 km/h	2.83 ± 0.89	2.66 ± 0.97	2.76 ± 1.11	
		4.5 km/h	2.91 ± 0.53	3.29 ± 0.97	3.57 ± 0.96	
			59.47 ± 3.82	58.82 ± 3.42	55.35 ± 3.48*+	
			26.70 ± 2.55	25.25 ± 4.00	23.90 ± 2.07*	
			50.31 ± 6.45	56.15 ± 9.10*	64.05 ± 14.12*	
Segment Motions	Acc pelvis AP RoM [m/s <sup>2</sup> ]		3.71 ± 0.67	4.01 ± 0.73*	<b>4.27 ± 0.73*+</b>	
			(0.53)			
		4.5 km/h	4.72 ± 1.08	<b>5.32 ± 1.10*</b>	<b>5.70 ± 1.04*+</b>	
			(0.59)			
			38.99 ± 6.89	41.59 ± 7.00	47.75 ± 11.84	
			2.35 ± 0.35	2.52 ± 0.38	2.63 ± 0.42*	
		4.5 km/h	3.08 ± 0.53	3.36 ± 0.58	<b>3.47 ± 0.58*</b>	
			(0.37)			
			63.28 ± 15.93	68.45 ± 19.77	65.75 ± 14.79	
			720.82 ± 56.69	712.15 ± 48.15	692.17 ± 51.53*	
	41.07 ± 3.61	37.38 ± 3.10*	<b>33.48 ± 3.31*+</b>			
	(3.99)					
	1.5 km/h	22.65 ± 2.14	21.18 ± 1.54	19.15 ± 3.15*		
	4.5 km/h	59.49 ± 6.16	<b>53.58 ± 5.05*</b>	<b>47.82 ± 3.89*+</b>		
	(4.33)					
EMG	Soleus – terminal stance		0.21 ± 0.07	0.20 ± 0.06	0.19 ± 0.08*	
			0.18 ± 0.03	0.18 ± 0.03	0.16 ± 0.03*+	
			0.15 ± 0.03 (0.02)	0.14 ± 0.03	<b>0.12 ± 0.03*</b>	

\* Significantly different from 0.3 kg ( $p < 0.05$ ).

+ Significantly different from 1.55 kg ( $p < 0.05$ ).

Bold: change larger than the average intra subject variability indicated between brackets at baseline.

Loaded conditions are compared to baseline condition. The table lists significant main effects (independent of speed) and significant interaction effects with speed, but only at speeds that are significant in pair wise comparisons.

in ML direction decreased significantly ( $p = 0.037$  and  $p = 0.007$ ), though pair wise comparisons revealed no significant changes.

The overall activity of the tibialis anterior has a significant change ( $p = 0.013$ ), though a clear trend is not visible

(see Table 8). And the vastus lateralis has a significant interaction effect with phase and speed ( $p = 0.004$ ), but pair wise comparisons did not reveal significant changes.

None of the significant changes exceeded the average intra-subject variability.

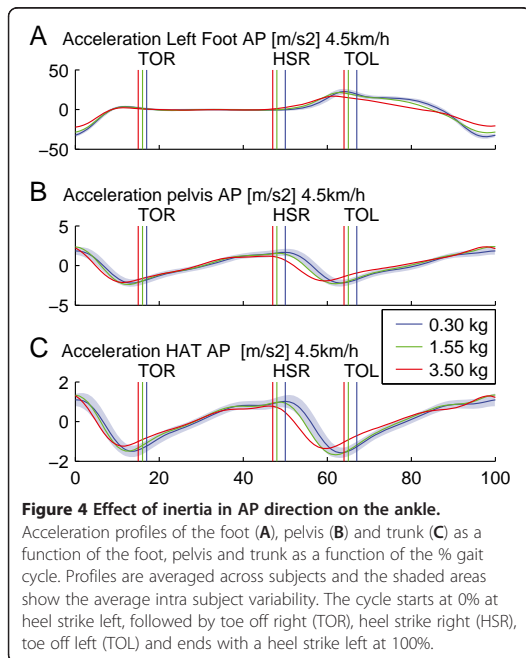


**Figure 4** Effect of inertia in AP direction on the ankle. Acceleration profiles of the foot (A), pelvis (B) and trunk (C) as a function of the foot, pelvis and trunk as a function of the % gait cycle. Profiles are averaged across subjects and the shaded areas show the average intra subject variability. The cycle starts at 0% at heel strike left, followed by toe off right (TOR), heel strike right (HSR), toe off left (TOL) and ends with a heel strike left at 100%.

## Discussion

We assessed the effect of adding inertia during walking on a treadmill in order to assess the effect of a gait training robot on gait. This study is novel in that we decoupled the inertia from gravitational effect and that we decoupled the inertia in different directions. We conducted two experiments, one with adding inertia to the ankle in anterior-posterior direction and one with adding inertia to the pelvis in AP and ML direction.

### Effect of the apparatus

In both experiments we first assessed the effect of the apparatus with minimum added inertia with free walking. The overall effect of the apparatus is negligible in both experiments. There were some significant changes, but these were very relatively small (few percent) and few in number: 11 for the ankle experiment and 10 for the pelvis experiment.

Most of these significant changes involve slow walking. All the loaded conditions, including the baseline conditions were randomized, but the free walking conditions were not randomized. Every subject started with slow walking. It is likely that the subjects were not completely familiarized with walking on the treadmill during the first trial i.e. free walking at slow speed. This could account for the significant interaction effects (load  $\times$  speed) that were found in the baseline validation.

### Effect of AP load on ankle

Adding inertia to the ankle during walking on a treadmill caused several significant changes. We hypothesized an increase in effort by the subject in order to maintain gait patterns. We did see a significant increase in energetics; this was not accompanied by an increase in muscle activity of the left (loaded) leg. This can be explained by the fact that muscle activity of the right leg increased, however this was not investigated. An argument in favor of this explanation could lie in the fact that the pelvis and hat segment show increased acceleration mainly during the terminal swing phase of the left leg. Since the left leg is swinging, effort for increased acceleration is likely to be caused by the right leg.

Adding 1.55 kg inertia to the ankle caused an increased in metabolic rate of 5.7%, which is a little less than the 7.6% that Royer and Martin found when applying a weight of 1.2 kg to the ankle and 0.8 kg to the knee [13]. They also found a significant increase of the soleus activity, where we found a small decrease. In our study the added load did not require vertical acceleration during push-off, whereas the extra weight in their study did require extra effort in vertical acceleration.

The muscle activity of the loaded leg remained unchanged largely, except for a few decreases: The first is that of the soleus in terminal stance, which indicates a reduced effort in push off, which is also visible in the reduced plantar flexion range of motion. Consequently the foot acceleration decreases and the stride length decreases. Contrary to our hypothesis the subject reduces the effort to accelerate the foot and its extra inertia, and 'accepts' changed gait patterns. The second reduction of muscle activity is the tibialis anterior in swing phase, indicating a reduced effort to lift the toe, which is explained by a reduced push off: if the plantar flexion is reduced, less effort is needed to lift the toes for sufficient ground clearance. Another consequence of the decreased acceleration is the significant increase in the swing time for the left leg: it takes longer before the foot touches the ground. Also this change is larger than the ISV, and therefore stated as 'appreciable'.

Adding 1.55 kg caused only an appreciable change in acceleration range of motion of the pelvis and left foot at high speeds only; the other 29 parameters remained unaffected. In both cases the changes just exceed the average intra subject variability. Therefore we conclude that walking with 1.55 kg added to the ankle in AP direction resembles normal walking.

Adding 3.5 kg also caused appreciable changes at low speeds and especially the changes of the pelvis and foot acceleration RoM at high speeds are much larger than the average intra subject variability. Therefore we conclude that walking with 3.5 kg added to the ankle in AP direction does not resemble normal walking.

**Table 7 Significant main effects and speed interaction effects of inertia added to the pelvis in AP direction**

Measure		Speed	X 0.7 kg	X 4.3 kg	X 10.2 kg	
<b>Energetics</b>						
Gait parameters	Stance time left [s]	1.5 km/h	1.43 ± 0.17	1.40 ± 0.16	1.41 ± 0.16	
		4.5 km/h	0.74 ± 0.04	0.74 ± 0.03	0.73 ± 0.03	
Joint- & Segment angles	Hip abduction RoM [deg]		12.24 ± 2.59	11.84 ± 2.40*	11.32 ± 2.27*+	
	Hip flexion RoM [deg]		37.04 ± 2.98	36.82 ± 2.54	36.14 ± 2.44*+	
	Knee flexion RoM [deg]		61.35 ± 5.54	61.06 ± 4.86	59.93 ± 4.67	
	Back sagittal flexion RoM [deg]		3.94 ± 0.96	4.54 ± 1.08*	5.29 ± 1.36*+	
Segment Motions	Pos pelvis AP RoM [mm]	1.5 km/h	4.25 ± 0.97	4.63 ± 0.99	4.98 ± 0.92*	
		4.5 km/h	3.64 ± 1.16 (1.56)	4.45 ± 1.61*	<b>5.60 ± 2.07*+</b>	
	Acc pelvis AP RoM [m/s <sup>2</sup> ]			49.14 ± 6.05	46.75 ± 5.35	43.03 ± 5.29*+
				3.88 ± 0.58 (0.56)	3.56 ± 0.41	<b>3.06 ± 0.33*+</b>
	Pos HAT AP RoM [mm]	4.5 km/h	5.04 ± 0.80 (0.57)	4.62 ± 0.62	<b>3.85 ± 0.59*+</b>	
				37.37 ± 4.26	36.10 ± 4.89	33.89 ± 4.76*
	Acc HAT AP RoM [m/s <sup>2</sup> ]			2.67 ± 0.29 (0.36)	2.55 ± 0.24	<b>2.24 ± 0.14*+</b>
				1.5 km/h	1.78 ± 0.28	1.66 ± 0.13
	EMG	Vastus lateralis - mid stance	4.5 km/h	3.55 ± 0.38 (0.35)	3.45 ± 0.40	<b>2.95 ± 0.19*+</b>
					0.23 ± 0.05	0.23 ± 0.05*
Vastus lateralis - terminal swing				0.06 ± 0.03	0.05 ± 0.02	0.06 ± 0.03*
				0.13 ± 0.04	0.14 ± 0.04	0.14 ± 0.04*
Soleus - mid stance			0.13 ± 0.04	0.14 ± 0.04*	0.14 ± 0.04*	

\* Significantly different from 0.3 kg ( $p < 0.05$ ).

+ Significantly different from 1.55 kg ( $p < 0.05$ ).

Bold: change larger than the average intra subject variability indicated between brackets at baseline.

Loaded conditions are compared to baseline condition. The table lists significant main effects (independent of speed) and significant interaction effects with speed, but only at speeds that are significant in pair wise comparisons.

### Effect of AP load on pelvis

We assessed the effect of adding inertia to the pelvis in AP direction during walking on a treadmill. We hypothesized that the effort remains unchanged and this is confirmed by the fact that energetics remain unchanged. The EMG activity does show significant changes, but, though significant, the changes are very small, and do not exceed the average intra subject variability.

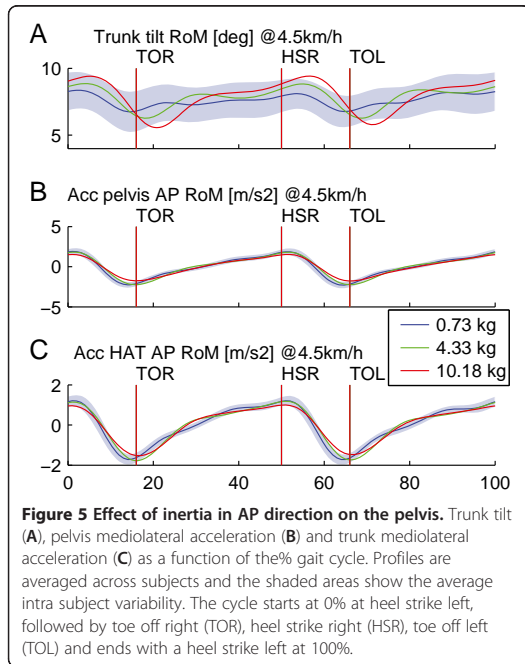
As hypothesized the pelvis motions decrease due to added inertia in AP direction. Though the decreases are less than the average intra subject variability, the pelvis position- and acceleration RoM decrease significantly. As the trunk is connected to pelvis also the trunk motions decrease significantly. However the sagittal rotation between the trunk and the pelvis, the back sagittal flexion increases. A possible explanation is that the pelvis shows more sagittal rotation, this however was not investigated in the study. The inertial forces due to the added inertia

may elicit a moment in the sagittal plane, causing the increased rotation.

Of all significant changes only the AP acceleration of the pelvis and hat segment and the sagittal rotation of the back exceed the average intra subject variability, only when 10.2 kg was attached. Therefore we consider walking with 4.3 kg to be similar to normal walking, whereas 10.2 kg does not resemble normal walking.

### Effect of ML load on pelvis

We assessed the effect of adding inertia to the pelvis in mediolateral direction during walking on a treadmill. We hypothesized that the ML motions of the pelvis would decrease, and correspondingly adding inertia did decrease the range of motion of the pelvis and HAT segment in ML direction significantly. These changes however are small and did not prove to be significant in pair wise



comparisons. Therefore we conclude that 5.3 kg can be added on the pelvis in ML direction without affecting the gait.

### Weber fractions

During the experiments subjects claimed that they did perceive the inertia, in several condition of low and high inertia. This can be explained by the Weber fraction [19]. The smallest noticeable difference in weight (the least difference that the test person can still perceive as a difference), is proportional to the starting value of the weight. Based on this, one could estimate what would be the just noticeable difference (JND) of added inertia, simply by taking the Weber fraction of the mass of the leg. For mass the Weber fraction is 1/10 [19,20]. Applying this to the mass distribution of the human body gives a JND of 3.2 kg for the trunk and 0.15 kg for the foot (see Table 9). In our study the applied inertia was more than the JND except for the baseline and the pelvis ML 2.3 kg condition.

**Table 8** Significant main effects and speed interaction effects of inertia added to the pelvis in ML direction

	Z 0.6 kg	Z 2.3 kg	Z 5.3 kg
Acc pelvis ML RoM [m/s <sup>2</sup> ]	1.61 ± 0.22	1.57 ± 0.24	1.54 ± 0.20
Acc HAT ML RoM [m/s <sup>2</sup> ]	1.39 ± 0.23	1.37 ± 0.23	1.32 ± 0.20
Tibialis anterior	0.12 ± 0.02	0.11 ± 0.02	0.12 ± 0.02*

\* Significantly different from 0.3 kg (p < 0.05).

This can explain why subject did perceive the difference even if physical measurement did not.

### Comparisons between experiments

In our experiments we found that adding inertia to the ankle causes more effect than adding the same inertia to the pelvis. Browning found similar results [12], with added weights, meaning that the found effects cannot be ascribed to the gravitational component only. An explanation is given by the fact that the acceleration of the foot is ten times larger than the acceleration of the pelvis in AP direction. Similarly, the acceleration of the pelvis in forward direction is three times higher than the acceleration of the pelvis in ML direction.

As hypothesized the effects are larger at high speeds. In the ankle experiment four appreciable effects at high speeds are found, only one for low speed. In the pelvis experiment for AP loading, three appreciable effects at high speeds are found, none for low speed.

### Comparison with other studies

In the pelvis experiment we applied AP inertia up to 10.2 kg and ML inertia of 5.3 kg which is approximately 13% and 7% of the body mass. Grabowski applied inertia of 25% of body weight in all directions and found an increase in metabolic rate (+25%). In our study the metabolic rate remains unchanged when applying inertias to the pelvis in the horizontal plane only. McGowan and colleagues applied inertias equal to 25% and 50% of the body mass and found an increase of soleus activity at the late stance of 17% and 43%. They found that the soleus is the primary contributor to forward trunk propulsion [10] and that the soleus and gastrocnemius both contribute in both support. In our study we reported no change of muscle activity in terminal stance, when adding 10.2 kg in AP direction or 5.2 kg in ML direction. However we did see a significant increase of both soleus and gastrocnemius in mid stance. McGowan applied inertia in all directions including vertical hence affecting the AP component of propulsion and the vertical component of propulsion, whereas we applied inertia only in one direction, only affecting the horizontal component of propulsion. Comparing our results with found results from Grabowski and McGowan suggests that vertical

**Table 9** Just noticeable difference for body segments according to the Weber fraction

	Weight percentage	Weight [kg] (75 kg bodyweight)	JND [kg] according to Weber fraction (1/10)
Trunk	43%	32.25	3.225
Upper leg	12%	9	0.9
Lower leg	5%	3.75	0.375
Foot	2%	1.5	0.15

motion of the pelvis may be the degree of freedom that is most sensitive to added inertia.

To find requirements for gait training robots, we started with applying inertia on one segment in one or two directions. Since nearly all robotic gait trainers have an interface to the lower shank and the pelvis, we applied inertia to the ankle and the pelvis. To obtain a complete set of requirements for gait training robots, the effect of inertia added to the knee should be investigated, as well as the effect of combined inertia's added to the ankle, knee and pelvis.

## Conclusion

In order to allow normal walking in a gait training robot, the robot should be transparent. In our study we quantified the requirements for transparent walking. We assume that when energetics, kinematics and gait parameters are unaffected, transparency in gait training is guaranteed. We found that inertia up to 2 kg to the ankle or 6 kg added to the pelvis have negligible effect on energetics, kinematics and gait parameters. Therefore, for gait training robots to be transparent, they should display inertias less than the found thresholds.

## Additional file

**Additional file 1: Movie of adding inertia to the pelvis in anterior-posterior and lateral direction independently.**

## Competing interests

Jos Meuleman works at Moog, working on the design of a gait training robot.

## Authors' contributions

JM conducted the research, data analysis and writing. EA and HK contributed in the design of the study and writing. All authors read and approved the final manuscript.

## Acknowledgements

Authors would like to thank Wybren Terpstra and Thijs Lohuis for their contribution in the execution of the experiment and their preliminary analysis of the data. This study was supported by a grant from Dutch Ministry of Economic affairs and Province of Overijssel, the Netherlands (grant: PID082004).

## Author details

<sup>1</sup>Moog Robotics, Nieuw-Vennep, The Netherlands. <sup>2</sup>Department of Biomechanical Engineering, University of Twente, Enschede, The Netherlands. <sup>3</sup>Biomechanical Engineering, Delft University of Technology, Delft, The Netherlands.

Received: 16 March 2012 Accepted: 10 April 2013

Published: 19 April 2013

## References

1. Colombo G, Joerg M, Schreiber R, Dietz V: Treadmill training of paraplegic patients using a robotic orthosis. *J Rehabil Res Dev* 2000, **37**:693-700.
2. Veneman JF, Kruidhof R, Hekman EE, Ekkelenkamp R, Van Asseldonk EH, van der Kooij H: Design and evaluation of the LOPES exoskeleton robot for interactive gait rehabilitation. *IEEE Trans Neural Syst Rehabil Eng* 2007, **15**:379-386.
3. van Asseldonk EHF, Veneman JF, Ekkelenkamp R, Buurke JH, van der Helm FCT, van der Kooij H: The Effects on Kinematics and Muscle Activity of Walking in a Robotic Gait Trainer During Zero-Force Control. *Neural Syst Rehabil Eng IEEE Trans* 2008, **16**:360-370.
4. Emken J, Harkema S, Beres-Jones J, Ferreira C, Reinkensmeyer D: Feasibility of manual teach-and-replay and continuous impedance shaping for

robotic locomotor training following spinal cord injury. *IEEE Trans Biomed Eng* 2008, **55**:322-334.

5. Emken J, Reinkensmeyer D: Robot-enhanced motor learning: accelerating internal model formation during locomotion by transient dynamic amplification. *IEEE Trans Neural Syst Rehabil Eng* 2005, **13**:33.
6. Kwakkel G, Kollen BJ, Krebs HI: Effects of robot-assisted therapy on upper limb recovery after stroke: a systematic review. *Neurorehabil Neural Repair* 2008, **22**:111-121.
7. Linde RQ, Lammertse P: Haptic Master - a generic force controlled robot for human interaction. *Ind Robot Int J* 2003, **30**:515-524.
8. Buerger SP, Hogan N: Complementary Stability and Loop Shaping for Improved Human - Robot Interaction. 23 IEEE Transactions on Robotics 232-244 (2007). doi:10.1109/TRO.2007.892229.
9. Grabowski A, Farley CT, Kram R: Independent metabolic costs of supporting body weight and accelerating body mass during walking. *J Appl Physiol* 2005, **98**:579-583.
10. McGowan CP, Neptune RR, Kram R: Independent effects of weight and mass on plantar flexor activity during walking: implications for their contributions to body support and forward propulsion. *J Appl Physiol* 2008, **105**:486-494.
11. De Witt JK, Hagan RD, Cromwell RL: The effect of increasing inertia upon vertical ground reaction forces and temporal kinematics during locomotion. *J Exp Biol* 2008, **211**:1087-1092.
12. Browning RC, Modica JR, Kram R, Goswami A: The effects of adding mass to the legs on the energetics and biomechanics of walking. *Med Sci Sports Exerc* 2007, **39**:515-525.
13. Royer TD, Martin PE: Manipulations of leg mass and moment of inertia: effects on energy cost of walking. *Med Sci Sports Exerc* 2005, **37**:649-656.
14. Aaslund MK, Moe-Nilssen R: Treadmill walking with body weight support: Effect of treadmill, harness and body weight support systems. *Gait posture* 2008, **28**:303-308.
15. Adams RJ, Hannaford B: Control law design for haptic interfaces to virtual reality. In *Book Control law design for haptic interfaces to virtual reality*. 2002. (Editor ed. Aeds.). City.
16. Furuta K, Kosuge K, Shiote Y, Hatano H: Master-slave manipulator based on virtual internal model following control concept, Robotics and Automation Proceedings 1987 IEEE International Conference. 1987:567-572. on; Mar 1987.
17. Hermens H, Frenks B, Merletti R, Stegeman D, Blok J, Rau G, Disselhorst-Klug C, Hägg G: *European Recommendations for Surface Electromyography*. 1999.
18. Zeni JA Jr, Richards JG, Higginson JS: Two simple methods for determining gait events during treadmill and overground walking using kinematic data. *Gait Posture* 2008, **27**:710-714.
19. Ross HE, Brodie EE: Weber fractions for weight and mass as a function of stimulus intensity. *Quarterly J Exp Psychology Sect Human Exp Psychology* 1987, **39**:77-88.
20. Ross HE, Brodie EE, Benson AJ: Mass-discrimination in weightlessness and readaptation to earth's gravity. *Expe Brain Res* 1986, **64**:358-366.

doi:10.1186/1743-0003-10-40

Cite this article as: Meuleman et al.: The effect of directional inertias added to pelvis and ankle on gait. *Journal of NeuroEngineering and Rehabilitation* 2013 **10**:40.

Submit your next manuscript to BioMed Central and take full advantage of:

- Convenient online submission
- Thorough peer review
- No space constraints or color figure charges
- Immediate publication on acceptance
- Inclusion in PubMed, CAS, Scopus and Google Scholar
- Research which is freely available for redistribution

Submit your manuscript at  
www.biomedcentral.com/submit





APPENDIX **C**

**LOPES II — Design and  
Evaluation of an Admittance  
Controlled Gait Training  
Robot with Shadow-Leg  
Approach**

This manuscript was submitted to Transactions on Neurosystems and Rehabilitation Engineering in 2015.

# LOPES II — Design and Evaluation of an Admittance Controlled Gait Training Robot with Shadow-Leg Approach

Jos Meuleman, *Member, IEEE*, Edwin van Asseldonk, Gijs van Oort, Hans Rietman, Herman van der Kooij, *Member, IEEE*

**Abstract**— Robotic gait training is gaining ground in rehabilitation. Room for improvement lies in reducing donning and doffing time, making training more task specific and facilitating active balance control, and by allowing movement in more degrees of freedom. Our goal was to design and evaluate a robot that incorporates these improvements. LOPES II uses an end-effector approach with parallel actuation and a minimum amount of clamps. LOPES II has eight powered degrees of freedom (hip flexion/extension, hip abduction/adduction, knee flexion/extension, pelvis forward/aft and pelvis mediolateral). All other degrees of freedom can be left free and pelvis frontal and transversal rotation can be constrained. Furthermore arm swing is unhindered. The end-effector approach eliminates the need for exact alignment, which results in a donning time of 10–14 minutes for first-time training and 5–8 minutes for recurring training. LOPES II is admittance controlled, which allows for the control over the complete spectrum from low to high impedance. When the powered degrees of freedom are set to minimal impedance, walking in the device resembles free walking, which is an important requisite to allow task-specific training. We demonstrated that LOPES II can provide sufficient support to let severely affected patients walk and that we can provide selective support to impaired aspects of gait of mildly affected patients.

**Index Terms**—gait training, admittance control, robotics, haptics, zero impedance, stroke, spinal cord injury

## I. INTRODUCTION

SINCE the end of the 20th century gait training robots have been developed [1], [2]. These devices reduce the physical workload for the therapist. Studies on effectiveness have shown contradictory results [3]–[7]. Recent meta-analyses have shown that for spinal chord injury (SCI) patients robotic-aided gait training has no beneficial effect compared to conventional therapy [8], but for stroke survivors robotic gait training is beneficial especially in the sub-acute phase and for severely impaired patients [6], [9].

J.H. Meuleman is with Moog and Department of Biomechanical Engineering of MIRA, University of Twente, The Netherlands, [jmeuleman@moog.com](mailto:jmeuleman@moog.com)

E.H.F. van Asseldonk and G. van Oort are with Department of Biomechanical Engineering of MIRA, University of Twente, The Netherlands. [E.H.F.vanAsseldonk@utwente.nl](mailto:E.H.F.vanAsseldonk@utwente.nl)  
[g.vanoort@utwente.nl](mailto:g.vanoort@utwente.nl)

J.S. Rietman is with Roessingh Research and Development, and Department of Biomechanical Engineering of MIRA, University of Twente, The Netherlands

H. v.d. Kooij is with Department of Biomechanical Engineering of MIRA, University of Twente, The Netherlands and with the Department of Biomechanical Engineering, Delft Technical University, The Netherlands, [h.vanderkooij@utwente.nl](mailto:h.vanderkooij@utwente.nl)

To improve the efficacy, gait training robots should encourage the patient to actively participate [10], [11]. This can be achieved by an ‘Assist-As-Needed’ (AAN) approach [12]–[15]. For severely affected patients, this implies that the robot should provide much assistance. This can be achieved with feedforward force [16], [17] or with high stiffness (high impedance). For mildly affected patients, the robot should behave transparently (low impedance) and provide assistance only on aspects that require support. Robot mechanics and control are key-drivers in facilitating AAN [18].

Implementation of AAN requires the robot mechanics to allow free motions in all Degrees of Freedom (DoFs) of gait, and when needed, to provide support in most DoFs. Hindering free motions or constraining DoFs causes changes in gait kinematics [4], [19]. Abduction and pelvis translations are constrained in e.g., the first generation Lokomat [1] and the Reo Ambulator [20]; Pelvis rotations are constrained in most devices e.g., Lopes I [21], Lokomat and Reo Ambulator. ALEX allows for pelvis vertical rotation [22], but not for pelvis anterior/posterior translation and other rotations. The PAM and POGO allows for free motion in all DoFs [17]. *Free motions* also means that arm swing should be possible, since it is part of normal walking and it contributes to the overall stability of human gait [23]. In most exoskeleton gait training robots arm swing is obstructed by the presence of mechanics beside the hip joints [4].

The interaction forces between robot and patient should be force controlled to implement both low and high impedance control [11], [24], [25]. The Lokomat was originally position controlled (high impedance), later force control was applied to the Lokomat [26]. This reduced the impedance of the Lokomat, however the behavior is not sufficiently transparent [10]. Several devices have been designed with low-impedance control as starting point, however, they all compromise on high impedance support: The stiffness of the Series Elastic Actuation in Lopes I is limited [21], [27], and therefore the high impedance mode is not stiff enough for training severely impaired patients. Similarly the PAM and POGO perform well in the low impedance control [17], but the stiffnesses are limited [28] and insufficient for high impedance control in gait training. Sulzer et al. [29] focused on low impedance for an active knee support, compromising high impedance support. AAN has been tested successfully on stroke-survivors with mild to moderate impairment with the single-sided exoskeleton ALEX [30]. The challenge is to develop a gait training robot

that is both sufficiently transparent and sufficiently stiff. Little has been published on the required transparency and stiffness. Regarding the required transparency, we have previously assessed the maximum allowable inertia added to the pelvis and ankle that do not give significant changes in kinematics during walking at  $4.5\text{km/h}$  [31].

Another aspect that needs improvement to optimize robot-aided gait training is the donning and doffing time. To increase the usability of gait training robots in practice, the donning time should be reduced. Little has been published about donning time of gait training robots. Nilsson et al. [32] reported a donning time of 15–20 minutes for the HAL robot, but this includes application of EMG. The donning time of the PAM and POGO is up to 30 min [17]. In interviews users of the Lokomat and Lopes I reported donning times of 20 minutes for the first training (including limb measurement and cuff selection) and 10–15 minutes for recurring trainings. These donning times are considerable given the duration of training sessions (30–60 minutes). In exoskeleton robots the long doffing/donning times are caused by the need to precisely align the robot joint axes with the human joints to prevent damage and uncomfortable man-machine interaction [33]. Improving the donning time is likely to be less enduring for both patient and physiotherapist.

Our goal was to design and evaluate a gait training robot suitable for clinical training of severely and mildly affected patients. This implies that donning should be quick, multiple DoFs should be free and the controller must be able to switch between low impedance (no support) and high impedance (full support).

The paper is structured as follows: In section II we discuss the requirements for the gait training robot. Section III describes the mechatronic design of LOPES II. Section IV describes the controller. Section V describes the validation of the technical requirements and the clinical feasibility of LOPES II. Section VI is the discussion. Finally conclusions are drawn in section VII.

## II. REQUIREMENTS

The user requirements were gathered with observations, interviews and group sessions with physiotherapists, stroke survivors, researchers and rehabilitation physicians. The main user requirements are *a)* quick donning and doffing; *b)* allow for motions occurring in a variability of (pathological) gait (e.g., hip-hiking and circumduction); *c)* provide Assist-As-Needed for patients with Functional Ambulation Category (FAC) 0–5; and *d)* ensure safety. The requirements are quantified in the following sections.

### A. Donning time

According to therapists and rehabilitation physicians, the time needed from the start of the preparation to the start of the training (donning time) should be less than ten minutes for first time patients; this includes measurements of limbs and selecting proper clamps. For recurring training the goal for the donning time is under five minutes.

TABLE I: Requirements per degree of freedom in terms of range of motion, torque and speed (powered DoFs only)

DoF	RoM [deg; m]	Force/ Torque [N; Nm]	Speed [rad/s; m/s]
Pelvis anterior/posterior	$\pm 0.2$	500	0.3
Pelvis mediolateral	$\pm 0.15$	500	0.3
Pelvis up / down	$\pm 0.1$	1000 <sup>a</sup>	
Pelvis sagittal rotation	$\pm 6$		
Pelvis frontal rotation	$\pm 10$		
Pelvis transversal rotation	$\pm 15$		
Hip abduction / adduction	20 / 20	70	
Hip flexion / extension	40 / 30	70	3.2
Hip endorotation / exorotation	15 / 15		
Knee extension / flexion	0 / 75	70	7.3
Foot endorotation / exorotation	10 / 20		
Ankle dorsiflexion/ plantarflexion	25 / 35		
Ankle inversion / eversion	10 / 10		

<sup>a</sup>Upward only (body weight support)

### B. DoF requirements

Table I lists the requirements per DoF. For the joint excursion limits we used the 95% interval of data from normal walking [34], [35] and from paretic gait [36]–[38]. For the pelvis translations we increased the range of motion to allow for acceleration/deceleration and drifting sideways.

Transparent behavior of the robot implies that the patient should be able to move freely with minimal resistance (impedance) of the robot [24]. With control strategies the robot impedance can be compensated for largely, but not completely. The remaining impedance can be implemented as an inertia, a damper or a combination of both. If the remaining impedance is sufficiently low, the gait pattern will not notably be affected. Little has been published on the maximum allowable impedances for gait training; we only have data about impedance expressed in terms of inertia: for pelvis anterior posterior and lateral motions is 6 kg and for the foot anterior translation it is 2 kg [31]. For the knee it is unspecified, but since the accelerations of the knee are less than that of the foot, but more than that of the hip it is estimated at 4 kg.

### C. Anthropometric data

To cover a wide population, we used several anthropometric datasets [39]. We aimed to cover 99% ( $\mu \pm 3\sigma$ ) of the populations of Europe and North America (see Table II).

## III. DESIGN DESCRIPTION

In order to minimize the moving mass of the robot, we incorporated fixed base actuation in LOPES II. We used a structure of push-pull rods, to transfer the motor torques to the patient, since they are light-weight and stiff. The shadow leg [41] serves as an intermediate body between motors and patient (see Fig. 1). Each motor is connected to a single segment of the shadow leg. The segments of the shadow leg are connected to the segments of the patient leg (Fig. 1). The angles of the shadow leg are directly related to the angles

of the patient leg, and thus given the patient limb lengths and angles of the shadow leg, the patient joint angles can be calculated exactly [42].

The shadow leg offers several advantages. The first is that a minimal amount of clamps are needed to control the patient's leg. We chose to have clamps at the feet, at the lower legs just below the knees, and at the pelvis (see Fig. 1). The second advantage is that, due to the minimum amount of clamps and the location of the shadow leg behind the patient, a small misalignment of the rods (i.e., not pointing exactly to the patient joints) will not cause any strains in the patient. Also these misalignments have only little effect on the calculated joint angles, e.g., on a lower leg of 400 mm, a vertical misalignment of 10 mm on the knee joint gives a 2.5% error in the calculated shank and thigh angle. Since all mechanics are located behind the patient, the arm swing is unhindered. The last advantage is that a physical end stop can be incorporated in the shadow leg to prevent hyper-extension of the knee.

For actuation we used Moog Control Loading actuators CL-R-E-/MD/40Nm (C40) for thigh flexion and abduction and pelvis lateral motion and CL-R-E-/MD/100Nm (C100) for the shank flexion and the pelvis anterior posterior motion [43]. We used a gearing with rods between the actuators and the human segments (see Tab. III).

The actuators are linked to the segments as follows: The shadow hip is attached to a stage that is actuated in the horizontal plane (d and e in Fig. 1), this way pelvis horizontal forces are applied to the patient. Thigh flexion of the shadow leg (actuated by b in Fig. 1) pushes the shadow knee and thus the patient knee forward. Shank rotation of the shadow leg (actuated by a in Fig. 1) translates the shadow ankle and thus

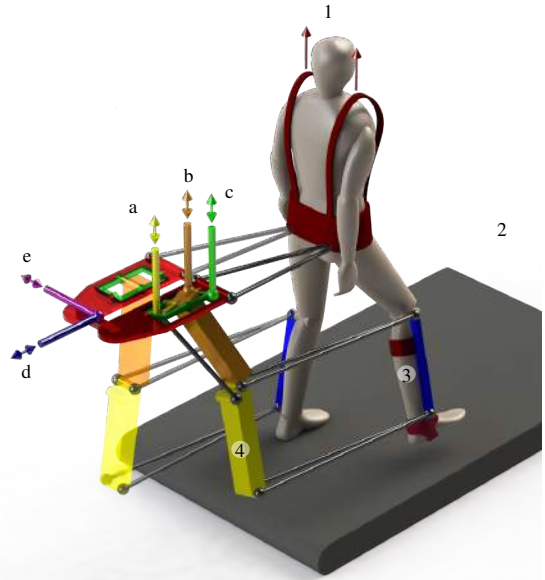


Fig. 1: Schematic overview of LOPES II with the shadow leg. The patient is placed on a treadmill (2) and attached to the harness with body weight support (1). The patient is clamped below the knees and at the feet. The clamps are connected to a leg guidance (3), which is connected to the shadow leg (4) with horizontal push pull rods. The shadow leg is actuated in shank flexion/extension (a), thigh flexion/extension (b) and abduction/adduction (c). The shadow leg is suspended on a stage connected to the patient's pelvis with rods, actuated in pelvis forward/aft- (d) and mediolateral direction (e).

TABLE II: Anthropometric data covering 99% of the European and North-american population

	Min	Max
Stature [mm]	1410 <sup>a</sup>	2088 <sup>b</sup>
Mass [kg]	36 <sup>c</sup>	138 <sup>d</sup>
Shank Length [mm]	347 <sup>e</sup>	514 <sup>e</sup>
Thigh Length [mm]	345 <sup>e</sup>	512 <sup>e</sup>

<sup>a</sup>Dutch 2004 (60 plus), female

<sup>b</sup>Dutch 2004 (20-30 years), male

<sup>c</sup>Dutch 2003 (31-65 years), male

<sup>d</sup>Dutch 2003 (31-65 years), male

<sup>e</sup>Values derived from stature [40]

TABLE III: Actuation of the LOPES II.

DoF	Actuator	Gearing	Force / Torque at segment <sup>a</sup>
Pelvis AP	C100	0.4 m	250 N
Pelvis ML	C40	0.2 m	200 N
Abduction	C40	2/3	60 Nm
Thigh flexion	C40	2/3	60 Nm
Shank flexion	C100	3/2	66 Nm

<sup>a</sup>force torque values are continuous. The motor and drive are capable of delivering a peak torque that is double the continuous torque, for a short period (< 1sec).

moves the patient ankle forward and backward. By applying abduction to the shadow leg (c in Fig. 1), the shadow ankle moves outward, and thus patient foot is pulled outward.

The rods pointing towards the ankle are connected to a foot bracket with a spherical gimbal, which has the center of rotation in the ankle joint. This assures that force from the ankle rods are exerted in the center of the ankle without imposing torques on the foot (see Fig. 2). At the pelvis a similar mechanism has been implemented to apply forces on the hip joints and allow for pelvic rotations in all three directions. At the end of the rods, near the patient, force sensors are mounted to measure the force between the patient and LOPES II (see Fig. 3).

The patient is suspended from a harness ((1) in Fig. 1), connected to pneumatic bodyweight support system (BWS). A near-constant upward force is applied to the harness by controlling the air-pressure in the BWS. Furthermore, the BWS contains a settable end-stop that limits the downward displacement of the harness to prevent falling.

Fig. 3 shows LOPES II as installed the Roessingh rehabilitation center in Enschede, the Netherlands. A second system has been installed in the Sint Maartenskliniek in Nijmegen,

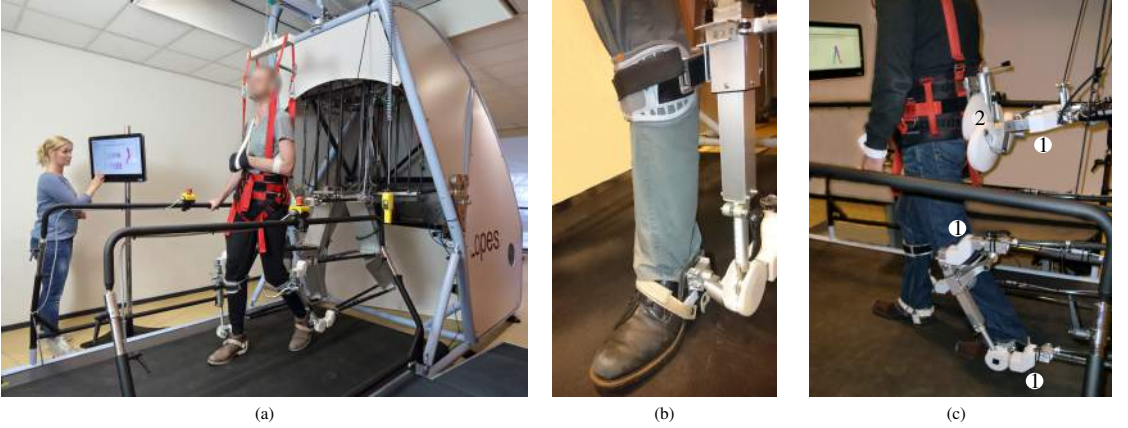


Fig. 3: LOPES II installed at rehabilitation center Roessingh, Enschede, the Netherlands (a). The patient is connected to LOPES II with a harness, clamps just below the knees, and foot brackets (b). Force sensors (1) are located closely to the patient, and the spherical gimbal at the pelvis (2) allows for rotations of the pelvis (c).

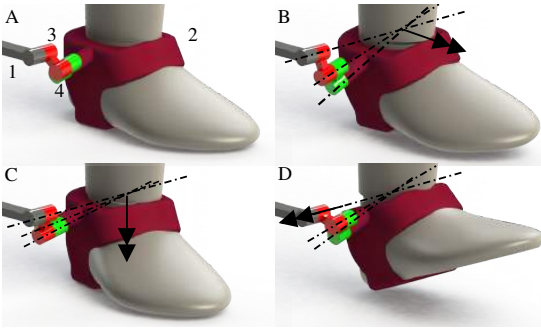


Fig. 2: Spherical gimbal connection of the ankle joint. The rod from the shadow leg (1) is connected to the foot bracket (2) with two segments (3, 4). The connections between the components are revolute joints, with axes intersecting in the ankle joint. This allows for rotation of the foot about the three principal axes: inversion / eversion (B), foot endorotation / exorotation (C) and plantarflexion / dorsiflexion (D).

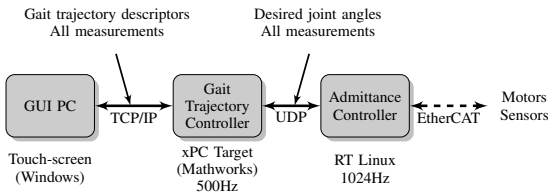


Fig. 4: The three computers used for controlling LOPES II.

the Netherlands.

TABLE IV: List of available sliders for adjusting the gait trajectory and support.

Gait subtask	Support Adjustment	Parameter adjustment
General	Yes	Walking velocity Hip extension offset
Weight shift	Yes	Amplitude <sup>a</sup> Timing Duration <sup>a</sup> Step width
Foot clearance	Yes <sup>a</sup>	Knee flexion in mid swing <sup>a</sup>
Stance	Yes <sup>a</sup>	Knee flexion in mid stance <sup>a</sup>
Prepositioning	Yes <sup>a</sup>	Knee flexion in end swing <sup>a</sup>
Step length	Yes <sup>a</sup>	Step length <sup>a</sup>

<sup>a</sup>adjustable for left and right leg separately

#### IV. CONTROLLER DESCRIPTION

LOPES II is controlled by three interconnected computers, as shown in Fig. 4. The graphical user interface is a touch screen PC with which the operator can optimize the gait trajectory for each patient. Additionally it provides real-time feedback and allows for post analysis of recorded data. The gait trajectory controller generates patient-specific gait patterns and support patterns. The admittance controller converts the gait and support patterns to actuator set points and processes data from the sensors. In the following sections, the three computers are discussed in detail.

##### A. User interface

In the graphical user interface (GUI) the gait is divided in subtasks, based on the *gait prerequisites* [44] (see Table IV). The amount of support (expressed as a percentage of the maximum support) and the reference trajectory can be adjusted for each gait subtask and each leg individually. This *selective support* [45] makes it possible to give support on only one

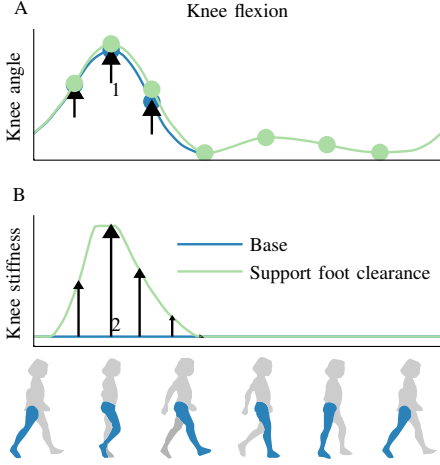


Fig. 5: Reference trajectory for the knee angle (A) and the support on the knee angle (B). The key events are plotted as dots in the angle trajectory. If the foot clearance is increased, specific key events are displaced (arrow 1), resulting in a modified reference trajectory for knee flexion in swing phase. If the support for foot clearance is increased, the stiffness of knee spring increases in swing phase (arrow 2).

subtask while giving complete freedom for the patient on the other subtasks, e.g., only supporting the patient in lifting his left foot during swing phase.

### B. Gait trajectory controller

The gait trajectory is generated by a Simulink model running on an embedded xPC Target PC (Mathworks Inc., Natick, MA, USA). For each joint, a trajectory is generated as a piecewise third order polynomial fitted between *key events* as described in [46]. The key event positions (timing and amplitude), and thus the trajectories, are dependent on walking velocity and patient length. The subtasks of gait are linked to the key events such that when the operator adjusts a parameter of a subtask, specific key events move relatively to their original location (see arrow 1 in Fig. 5), resulting in a modified gait trajectory for DoFs that are related to the specific subtask.

The joint trajectories are sent to the Admittance Controller which interprets them as the equilibrium position of a (critically damped) virtual spring. The spring stiffness  $K$  is related to the desired support  $G$  (in percent) by  $K = K_{\max} \left(\frac{G}{100}\right)^2$  with  $K_{\max}$  a predefined maximum stiffness (see Table V). The reason for the nonlinearity is that, since  $K_{\max}$  is high,  $\frac{1}{2}K_{\max}$  still *feels* very stiff; while we wanted 50% of the stiffness to feel significantly less stiff than 100% stiffness. Although algorithms exist to automatically adjust the stiffness [45], [47], we have used manually adjustable guidance as this was a specific request by the therapists.

As already stated in section IV-A, the support can be adjusted for each gait subtask individually, resulting in a gait-phase dependent stiffness. This results in a time-varying stiffness (see Fig. 5B).

Apart from generating the gait trajectories and stiffness trajectories, the Simulink model also has various safety checks and a state machine for the transitions between different modes (self test, motors off, standing still, training etc.).

### C. Admittance Controller

For the control of the actuators we use an admittance controller since it has the capability of displaying low and high impedance [48]. An overview of the admittance controller and its relation with the gait trajectory controller and mechanics is given in Fig. 6. In this section the components of the controller are discussed.

The central component of the admittance controller is the mass model ( $M^{-1}$ ), which converts the measured and virtual forces to a desired acceleration. The mass model of LOPES II displays virtual point masses in Cartesian coordinates i.e., the pelvis anterior/posterior translation (AP), the pelvis mediolateral translations (ML), the knee AP translation and the foot AP and ML translation. Since the controller uses segment coordinates, the mass matrix is a non-diagonal eight by eight matrix. This implies that forces in one DoF generate accelerations in several DoFs. For each DoF the value of the virtual mass is automatically adjusted depending on the phase of the gait. Higher virtual mass are used in stance to assure contact stability [49], and lower virtual masses are permitted in swing phase to allow for more transparency. The virtual masses and dampers in LOPES II admittance controller are tuned such that the system shows no oscillations in operation (see Table V). A leg in swing phase has low virtual mass on the foot (2 kg) and knee (5 kg), which is close to the maximum allowable inertias. The virtual masses of the foot and the knee are increased during stance phase to 12 kg and 15 kg respectively. Since the accelerations of the foot and the knee are relatively low in stance, this increased virtual mass is not perceived by the subject. For the pelvis the inertia is 40 kg, nearly seven times higher than desired. The Coulomb dampers are applied on the segments.

Haptic effects are implemented as virtual springs and dampers in the renderer. The springs are used to apply guidance forces; the dampers are used to damp oscillations. All effects can be limited in the force they exert on the virtual model. A limited damper therefore is called a Coulomb damper, since the behavior is similar to Coulomb friction when the damper is limited in force. The gait trajectory controller calculates the desired support in terms of the spring stiffness and joint trajectories.

The accelerations calculated by the mass model ( $a^U$ ) require limiting to assure that the model position, velocity and acceleration (pva) does not exceed predefined limits e.g., speed limit of actuators and joint excursion limits. The limited model accelerations ( $a^L$ ) are integrated to model velocities and positions. The model pva serves as setpoints for the motor controllers. The actuators and sensors in LOPES II are not directly coupled to the patient segments or joints like in most exoskeletons, but through a structure of rods. This results in a non-linear relationship between sensors and motor pva on the one hand and patient segment pva on the other hand.

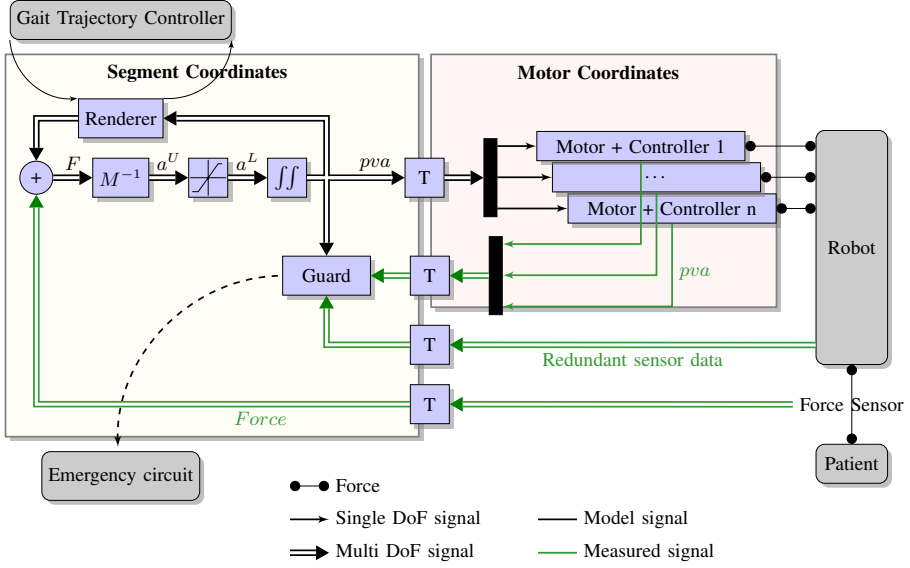


Fig. 6: Admittance controller layout of LOPES II and its relation with its peripherals. The gait controller sets the stiffnesses and positions for the guidance springs in the renderer, which calculates the supporting forces for the patient based on the spring positions and the measured positions. The sum of the renderer force and the measured force are the input for the virtual mass ( $M^{-1}$ ). The resulting model acceleration in segment coordinates ( $a^U$ ) is fed through a limiter to assure the model positions, velocities and accelerations (pva) stay within bounds. The model pva are transformed ( $T$ ) to motor coordinates to serve as set points for the individual motor controllers, which control the robot, which interacts with the patient. The guard triggers the emergency circuit if the errors between the measured pva and model pva, and the errors between measured motor angles with redundant sensor angle data.

TABLE V: Required and realized impedance of LOPES II in terms of inertia and damping and stiffness

DoF	Required mass	Virtual mass	Coulomb <sup>a</sup>	Maximum stiffness
Pelvis AP	6 kg	40 kg	5 N	5 N/mm <sup>b</sup>
Pelvis ML	6 kg	40 kg	5 N	20 N/mm
Knee AP	4 kg	5 kg <sup>c</sup>		
Foot AP	1.5 kg	2 kg <sup>d</sup>		
Foot ML	1.5 kg	2 kg <sup>d</sup>		
Abduction			0.5 Nm	1500 Nm/rad
Thigh flexion			0.5 Nm	1500 Nm/rad
Shank flexion			0.1 Nm	
Knee flexion				1500 Nm/rad

<sup>a</sup>Implemented as a virtual viscous damper with a maximum force

<sup>b</sup>The controller is capable of rendering higher stiffness (>20 N/mm), but we chose 5 N/mm since this felt more in balance with the stiffnesses of the other DoFs

<sup>c</sup>Inertia in swing phase; Inertia in stance phase is 15 kg

<sup>d</sup>Inertia in swing phase; Inertia in stance phase is 12 kg

The Admittance Controller performs real-time transformation ( $T$  blocks in Fig. 6) between motor and sensor data (force, position), and segment data. Subsequently each actuator has its own controller which controls the actuators in velocity mode,

with a bandwidth of > 100Hz.

The guard compares the model pva with the measured pva. When the difference between model and measured pva exceeds predefined limits, the guard triggers the emergency circuit to stop the system. Similarly the guard compares the measured motor angles with redundant sensor angles to assure validity of the motor encoders.

## V. EVALUATION AND RESULTS

### A. Position Accuracy

Since the position sensors of LOPES II are not collocated with the patient's segments, we want to verify whether the patient's segment angles are calculated correctly. Structural compliance may harm the accuracy of the calculated segment angles. We used an optical tracking system (Visualeyez VZ4000, PTI, Burnaby, Canada) to determine the accuracy of segment positions and angles calculated by LOPES II based on the motor angles (LOPES controller data). We applied cluster markers (frames with three markers) on the feet, lower legs, upper legs and sternum. Individual markers were put on the knee (lateral epicondyle) and hip (greater trochanter). We put additional markers on mechanical structure close to the patient i.e., the leg guidance (see Fig. 1 (3)) and on the rods that are connected to the pelvis.

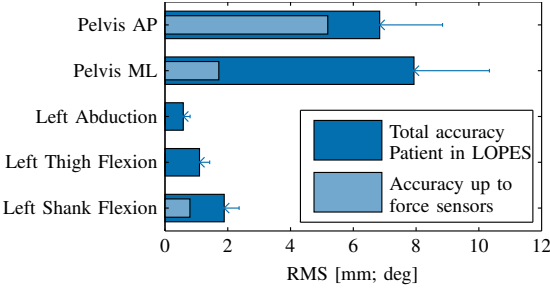


Fig. 7: Dark blue: Root mean square error between LOPES controller data (segment angles and position calculated by LOPES II) and angles and positions derived from markers on the subject; Light blue: RMSE between LOPES controller data and markers on the LOPES structure (near the clamps).

Two healthy subjects walked at two speeds (1.5 km/h and 2.5 km/h) in LOPES II with different support levels (0%, 10% and 100%). The optical tracking data was sampled at a rate of 90 Hz. In post processing data was filtered for spikes (50 mm), gaps up to 30 samples were interpolated, data was low-pass filtered with a second-order Butterworth filter at 10 Hz. The LOPES controller data (recorded at 1024 Hz) and optical data were re-sampled to 100 Hz, synchronized and cut into steps. Segment angles and positions were calculated from the positions of the markers on the subject (subject marker data). We also calculated the segment angles and positions from the markers on the LOPES structure (LOPES marker data).

To assess the inaccuracies we calculated the root mean square error (RMSE) between LOPES controller data and LOPES marker data. Subsequently we calculated the position accuracy up to the clamps i.e., the RMSE between the LOPES controller data and LOPES marker data, to assess the inaccuracy caused by the control loop and mechanical structure (e.g., free play and mechanical compliance).

The RMSE between LOPES controller data and subject marker data is 1–2 degrees for the segment rotations and 7–8 mm for pelvis translations (see Fig. 7). Although the subjects are firmly strapped in LOPES II, a great part of the error can be attributed to the clamps and human tissue: for the pelvis ML translation, the position accuracy up to the clamps is 2 mm. Therefore we conclude that the compliance of the harness and human tissue are the main contributors of the position inaccuracy. In AP direction, the position accuracy up to the harness is 5 mm. In AP direction, the connection is much stiffer than in ML direction, and only accounts for 2 mm of the inaccuracy. For the shank, the accuracy up to the clamps is 1 degree, which is half of the total position accuracy of the shank rotation.

### B. Minimal Impedance

The minimal impedance mode (MI) of LOPES II (0% support) was evaluated by comparing gait patterns of the subjects walking in minimal impedance mode in LOPES II with free walking (FW) on a treadmill. We used the same

TABLE VI: Correlation (top) and RMSE (bottom) of gait patterns between free walking and minimal impedance walking for two subjects at two speeds.

	S1		S2	
	1.5 km/h	2.5 km/h	1.5 km/h	2.5 km/h
Pelvis AP	0.84	0.33	0.91	0.62
Pelvis ML	1	0.82	0.96	0.99
Trunk AP	0.75	0.61	0.86	0.35
Trunk ML	1	0.80	0.93	0.95
Left abduction	0.95	0.84	0.93	0.88
Left hipflexion	1	0.98	0.99	1
Left kneelexion	0.99	– <sup>a</sup>	0.99	0.99
Left plantarflexion	0.87	– <sup>a</sup>	0.9	0.82
Pelvis AP [mm]	12.3	11.9	9.2	10.9
Pelvis ML [mm]	3.4	11.0	7.2	2.7
Trunk AP [mm]	4.3	5.0	4.9	5.7
Trunk ML [mm]	11.5	12.9	14.4	5.7
Left abduction [deg]	1.3	1.6	1.6	1.5
Left hipflexion [deg]	1.0	2.6	1.2	1.4
Left kneelexion [deg]	2.4	– <sup>a</sup>	2.3	2.7
Left plantarflexion [deg]	3.5	– <sup>a</sup>	3.7	4.6

<sup>a</sup>Too many missing markers on the left shank

marker layout and walking velocities as described in section V-A.

Gait patterns in minimal impedance mode resemble gait patterns of free walking (Fig. 8). For the joint angles and trunk and pelvis ML motion, the correlation between minimal impedance and free walking is high ( $> 0.8$ , see table VI), and the RMSE of the difference of the gait patterns is a few degrees. For trunk and pelvis AP motion the correlation is lower, especially at higher speeds.

An explanation for the difference in correlation between pelvis AP and ML motion can be found in the acceleration. The acceleration in AP direction is higher [31] and consequently the interaction forces (needed to accelerate the virtual mass) are higher. This is confirmed by the force patterns in Fig. 8 and the peak-to-peak values of the interaction forces (see Table VII). For the joints the interaction torques are considerably lower during swing than during stance (see Tab. VII). Although the accelerations of the swing leg are higher than the accelerations of the stance leg, the virtual mass during swing is considerably lower than during stance (see Tab. V), and therefore the interaction forces are lower.

### C. Donning time

We recorded the donning time for several stroke patients (N=13) with Functional ambulation category (FAC) scores ranging from 0 to 4. The donning procedure for patients who perform training with LOPES II for the first time consists of five steps: 1) the therapist measures the length of the upper leg, lower leg and foot length; 2) the measured data and other patient data e.g., weight, posture is fed into computer; 3) the patient is prepared to get into LOPES II i.e., getting to stand from wheelchair, optionally apply a sling for the paretic arm and put into standing position. For patients with FAC 0

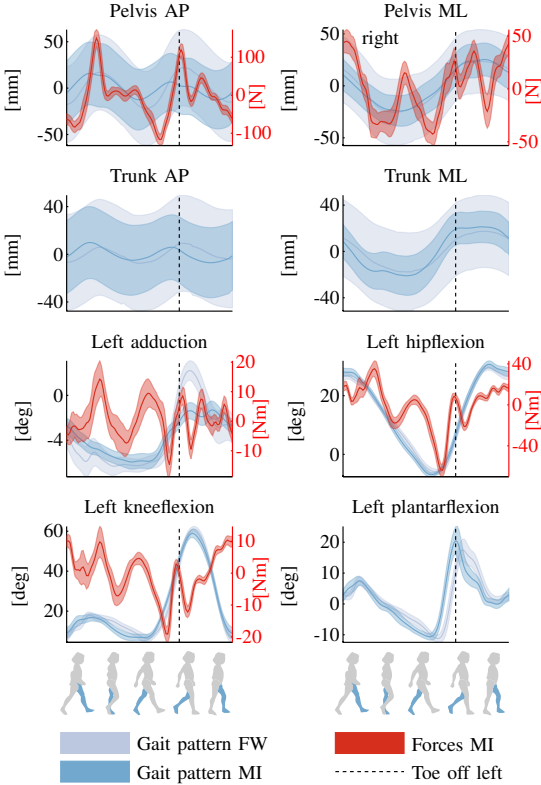


Fig. 8: Gait pattern of subject 2 at 2.5 km/h free walking outside LOPES II on a treadmill (FW) (light blue), and in LOPES II with minimal impedance (MI) (dark blue); and interaction forces in MI are plotted red; Toe-off left is indicated by the dashed line; at the left of the toe-off line, the left leg is in stance; at the right of the toe-off line, the left leg is in swing.

TABLE VII: Peak-to-peak interaction forces/torques in minimal impedance walking for two subjects at two speeds. For abduction, hip flexion and knee flexion, the interaction torques are split in swing phase (Sw.) and stance phase (St.)

		S1		S2	
		1.5 km/h	2.5 km/h	1.5 km/h	2.5 km/h
Pelvis AP [N]		107.6	169.2	125.7	266.8
Pelvis ML [N]		55.2	76.1	52.0	87.6
Left abduction [Nm]	Sw.	3.3	7.8	5.4	18.1
	St.	14.2	13.6	8.4	28.9
Left hipflexion [Nm]	Sw.	20.6	33.3	21.9	39.8
	St.	32.9	69.1	41.3	99.3
Left kneeflexion [Nm]	Sw.	8.4	8.7	12.8	22.6
	St.	9.0	21.1	14.2	29.2

the harness is applied in the wheelchair and the body weight support (BWS) system is used to lift the patient out of the wheelchair into LOPES II. Additionally the leg guidance (Fig. 1) is set to the length of the lower leg; 4) the therapist firmly

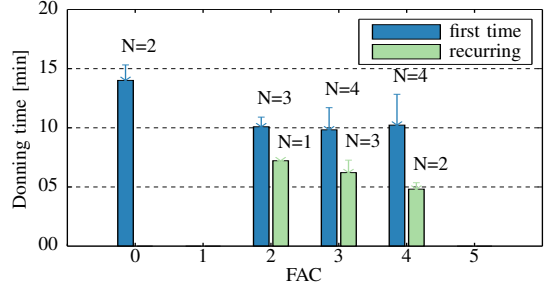


Fig. 9: Donning time grouped by FAC score and separated in first training and recurring training. For FAC 0 a lift was used to transfer the patients from wheelchair to LOPES II.

straps the patient in LOPES II. This is done while the patient is standing, if needed the BWS is used; 5) LOPES II is put in an active mode from which the training can start.

For recurring training, steps one and two of the donning procedure are not needed, since the settings are stored in the database, resulting in a shorter donning time. Therefore we did a recording of the recurring donning time for six patients.

The average first donning time is eleven minutes and two seconds. The average recurring donning time is six minutes and four seconds (see Fig. 9). For patients with FAC 2–4 the donning time for first training meets the goal of 10 minutes. For patients with FAC 0 donning time was longer (14–15 minutes), due to the use of the lift. For recurring trainings (no limb measurement needed) the donning time was 5–8 minutes. This approaches the desired donning time of 5 minutes for recurring patients. A limitation is that no data was available of recurring training of FAC 0 patients. There seems to be a trend that a higher FAC score shortens the donning time, but there were too few measurements to statistically confirm this trend.

#### D. Pilots with patients

We performed exploratory studies with stroke survivors and SCI patients. We will discuss two extreme cases: a mildly impaired stroke survivor (FAC 5) and a severely impaired SCI patient (lesion level C1, FAC 0).

A stroke survivor (FAC 5) walked in LOPES II at 1.5 km/h, first with 10% support and 0% BWS. The subject showed a stiff-knee gait on the right leg and used a little circumduction (5 degrees abduction) as compensation strategy. Subsequently we applied selective support on the foot clearance, i.e., support (high stiffness) on the paretic knee flexion during the swing phase. The paretic knee showed an increased knee flexion from 42 to 51 degrees (see Fig. 10). Despite the increased support in knee flexion during the swing phase, the interaction torque did not increase. This can be attributed to an intuitive response of the subject to minimize the interaction force. Though the support occurred only during the swing phase, the pelvis ML translation increased to the paretic side and the paretic adduction increased during stance phase of the paretic

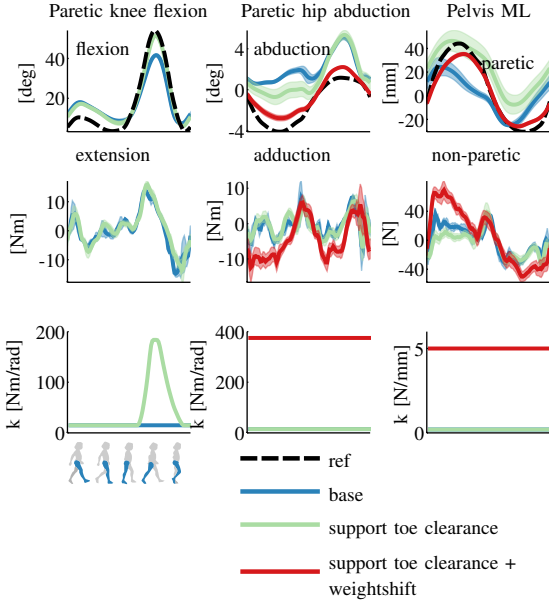


Fig. 10: Assist-As-Needed with a chronic stroke survivor (FAC 5), 1.5 km/h. Joint angles, interaction torques and virtual spring stiffness are shown for different support conditions. The spring stiffness is denoted by ‘k’, the spring’s reference trajectory denoted by ‘reference’. For clarity we omitted the support toe clearance plus weight shift (red line) for knee flexion plots, since the lines are similar to the lines of support toe clearance.

leg. This indicates that the subject took more weight on the paretic leg, during support on toe clearance.

Next we added selected support on the weight shift. This means that the stiffness for pelvis ML and for the abduction/adduction of both legs was increased for the complete gait cycle. The pelvis ML motions increased (see Fig. 10). Contrary to the support on foot clearance, the subject did not minimize the interaction forces. Due to the increase in stiffness in abduction, the paretic abduction decreased to 2 degrees, partially canceling the circumduction.

A SCI patient (FAC 0; 114 kg) walked in LOPES II with a general support of 80% and 40% bodyweight support (BWS) at 0.7 km/h (see Fig. 11). The patient’s joint angles and pelvis translations followed the reference trajectories. Since the support is implemented as springs, the interaction forces are largely proportional to the tracking errors. This is reflected in the pelvis AP force: the subject was leaning backward (negative interaction force). Consequently the measured trajectory of pelvis AP was a little behind its reference trajectory. This also resulted in more abduction of the left leg, especially during left stance phase: interaction torque of -40 Nm and a tracking error of 2 degrees. In swing the subject is able to follow the reference trajectory: the interaction torque and tracking error approach zero.

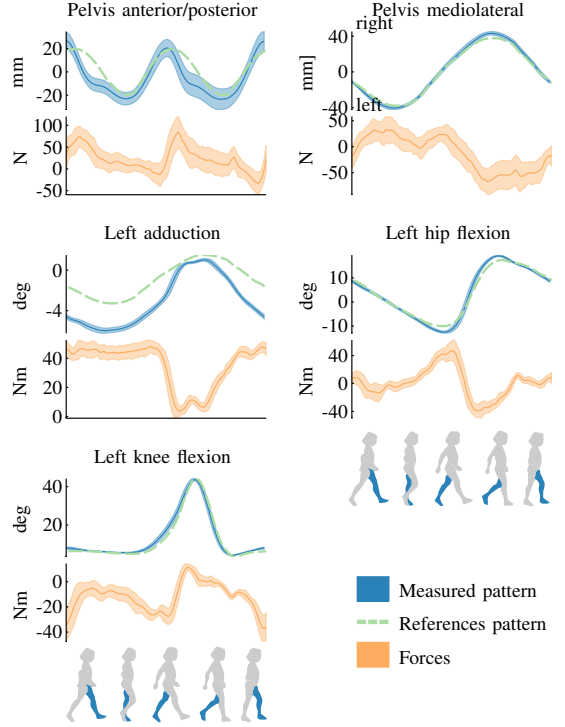


Fig. 11: Gait pattern and interaction forces of a 114 kg SCI patient (FAC 0) walking in LOPES II with 80% support and 40% bodyweight support at 0.7 km/h.

## VI. DISCUSSION

In this paper we discussed the design, the technical validation and the preliminary evaluation with patients of a shadow leg based robotic gait trainer with admittance control. We demonstrated that LOPES II is suitable for Assist-As-Needed training and that the required donning time is acceptable for clinical practice.

LOPES II uses the new shadow-leg concept. In this concept the motors are not collocated with the patient’s segments, but are coupled to the segments with a structure of rods and levers. The mechanics are located behind the patient. This implies that mildly impaired patients have the freedom to walk with arm swing; the more severely impaired, can use the side railing to aid in balance support.

Despite this complex structure, LOPES II calculates the subject segment angles with an accuracy of  $\pm 2$  degrees. A considerable part of the error can be attributed to the compliance between the robotic structure and the subject (see Fig. 7). A stiffer connection between the LOPES structure and the subject’s skeleton would improve the agreement between LOPES data and the subject marker data, and consequently the position accuracy. The most compliant elements between LOPES II and the subject’s skeleton are human tissue and the harness. In other words, if the position accuracy should be

improved the main focus should be on stiff clamping. At the pelvis translations the accuracy is 7–8 mm. Here the effect of the compliance of the harness is considerable especially in the ML direction. A stiffer clamping of the harness, will improve the position accuracy considerably.

Neckel et al. [50] investigated the position accuracy of the Lokomat in terms of Cartesian joint positions, by comparing optical tracking data with Lokomat data. They found an average error (offset), projected on the sagittal plane, of 12 mm for the left hip and 18 mm for the right hip. Assuming a 400 mm upper leg, this results into a hip flexion error of 1.7 – 2.6 degrees for the Lokomat. Therefore we conclude that the position accuracy of LOPES II, despite the non-collocated motors with the complex structure, is similar to that of Lokomat.

To cover the complete spectrum from low to high impedance, we used an Admittance Controller. The minimal impedance of LOPES II is reflected by an inertia (see Tab. V). This means that the patient has to apply force to LOPES II to accelerate the virtual mass. If the virtual mass is sufficiently low, the forces the patient has to apply are negligible. In an earlier study we found that gait patterns are not noticeably affected when an inertia of less than 2 kg is added to the ankle [31]. For the ankle motions, the achieved inertias in swing-phase are the required 2 kg, whereas in stance phase, the inertias are considerably higher than required to maintain contact stability. This has minimal effect on free walking, since the leg has a high impedance during stance. Similarly for the knee, the admittance controller adds 5 kg of inertia during swing phase, whereas we estimated that 4 kg was allowed.

The scaling of the inertia is reflected in the interaction forces. During stance the interaction forces are considerably higher than in swing (see Tab. VII). We believe that for transparency, the interaction forces during swing phase are more important, since the impedance of the leg is lower, and the desired accelerations of the leg are higher. The range of interaction torques of LOPES II in swing are 8–23 Nm for the knee flexion, and for the hip flexion 20–40 Nm. The torques increase with speed, but also show large differences between the two subjects.

Reference material for interaction torques is scarce. For the Lokomat in zero impedance mode, Riener et al. [11] reported interaction torques of 38–42 Nm for the hip and 25–28 Nm at the knee at a speed of 2 km/h. Van Dijk et al. [51] experimented on reduction of the interaction forces on Lopes I. The baseline peak-to-peak interaction torques at the hip and knee are 6 Nm and 17 Nm respectively. Using dynamics compensation and acceleration feed-forward, the RMS of the interaction forces at the thigh reduced with 35-39%, but at the shank the change in interaction force was negligible. Direct comparison of our results with these two studies is difficult. In the Lokomat study the interaction torques are not recorded directly, but reconstructed from forces measured at the suspension of the actuators. Van Dijk et al. [51] did record direct interaction forces, but they did not convert the forces to joint torques. The joint torques that are reported are measured in the series elastic actuators. Dynamics of the mechanics between the SEA and the subjects negatively affect

the interaction torques. Therefore we conclude that LOPES II has lower interaction torques than the Lokomat and higher interaction torques than Lopes I.

A second criterion for transparency is how much gait patterns in minimal impedance mode resemble the patterns of free walking. The joint angle patterns in minimal impedance mode are similar to free walking (see Fig. 8). This is reflected in a high correlation (0.84–1) and a low RMSE of a few degrees on the joint rotations which is similar to the normal intra-subject-variability of normal walking [46]. However for pelvis and trunk AP translation the deviations in amplitude and phase are larger, resulting in lower correlations (0.33–0.91). This is not surprising considering the fact that the inertia (40 kg) is nearly seven times higher than required (6 kg [31]). The RMSE values are considerable (4–12 mm), however they are less than the within-subject standard deviation of the patterns (see Fig. 8).

For the pelvis- and trunk ML the correlations are high (0.8–1), despite the fact that also for the pelvis ML translation, the inertia is seven times higher than required. This is explained by the fact that the acceleration in ML direction are lower compared to AP direction [31], and consequently the inertial forces are lower (see Fig. 8). Therefore the transparency in ML direction is higher than in AP direction. However, still the RMSE values in ML direction are considerable (3-14 mm), indicating that there is room for improvement of the transparency.

Based on the relatively low interaction forces and the high correlation of gait patterns with free walking, we conclude that LOPES II has a reasonable transparency in minimal impedance mode. In the minimum impedance mode, LOPES II displays an inertia (non zero impedance) and therefore the interaction forces are required to accelerate this virtual mass. The transparency may be improved further by reduction of the virtual mass, especially in the pelvis AP direction, or to provide a feed forward on the acceleration of the virtual mass [51].

For clinical application of robotic aided gait training it is paramount that the donning time is short. The donning time for LOPES II is 10–15 minutes for first training (see Fig. 9). Recurring donning time is 5–8 minutes for patients FAC 2–4. For the severely impaired, the first donning time and probably also the recurring donning time (although not measured) are higher than desired. This can be attributed to the fact the donning severely impaired patients includes the process of lifting out of the wheelchair. The donning time for the more severely affected patients can be shortened by improving the process of lifting the subject out of the wheelchair.

The goal was to provide robotic gait training for a wide range of patients from mildly to severely impaired. LOPES II was shown to be powerful and stiff enough to enforce a walking pattern on a severely affected patient (SCI lesion level C1; FAC0; 114 kg). We also demonstrated that, on the other side of the spectrum, LOPES II can provide selective support to a mildly affected patient (FAC5). This resulted in the anticipated effect on the supported aspect of gait. The patient seemed to adapt to support on toe clearance since the interaction torques did not change. Remarkably the stroke

survivor also showed minor changes in aspects of walking that were not supported directly. We assume that when subjects receive selective support, they adapt different aspects of their gait pattern, also aspects that are not supported directly, to find a new optimal gait pattern. For this process the minimal impedance of LOPES II is paramount, since it gives the patient the freedom to adapt his gait pattern. This showed that LOPES II is capable of providing Assist-As-Needed.

## VII. CONCLUSION

The robotic gait trainer LOPES II has been designed to meet the requirements stated by physiotherapists, patients, researchers and rehabilitation physicians. The main goals were to facilitate Assist-As-Needed training and realize short donning time. We have built a device with has eight admittance controlled Degrees of Freedom (DoFs) to cover the spectrum of low and high impedance. Additionally free motion is allowed in the remaining DoFs of gait. The mechanical structure of the shadow-leg does not require exact joint alignment and uses a minimal amount of clamps. This allows for a short donning time. LOPES II can apply maximum support to severely impaired patients and minimum support to healthy subjects. With the gait controller selective support can be applied to specific aspects of gait. We conclude that LOPES II is suitable for Assist-As-Needed training. This makes LOPES II promising for clinical application. Clinical studies are needed to answer the questions how gait training with the LOPES II compares with conventional therapy or other gait training robots, in terms of effectiveness and cost.

## ACKNOWLEDGMENTS

This study was supported by a grant from Dutch Ministry of Economic affairs and Province of Overijssel, the Netherlands (grant: PID082004).

## REFERENCES

- [1] G. Colombo, M. Joerg, R. Schreier, and V. Dietz, "Treadmill training of paraplegic patients using a robotic orthosis," *Journal of Rehabilitation Research and Development*, vol. 37, no. 6, pp. 693–700, 2000.
- [2] S. Hesse and D. Uhlenbrock, "A mechanized gait trainer for restoration of gait," *Journal of Rehabilitation Research and Development*, vol. 37, no. 6, pp. 701–708, 2000.
- [3] T. G. Hornby, D. D. Campbell, J. H. Kahn, T. Demott, J. L. Moore, and H. R. Roth, "Enhanced gait-related improvements after therapist- versus robotic-assisted locomotor training in subjects with chronic stroke: a randomized controlled study," *Stroke; a journal of cerebral circulation*, vol. 39, no. 6, pp. 1786–92, Jun. 2008.
- [4] J. Hidler, D. Nichols, M. Pelliccio, K. Brady, D. D. Campbell, J. H. Kahn, and T. G. Hornby, "Multicenter randomized clinical trial evaluating the effectiveness of the lokomat in subacute stroke," *Neurorehabilitation and Neural Repair*, vol. 23, no. 1, pp. 5–13, 2009.
- [5] B. Husemann, F. Müller, C. Krewer, S. Heller, and E. Koenig, "Effects of locomotion training with assistance of a robot-driven gait orthosis in hemiparetic patients after stroke: a randomized controlled pilot study," *Stroke*, vol. 38, no. 2, pp. 349–354, 2007.
- [6] M. Pohl, C. Werner, M. Holzgraefe, G. Kroczeck, J. Mehrholz, I. Wingendorf, G. Hoölig, R. Koch, and S. Hesse, "Repetitive locomotor training and physiotherapy improve walking and basic activities of daily living after stroke: a single-blind, randomized multicentre trial (DEutsche GAntrainerStudie, DEGAS)," *Clinical rehabilitation*, vol. 21, no. 1, pp. 17–27, Jan. 2007.
- [7] G. Morone, M. Iosa, M. Bragoni, D. De Angelis, V. Venturiero, P. Coiro, R. Riso, L. Pratesi, and S. Paolucci, "Who may have durable benefit from robotic gait training?: a 2-year follow-up randomized controlled trial in patients with subacute stroke," *Stroke; a journal of cerebral circulation*, vol. 43, no. 4, pp. 1140–2, Apr. 2012.
- [8] E. Swinnen, S. Duerinck, J.-P. Baeyens, R. Meeusen, and E. Kerckhofs, "Effectiveness of robot-assisted gait training in persons with spinal cord injury: a systematic review," *Journal of rehabilitation medicine*, vol. 42, no. 6, pp. 520–6, Jun. 2010.
- [9] J. Mehrholz, B. Elsner, C. Werner, J. Kugler, and M. Pohl, "Electromechanical-assisted training for walking after stroke ( Review )," *The Cochrane Library*, no. 7, 2013.
- [10] A. Schüick, R. Labruyere, H. Vallery, R. Riener, and A. Duschau-Wicke, "Feasibility and effects of patient-cooperative robot-aided gait training applied in a 4-week pilot trial," *Journal of neuroengineering and rehabilitation*, vol. 9, no. 1, p. 31, May 2012.
- [11] R. Riener, L. Lünenburger, S. Jezernik, M. Anderschitz, G. Colombo, and V. Dietz, "Patient-cooperative strategies for robot-aided treadmill training: first experimental results," *IEEE transactions on neural systems and rehabilitation engineering : a publication of the IEEE Engineering in Medicine and Biology Society*, vol. 13, no. 3, pp. 380–94, Sep. 2005.
- [12] L. L. Cai, A. J. Fong, C. K. Otoshi, Y. Liang, J. W. Burdick, R. R. Roy, and V. R. Edgerton, "Implications of Assist-As-Needed Robotic Step Training after a Complete Spinal Cord Injury on Intrinsic Strategies of Motor Learning," *The Journal of Neuroscience*, vol. 26, no. 41, pp. 10564–10568, 2006.
- [13] M. D. Ziegler, H. Zhong, R. R. Roy, and V. R. Edgerton, "Why variability facilitates spinal learning," *The Journal of neuroscience : the official journal of the Society for Neuroscience*, vol. 30, no. 32, pp. 10720–6, Aug. 2010.
- [14] J. Cao, S. Q. Xie, R. Das, and G. L. Zhu, "Control strategies for effective robot assisted gait rehabilitation: The state of art and future prospects," *Medical Engineering & Physics*, vol. 36, no. 12, pp. 1555–1566, Sep. 2014.
- [15] J. L. Emken, J. E. Bobrow, and D. J. Reinkensmeyer, "Robotic movement training as an optimization problem: Designing a controller that assists only as needed," in *Rehabilitation Robotics, 2005. ICORR 2005. 9th International Conference on*, 2005, pp. 307–312.
- [16] S. K. Agrawal and A. Fattah, "Gravity-balancing of spatial robotic manipulators," *Mechanism and Machine Theory*, vol. 39, no. 12, pp. 1331–1344, Dec. 2004.
- [17] D. Aoyagi, W. E. Ichinose, S. J. Harkema, D. J. Reinkensmeyer, and J. E. Bobrow, "A robot and control algorithm that can synchronously assist in naturalistic motion during body-weight-supported gait training following neurologic injury," *Neural Systems and Rehabilitation Engineering, IEEE Transactions on*, vol. 15, no. 3, pp. 387–400, Sep. 2007.
- [18] A. Pennycott, D. Wyss, H. Vallery, V. Klamroth-marganska, and R. Riener, "Towards more effective robotic gait training for stroke rehabilitation : a review," *Journal of neuroengineering and rehabilitation*, pp. 1–13, 2012.
- [19] J. F. Veneman, J. Menger, E. H. van Asseldonk, F. C. van der Helm, and H. van der Kooij, "Fixating the pelvis in the horizontal plane affects gait characteristics," *Gait Posture*, vol. 28, no. 1, pp. 157–163, 2008.
- [20] Motorika, "REO Ambulator." 2015. [Online]. Available: <http://www.motorika.com/?categoryId=90004>
- [21] J. F. Veneman, R. Kruidhof, E. E. G. Hekman, R. Ekkelenkamp, E. H. F. Van Asseldonk, and H. van der Kooij, "Design and Evaluation of the LOPES Exoskeleton Robot for Interactive Gait Rehabilitation," *Neural Systems and Rehabilitation Engineering, IEEE Transactions on*, vol. 15, no. 3, pp. 379–86, Sep. 2007.
- [22] S. K. Banala, S. H. Kim, S. K. Agrawal, and J. P. Scholz, "Robot Assisted Gait Training With Active Leg Exoskeleton (ALEX)," *IEEE transactions on neural systems and rehabilitation engineering*, vol. 17, no. 1, pp. 2–8, 2009.
- [23] S. M. Bruijn, O. G. Meijer, P. J. Beek, and J. H. van Dieën, "The effects of arm swing on human gait stability," *The Journal of Experimental Biology*, vol. 213, no. 23, pp. 3945–3952, Dec. 2010.
- [24] E. H. F. van Asseldonk, J. F. Veneman, R. Ekkelenkamp, J. H. Buerke, F. C. T. van der Helm, and H. van der Kooij, "The Effects on Kinematics and Muscle Activity of Walking in a Robotic Gait Trainer During Zero-Force Control," *Neural Systems and Rehabilitation Engineering, IEEE Transactions on*, vol. 16, no. 4, pp. 360–370, Aug. 2008.
- [25] H. Vallery, A. Duschau-wicke, and R. Riener, "Generalized Elasticities Improve Patient-Cooperative Control of Rehabilitation Robots," in *International Conference on Rehabilitation Robotics, 2009*, pp. 535–541.
- [26] M. Bernhardt, M. Frey, G. Colombo, and R. Riener, "Hybrid force-position control yields cooperative behaviour of the rehabilitation robot

- LOKOMAT," in *Rehabilitation Robotics, 2005. ICORR 2005. 9th International Conference on*, 2005, pp. 536–539.
- [27] H. Vallery, J. Veneman, E. van Asseldonk, R. Ekkelenkamp, M. Buss, and H. van Der Kooij, "Compliant actuation of rehabilitation robots," *Robotics & Automation Magazine, IEEE*, vol. 15, no. 3, pp. 60–69, 2008.
- [28] D. J. Reinkensmeyer, D. Aoyagi, J. L. Emken, J. a. Galvez, W. Ichinose, G. Kerdanyan, S. Maneeekobkunwong, K. Minakata, J. a. Nessler, R. Weber, R. R. Roy, R. D. Leon, J. E. Bobrow, S. J. Harkema, and V. R. Edgerton, "Tools for understanding and optimizing robotic gait training," *The Journal of Rehabilitation Research and Development*, vol. 43, no. 5, p. 657, 2006.
- [29] J. S. Sulzer, R. a. Roiz, M. a. Peshkin, and J. L. Patton, "A Highly Backdrivable, Lightweight Knee Actuator for Investigating Gait in Stroke." *IEEE transactions on robotics : a publication of the IEEE Robotics and Automation Society*, vol. 25, no. 3, pp. 539–548, Jun. 2009.
- [30] S. Srivastava, P.-C. Kao, S. H. Kim, P. Stegall, D. Zanotto, J. Higginson, S. Agrawal, and J. Scholz, "Assist-as-Needed Robot-Aided Gait Training Improves Walking Function in Individuals Following Stroke." *IEEE transactions on neural systems and rehabilitation engineering : a publication of the IEEE Engineering in Medicine and Biology Society*, vol. 4320, no. c, pp. 1–9, Oct. 2014.
- [31] J. H. Meuleman, E. H. van Asseldonk, and H. van der Kooij, "The effect of directional inertias added to pelvis and ankle on gait." *Journal of neuroengineering and rehabilitation*, vol. 10, no. 1, p. 40, Apr. 2013.
- [32] A. Nilsson, K. S. Vreede, V. Häglund, H. Kawamoto, Y. Sankai, and J. Borg, "Gait training early after stroke with a new exoskeleton the hybrid assistive limb : a study of safety and feasibility," *Journal of neuroengineering and rehabilitation*, vol. 11, no. 92, 2014.
- [33] A. Schiele, "Ergonomics of exoskeletons: Objective performance metrics," in *EuroHaptics conference, 2009 and Symposium on Haptic Interfaces for Virtual Environment and Teleoperator Systems. World Haptics 2009. Third Joint*, 2009, pp. 103–108.
- [34] D. A. Winter, *The biomechanics and motor control of human gait*. University of Waterloo Press, 1987.
- [35] D. G. Wright, S. M. Desai, and W. H. Henderson, "Action of the Subtalar and Ankle-Joint Complex during the Stance Phase of Walking," *J Bone Joint Surg Am*, vol. 46, pp. 361–382, Mar. 1964.
- [36] D. C. Kerrigan, E. P. Prates, S. Rogan, and P. O. Riley, "Hip hiking and circumduction: quantitative definitions," *American Journal of Physical Medicine & Rehabilitation*, vol. 79, no. 3, pp. 247–252, 2000.
- [37] D. C. Kerrigan, M. E. Karvosky, and P. O. Riley, "Spastic paretic stiff-legged gait: joint kinetics," *American Journal of Physical Medicine & Rehabilitation*, vol. 80, no. 4, pp. 244–249, 2001.
- [38] C. M. Kim and J. J. Eng, "Magnitude and pattern of 3D kinematic and kinetic gait profiles in persons with stroke: relationship to walking speed," *Gait Posture*, vol. 20, no. 2, pp. 140–146, 2004.
- [39] TU Delft, "DINED," 2015. [Online]. Available: <http://dined.io.tudelft.nl/dined/#>
- [40] D. A. Winter, *Biomechanics and Motor Control of Human Movement*. Nueva York, EUA : Wiley, 1990.
- [41] J. H. Meuleman and P. Lammertse, "Rehabilitation apparatus with a shadow leg," 2014. [Online]. Available: <http://www.google.com/patents/WO2014090414A1?cl=en>
- [42] J. H. Meuleman, E. van Asseldonk, and H. van der Kooij, "Novel actuation design of a gait trainer with shadow leg approach," in *Rehabilitation Robotics (ICORR), 2013 IEEE International Conference on*, Seattle, 2013.
- [43] MOOG, "Moog Control Loading Solutions," p. 5, 2009. [Online]. Available: <http://www.moog.com/literature/ICD/Moog-Test-ControllLoadingSolutions-Overview-en.pdf>
- [44] J. Perry, *Gait Analysis: Normal and Pathological Function*. SLACK Incorporated, 1992, vol. 12.
- [45] B. Koopman, E. H. F. van Asseldonk, and H. van der Kooij, "Selective control of gait subtasks in robotic gait training: foot clearance support in stroke survivors with a powered exoskeleton," *Journal of Neuroengineering and Rehabilitation*, vol. 10, no. 1, p. 3, Jan. 2013.
- [46] —, "Speed-dependent reference joint trajectory generation for robotic gait support," *Journal of Biomechanics*, vol. 47, no. 6, pp. 1447–1458, Apr. 2014.
- [47] E. H. F. V. Asseldonk, B. Koopman, J. H. Buurke, C. D. Simons, H. V. D. Kooij, E. H. F. van Asseldonk, and H. van der Kooij, "Selective and adaptive robotic support of foot clearance for training stroke survivors with stiff knee gait," in *Rehabilitation Robotics, 2009. ICORR 2009. IEEE International Conference on*, 2009, pp. 602–607.
- [48] R. van der Linde and P. Lammertse, "The HapticMaster, a new high-performance haptic interface," *Proc.*, pp. 1–5, 2002.
- [49] R. Adams, M. Moreyra, and B. Hannaford, "Stability and performance of haptic displays: Theory and experiments," *Proceedings ASME International ...*, 1998.
- [50] N. Neckel, W. Wisman, and J. Hidler, "Limb alignment and kinematics inside a Lokomat robotic orthosis." *Conference proceedings : ... Annual International Conference of the IEEE Engineering in Medicine and Biology Society. IEEE Engineering in Medicine and Biology Society. Annual Conference*, vol. 1, pp. 2698–701, Jan. 2006.
- [51] W. van Dijk, H. van der Kooij, B. Koopman, and E. van Asseldonk, "Improving the transparency of a rehabilitation robot by exploiting the cyclic behaviour of walking," in *ICORR*, 2013.



APPENDIX **D**

# Rehabilitation Apparatus with a Shadow Leg

international patent application number WO2014/090414 publication data  
June 19, 2014

(12) INTERNATIONAL APPLICATION PUBLISHED UNDER THE PATENT COOPERATION TREATY (PCT)

(19) World Intellectual Property  
Organization  
International Bureau



(10) International Publication Number  
**WO 2014/090414 A1**

(43) International Publication Date  
19 June 2014 (19.06.2014)

- (51) International Patent Classification:  
A61H 1/02 (2006.01) A61H 3/00 (2006.01)
- (21) International Application Number:  
PCT/EP2013/053354
- (22) International Filing Date:  
20 February 2013 (20.02.2013)
- (25) Filing Language: English
- (26) Publication Language: English
- (30) Priority Data:  
1222322.8 12 December 2012 (12.12.2012) GB
- (71) Applicant: MOOG BY [NL/NL]; PO Box 187, NL-2150 AD Nieuw-Vennep (NL).
- (72) Inventors: MEULKMAN, Jos; Talmalaan 9, NL-2121CR Bennebroek (NL). LAMMERTSE, Piet; Graaf Aelbrechtlaan, NL 1181 SW Amstelveen (NL).
- (74) Agent: WITHERS & ROGERS LLP; 4 More London Riverside, London SE1 2EW (GB).
- (81) Designated States (unless otherwise indicated, for every kind of national protection available): AE, AG, AI, AM,

AO, AT, AU, AZ, BA, BB, BG, BH, BN, BR, BW, BY, BZ, CA, CH, CL, CN, CO, CR, CU, CZ, DE, DK, DM, DO, DZ, EC, EE, EG, ES, FI, GB, GD, GE, GH, GM, GT, HN, HR, HU, ID, IL, IN, IS, JP, KE, KG, KM, KN, KP, KR, KZ, LA, LC, LK, LR, LS, LT, LU, LY, MA, MD, ME, MG, MK, MN, MW, MX, MY, MZ, NA, NG, NI, NO, NZ, OM, PA, PE, PG, PH, PL, PT, QA, RO, RS, RU, RW, SC, SD, SE, SG, SK, SL, SM, ST, SV, SY, TH, TJ, TM, TN, TR, TT, TZ, UA, UG, US, UZ, VC, VN, ZA, ZM, ZW.

(84) Designated States (unless otherwise indicated, for every kind of regional protection available): ARIPO (BW, GH, GM, KE, LR, LS, MW, MZ, NA, RW, SD, SI, SZ, TZ, UG, ZM, ZW), Eurasian (AM, AZ, BY, KG, KZ, RU, TJ, TM), European (AL, AT, BE, BG, CH, CY, CZ, DE, DK, EE, ES, FI, FR, GB, GR, HR, HU, IE, IS, IT, LT, LJ, LV, MC, MK, MT, NL, NO, PL, PT, RO, RS, SE, SI, SK, SM, TR), OAPI (BF, BJ, CF, CG, CI, CM, GA, GN, GQ, GW, ML, MR, NE, SN, TD, TG).

Published:  
— with international search report (Art. 21(3))

(54) Title: REHABILITATION APPARATUS WITH A SHADOW LEG

(57) Abstract: A gait rehabilitation apparatus (12) uses a mechanical shadow leg (42) positioned behind the biological leg (18) to provide forces and guide the biological leg in use.

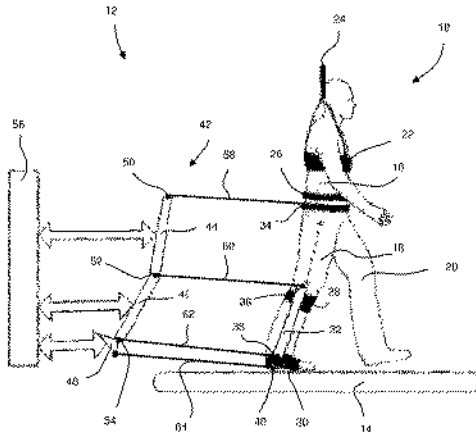


Fig. 1

WO 2014/090414 A1

## D.1 Rehabilitation apparatus

The present invention is concerned with an apparatus for driving and/or supporting a limb and an associated method. More specifically, the present invention is concerned with a mechanical apparatus for gait rehabilitation by guiding and / or applying forces to a limb of a human or animal subject.

Medical conditions such as brain damage (stroke) and nerve damage (spinal cord injury) caused by accident or injury can result in the temporary loss or impairment of use of a subject's limbs. For example, the legs may be limited in their use such that the subject finds it difficult to walk. Following such injury or illness, a period of rehabilitation is typical during which nerve and / or muscle damage is repaired.

Such rehabilitation has been traditionally provided by a physiotherapist or physical therapist manually interacting with the subject. For example, the subject may walk on a treadmill or along a set path during which activity the physiotherapist will manually support and manipulate the subject's legs in order to provide the desired motion and feedback. By this process muscles and nerves can be gradually repaired.

Methods which involve the direct interaction of a physiotherapist, or require the physiotherapist to support and / or guide the subject are not ideal because they may result in uneven or unpredictable forces on the subject. It may also be uncomfortable for the therapist to undergo such activity for extended periods, potentially with numerous subjects. Fatigue or strength of the physiotherapist often is the limiting factor in therapy

An alternative to the above mentioned method is to provide a mechanical gait rehabilitation robot. Mechanical gait rehabilitation robots are known in the art.

WO2012/062283 discloses a device which uses a number of flexible cords in tension to support a subject's limbs during rehabilitation. Another example of such a device can be seen in US7998040. Although such devices can apply uni-directional forces to the subject (with the cords in tension), they are not able to provide forces in the opposite direction (a flexible cord cannot carry a compressive force), or in other directions (e.g. sideways to retain the subject's leg in a set path).

US6666798 discloses an apparatus for rehabilitation in which a therapist is connected to a subject via a set of rigid links. This system is provided to free the physiotherapist's hands, and still requires the physiotherapist to bear the weight of, and guide, the subject's legs. Therefore the inherent lack of repeatability and potential for injury to the physiotherapist is

still present. The disclosure is also only concerned with lower leg rehabilitation, having the ankle and knee connected to the therapist. Therefore rehabilitation of the upper leg is not considered.

Prior art document CN101862255B discloses a known type of rehabilitation apparatus which has a mechanical leg at the side of the patient's leg. A problem with this type of apparatus is that it needs to be provided with extendible leg members in order to account for various different sizes of patient. As such, this apparatus is particularly complicated and time consuming to set up for each individual patient.

It is an aim of the present invention to overcome or at least alleviate the above mentioned problems with the prior art.

According to a first aspect of the invention there is provided a gait rehabilitation apparatus comprising an articulated mechanical shadow leg configured to mimic the movement of a biological leg, a first member extending from the shadow leg and having a first biological leg attachment formation defined thereon, wherein the first member extends in a substantially anteroposterior direction relative to the shadow leg in use.

Advantageously, the provision of an articulated, mechanical shadow leg positioned behind the leg of the subject allows for controlled, repeatable and reliable movement to be introduced. The joints of the shadow leg can be arranged so that only desired motion of the subject is permitted. Furthermore, because the shadow leg is positioned behind the subject's leg, various different sizes of subject can be accommodated. Evidently, the position of the first member will change depending on the size of the patient, however, this would not be significant enough to seriously affect the kinematics of the mechanism.

Preferably, there is provided a second member extending from the shadow leg and having a second biological leg attachment formation defined thereon; wherein the second member extends in a substantially anteroposterior direction relative to the shadow leg in use.

Preferably, the articulated shadow leg comprises an upper leg portion articulated about a shadow hip joint at an upper end in use.

Preferably, the first member extends from proximate the shadow hip joint, and the second member extends proximate a knee region of the shadow leg.

Preferably, the articulated shadow leg comprises a lower leg portion articulated about a shadow knee joint at an upper end in use.

Preferably, the first member extends from proximate the shadow knee

joint, and the second member extends proximate an ankle region of the shadow leg.

Preferably, the articulated shadow leg comprises a foot portion articulated about a shadow ankle joint at an upper end in use.

Preferably, the first member extends from proximate the shadow ankle joint, and the second member extends proximate a foot region of the shadow leg.

Preferably, there is provided a third member extending from the shadow leg and having a third biological leg attachment formation defined thereon; wherein the third member extends in a substantially anteroposterior direction relative to the shadow leg in use.

Preferably, the articulated shadow leg comprises an upper leg portion articulated about a shadow hip joint at an upper end in use; and, a lower leg portion connected to the upper leg portion and articulated about a shadow knee joint at an upper end in use.

Preferably, the first member extends from proximate the shadow hip joint, the second member extends proximate the shadow knee joint and the third member extends proximate an ankle region of the shadow leg.

Preferably, a fourth member is provided extending from the shadow leg and having a fourth biological leg attachment formation defined thereon; wherein the fourth member extends in a substantially anteroposterior direction relative to the shadow leg in use.

Preferably, the articulated shadow leg comprises a foot portion connected to the lower leg portion and articulated about a shadow ankle joint at an upper end in use.

Preferably, the fourth member extends proximate a foot region of the shadow leg.

According to a second aspect of the present invention, there is provided a method of gait rehabilitation comprising the steps of providing an articulated mechanical shadow leg configured to mimic the movement of a biological leg, providing a first member connected to the shadow leg, providing a second member connected to the shadow leg, attaching the first and second members to the biological leg of a subject such that the first and second members extend in a substantially anteroposterior direction and, using the shadow leg to guide and / or provide force input to the biological leg.

An example gait rehabilitation apparatus and method in accordance with the present invention will now be described with reference to the accompanying figures in which:-

FIGURE D.1 is a side schematic view of an embodiment of a gait rehabilitation apparatus in accordance with the present invention; and

FIGURE D.2 is a further schematic side view of the apparatus of Figure D.1.

With reference to Figure D.1, a subject 10 is attached to an apparatus 12 in accordance with the present invention. The subject 10 is supported by, and walking on a treadmill 14. Such treadmills are well known in the art. The subject 10 has a torso 16, a right leg 18 and a left leg 20.

The apparatus 12 of the present invention comprises a torso harness 22, which wraps around the subject's torso 16. The harness 22, and therefore at least some of the weight of the subject 10 is supported from a mounting point 24 directly above the subject 10. In the event that the subject cannot support their own weight, the harness 22 provides some assistance.

A waistband 26 is positioned around the mid-section of the subject's torso 16. The waistband is an adjustable belt of material which can be securely fastened to the patient. A leg strap 28 is wrapped around the subject's leg just below the knee. The leg strap also comprises an adjustable strip of material. Finally, a foot harness 30 is positioned around the subject's foot. The foot harness 30 is a cradle in which the foot rests, and comprises a stiff inflexible member extending from the ankle to the base of the foot. The foot harness 30 is attached to the foot such that it moves therewith rotationally and translationally.

A substantially inflexible lower leg member 32 is attached to, and positioned between, the leg strap 28 and the ankle region of the side member of the foot harness 30. The member 32 is adjustable in length as will be discussed below. The lower leg member 32 reacts excessive side-to-side forces cause by misalignment of the knee and ankle which would put the knee under significant stress. It also reacts any tangential forces on the knee which may move the leg strap 28.

An attachment point 34 is provided at the lower part of the subject's back on the waistband 26. A second attachment point 36 is provided at an upper end of the member 32 and is coincident with the flexion/extension axis of the subject's knee. A third attachment point 38 is provided proximate a lower end of the member 32, at the top of the foot harness 30 and is oriented to be substantially coincident with the flexion/extension axis of the subject's ankle. The member 32 is adjusted during fitting to ensure that the attachment points 36 and 38 align with the knee and ankle respectively. Finally, a fourth attachment point 40 is provided at the base of the subject's foot proximate the heel.

The apparatus 12 comprises a shadow leg 42 comprising an upper leg member 44, a lower leg member 46 and a foot member 48.

The upper leg member 44 is a stiff, elongate member of approximately the same length of an average human thigh. The upper leg member 44 is connected at its top end to a support (not shown) by a shadow hip joint 50 which allows articulation about an axis perpendicular to the page (and therefore equivalent to the extension / flexion movement of the subject's hip when walking).

At the opposite, lower end of the upper leg member 44, there is provided a shadow knee joint 52 which connects the upper leg member 44 and the lower leg member 46. The shadow knee joint 52 is a rotational joint which also has an axis of rotation perpendicular to the page (and therefore equivalent to the extension / flexion movement of the subject's knee when walking).

At the lower end of the lower leg member 46, there is provided a shadow ankle joint 54 which again has an axis of rotation perpendicular to the page, per the subject's ankle in flexion / extension. The shadow ankle joint 54 connects the lower leg member 46 to the foot member 48.

Members 44, 46 and 48 each define together a shadow leg 42 which can be articulated by a suitable actuation system which is shown schematically at 56. The actuation system 56 is capable of applying forces and/or motion constraints to the members 44, 46 and 48. The actuation system 56 may take the form of an automated control system employing various electric motors or hydraulic or pneumatic cylinders. It is within the skill of the notional skilled person to provide a suitable actuation system for movement of the shadow leg 42.

Because the dimensions of the subject's legs are known, a geometric transformation can be provided as part of the automated control system which can relate movement of the shadow leg to movement of the subject's leg. In other words, for a required movement of the subject's leg, the system can calculate through which angles to actuate the shadow leg to produce the desired result.

The shadow leg 42 and the right leg 18 of the subject 10 are connected by a plurality of members extending in an anteroposterior direction. A first member 58 extends from the shadow hip joint 50 to the attachment point 34 at the lower back of the subject 10. A second member 60 extends from the shadow knee joint 52 to the attachment point 36 at the knee of the subject 10. A third member 62 extends from the shadow ankle joint 54 to the attachment point 38 at the ankle of the subject 10. A fourth member

64 extends from the bottom of the shadow foot 48 to the fourth attachment point 40 at the base of the foot of the subject 10. Each member 58, 60, 62, 64 is rotatably mounted to the shadow leg 42 for rotation about axes parallel to the joints therein.

Each of the members 58, 60, 62 and 64 are elongate, stiff members constructed from e.g., metal or a composite. Each member is the generally the same length, and as such the motion of the shadow leg 42 and biological leg 18 are constrained together. The member 60 is provided with some minor adjustability to ensure that when the shadow leg is fully extended, so is the subject's knee. This provides a mechanical stop on knee over-extension (which can be very harmful if permitted).

The members are of a length longer than the members of the shadow leg 44, 46, 48 and are about 1m long.

The motion of the shadow leg 42 and biological leg 18 is demonstrated with respect to Figure D.2, in which the shadow leg 42 and the biological leg 18 have both advanced to a further position shown in hidden line.

It will be noted that advantageously, the size of the subject 10 is not important. Should a larger or smaller subject be installed within the apparatus then the members 58, 60, 62 and 64 may spread apart slightly depending on the relative size of the subject's leg, however, because the members 58, 60, 62 are relatively long, the kinematics of the device will remain substantially the same. The fact that each of the members 58, 60, 62 and 64 are of a length that is longer than either the upper or lower leg members 44, 46 means that this change in size of the subject 10 has little effect on the relative movement of the patient's leg as compared to the shadow leg.

Variations fall within the scope of the present invention. For example, instead of the subject 10 being placed on the treadmill 14, the apparatus 12 may be mobile, i.e., mounted on a trolley or other mobile device such that the patient can walk around freely whilst being rehabilitated.

The shadow leg 42 has mechanical restraints imparted thereon in order to avoid any excessive articulation of the subject's joints. For example, the knee joint 52 is limited by mechanical end stop to 180 degrees or thereabouts such that the patient 10 cannot hyperextend their knee.

The functionality of the torso harness may be integrated into the waistband, to support the subject at the waist instead of the torso.

## D.2 Claims

1. A gait rehabilitation apparatus comprising: an articulated mechanical shadow leg configured to mimic the movement of a biological leg; a first member extending from the shadow leg and having a first biological leg attachment formation defined thereon; wherein the first member extends in a substantially anteroposterior direction relative to the shadow leg in use.

2. A gait rehabilitation apparatus according to claim 1, comprising: a second member extending from the shadow leg and having a second biological leg attachment formation defined thereon; wherein the second member extends in a substantially anteroposterior direction relative to the shadow leg in use

3. A gait rehabilitation apparatus according to claim 2, in which the articulated shadow leg comprises an upper leg portion articulated about a shadow hip joint at an upper end in use.

4. A gait rehabilitation apparatus according to claim 3, in which the first member extends from proximate the shadow hip joint, and the second member extends proximate a knee region of the shadow leg.

5. A gait rehabilitation apparatus according to claim 2, in which the articulated shadow leg comprises a lower leg portion articulated about a shadow knee joint at an upper end in use.

6. A gait rehabilitation apparatus according to claim 5, in which the first member extends from proximate the shadow knee joint, and the second member extends proximate an ankle region of the shadow leg.

7. A gait rehabilitation apparatus according to claim 2, in which the articulated shadow leg comprises a foot portion articulated about a shadow ankle joint at an upper end in use.

8. A gait rehabilitation apparatus according to claim 7, in which the first member extends from proximate the shadow ankle joint, and the second member extends proximate a foot region of the shadow leg.

9. A gait rehabilitation apparatus according to claim 2, comprising: a third member extending from the shadow leg and having a third biological leg attachment formation defined thereon; wherein the third member extends in a substantially anteroposterior direction relative to the shadow leg in use.

10. A gait rehabilitation apparatus according to claim 9, in which the articulated shadow leg comprises: an upper leg portion articulated about a shadow hip joint at an upper end in use; and, a lower leg portion connected

to the upper leg portion and articulated about a shadow knee joint at an upper end in use.

11. A gait rehabilitation apparatus according to claim 10, in which the first member extends from proximate the shadow hip joint, the second member extends proximate the shadow knee joint and the third member extends proximate an ankle region of the shadow leg.

13. A gait rehabilitation apparatus according to claim 11, comprising: a fourth member extending from the shadow leg and having a fourth biological leg attachment formation defined thereon; wherein the fourth member extends in a substantially anteroposterior direction relative to the shadow leg in use.

14. A gait rehabilitation apparatus according to claim 13, in which the articulated shadow leg comprises a foot portion connected to the lower leg portion and articulated about a shadow ankle joint at an upper end in use.

15. A gait rehabilitation apparatus according to claim 14, in which the fourth member extends proximate a foot region of the shadow leg.

16. A method of gait rehabilitation comprising the steps of: providing an articulated mechanical shadow leg configured to mimic the movement of a biological leg; providing a first member connected to the shadow leg; providing a second member connected to the shadow leg; attaching the first and second members to the biological leg of a subject such that the first and second members extend in a substantially anteroposterior direction; and, using the shadow leg to guide and / or provide force input to the biological leg.

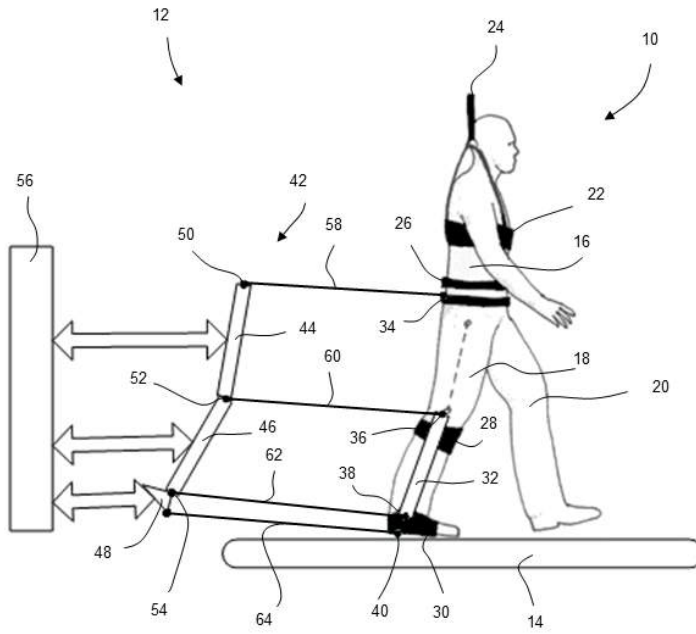


Figure D.1

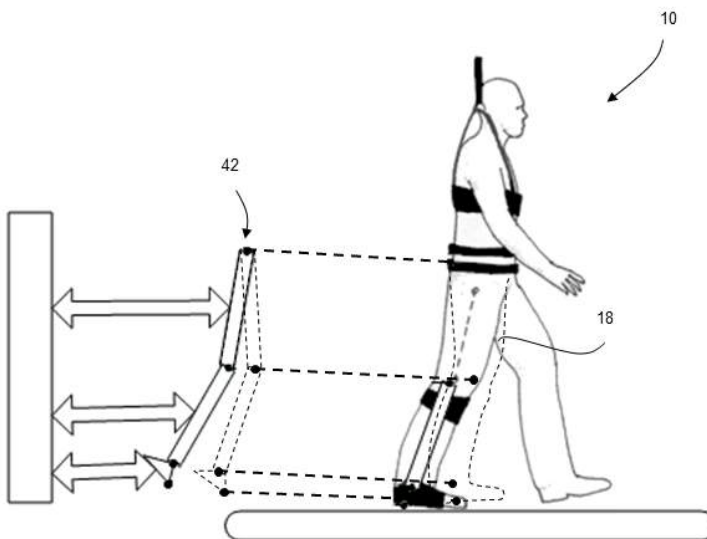


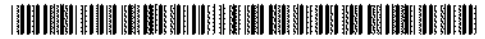
Figure D.2



APPENDIX **E**

# Parallel Rectangular Manipulator

international patent application number WO2014/161726, publication date  
October 9, 2014



- (51) International Patent Classification:  
B25J 9/10 (2006.01) F16H 21/18 (2006.01)
- (21) International Application Number:  
PCT/EP2014/055651
- (22) International Filing Date:  
20 March 2014 (20.03.2014)
- (25) Filing Language: English
- (26) Publication Language: English
- (30) Priority Data:  
1305989.4 3 April 2013 (03.04.2013) GB
- (71) Applicant: MOOG BV [NL/NL]; PO Box 187, NL-2150 AD Nieuw-Vennep (NL).
- (72) Inventor: MEULEMAN, Jos; Tahndalaan 9, NL-2121CR Beunbroek (NL).
- (74) Agent: SANGER, Phillip; WITHERS & ROGERS LLP, 4 More London Riverside, London SE1 2AU (GB).
- (81) Designated States (unless otherwise indicated, for every kind of national protection available): AE, AG, AL, AM,

AO, AT, AU, AZ, BA, BB, BG, BH, BN, BR, BW, BY, BZ, CA, CH, CL, CN, CO, CR, CU, CZ, DE, DK, DM, DO, DZ, EC, EE, EG, ES, FI, GB, GD, GE, GH, GM, GT, HN, HR, HU, ID, IL, IN, IR, IS, JP, KE, KG, KN, KP, KR, KZ, LA, LC, LK, LR, LS, LT, LU, LY, MA, MD, ME, MG, MK, MN, MW, MX, MY, MZ, NA, NG, NI, NO, NZ, OM, PA, PE, PG, PH, PL, PT, QA, RO, RS, RU, RW, SA, SC, SD, SE, SG, SK, SL, SM, ST, SV, SY, TH, TJ, TM, TN, TR, TT, TZ, UA, UG, US, UZ, VC, VN, ZA, ZM, ZW.

(84) Designated States (unless otherwise indicated, for every kind of regional protection available): ARIPO (BW, GH, GM, KE, LR, LS, MW, MZ, NA, RW, SD, SL, SZ, TZ, UG, ZM, ZW), Eurasian (AM, AZ, BY, KG, KZ, RU, TJ, TM), European (AL, AT, BE, BG, CH, CY, CZ, DE, DK, EE, ES, FI, FR, GB, GR, HR, HU, IE, IS, IT, LT, LJ, LV, MC, MK, MT, NL, NO, PL, PT, RO, RS, SE, SI, SK, SM, TR), OAPI (BF, BJ, CF, CG, CI, CM, GA, GN, GQ, GW, KM, ML, MR, NE, SN, TD, TG).

Published: — with international search report (Art. 21(3))

(54) Title: MANIPULATOR MECHANISM

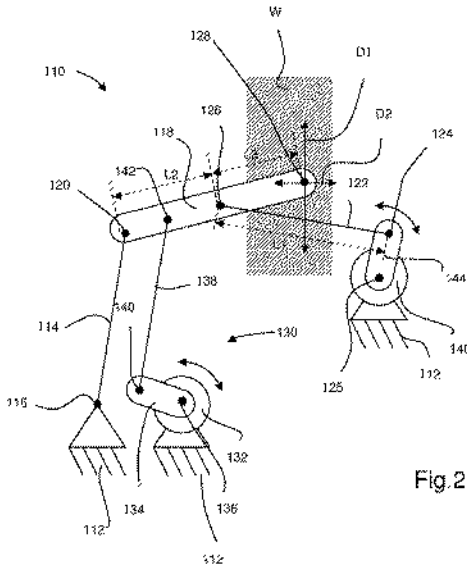


Fig. 2

(57) Abstract: A manipulator (110) for e.g. gait training is constructed from an Evans mechanism with an additional degree of freedom to provide a two dimensional workspace.

WO 2014/161726 A1

## E.1 Manipulator mechanism

The present invention is concerned with a manipulator. More specifically the present invention is concerned with a 2 degree of freedom manipulator comprising an end effector which can be moved in an uncoupled sense in two substantially perpendicular linear directions in a planar workspace.

Two degree of freedom manipulators have many uses. For example, they may be used in the manipulation of an end effector such as a robot arm or machine tool in order to pick and place an object, or perform a manufacturing operation on a component.

Another application for two degree of freedom manipulators is in the use of rehabilitation robots in order to provide support and/or assistive forces to a patient undergoing rehabilitation. Such manipulators are attached to a body part of the subject and can be used to provide assistive forces and support during a rehabilitation exercise such as gait training.

For example, a 2DOF manipulator may be connected to a subject's pelvis to support their weight and provide predetermined gait cues to assist in walking. One such manipulator is shown in US2007/0016116. In this document, a pair of pneumatically driven manipulators apply forces to the subject's pelvis with an arrangement of cylinders. In particular, fore-aft movement of the subject is provided by pneumatic cylinders mounted in the fore-aft direction, and lateral movement is provided by laterally orientated pneumatic cylinders. A problem with this arrangement is that the lateral cylinders mean that the manipulator is quite wide. This makes it more difficult to install, and the laterally extending pneumatic cylinders may clash with the subject's arms during normal gait motion. Also, the workspace is quite small compared to the size of the manipulator.

A different, known, 2DOF manipulator comprises a 2D Cartesian slide-way arrangement in which a carriage is slidable on a first rail in a first direction, which first rail is slideable between two further parallel rails in a second direction, perpendicular to the first. Such systems have certain disadvantages.

One disadvantage is that there is a significant amount of equipment surrounding and within the workspace. This is generally undesirable in many applications, as the manipulator and the workpiece or subject may clash, and in the event that the manipulator is used for gait training, the rails may clash with the subject's arms.

Another disadvantage with such systems is that sliding joints between

components are generally undesirable because they are prone to contamination and wear.

Also, in such a system a motor is provided to move the carriage on the first rail. The provision of a motor attached to the first rail, and arranged to move the carriage, means that the first rail has a high inertia, which is undesirable when being moved on the parallel rails.

It is an object of the present invention to overcome or at least mitigate the above referenced problems.

According to the first aspect of the invention, there is provided a manipulator comprising: a frame; a first link; a second link; and, a first coupler; arranged to form an Evans straight-line mechanism such that a point on the first coupler describes a substantially straight line in a first direction for a part of its locus; wherein the second link is attached to the frame via a crank, such that actuation of the crank moves the point on the first coupler in a substantially straight line in a second direction, perpendicular to the first direction.

The invention provides an Evans mechanism in which an additional degree of freedom is provided at the mounted end of one of the driver arms. The actuation of the additional crank provides motion in the degree of freedom perpendicular to the normal linear degree of freedom of the Evans mechanism. This arrangement has many advantages. Firstly, the majority of the mechanism is placed outside of the workspace and rearwardly thereof. Secondly the arrangement only uses rotational joints, which do not suffer the disadvantages of linear joints per the prior art.

Preferably: L1 is the distance along the second link (122; 222) between an axis of rotation with the coupler (118; 218) and an axis of rotation with the crank (144; 248); L2 is the distance along the coupler (118; 218) between an axis of rotation with the first link (114; 214); L3 is the distance along the coupler (118; 218) between the axis of rotation with the coupler (118; 218) and the end point (128; 228); in which the manipulator is configured such that L2 is within 10% of the value determined by  $L2 = L1 * L3$ .

This provides a good approximation to a straight line throughout a significant portion of the travel of the end point.

Preferably the mechanism comprises a first actuation assembly having a first motor configured to articulate the manipulator to move the point on the first coupler in the first direction. Preferably the first actuation assembly comprises a third link, driven by a first actuation assembly crank, which is driven by the first motor, in which the third link is arranged to drive the first coupler.

Preferably the third link is attached to the first coupler between the first link and the second link.

Preferably the manipulator comprises: a second coupler connected to the first coupler and configured to move therewith; and, an end effector connecting the first and second couplers.

This provides a more stable mechanism, and allows an end effector to be used which transfers torques as well as point forces. Preferably the first and second couplers are connected by a coupler connector spaced from the end effector. Preferably the first and second couplers are connected by the end effector and coupler connector so as to form two parallel sides of a parallel linkage.

The manipulator may comprise a further second link connected to the second coupler, wherein the further second link is attached to the frame via a further crank, such that actuation of the crank moves a point on the second coupler in a substantially straight line in the second direction.

Preferably the crank and the further crank are arranged for synchronised motion. The crank and the further crank may be driven by a common actuation assembly, for example the first motor may drive the first crank and the further crank via a common pushrod.

An example manipulator in accordance with the present invention will now be described with reference to the following figures.

Figure E.1 is a side schematic view of a known Evans mechanism.

Figure E.2 is a side schematic view of a first mechanism in accordance with the present invention.

Figures E.3a to E.3b are schematic views of the range of motion of the mechanism of Figure E.2.

Figure E.4 is a side schematic view of a second mechanism in accordance with the present invention.

Figure E.5 is a side schematic view of an application of the mechanism of Figure E.4.

Turning to Figure E.1, a known Evans mechanism 10 is shown schematically. The Evans mechanism 10 comprises a frame 12 which is fixed in use. The different areas of the frame 12 in Figure E.1 are rigidly attached to each other.

A first link 14 is provided, and pivotably connected to the frame 12 at a first joint 16 positioned at a first end of the first link 14.

A coupler 18 is provided which is pivotably connected via a second rotational joint 20 to the first link 14 at a second end of the first link 14 and a first end of the coupler 18.

A second link 22 is pivotably connected to the frame 12 via a third rotational joint 24 at a first end thereof. A second end of the second link 22 is pivotably connected to the coupler 18 via a fourth rotational joint 26.

In Figure E.1, L1 is the distance between the third and fourth joints 24, 26 on the second link 22. L2 is the distance from the second joint 20 to the fourth joint 26 on the coupler 18 and L3 is the distance between the fourth joint 26 and the end point 28 (i.e. the point which is to be manipulated). The mechanism is configured such that  $L22 = L1 * L3$ , which provides the most accurate straight line motion for the end point 28.

The first rotational joint 16 and the third rotational joint 24 connecting the links 14, 22 with the frame 12 are spaced apart. It will also be noted that the rotational joints 16, 20, 24, 26 are positioned such that the first and second links 14, 22 are approximately 90 degrees to each other.

The frame 12, first and second links 14, 22 and the coupler 18 form a four bar link mechanism known in the art as an Evans mechanism. The coupler 18 extends from the first rotational joint 20 past the fourth rotational joint 26 to an end point 28. When the first link 14 rotates clockwise about the first rotational joint 14, and the second link 22 rotates about the third rotational joint 24, linear motion of the end point 28 in direction D1 results.

The geometry of the mechanism (as described by  $L22 = L1 * L3$ ) dictates that for a significant part of the locus of the endpoint 28 during actuation, a substantially, or an approximation of linear motion is observed. Should the mechanism be actuated far beyond the position shown in Figure E.1, then the path of the end point 28 will deviate away from linear direction D1 and become curved, however for a significant proportion of the movement of the mechanism, the path is linear. As such, the Evans mechanism is also known as a “straight line mechanism”.

The Evans mechanism may be actuated in several ways. In the embodiment shown in Figure E.1, the Evans mechanism 10 is actuated by a separate actuation assembly 30.

The actuation assembly 30 comprises a first motor 32 which is mounted to the frame 12. The motor 32 forms a fifth rotational joint 36, about which a crank 34 is driven. A third link 38 is attached to a free end of the crank 34 via a sixth rotational joint 40 and to the coupler at a seventh rotational joint 42. The seventh rotational joint 42 is positioned between the second rotational joint 20 and the fourth rotational joint 26 on the coupler 18. Using the actuation assembly 30 the motor 32 can drive the crank 34 which in turn will push or pull the coupler 18 via the third link 38 to actuate the Evans mechanism and drive the end point 28 along in direction D1.

It will be noted that other types of actuation assembly are possible, for example, rotation of the first or second links 14, 22 can be achieved by providing motors at the first or third rotational joints 16 or 24. Provision of a motor at the joint 16 may be problematic depending on the range of motion used- at a position where the coupler 18 and the second link 22 are parallel, rotation of the joint 16 would not be possible via a torque about the centre of rotation of the joint.

The Evans mechanism of Figure E.1 can be used as a one degree of freedom manipulator. The present invention provides a 2 degree of freedom mechanism. This is achieved by the arrangement shown in Figure E.2. The reference numerals shown in Figure E.2 are similar to those shown in Figure E.1 for common features, albeit incremented by 100.

A two degree of freedom mechanism 110 in accordance with the present invention comprises a frame 112, a first link 114 connected to the frame 112 via a first rotational joint 116 and connected to a coupler 118 via a second rotational joint 120. A second link 122 is provided being connected to the coupler 118 via a fourth rotational joint 126. An actuation assembly 130 is provided, being substantially similar to the actuation assembly 30, having a first motor 132 defining a fifth rotational joint 136, a first crank 134 driven by the motor and a third link 138 connected between a sixth rotational joint 140 on the crank and a seventh rotational joint 142 on the coupler 118.

Instead of being directly attached to the frame 112, the second rotational link 122 is connected to a second crank 144 at a third rotational joint 124, which crank in turn is driven by a second motor 146 which is mounted on the frame 112, the second motor forming an eighth rotational joint 125.

With the second crank 144 in a stationary position, the mechanism 110 acts in substantially the same manner as the Evans mechanism of Figure E.1. The end point 128 of the coupler 118 moves in direction D1 when the mechanism is actuated by the first motor 132.

Per Figure E.1, L1 is the distance between the third and fourth joints 124, 126 on the second link 122. L2 is the distance from the second joint 120 to the fourth joint 126 on the coupler 118 and L3 is the distance between the fourth joint 126 and the end point 128 (i.e. the point which is to be manipulated). The mechanism is configured such that  $L2 = L1 * L3$ , which provides the most accurate straight line motion for the end point 128.

However, it will be noted that the second crank 144 can also be driven in order to move the end point 128 of the coupler 118 in a direction D2, which is substantially perpendicular to the direction D1. As such a two-

dimensional workspace  $W$  is formed in which the end point 128 is moved linearly in two, normal, directions.

It will be noted that for the range of movement around the position shown in Figure E.2, D1 and D2 are substantially straight and perpendicular. Movement out of the workspace  $W$  will result in progressively less rectilinear behaviour.

Turning to Figure E.3a, a mechanism similar to that of Figure E.2 is shown with its range of movement through a finite number of angles of both the degrees of freedom of the first and second cranks 134, 144. It will be noted in Figure E.3a that the first crank 134 is attached to the frame at the same point as the first link 114, but this does not significantly affect the kinematics of the mechanism.

The angle  $\theta_1$  represents the angle of the first crank 134 from its central position shown in Figure E.3a, and the angle  $\theta_2$  represents the angle of the second crank 144 about its central position shown in Figure E.3a.

Figure E.3a shows the mechanism 110 at a position within the workspace  $W$ . Turning to Figure E.3b, the mechanism 110 is shown at a first corner of the workspace  $W$ , beyond which point the motion of the end point 128 becomes less linear. At the position of Figure E.3b,  $\theta_1$  is at -30 degrees and  $\theta_2$  at 40 degrees. Similarly, in Figures E.3c ( $\theta_1=-30, \theta_2=-40$ ), E.3d ( $\theta_1=30, \theta_2=40$ ) and E.3e ( $\theta_1=30, \theta_2=-40$ ) the mechanism 110 is shown at the extreme of movement after which its motions becomes significantly less linear i.e. outside of the defined workspace  $W$ .

As can be seen by the gridlines in each of Figures E.3a to E.3e, motion of the end point 128 is relatively rectilinear and provides a good approximation to a 2 degree of freedom manipulator, such as the Cartesian slide manipulator mentioned earlier.

In the embodiments of Figures E.2 and E.3a to E.3e, it may be desirable to attach a pushrod to the endpoint 128 in direction D1 (away from the mechanism 110). For example in a gait rehabilitation robot, a pushrod can be attached to the lower back of the subject. As mentioned, such robots need to guide the subject, and as such must resist forces from the subject to the mechanism.

For provision of such a pushrod, it may be desirable to lock the rotation of the endpoint or to place the effective point outside the mechanism. For this purpose, referring to Figure E.4, there is shown a mechanism 210 which is better suited to reacting the forces from the subject via a pushrod by locking the rotation of an end effector. The mechanism has some compo-

nents in common with the mechanism 110 as shown in Figure E.2. These will be numbered 100 greater.

The mechanism 210 comprises a frame 212, to which a first link 214 is pivotably attached via a first rotational joint 216 at a first end and pivotably attached via a second rotational joint 220 to a first coupler 218 at the second end.

A second link 222 is connected to a first rocker 248 (to be described in more detail below) via a third rotational joint 224 and to the first coupler 218 via a fourth rotational joint 226. As with the mechanism 110 an actuation assembly 230 comprising a first motor 232 defining a fifth rotational joint 236, a first crank 234 driven by the first motor 232 and a third link 238 connected to the crank 234 via a sixth rotational joint 240 and to the coupler 218 via a seventh rotational joint 242.

A second actuation assembly 252 is provided comprising a motor 254 connected to the frame 212 and defining an eighth rotational joint 225. The assembly 252 comprises a crank 256 and a push rod 258 connected to the crank 256 via a ninth rotational joint 259.

The first rocker 248 is a member mounted for rotation to the frame 212 via a tenth rotational joint 250. The rocker 248 is driven in rotation about the tenth rotational joint 250 by the push rod 258 which is connected to the rocker 248 via an eleventh rotational joint 260. Each of the joints 224, 250, 260 on the first rocker 248 are spaced apart so as to define the vertices of a triangle.

A second rocker 262 is provided, identical to the first rocker but spaced therefrom, being attached to the frame 212 via a twelfth rotational joint 264. The push rod 258 extends beyond the first rocker 248 to drive the second rocker 262 at a thirteenth rotational joint 265. The second rocker also comprises a fourteenth rotational joint 276 as will be described below.

A second coupler 266 is provided, being generally offset and parallel to the first coupler 218. The second coupler 266 is connected to the first coupler 218 via a first intermediate link 268 and an end effector 284 (i.e. a pushrod), so as to form a parallel linkage (i.e. the opposing members are always parallel). The first intermediate link 268 is joined to the first rocker 218 via an fifteenth rotational joint 270, proximate the joint 220 and to the second rocker 262 via a sixteenth rotational joint 272. The second coupler 266 is driven by a fourth link 274 which attaches to the second rocker 262 via the fourteenth rotational joint 276, and to the second coupler 266 via a seventeenth rotational joint 278.

The end effector 284 is connected to the first coupler 218 via an eigh-

teenth rotational joint 228 and to the second coupler 266 via a nineteenth rotational joint 280.

In use the mechanism 210 can be actuated in much the same way as the mechanism of Figure E.2. With the second motor 254 stationary, the first motor 232 drives the end effector 284 per a normal Evans mechanism i.e. in linear direction D1. It will be noted that the two couplers 218, 266 remain parallel throughout the range of motion as they are constrained by the first intermediate member 268 and the end effector 284.

Motion in direction D2 is provided by the motor 254 which drives the rockers 248, 262 to provide a vertical force through the second and fourth links 222, 274. A benefit of this particular arrangement is that the end effector 284 remains horizontal and parallel to direction D1, so that it can resist any rotational motion as required. In other words the mechanism 210 is capable of applying forces to all and any point on the end effector 284. It can be made any suitable shape to provide the desired location of the point of actuation. The system is also inherently stiffer, which is advantageous.

It will be noted that as an alternative to the rockers 248, 262, a pair of synchronised motor / crank assemblies could be used.

Turning to Figure E.5, the mechanism 210 is shown connected to a harness 300 for a rehabilitation patient. The mechanism 210 is arranged in the horizontal plane as shown, such that the height of the subject or patient is in a direction perpendicular to the page. As such D1 is in a fore aft direction of the subject and D2 is in a left right direction. It will be noted that the frame 212 can be provided in a stationary fashion with the subject walking on a treadmill, or alternatively can be moveable, in order to provide the ability to the patient or subject to walk. In particular during gait rehabilitation, the systems can be used to support the patient and/or provide input forces as required. In particular, the mechanism of the present invention is particularly well-suited to use with systems which utilise admittance control, so that it can be configured to be effectively transparent or provide restorative or input forces as required.

## E.2 Claims

1. A manipulator (110; 210) comprising: a frame (112; 212); a first link (114; 214); a second link (122; 222); and, a first coupler (118; 218); arranged to form an Evans straight-line mechanism such that a point (128; 228) on the first coupler describes a substantially straight line in a first direction

(D1) for a part of its locus; wherein the second link (122; 222) is attached to the frame via a crank (144; 248), such that actuation of the crank moves the point on the first coupler in a substantially straight line in a second direction (D2), perpendicular to the first direction.

2. A manipulator (110; 210) according to claim 1, in which: L1 is the distance along the second link (122; 222) between an axis of rotation with the coupler (118; 218) and an axis of rotation with the crank (144; 248); L2 is the distance along the coupler (118; 218) between an axis of rotation with the first link (114; 214); L3 is the distance along the coupler (118; 218) between the axis of rotation with the coupler (118; 218) and the end point (128; 228); in which the manipulator is configured such that  $L2$  is within 10% of the value determined by  $L2 = L1 * L3$ .

3. A manipulator (110; 210) according to claim 1 or 2, comprising a first actuation assembly having a first motor (132; 232) configured to articulate the manipulator to move the point on the first coupler in the first direction.

4. A manipulator (110; 210) according to claim 3, in which the first actuation assembly comprises a third link (138; 238), driven by a first actuation assembly crank (134; 234), which is driven by the first motor (132; 232), in which the third link is arranged to drive the first coupler.

5. A manipulator (110; 210) according to claim 4, in which the third link is attached to the first coupler (118; 218) between the first link (114; 214) and the second link (122; 222).

6. A manipulator (210) according to any preceding claim, comprising: a second coupler (266) connected to the first coupler (218) and configured to move therewith; and, an end effector (284) connecting the first and second couplers.

7. A manipulator (210) according to claim 6, in which the first and second couplers are connected by a coupler connector (268) spaced from the end effector.

8. A manipulator (210) according to claim 7, in which the first and second couplers (218, 266) are connected by the end effector (284) and coupler connector (268) so as to form two parallel sides of a parallel linkage.

9. A manipulator (210) according to any of claims 6 to 8, comprising a further second link (274) connected to the second coupler (266), wherein the further second link (274) is attached to the frame via a further crank (262), such that actuation of the crank moves a point on the second coupler in a substantially straight line in the second direction (D2).

10. A manipulator (210) according to claim 9, in which the crank (248) and the further crank (262) are arranged for synchronised motion.

11. A manipulator (210) according to claim 9 or 10, in which the crank (248) and the further crank (262) are driven by a common actuation assembly.

12. A manipulator (210) according to claim 11 when dependent upon claim 4, in which the first motor drives the first crank (248) and the further crank (262) via a common pushrod (258).

13. A rehabilitation apparatus comprising a manipulator according to any preceding claim.

14. A gait training apparatus comprising a manipulator according to any of claims 1 to 12.

15. A manipulator, rehabilitation apparatus and / or gait training apparatus as described herein, with reference to, or in accordance with, the accompanying drawings.



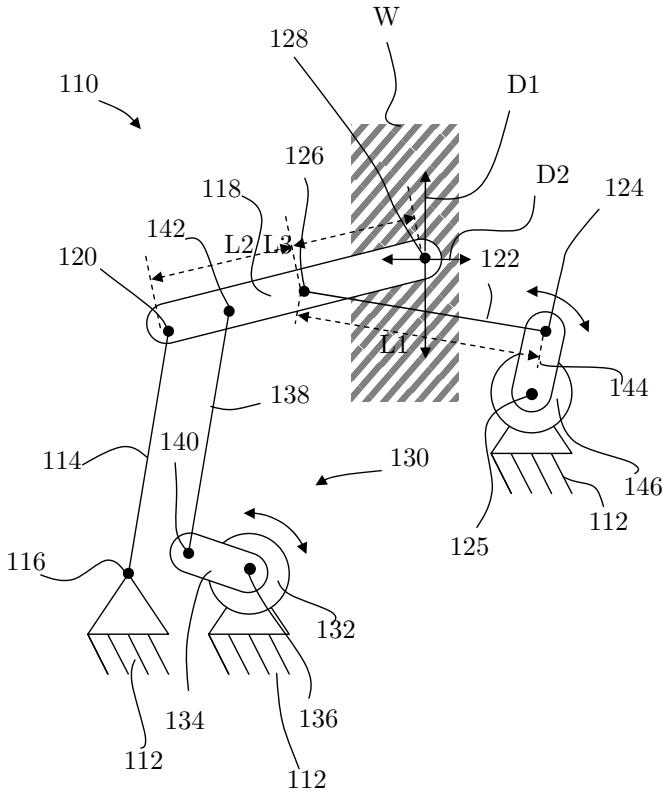


Figure E.2

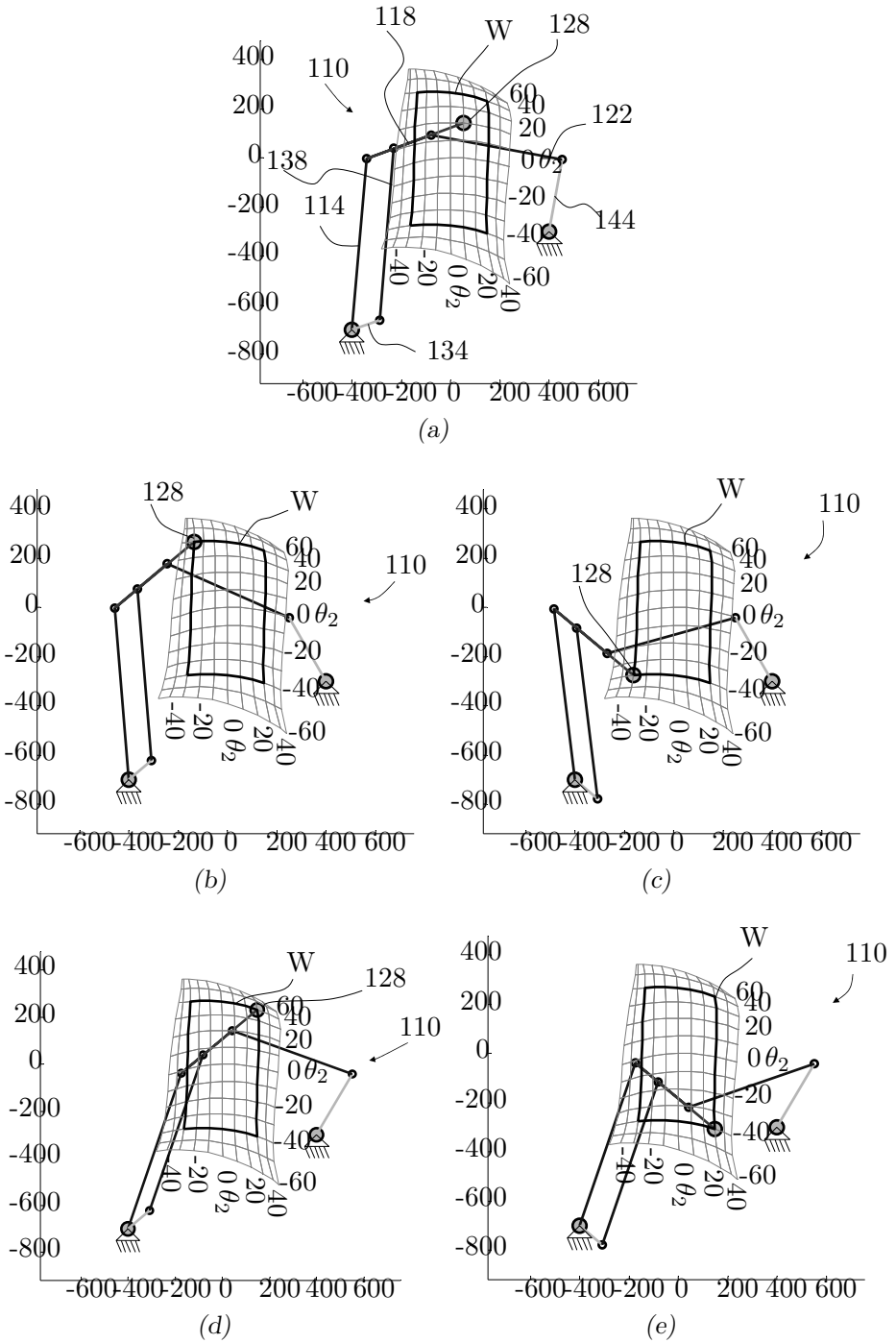


Figure E.3

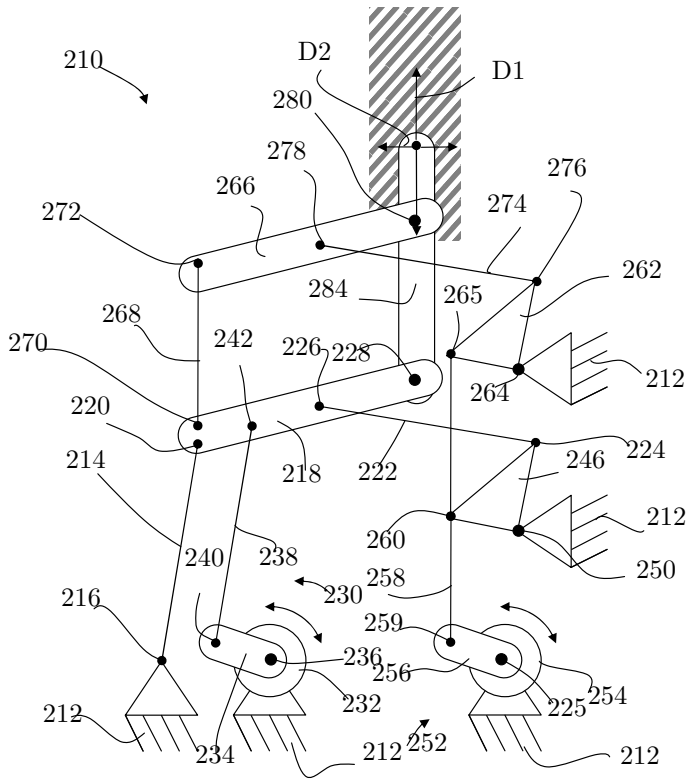


Figure E.4

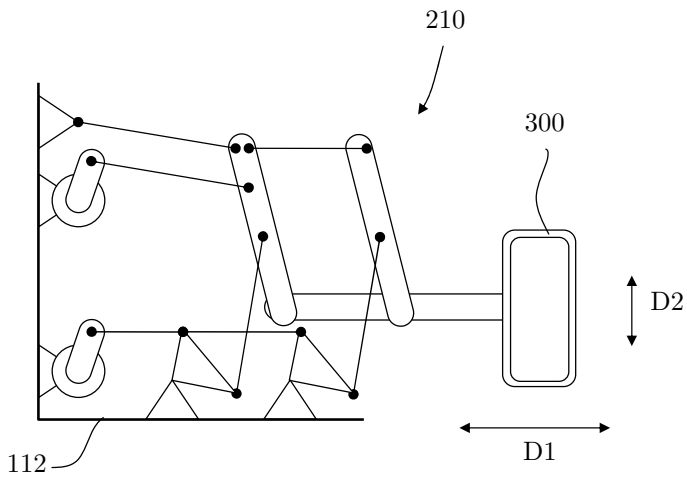
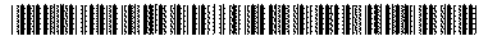


Figure E.5

APPENDIX **F**

# Short Skewed Axis Gimbal

international patent application number WO2014/161726, publication date  
October 9, 2014



- (51) International Patent Classification:  
A61H 1/02 (2006.01)
- (21) International Application Number:  
PCT/EP2014/056368
- (22) International Filing Date:  
28 March 2014 (28.03.2014)
- (25) Filing Language:  
English
- (26) Publication Language:  
English
- (30) Priority Data:  
1305984.5 3 April 2013 (03.04.2013) GB
- (71) Applicant: MOOG BV [NL/NL]; PO Box 187, NL-2150  
AD Nieuw-Vennep (NL).
- (72) Inventor: MKULEMAN, Jos; Tahmalaan 9, NL-2121CR  
Beunbrack (NL).
- (74) Agent: WITHERS & ROGERS LLP; 4 More London  
Riverside, London SE1 2AU (GB).
- (81) Designated States (unless otherwise indicated, for every  
kind of national protection available): AE, AG, AL, AM,

AO, AT, AU, AZ, BA, BB, BG, BH, BN, BR, BW, BY, BZ, CA, CH, CL, CN, CO, CR, CU, CZ, DE, DK, DM, DO, DZ, EC, EE, EG, ES, FI, GB, GD, GE, GH, GM, GT, HN, HR, HU, ID, IL, IN, IR, IS, JP, KE, KG, KN, KP, KR, KZ, LA, LC, LK, LR, LS, LT, LU, LY, MA, MD, ME, MG, MK, MN, MW, MX, MY, MZ, NA, NG, NI, NO, NZ, OM, PA, PE, PG, PH, PL, PT, QA, RO, RS, RU, RW, SA, SC, SD, SE, SG, SK, SL, SM, ST, SV, SY, TH, TJ, TM, TN, TR, TT, TZ, UA, UG, US, UZ, VC, VN, ZA, ZM, ZW.

(84) Designated States (unless otherwise indicated, for every kind of regional protection available): ARIPO (BW, GH, GM, KE, LR, LS, MW, MZ, NA, RW, SD, SI, SZ, TZ, UG, ZM, ZW), Eurasian (AM, AZ, BY, KG, KZ, RJ, TJ, TM), European (AL, AT, BE, BG, CH, CY, CZ, DE, DK, EE, ES, FI, FR, GB, GR, HR, HU, IE, IS, IT, LT, LJ, LV, MC, MK, MT, NL, NO, PL, PT, RO, RS, SE, SI, SK, SM, TR), OAPI (BF, BJ, CF, CG, CI, CM, GA, GN, GQ, GW, KM, ML, MR, NE, SN, TD, TG).

Published:  
— with international search report (Art. 21(3))

(54) Title: MECHANICAL LINKAGE

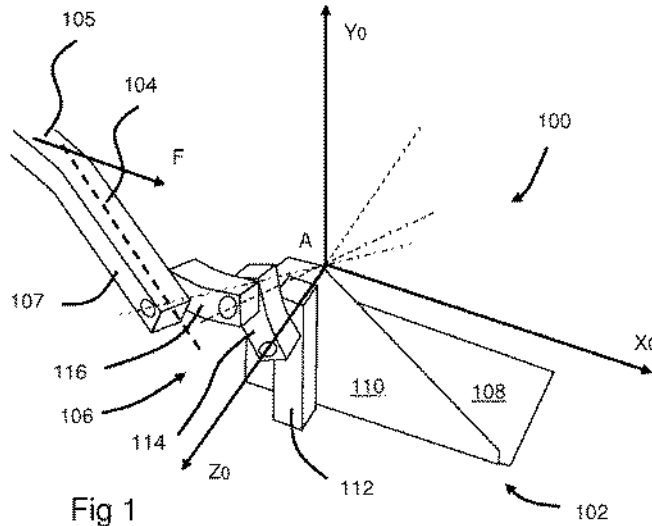


Fig 1

(57) Abstract: A linkage (100, 200) having a plurality of small angle links (114, 116; 208, 212) with axes of rotation directed to a single point to allow movement of an recipient object without moving the point of action of an applied force (F).

WO 2014/161797 A1

## F.1 Mechanical linkage

The present invention concerns a mechanical linkage. More specifically, the present invention concerns a gimbal-type linkage for the transference of force between two points whilst permitting limited movement of a force recipient in selected degrees of freedom.

It is often desirable to transfer a force between an actuator and a recipient in a mechanical system. In particular, it is often desirable to exert the force on a virtual point which may not be accessible in reality.

For example in the field of rehabilitation robots for victims of neurological disorders, the actuator needs to be able to provide both actuating and supporting forces to move and support patient limbs. This may be done, for example, by using a rod attached at one end to an actuator, and at the other end to the limb of a subject, such as an arm or leg.

The connection between the rod and the subject's limb may be achieved in several ways. For example, the rod may be rigidly attached to a strap or brace which secures around the limb. This type of connection does not allow any free movement between the rod and limb, and as such movement of the limb in all six degrees of freedom is dependent upon movement of the rod.

This is problematic in rehabilitation. The aim is to progress the subject towards self supporting motion, and allowing some movement is beneficial as the feeling of freedom of movement inspires the subject to exercise control.

A spherical or Cardan joint may be provided between the rod and strap, however this only provides freedom in two rotational degrees of freedom, about the centre of the physical joint. In the event that the force is applied to a joint, for example an ankle, this can be problematic, as once the ankle joint rotates about the spherical joint, the line of direction of force from the rod is no longer coincident with the centre of rotation of the ankle. This is not ideal, as it creates a moment on the ankle which resists movement back to the nominal, aligned position and therefore resists the subject's efforts to correct their gait.

What is required is a connection which allows transmission of a force from an actuator to a recipient, but minimises constraint free rotation of the recipient.

It is an aim of the present invention to overcome, or at least mitigate the above referenced problems.

According to a first aspect of the invention there is provided an assem-

bly for transferring a force from a force provider to a recipient object, the assembly comprising: a force provider; a recipient object; a linkage configured to transfer a force from the force provider to the recipient object, the linkage comprising a first link and a second link; the first link having a first rotational joint defining a first link axis, and a second rotational joint defining a second link axis, the first and second link axes being at a first link angle to each other, which first link is pivotally attached to the recipient object for rotation about the first axis; and, the second link having a third rotational joint defining a third link axis, and a fourth rotational joint defining a fourth link axis, the third and fourth link axes being at a second link angle to each other, the second link being pivotally attached to the first link such that the second and third link axes coincide, the second link being pivotally mounted at the fourth link axis to transfer a force from the force provider, in which the first, second, third and fourth axes intersect at a predetermined point such that the recipient object can rotate about the predetermined point by articulation of the linkage; in which the first and second link angles are each less than 45 degrees.

Advantageously, this gimbal-like mechanism allows forces to be applied by the force provider to the predetermined point. The recipient object can articulate the linkage to move about the predetermined point, but importantly the force remains acting through that point during articulation of the linkage. Therefore forces can be applied in a desired direction, and movement of the recipient object is permitted without distortion of the force, or production of undesirable torques. The use of small angle links (less than 45 degrees) allows for a reasonable range of movement whilst keeping the arrangement compact. Preferably the sum of the internal angles of the links should be less and 90 degrees for this reason. The angles may be selected to provide a limited range of motion as desired- for example to prevent over-articulation in the case of a rehabilitation robot.

Preferably the force provider is a push-pull rod driven by an actuator, such as a linear actuator or preferably a rotational actuator with a crank.

As mentioned, preferably the push-pull rod and the actuator are configured to exert a force through the predetermined point.

Preferably the rotational joints are defined by bores in the links having common shafts extending therethrough. This allows for simple assembly.

Preferably each link comprises a body having a mid section, a first end section and a second opposite end section, the end sections being angled with respect to the mid section. The rotational joints of the links may

then be defined normal to respective end sections such that the sections are angled to provide the link angles.

Preferably the links are constructed from generally tubular bodies, e.g. extruded bodies. This makes them light.

The linkage may comprise a third link having a fifth rotational joint defining a fifth link axis, and a sixth rotational joint defining a sixth link axis, the fifth and sixth link axes being at a third link angle to each other, the third link being pivotably attached to the second link such that the second and third link axes coincide, the third link being pivotably mounted at the sixth link axis to transfer a force from the force provider. The linkage may comprise more than three links.

The invention also provides a rehabilitation apparatus comprising a linkage according to the first aspect, in which the recipient object is a support for a body part. For example for a leg, arm or torso.

Preferably the support for a body part is configured to receive a body part proximate a joint to as to align an axis of rotation of the joint with the predetermined point of the linkage. This keeps the point of action of the rehabilitation force on the joint.

More preferably the support for a body part is configured to receive a body part proximate a joint to as to align a centre of rotation of the joint with the predetermined point of the linkage.

The force provider may be configured to exert a force in a first direction, in which the first link axis is oriented at 80 to 100 degrees to the exerted force. Preferably it is oriented at 90 degrees.

Preferably the support is a foot support, and the force provider is configured to exert the force in a fore-aft direction of a subject in use.

Preferably the first link is connected to the support at a lateral side of the subject's foot in use.

An example linkage in accordance with the present invention will now be described with reference to the accompanying figures, in which:

Figure F.1 is a perspective view of a part of a gait training apparatus comprising a first linkage in accordance with the present invention;

Figure F.2 is a detail view of a component of the linkage of Figure F.1;

Figure F.3 is a perspective view of the linkage of Figure F.1;

Figure F.4 is a side view of the linkage of Figure F.1;

Figures F.5a and b are schematic views of a second linkage in accordance with the present invention;

Figures F.6a and b are schematic views of the linkage of Figures F.5a and b in a second position;

Figures F.7a and b are schematic views of the linkage of Figures F.5a and b in a third position;

Figure F.8 is a diagram of the workspace and range of motion of a gait rehabilitation robot for the ankle degree of freedom;

Figure F.9 is a diagram of the workspace and range of motion of a gait rehabilitation robot for the torso degree of freedom;

Figure F.10 is a schematic perspective view of a further part of a gait training apparatus comprising a third linkage in accordance with the present invention.

Referring to Figure F.1, there is shown a gait training assembly 100 comprising a foot brace 102, a push rod 104 and a linkage 106.

The foot brace 102 comprises a base plate 108 configured to support the underside of a human foot (not shown), and a side plate 110 extending perpendicularly and vertically therefrom to support the outer side of the foot. The side plate 110 comprises a support member 112 also extending vertically from the base plate 108 on the outer side of the side plate 110.

A global coordinate system is shown in Figure F.1 having axes X0, Y0, Z0. The foot brace 102 is arranged to hold a human foot with the centre of the ankle joint (modelled as a spherical joint for simplicity) A at the centre of the global coordinate system.

The pushrod 104 has a main portion 105 connected to an actuator (not shown) arranged to provide a force in direction F, which is generally parallel to X0. An end portion 107 of the pushrod 104 is at an angle to the main portion 105 as shown in Figure F.3.

The linkage 106 comprises a first link 114 and a second link 116. The links 114, 116 in this embodiment are similar, and as such only the link 114 will be described here with reference to Figure F.2.

The link 114 comprises a tubular, prismatic body 115 having a hollow square cross-section. The link defines a first end 124 and a second end 132. The body 115 comprises a first end portion 118, a second end portion 120 and a middle part 122 joining the first and second end portions 118, 120. A first pair of bores 128, 130 extend through the first end portion proximate the first end 124 of the body 115. The bores 128, 130 define a first axis 126 normal to the surfaces of the body 115 in which the bores 128, 130 are defined. Similarly a second pair of bores 136, 138 extend through the second end portion proximate the second end 132 of the body 115. The bores 136, 138 define a second axis 134 normal to the surfaces of the body 115 in which the bores 138, 136 are defined. The first and second end

portions 118, 120 are angled to the middle part 122 at an angle  $\theta/2$  such that the axes 126, 134 are at an included angle of  $\theta$  to each other.

Referring to Figure F.3, the first link 114 is connected to the support member 126 via a first rotational joint 138, which comprises a shaft engaged in the aligned bores 128, 130 of the link 114. The axis 126 of the first link 114 is aligned with the global axis Z0 such that the first link 114 can rotate relative to the foot brace 102.

The second link 116 is connected to the second end portion 120 of the first link 114 by a second rotational joint 140 which allows the first and second links 114, 116 to rotate relative to one another about the second axis 134 of the first link 114, and a first axis 126 of the second link 116, which are aligned.

The end portion 107 of the pushrod 104 is connected to the second link 116 by a third rotational joint 142 for rotation about a second axis 134 of the second link 116.

In the configuration shown in Figures F.3 and F.4 (i.e. with the links in-line), the links 114, 116 span an angle of  $2\theta$  relative to the axis 126.

Referring to Figures F.5a and b, a schematic representation of a second assembly 200, which works on the same principle as the first assembly 100. The assembly 200 comprises a foot brace 202 holding a human foot 2. The ankle joint of the human foot 2 is coincident with the global coordinate system X0, Y0, Z0 having an origin O.

A linkage 204 comprises a first joint connected to the foot brace 202 defining a first axis 206 (aligned with Z0 in Figures F.5a and b). A first link 208 is connected to rotate about the first axis 206, and is connected to a second joint defining a second axis 210. A second link 212 is connected to rotate about the second axis 208 relative to the first link 208, and is connected to a third joint defining a third axis 214. The second link is thereby rotationally connected to a pushrod 216.

The axes 206, 210 and 214 intersect at a common point which is coincident with the origin O of the ankle. The links 208, 212 therefore form a gimbal-like mechanism permitting movement of the foot 2 in a controlled manner.

The foot 2 in Figures F.5a and b is in a neutral, or static position, and as can be seen, force F when applied to the pushrod 216 in a direction generally aligned with X0 will urge the foot forwards via the brace 202. The pushrod 216 is configured such that the force F acts through the centre of rotation O of the ankle. Therefore the subject does not feel any torque on the ankle.

Turning to Figures F.6a and b, the foot 2 has undergone an endorotation of  $\alpha$  degrees about the vertical axis Y0, thus providing new foot axes X0, Z0 each of which are rotated by  $\alpha$  degrees from the global axes X0, Z0.

Because of the constraint of the first joint defining axis 206 to the brace 202, the axis 206 rotates with the foot axis Z0 by  $\alpha$  degrees. Although this is the case, articulation of the links 208, 212 means that the pushrod 216 (and therefore the axis 214) remains in the same position. Therefore the force F can still be applied in the same direction, through the origin O of the ankle joint. This allows the foot to undergo exorotation and endorotation whilst the rehabilitation is taking place. During walking, the subject ankle undergoes a few degrees of endo-exorotation (this is normal). By allowing this rotation, gait is allowed to occur naturally without unnecessary restriction on this movement. There is the possibility to apply corrective forces on the ankle, e.g. increase step length or to place the foot more outward, without applying endo exorotation. Exo- and endo-rotation does not result in any forces being applied which are not coincident with the origin O of the ankle. In particular, no forces which oppose movement of the ankle back to the neutral position shown in Figures F.5a and b are applied.

It will be noted that the range of movement of the mechanism is limited by the included angles  $\theta$  of the links 208, 212.

Turning to Figures F.7a and b, the foot 2 has undergone an inversion of  $\beta$  degrees about the horizontal axis X0, thus providing new foot axes Y0, Z0 each of which are rotated by  $\beta$  degrees from the global axes Y0, Z0.

Because of the constraint of the first joint defining axis 206 to the brace 202, the axis 206 rotates with the foot axis Z0 by  $\beta$  degrees. Although this is the case, articulation of the links 208, 212 means that the pushrod 216 (and therefore the axis 214) remains in the same position. Therefore the force F can still be applied in the same direction, through the origin O of the ankle joint. This allows the foot to undergo inversion and eversion whilst the rehabilitation is taking place. Inversion and eversion does not result in any forces being applied which are not coincident with the origin O of the ankle. In particular, no forces which oppose movement of the ankle back to the neutral position shown in Figures F.5a and b are applied.

Again, it will be noted that the range of movement of the mechanism is limited by the included angles  $\theta$  of the links 208, 212.

As seen in the Figures, the point on at which the first link 208 is attached to the brace 202, is on the side of the foot (as opposed to the force F, which is applied from the rear of the foot towards the front). As such, the axis 206 of the attachment of the linkage 204 to the brace 202 is at 90 degrees to the

direction of the applied force  $F$ . Therefore the included angle  $\theta$  is less than 45 degrees (and is 17 degrees in this example). This provides a reasonable degree of movement of the foot 2, whilst ensuring that the linkage 204 is compact.

During rehabilitation, it is desirable to provide 25 degrees of dorsiflexion, and 35 degrees of plantarflexion (rotation about Z0). Due to this significant range of motion required, the first axis (which is highly unconstrained) is aligned to the ankle flexion axis (i.e. the first link is positioned at the side of the foot).

Turning to Figure F.8, the required range of motion for an ankle support is shown (for inversion / eversion and endo/exo rotation). Endo/exo rotation is shown on the horizontal axis, and inversion / eversion on the vertical axis.

The circular area 300 represents the range of motion provided by a linkage having two links each with  $\theta=12$  degrees. The circle has a diameter  $D$  of 24 degrees- i.e.  $2\theta$ . This means that a potential range of 24 degrees in either degree of freedom is possible.

10 degrees of ankle inversion and eversion (i.e. rotation about a horizontal fore-aft axis) are also desirable. It is desirable to provide a hard limit for inversion to avoid injury (the most common type of ankle sprains arise from inversion).

10 degrees of endorotation and 20 degrees of exorotation are also required for normal gait.

The required workspace 302 is also shown (as defined by the range of motion above). It is rectangular because the range of angular motion is specified by the design and geometry of the linkage. The workspace is a two-dimensional area because it is possible to undergo two types of motion simultaneously (because the ankle is effectively a ball joint).

By configuring the linkage appropriately, a centre 304 of the circular workspace 300 can be moved such that it is at 5 degrees exorotation (i.e. the mid-point of the exo-endo rotation range), and 10 degrees inversion. Usefully, this positions almost all of the required workspace 302 within the range of motion of the linkage, and also provides a hard limit of around -10 degrees inversion (although in reality this is dependent upon simultaneous endo/exo rotation).

The centre of the circle in Figure F.8 is the position of the links at which the axes 206 and 214 coincide. This can be determined by appropriate mechanical set up of the link axes during manufacture and assembly.

A similar example is shown in Figure F.9 for the human torso. In this

instance, the linkage is attached with its virtual centre on the hip joint. Two linkages may be used- one centred on each hip joint to provide full freedom of movement (this is described in more detail with reference to Figure F.10 below). The present invention is particularly advantageous because forces should be applied into the hip joint without producing torques on the pelvis.

In Figure F.9, the range of motion of the linkage is shown as area 400. Pelvis axial rotation is represented on the horizontal axis, and pelvis sagittal rotation on the vertical axis. With two links having  $\theta=17$  degrees, the diameter D is 34 degrees.

The desired degrees of freedom required by the pelvis during gait are as follows: (i) rotation of the pelvis in the frontal plane about a fore-aft axis (frontal rotation); (ii) rotation of the pelvis in the horizontal, transverse plane about a vertical axis (axial rotation); and (iii) rotation of the pelvis in the sagittal plane about a left-right axis (sagittal rotation).

The linkage is positioned behind the patient- at the side of the patient there is no available space, since in gait the subject's arms must be able to swing.

The range of motion required by the pelvis is as follows:

Frontal rotation =  $\pm 10$  degrees; Axial rotation =  $\pm 15$  degrees; Sagittal rotation = -26.9 to 22.6 degrees.

The above range provides a required workspace 402.

The linkage is assembled such that the axis equivalent to Z0 is aligned with the frontal axis of rotation (i.e. in a fore-aft direction), and positioned at the rear of the subject. In effect, the linkage does not therefore limit pure frontal rotation. This is not problematic, as during gait excessive frontal rotation is not a problem (it would be very difficult to achieve).

As mentioned above,  $\pm 15$  degrees axial rotation is required, and as such the minimum link angle (for two links)  $\theta = 15/2 = 7.5$  degrees.

One minor drawback of the linkage is that the centre point (the origin of the circle in Figure F.9) creates a slightly distracting sensation for the subject, and therefore it would not be desirable to have this in the normal range of motion. As such, it is offset by 10 degrees in axial rotation.

From the circle centre 404, the angle  $\theta$  is selected so that the circle 400 covers the required workspace 400. In this case  $\theta=17$  degrees.

Turning to Figure F.10, there is shown a gait training assembly 500 comprising a waist band 502, a first push rod 504, a first linkage 506, a second push rod 508 and a second linkage 510.

The waist band is configured to surround the abdomen of a subject to affix the linkages 506, 510 at the rear of the respective left and right hips.

The first linkage 506 comprises a first link 512 pivotably attached to the first push rod 504 about an axis 513 and a second link 514 pivotably attached to the first link 512 for rotation about an axis 515. The second link 514 is also pivotably attached to a bracket 516 downwardly depending from the waist band 502 for rotation about an axis 518.

Each link 512, 514 has an included angle of  $\theta$  between its respective axes of rotation, as with previous embodiments. All the axes 513, 515, 518 intersect at a hip joint centre of rotation H, and the assembly 500 is configured such that this imaginary intersection point is aligned with the subject's hip.

The second linkage 510 is configured in substantially the same way as the first linkage 506.

Variations fall within the scope of the present invention.

For example, more than two links may be provided for extra range of movement. The eventual number of links must be chosen for the specific application, as although an increased number of links would provide a more fluid motion, the stiffness of the linkage is decreased.

Another variation is a simple arrangement that points to the centre of mass of the pelvis- between the hips (instead of at each hip joint). With this setup you can apply forces to the centre mass without applying distracting torques on the subject.

The present invention can be used to apply forces to other joints, providing the axes are aligned to intersect at the centre of rotation of the subject's joint.

## F.2 Claims

1. An assembly for transferring a force from a force provider to a recipient object, the assembly comprising: a force provider; a recipient object; a linkage configured to transfer a force from the force provider to the recipient object, the linkage comprising a first link and a second link; the first link having a first rotational joint defining a first link axis, and a second rotational joint defining a second link axis, the first and second link axes being at a first link angle to each other, which first link is pivotably attached to the recipient object for rotation about the first axis; and, the second link having a third rotational joint defining a third link axis, and a fourth rotational joint defining a fourth link axis, the third and fourth link axes being at a second link angle to each other, the second link being

pivotably attached to the first link such that the second and third link axes coincide, the second link being pivotably mounted at the fourth link axis to transfer a force from the force provider, in which the first, second, third and fourth axes intersect at a predetermined point such that the recipient object can rotate about the predetermined point by articulation of the linkage; in which the first and second link angles are each less than 45 degrees.

2. A linkage according to claim 1, in which the force provider is a push-pull rod driven by an actuator.

3. A linkage according to claim 2, in which the push-pull rod and the actuator are configured to exert a force through the predetermined point.

4. A linkage according to any of claims 1 to 3, in which the rotational joints are defined by bores in the links having common shafts extending therethrough.

5. A linkage according to any of claims 1 to 4 in which each link comprises a body having a mid section, a first end section and a second opposite end section, the end sections being angled with respect to the mid section.

6. A linkage according to claim 5, in which the rotational joints of the links are defined normal to respective end sections such that the sections are angled to provide the link angles.

7. A linkage according to any of claims 1 to 6 in which the links are constructed from generally tubular bodies.

8. A linkage according to any of claims 1 to 7 in which the linkage comprises a third link having a fifth rotational joint defining a fifth link axis, and a sixth rotational joint defining a sixth link axis, the fifth and sixth link axes being at a third link angle to each other, the third link being pivotably attached to the second link such that the second and third link axes coincide, the third link being pivotably mounted at the sixth link axis to transfer a force from the force provider.

9. A rehabilitation apparatus comprising: a linkage according to any of claims 1 to 8, in which the recipient object is a support for a body part.

10. A rehabilitation apparatus according to claim 9, in which the support for a body part is configured to receive a body part proximate a joint to as to align an axis of rotation of the joint with the predetermined point of the linkage.

11. A rehabilitation apparatus according to claim 10, in which the support for a body part is configured to receive a body part proximate a joint to as to align a centre of rotation of the joint with the predetermined point of the linkage.

12. A rehabilitation apparatus according to any of claims 9 to 11, in which the force provider is configured to exert a force in a first direction, and in which the first link axis is oriented at 80 to 100 degrees to the exerted force.

13. A rehabilitation apparatus according to claim 12, in which the support is a foot support, and the force provider is configured to exert the force in a fore-aft direction of a subject in use.

14. A rehabilitation apparatus according to claim 13, in which the first link is connected to the support at a lateral side of the subject's foot in use.

15. An assembly for transferring a force as described herein with reference to, or in accordance with, the accompanying figures.

16. A rehabilitation apparatus as described herein with reference to, or in accordance with, the accompanying figures.

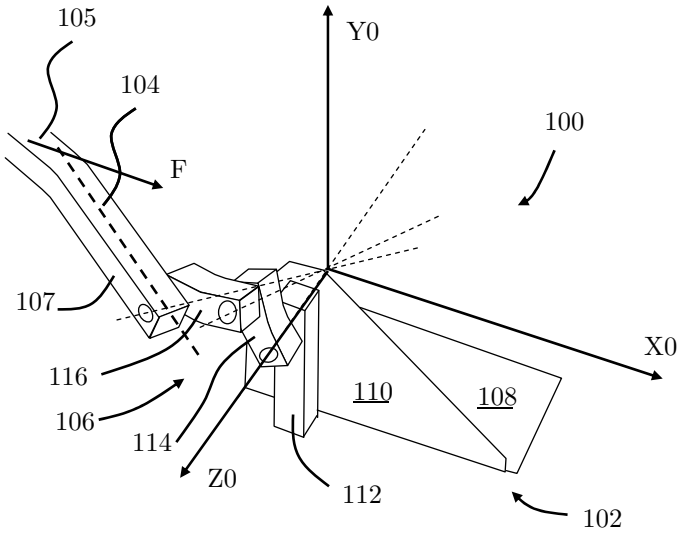


Figure F.1

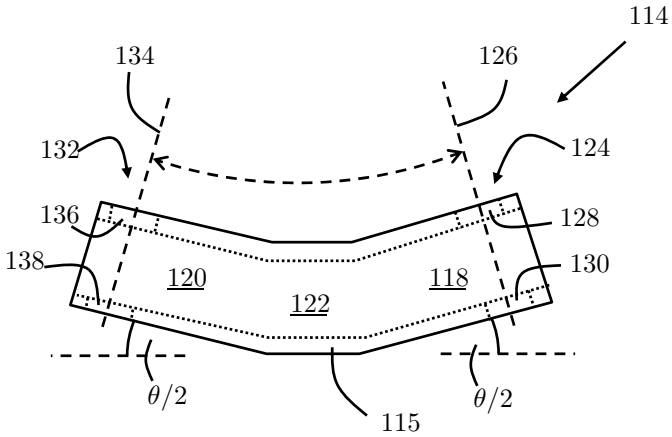


Figure F.2

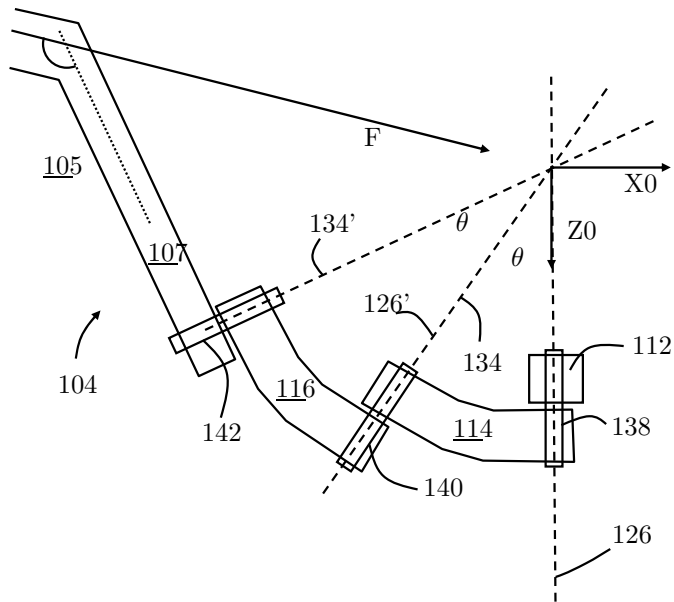


Figure F.3

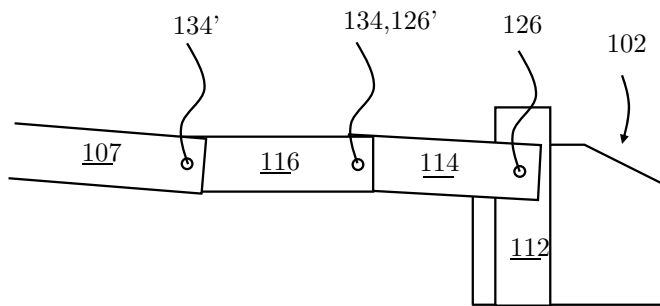


Figure F.4

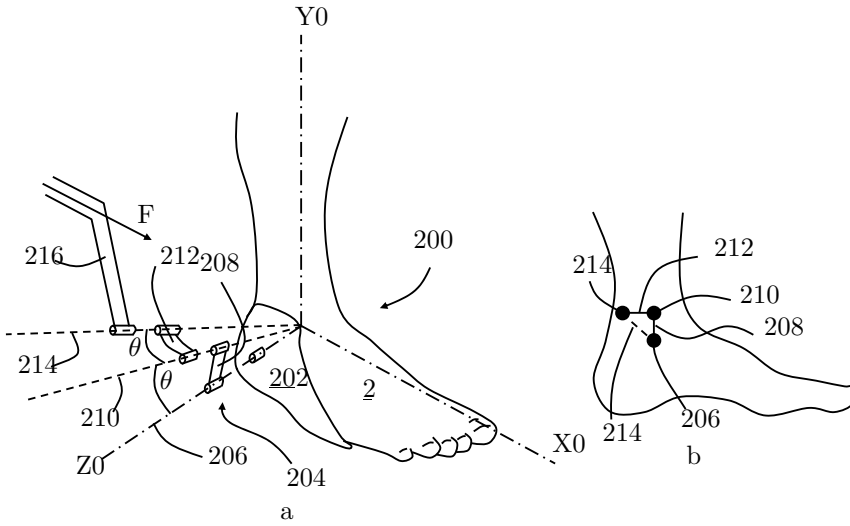


Figure F.5

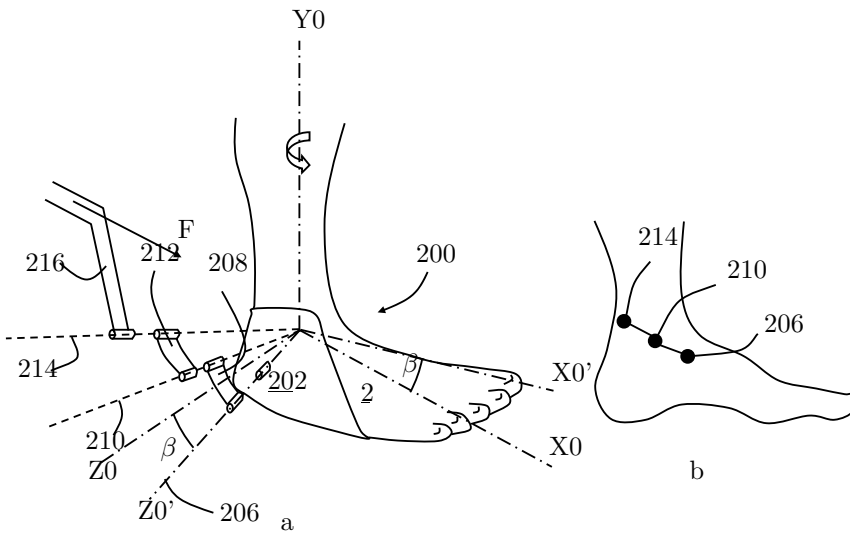


Figure F.6

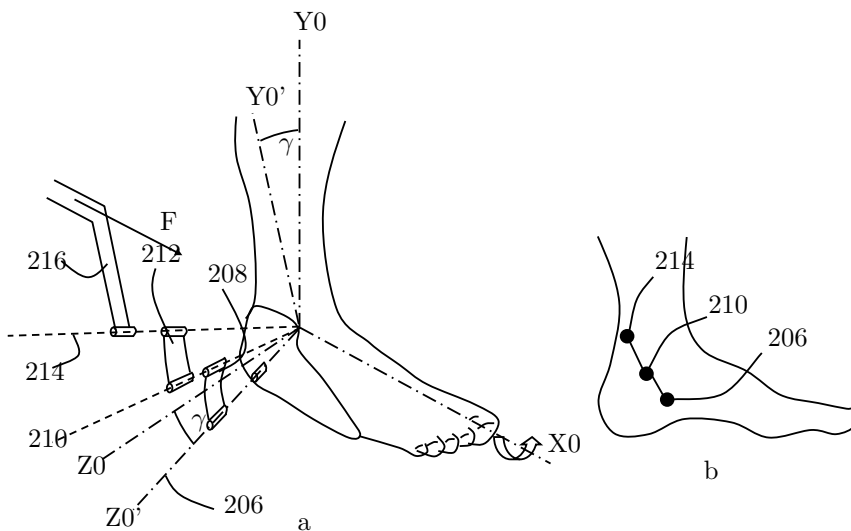


Figure F.7

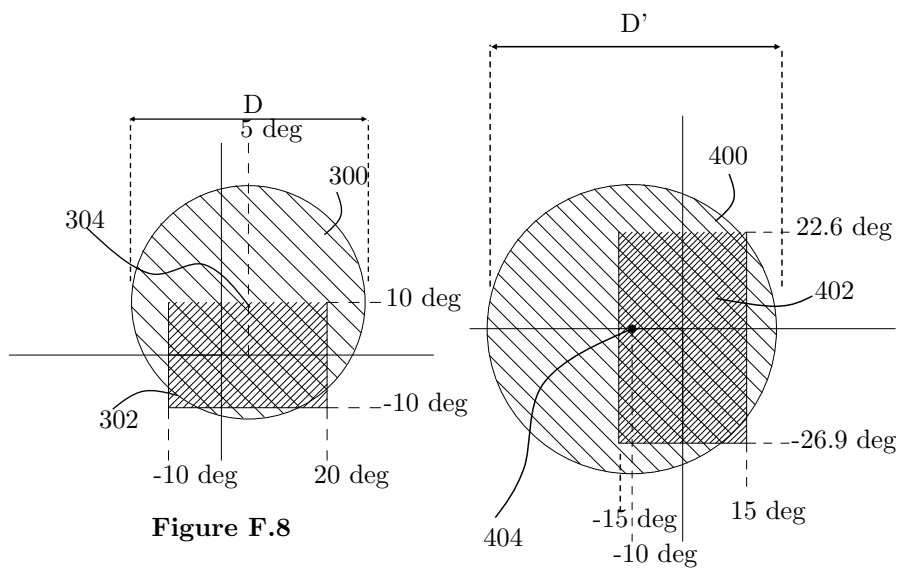


Figure F.8

Figure F.9

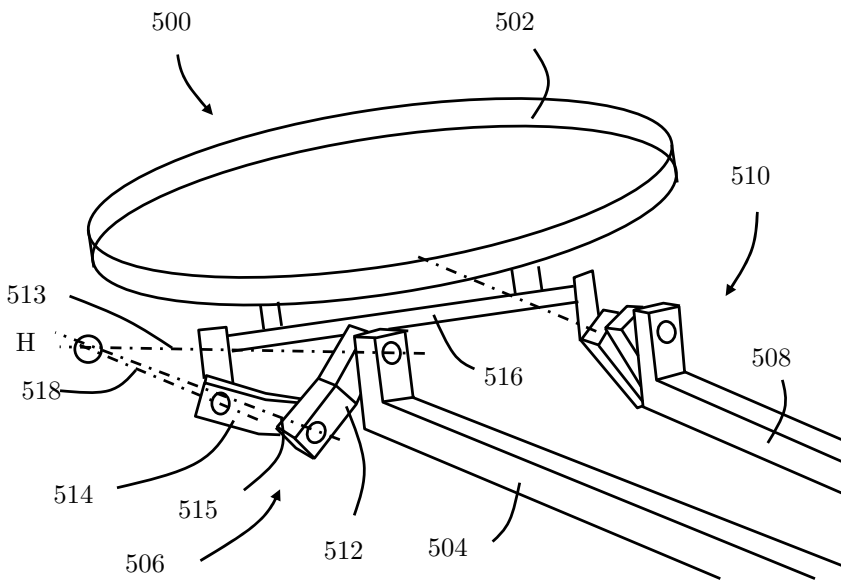


Figure F.10

# Proximal PD Controller Used as PVA Limiter

This chapter describes the theory of the Proximal PD (PPD) controller. The PPD controller is used as a limiter for position, velocity and acceleration in LOPES II. This work is based on work done by Piet Lammertse. We have added proof of robustness.

## G.1 The Problem

How to make sure that a servo system will not exceed position limits? In robots it is common practice that the robot has no-go areas, i.e., position limits that should not be exceeded. The main reasons are to prevent the robot to harm its environment and itself.

In admittance controlled robots the control loop uses virtual model of a moving mass and the motors of the robot are controlled such that the robot follows the moving mass. To prevent the robot to do damage to its environment and to itself, it is prudent that this model contains realistic and safe limits in terms of position, velocity and acceleration (pva). Using feasible limits means that the model limits are within the robot's performance limits, which may be limited by e.g. current limits, voltage limits, speed and acceleration. This reduces the control error, i.e. the difference between model pva and robot pva, and therefore it increases the controllability. Safe limits mean that the robot will not reach positions that are harmful for its environment. Admittance controlled robots use a

virtual model to generate setpoints for the servo system (see Fig. G.1). The model consists of a virtual mass, where the force input for the virtual mass is a sum of measured forces and forces from haptic effects, e.g. springs and dampers (Van der Linde and Lammertse, 2002). In the admittance controller the velocity and position are obtained through integration of the acceleration. To assure that neither of the states (pva) will violate a limit, the acceleration must be corrected.

Assuring that the acceleration limits are not exceeded is straightforward. Simply clipping the model acceleration is sufficient to guarantee that the acceleration set point is within limits. Also these limits can be asymmetric, such that for deceleration is different from the acceleration limit. Systems with friction can decelerate faster, therefore with an asymmetric limiter the full acceleration capacity is used.

A limitation of the velocity is also straight forward. Simply set the acceleration to zero as if the velocity is about to exceed its limit.

The challenge of the proper pva limiter is to obey the position limits. The goal is to decelerate the model (and model following robot) such that 1) the position limit is not violated i.e., the model does not go beyond a predefined position; while 2) the deceleration to stop the model does not violate the deceleration limit; such that 3) the limiter reacts ‘just in time’ i.e., the limiter is only active in the vicinity of the position limit; and such that 4) the limiter is stable i.e., will not cause oscillations or limit cycles.

## G.2 Parabolic Limiter

The ‘just in time’ requirement implies a constant maximum acceleration ( $\ddot{x}_{max}$ ). This means that, given the maximum deceleration and using the equations of motion, for each point with distance  $x$  from its limit, we can

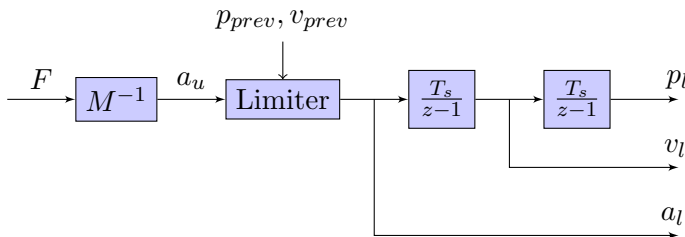


**Figure G.1:** Schematic overview of set point limitation for a force input model

define the maximum allowable speed at that point.

$$\dot{x}_{max} = \sqrt{2 |x| \ddot{x}_{max}} \quad (\text{G.1})$$

In the phase plot of position and velocity this is a parabolic curve (see figure G.2a).

So if we want to correct the actual speed ( $\dot{x}$ ) toward the local maximum speed, then we can define a corrective force (acceleration) proportional to the speed error:

$$\ddot{x}^L = -D (\dot{x} - \dot{x}_{max}) \quad (\text{G.2})$$

With  $D$  as the damping term. Substituting (G.1) in (G.2) gives:

$$\ddot{x}^L = -D \dot{x} - D \sqrt{2 |x| \ddot{x}_{max}} \quad (\text{G.3})$$

The derivative of this function is:

$$\frac{\partial \ddot{x}^L}{\partial \dot{x}} = -D \quad (\text{G.4})$$

$$\frac{\partial \ddot{x}^L}{\partial x} = \frac{-D}{\dot{x}_{max} \sqrt{|x|}} \quad (\text{G.5})$$

When using this algorithm the pva limiter is unstable, since a small position error in the vicinity of the end stop, causes a high control gain, therefore it parabolic curve is unsuitable as pva limiter.

## G.3 The Proximal PD Controller

### G.3.1 Introducing the Proximal PD Controller

For the limiting function we propose the Proximal PD controller (PPD) which is a parabolic curve far from the end stop and a linear PD controller in the vicinity of the end stop. We use the term ‘controller’ here for the function of set point limitation. This should not be confused with the controllers for the actuators.

$$\ddot{x}^L = -D \dot{x} - \frac{P x}{\sqrt{1 + |x|/r}} \quad (\text{G.6})$$

where  $r$  is defined by the maximum deceleration ( $a_{max}$ )

$$r = 2 a_{max} \left( \frac{D}{P} \right)^2 \quad (\text{G.7})$$

For convenience in further equations, we make the PPD (G.6) dimensionless by using:

$$\epsilon = \frac{x}{r} \quad (\text{G.8})$$

$$\ddot{\epsilon}^L = -2\zeta\omega\dot{\epsilon} - \omega^2 \frac{\epsilon}{\sqrt{1+|\epsilon|}} \quad (\text{G.9})$$

with:

$$\omega = \sqrt{P} \quad (\text{G.10})$$

$$\zeta = \frac{D}{2\omega} \quad (\text{G.11})$$

The linear curve and the parabolic curve intersect at  $\epsilon = \pm 1$  (see Fig. G.2a). For values of  $|\epsilon| \gg 1$  the PPD behaves as a parabolic, and for  $|\epsilon| \ll 1$  it behaves as a linear curve.

$$\ddot{\epsilon}^L = \begin{cases} -2\zeta\omega\dot{\epsilon} - \omega^2\epsilon & |\epsilon| \ll 1 \\ -2\zeta\omega\dot{\epsilon} - \omega^2\sqrt{|\epsilon|} & |\epsilon| \gg 1 \end{cases} \quad (\text{G.12})$$

The proximal PD Controller has the following properties: the D-term is constant, the derivative to position is bounded in for all positions, the acceleration and velocity are limited. These properties are proven in the following sections.

### G.3.2 Constant D-term

The derivative of the proximal PD controller to velocity is constant (see (G.13)). This means that the controller can be dimensioned with a constant and optimal damping term.

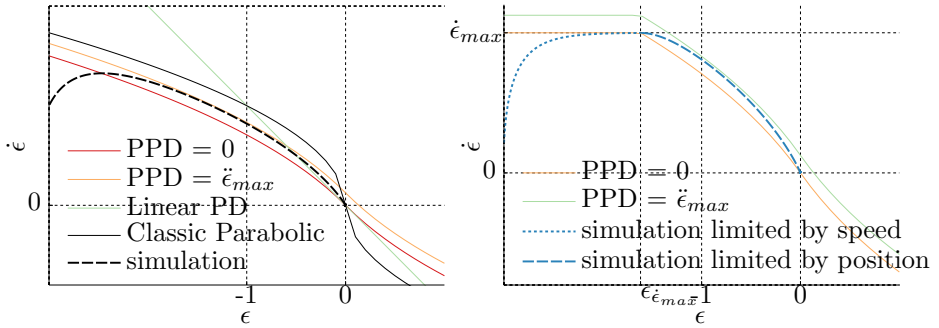
$$\frac{\partial \ddot{\epsilon}^L}{\partial \dot{\epsilon}} = -2\zeta\omega \quad (\text{G.13})$$

### G.3.3 Bounded P-term

The derivative to position is:

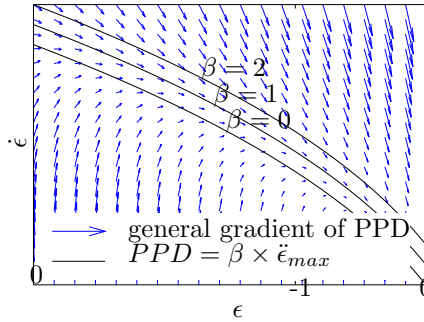
$$\frac{\partial \ddot{\epsilon}_\ell}{\partial \epsilon} = -\frac{\omega^2(|\epsilon| + 2)}{2(|\epsilon| + 1)^{3/2}} \quad (\text{G.14})$$

The derivative to  $\epsilon$  is finite



(a) PPD compared with a constant acceleration (black), and a linear PD controller (green).

(b) PPD with velocity limitation.



(c) Gradient of the PPD controller (blue), compared with constant torque lines (black);  $\beta = 0$  is the zero torque line,  $\beta = 1$  is the maximum deceleration curve.

**Figure G.2:** Phase plots of the Proximal PD controller (PPD)

$$\frac{\partial \ddot{\epsilon}^L}{\partial \epsilon} = \begin{cases} -\omega^2 & |\epsilon| \ll 1 \\ \frac{\omega^2 \text{sign}(\epsilon)}{2\sqrt{|\epsilon|}} & |\epsilon| \gg 1 \end{cases} \quad (\text{G.15})$$

In other words, the algorithm gradually changes from a maximum acceleration controller at large position errors (see (G.5)), to a linear PD controller at small position errors.

### G.3.4 Limiting the Velocity

The acceleration limit as calculated in (G.9) does not take into account the maximum velocity. On the zero PPD curve ( $\ddot{\epsilon}^L = 0$ ) we calculate the point where the velocity is maximum:

$$\epsilon_{\dot{\epsilon}_{max}} = \pm \mu \left( 1 + \sqrt{1 + 2/\mu} \right) \quad (\text{G.16})$$

with:

$$\mu = 2 \left( \frac{\zeta}{\omega} \dot{\epsilon}_{max} \right)^2 \quad (\text{G.17})$$

In (G.9) we limit the input value for  $\epsilon$ :

$$\ddot{\epsilon}^L = -2\zeta\omega\dot{\epsilon} - \omega^2 \frac{\epsilon_{PPD}}{\sqrt{1 + |\epsilon_{PPD}|}} \quad (\text{G.18})$$

with

$$\epsilon_{PPD} = \text{sign}(\epsilon) \min(|\epsilon|, \epsilon_{\dot{\epsilon}_{max}}) \quad (\text{G.19})$$

## G.4 Analysis of Robustness

When using a critically damped system ( $\zeta = 1$ ) the velocity and position stay within the predefined bounds ( $\dot{\epsilon} \leq \dot{\epsilon}_{max}$  and  $\epsilon \leq 0$ ) (see figure G.2b).

The calculation of the maximum accelerations is more complex. Looking at the numerical simulations (see figure G.2) the occurring accelerations seem to stay below the maximum acceleration curve, however this is insufficient proof. The maximum acceleration that occurs in the PPD is calculated with the following steps. First we calculate the gradient of the PPD (see figure G.2c):

$$\begin{aligned} \vec{\nabla}_{\epsilon_{PPD}}(\epsilon, \dot{\epsilon}) &= \left( \frac{\partial \epsilon_{PPD}}{\partial \epsilon}, \frac{\partial \epsilon_{PPD}}{\partial \dot{\epsilon}} \right) \\ &= \left( \dot{\epsilon}, -2\zeta\omega\dot{\epsilon} - \omega^2 \frac{\epsilon}{\sqrt{1 + |\epsilon|}} \right) \end{aligned} \quad (\text{G.20})$$

Furthermore we calculate the curve at which the PPD produces a constant value (see figure G.2c) :

$$\begin{aligned} -2\zeta\omega\dot{\epsilon} - \omega^2 \frac{\epsilon}{\sqrt{1 + |\epsilon|}} &= \ddot{\epsilon}_c \\ &= \beta \frac{-a_{max}}{r} \end{aligned} \quad (\text{G.21})$$

where  $\beta$  denotes the normalized constant PPD output. For  $\beta = 1$  the PPD produces the maximum acceleration ( $a_{max}$ ).

Now it is key to find the lowest constant acceleration curve (lowest value of  $\beta$ ) for which the gradient stays below the constant acceleration curve. The mathematical solution is quite complex and requires numerical solving. The solution is  $\beta = 1.0359$ . This means that the maximum acceleration that the PPD will produce is 3.6% higher than the predefined maximum acceleration. And it means that the used acceleration value in (G.7) must be 96.5% of the desired maximum deceleration.

## G.5 PPD in Practice

### G.5.1 Pseudo Code

Summarizing the PPD controller can be used as a set point limiter with the following rules.

1. Establish the maximum position, velocity and deceleration for a single DoF.
2. Correct the maximum deceleration with 96.5% to guarantee no excessive acceleration
3. Select the desired end stop stiffness  $P$ .
4. Calculate  $D$  with (G.10) and (G.11)
5. Calculate  $r$  with (G.7)
6. Calculate the position on the PPD curve at which the speed is maximum ( $p_{v_{max}}$ ) using (G.16) and  $r$

Then for each loop cycle, for each DoF do the following:

1. Calculate  $x$ , the distance to the endstop
2. Replace  $x$  with the minimum of  $x$  and  $x_{\dot{x}_{max}}$  to make sure the velocity limit will not be exceeded
3. Calculate the maximum acceleration ( $\ddot{x}^L$ ) with (G.6)
4. if the desired acceleration exceeds the maximum acceleration, limit the desired acceleration to the maximum acceleration

**Table G.1:** Set and derived parameters for the PVA limiter in the HapticMASTER

Set parameters		
Negative endstop ( $p_{min}$ )	-0.27	[m]
Positive endstop ( $p_{max}$ )	0.27	[m]
Maximum speed ( $v_{max}$ )	1	[m/s]
Maximum acceleration ( $a_{upperlimit}$ )	50	[m/s <sup>2</sup> ]
Maximum deceleration ( $a_{lowerlimit}$ )	50*1.0359	[m/s <sup>2</sup> ]
Endstop stiffness (P)	50000	[N/kgm]
Endstop damping ( $\zeta$ )	1	[]
Derived parameters		
$\omega$	707	[Hz]
$D$	1414	[Ns/kgm]
$r$	0.76	[mm]
$\mu$	6.76	[-]
$p_{v_{max}}$	0.011	[m]
$\epsilon_{v_{max}} (p_{v_{max}}/r)$	14.5	[-]

### G.5.2 Numerical Simulation of the HapticMASTER

A simulation of a HapticMASTER approaching its end stop is given in Fig. G.3. None of the limitations are violated: The peak accelerations are  $50 \text{ m/s}^2$  and  $-49.8 \text{ m/s}^2$ . The peak velocity is  $1 \text{ m/s}$ . The maximum position is  $0.27 \text{ m/s}$ .

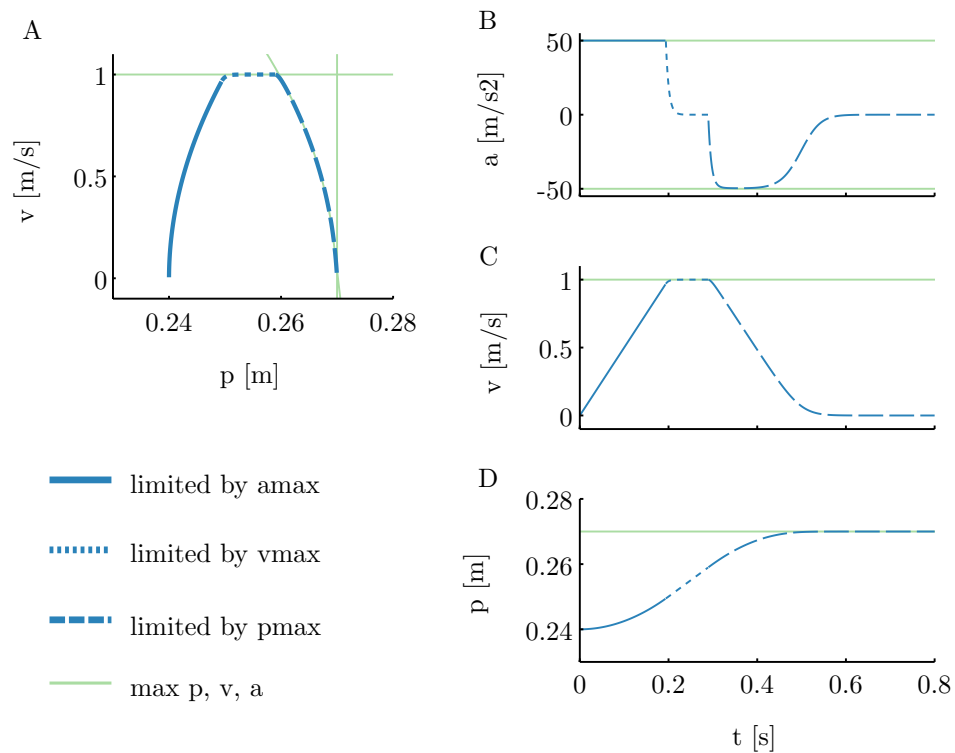


**Figure G.3:** Simulation of the PVA limiter in the HapticMASTER: velocity vs position (A), Acceleration vs time (B), Velocity vs time (B)



# System Usability Scale for LOPES II

This section lists the questionnaire we used to assess the usability of LOPES II. The questions are based on the System Usability Scale ([Brooke, 1996](#)). The questions are in dutch.

1. Ik denk dat ik de LOPES graag regelmatig wil gebruiken

Sterk mee oneens      Sterk mee eens

2. Ik vind de LOPES onnodig complex

Sterk mee oneens      Sterk mee eens

3. Ik vind de LOPES gemakkelijk te gebruiken

Sterk mee oneens      Sterk mee eens

4. Ik denk dat ik ondersteuning nodig heb van een technisch persoon om de LOPES te kunnen gebruiken

Sterk mee oneens      Sterk mee eens

5. Ik vind dat de verschillende functies in de LOPES erg goed geventueerd zijn

Sterk mee oneens      Sterk mee eens

6. Ik vind dat er teveel tegenstrijdigheden in de LOPES zaten

Sterk mee oneens      Sterk mee eens

7. Ik kan me voorstellen dat de meeste mensen zeer snel leren om de LOPES te gebruiken

Sterk mee oneens      Sterk mee eens

8. Ik vind de LOPES erg omslachtig in gebruik

Sterk mee oneens      Sterk mee eens

9. Ik voel me erg vertrouwd met de LOPES

Sterk mee oneens      Sterk mee eens

10. Ik moest erg veel leren voordat ik aan de gang kon gaan met de LOPES

Sterk mee oneens      Sterk mee eens

The answers to the questions are listed in figure [H.1](#).

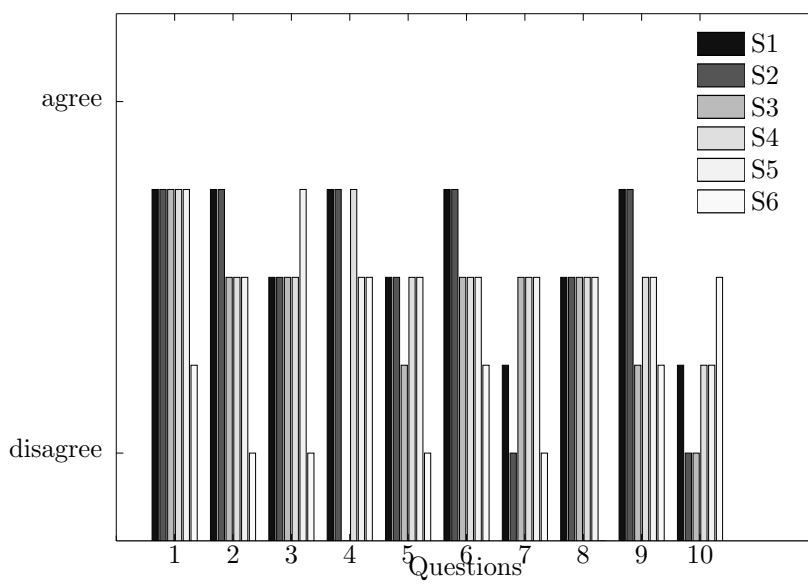


**Figure H.1:** Answers to the questions of six subjects.



# Dankwoord

Vrijwel elke promotie lijkt een one-manshow, maar is in feite met hulp van velen tot stand gekomen. Met dit onderzoek is het niet anders. Bij deze wil ik graag de mensen bedanken die hebben meegeholpen, meegedacht en meegewerkt.

Mijn promotie onderzoek heb ik kunnen uitvoeren terwijl ik in dienst was bij Moog. Daar heb ik mij, naast mijn normale werkzaamheden, de afgelopen jaren kunnen storten op de wetenschappelijke kant van het ontwikkelen van een looprobot. Weinig mensen hebben het geluk dat hun werkgever dit ondersteunt. Ik ben daarom Moog en mijn collega's ontzettend dankbaar dat ze mij de ruimte hebben gegeven aan mijn promotieonderzoek te werken. Vooral Piet en Harry wil ik daarvoor bedanken. Jullie hebben veel (lobby) werk verricht om te zorgen dat het LOPES project van start kon gaan. Jullie hebben in het begin zelfs mij moeten overtuigen dat een promotie onderzoek een goed idee was. En daar hebben jullie gelijk in gekregen.

Verderop zal ik nog terugkomen op mijn Moog-collega's, maar ik wil hier eerst een woord wijden aan Piet. Je bent de Founding Father van de afdeling en van vrijwel alle producten die we maken. Ook bij LOPES II heb je een groot stempel gedrukt op de processen, mechanische concepten en controller componenten. Maar ondanks je grote invloed zou jij het natuurlijk toch helemaal anders hebben gedaan. Misschien krijg je ooit nog je zin en bouw je toch nog een Lopes met een Turks muiltje.

In de zomer van 2009 begon mijn Lopes avontuur. Bij Moog had ik al wel ervaring met Ontwerpen, maar Wetenschappelijk Onderzoek was de afgelopen jaren wat onderbelicht. Gelukkig had ik op de UT veel steun aan Herman en Edwin en later ook Hans, die mij de fijne kneepjes van Onderzoek en Publiceren probeerden bij te brengen. Herman, ook voor jou moet het een avontuur zijn geweest om een wat oudere promovendus van buiten

aan te nemen. Een andere uitdaging kwam door de dubbele rollen die we hadden: jij als promotor, ik als promovendus; jij als klant, ik als leverancier. Dat zou wel eens lastig kunnen worden, dacht ik soms. Gelukkig is dit reuze meegevallen en kijk ik terug op een erg prettige samenwerking.

De wereld van de revalidatie was nieuw voor mij. Zo ook alle terminologie die fysiotherapeuten, revalidatieartsen en bewegingswetenschappers gebruiken. Voor het ontwikkelen van een looprobot moet je echter goed met hen kunnen communiceren. Edwin, jij hebt me snel wijsgemaakt in die wereld. En wel door me meteen in het diepe te gooien: Ik was koud op de UT, of we hadden interviews in Amsterdam, Nijmegen en Enschede, met alle specialisten op het gebied van revalidatie. Op de terugweg vertaalde jij dan nog even wat mij net allemaal was verteld. Daarnaast heb jij me geweldig geholpen met de opzet van de onderzoeken en de statistische analyses. Maar de grootste bijdrage zit toch wel in het redigeren. Altijd was je bereid om teksten te reviewen en daarmee te verbeteren. Ontzettend bedankt daarvoor!

Hans, we kenden elkaar al vanaf het begin van het project, maar pas later werd je mijn co-promotor. Heel erg bedankt voor de discussies en de bijdragen in het schrijven, waardoor LOPES II nog dichter bij een klinische toepassing is gekomen.

Ik heb een erg leuke tijd gehad op de UT. Dat komt vooral ook door de vakgroep. Etentjes, taart, discussies, 1-april-grappen bij Herman, nog meer taart, muziek maken, alweer taart, body-pump (om die taart weer kwijt te raken). Arno, Tjitske, Bram, Gijs, Bas, Carsten, en vele anderen, ontzettend bedankt.

In het begin van het project waren we op zoek naar het juiste concept voor LOPES II. Dit was de tijd van het iteratief ontwerpen, waarin we elke twee weken bij het Roessingh of de Sint Maartenskliniek stonden met een houtje-touwtje opstelling van buizen, autobanden en fietswielen. Dit proces is uitvoerig beschreven in hoofdstuk 4 in dit proefschrift. Wat ik hier nog wil benadrukken is dat je voor dit proces de juiste mensen moet hebben. Frans, fantastisch hoe je elke keer weer op basis van een vage potloodschets binnen een week een mechanisme kon maken wat we konden uitproberen. Rob en Alex, onmisbaar bij het verzinnen, uitvoeren en documenteren van de nieuwe concepten, en de integratie van de concepten in de test kar. En niet te vergeten, de mensen van het Roessingh en de Sint Maartenskliniek, die de moeite namen door de vreemde bouwsels heen te kijken en de input te geven die we nodig hadden om tot het juiste concept te komen. Willem,

Hennie, Bart, Jaap, Bertine, Martijn en Hans, bedankt voor jullie open blik en constructieve commentaar.

Het LOPES project is opgezet met een consortium van 5 partijen: Sint Maartenskliniek, Roessingh Research and Development, Universiteit Twente, Demcon en Moog. Demcon is net als Moog gespecialiseerd in het ontwikkelen van mechatronische systemen. Kort na aanvang van het project werd duidelijk dat er behoorlijke verschillen waren in werkwijze en visie tussen Moog en Demcon. Gelukkig zijn we er uitgekomen, mede dankzij Rini Zwikker, en hebben we alsnog prettig kunnen samenwerken. Vrijwel wekelijks ging ik op mijn vouwfietsje naar Oldenzaal om details van het ontwerp te bespreken. Met plezier denk ik terug aan de tijd dat we bij een whiteboard stonden en daar ontwerpuitdagingen trotseerden.

Toen bij Demcon de contouren van LOPES II helder begonnen te worden, werd het bij Moog tijd voor het ontwerpen van elektronica en software. Waar nodig trommelde Wouter hulp uit alle hoeken en gaten, al dan niet gelokt met snoepgoed. Wouter, Mark, Eyal, Piet, Karlijne, Arno, Johannes en Ben, ontzettend bedankt voor de fantastische samenwerking.

In maart 2013 was het eindelijk zover. LOPES II werd, met veel kunst en vliegwerk, geïnstalleerd bij het Roessingh. Hij was echter nog niet operationeel, er moest nog veel programmeerwerk worden verzet. Niet alleen door mijzelf, ook de UT moest nog een flink stuk software ontwikkelen. Daar had de UT gelukkig Gijs voor. Daar zaten we dan met zijn tweeën, in een hoekje in het Roessingh, met een half werkende machine. Vervelend? Integendeel! Ik heb erg veel plezier beleefd aan deze tijd, waarin we wiskundige puzzels probeerden op te lossen met creatieve ingevingen. Gijs, heel erg bedankt voor het meedenken, programmeren, tunen en natuurlijk nerd-snipen.

‘Iets later dan gepland, werden de twee prototypes begin 2014 dan toch eindelijk in gebruik genomen. Zoals dat gaat met prototypes zaten er nog wel wat kinderziektes in, waardoor er nog het nodige werk aan moest worden verricht. Graag wil ik de mensen van het Roessingh, RRD en de Sint Maartenskliniek bedanken voor hun geduld en samenwerking tijdens de pilot tests.

In het laatste half jaar van mijn promotie begon het vele schrijven. ‘Heelaas moest er tegelijkertijd een LOPES III worden ontwikkeld en gebouwd. Dit vergde ook veel tijd. Gelukkig hielden vooral Tom en Karlijne mij uit de wind, door een groot deel van de ontwikkeling van LOPES III op zich te nemen. Bedankt voor de fantastische samenwerking het en het jullie inzet om LOPES naar *the next level* te brengen.

Naast alle mensen met wie ik heb samengewerkt tijdens het LOPES project wil ik ook graag vrienden en familie bedanken voor de onontbeerlijke morele steun (“Hoe gaat het met je afstuderen?”) en voor, gewoon, er altijd zijn. In 1994 leerde ik Ralph en Floris kennen tijdens de start van de studie Werktuigbouwkunde aan de UT. Sindsdien zijn we elkaar niet uit het oog verloren. Ik ben erg blij dat jullie mijn paranimfen willen zijn. Kees en Leida, hartelijk dank voor het regelmatig opvangen van de kinderen van de twee carrière jagers. Pap en Mam, door de afstand zien we elkaar niet zo vaak, maar jullie ontzettend bedankt voor de morele steun en het ‘trots zijn’.

De meeste dank ben ik verschuldigd aan Martine en mijn kinderen. Promoveren is al een uitdaging en de reis afstand Bennebroek–Enschede maakte deze uitdaging nog groter. Vooral met drie jonge kinderen vergt dat regelen, goochelen met de tijd, prioriteiten stellen, en dus niet vergeten af en toe tijd voor elkaar maken. Martine, Gijs, Marie en Siebe, jullie zijn de grootste steun geweest in de afgelopen jaren, waarschijnlijk zonder dat jullie dat heel erg beseft hebben. Mijn promoveren was een leuk avontuur, maar nog leuker was het om na een paar dagen Enschede thuis te komen en dan verhalen te horen over school, speelafspraken en de lokale politiek, en mee te helpen met Lego bouwwerken en het ‘runnen van het gezin’. Martine, nu is het jouw tijd, sterker nog, je bent al hard bezig met jouw eigen ‘promotie. Ik hoop dat ik je in je politieke carrière net zo kan steunen zoals je mij hebt gesteund in mijn wetenschappelijke carrière.

Bennebroek, oktober 2015

# Biography

Jos Meuleman was born on April 9, 1976 in Amsterdam. After finishing highschool in Assen in 1994, he started his study Mechanical Engineering at the University of Twente. He did his master in Mechanical Automation and Mechatronics. His graduation project was the design of a six-dimensional force sensor, conducted at Fokker Control Systems.



After his graduation in 2001 he started working as design engineer at Fokker Control Systems, later named Moog. He first worked in the technology team support various projects. In 2004 he joined the Robotics department where force feedback systems were being developed. He worked on the development and exploitation of the HapticMASTER, an admittance controlled generic 3DoF haptic interface that is often used in research on arm movements e.g., for rehabilitation. He developed the Wristalyzer, a haptic device to perturb wrist flexion and extension and measure joint stiffness. In 2006 the Robotics department started the development of the Simodont, a haptic device for simulating dental procedures. Jos' role was to develop the mechatronics of the first proofs of principles and of several prototypes.

In 2009 the Lopes project started. Moog, University of Twente, Demcon, Roesssingh Research and Development and the Sint Maartens clinic teamed up to develop the follow-up of the Lopes I, which was developed by the University of Twente. In this project Jos was responsible for the concepts, system design, mechatronics and control of the new LOPES II. Simultaneously he started doing his PhD at the University of Twente on the development of LOPES II. Currently Jos is part of the team that develops the third generation of LOPES at Moog.



# List of Publications

## PEER REVIEWED PAPER, PUBLISHED

Jos H. Meuleman, Edwin H.F. van Asseldonk, and Herman van der Kooij. The effect of directional inertias added to pelvis and ankle on gait. *Journal of neuro-engineering and rehabilitation*, 10(1):40, April 2013.

## PEER REVIEWED PAPER, UNDER REVIEW

Jos H. Meuleman, Edwin H.F. van Asseldonk, Gijs van Oort, Hans Rietman and Herman van der Kooij. LOPES II — Design and Evaluation of an Admittance Controlled Gait Training Robot with Shadow-Leg Approach *Transactions on Neural Systems & Rehabilitation Engineering*

## CONFERENCE PROCEEDINGS

Jos H. Meuleman, Wybren Terpstra, Edwin H. F. van Asseldonk, and Herman van der Kooij. Effect of added inertia on the pelvis on gait. *IEEE ... International Conference on Rehabilitation Robotics : [proceedings]*, 2011

Jos H. Meuleman, Reinoud Kruithof, Edwin H F Van Asseldonk, and Herman Van Der Kooij. Pilot Study on Following and Resisting Forces on the Pelvis. In Marta Pons, José L.; Torricelli, Diego; Pajaro, editor, *Converging Clinical and Engineering Research on Neurorehabilitation*, pages 149 – 153. Springer, 2012.

Bram Koopman, Jos H. Meuleman, Edwin H.F. van Asseldonk, and Herman van der Kooij. Lateral balance control for robotic gait training. In *Rehabilitation Robotics (ICORR), 2013 IEEE International Conference on*, pages 1–6, 2013.

Jos H. Meuleman, E.H.F. van Asseldonk, and H. van der Kooij. Novel actuation design of a gait trainer with shadow leg approach. In *Rehabilitation Robotics (ICORR), 2013 IEEE International Conference on*, Seattle, 2013.

## INTERNATIONAL PATENT APPLICATIONS

Jos H. Meuleman and Piet Lammertse, Moog BV Rehabilitation apparatus with a shadow leg, 2014. application number: WO2014090414 A1 URL <http://www.google.com/patents/WO2014090414A1?cl=en>.

Jos H. Meuleman, Moog BV Manipulator mechanism, 2014. application number: WO2014161726 A1 URL <http://www.google.com/patents/WO2014161726A1?cl=en>.

Jos H. Meuleman, Moog BV Mechanical linkage, 2013. application number: WO2014161797 A1 URL <https://www.google.com/patents/WO2014161797A1?cl=en>.

# Admittance Control

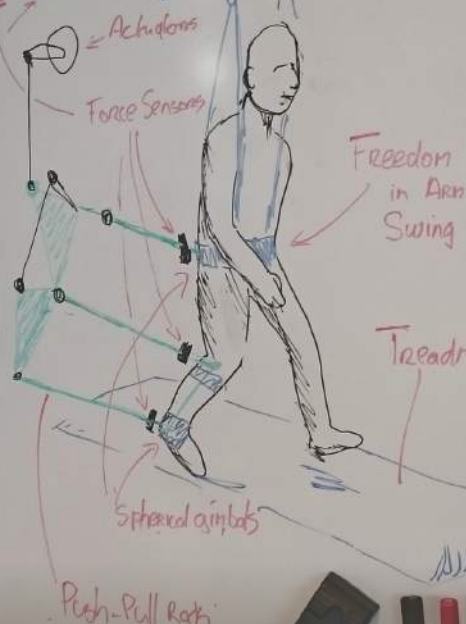


Body weight Support

# LOPES II

\* Assist As Needed

\* Quick Donning & Doffing



Treadmill



ISBN: 978-90-365-3965-4